Tennessee Valley Authority, Post Office Box 2000, Spring City, Tennessee 37381-2000

OCT 0 9 2001

10 CFR 50 Appendix H

U.S. Nuclear Regulatory Commission
ATTN: Document Control Desk
Washington, D. C. 20555

Gentlemen:

In the Matter of)
Tennessee Valley Authority)

Docket No.50-390

WATTS BAR NUCLEAR PLANT (WBN) UNIT 1 - REACTOR VESSEL SURVEILLANCE CAPSULE W TEST RESULTS AND REACTOR VESSEL FRACTURE TOUGHNESS (J-R) TEST RESULTS (TAC NO. MA8635)

In accordance with 10 CFR 50, Appendix H.IV.A, TVA is submitting the technical report "Analysis of Capsule W From the Tennessee Valley Authority Watts Bar Unit 1 Reactor Vessel Material Surveillance Program," approved September 10, 2001. This report was developed by BWXT Services, Inc. and details the tests results of Surveillance Capsule W withdrawn in Cycle 3 refueling outage. Based on the results of Capsule W and the results of Capsule U submitted October 13, 1998, the upper shelf energy (USE) values for the beltline materials are expected to be greater than 50 foot pounds (ft-lb) through end-of-life (EOL), 32 effective full power years (EFPY) as required by 10 CFR 50, Appendix G. Enclosure 1 provides the report for your review.

In addition to the above required report, Enclosure 2 provides a supplemental report entitled "Analysis of J-R Curves Generated from Capsule W 1/2T Compact Tension Specimens of the Tennessee Valley Authority Watts Bar Unit 1 Reactor Vessel Material Surveillance Program," approved September 24, 2001. This report provides the results of the reactor vessel fracture toughness (J-R) testing and an evaluation of the effects on TVA's equivalent margins analysis which was provided to NRC on October 15, 1993. The testing for the J-R Curve analysis was performed by BWXT Services, Inc. with procedures that were

D030

Printed on recycled paper

submitted to NRC for approval on July 10, 2001. NRC approved the use of those procedures in a letter dated August 1, 2001. Based on the evaluation of the J-R curves generated from 1/2T compact fracture specimens, it is concluded that the requirements of American Society of Mechanical Engineering (ASME) Section XI, Appendix X are met for neutron fluence values up to 1.23×10^{19} n/cm^2 (E>1.0 MeV) at EOL. The results of the October 15, 1993, equivalent margins analysis were also met with ample margin. This testing was performed in accordance with the WBN License Condition C.(5) and completes the portion of the License Condition for Capsule W supplemental testing.

There are no commitments identified in this letter. If you have any questions about these reports, please contact me at (423) 365-1824.

Sincerely,

Rebecca M. Mays

for P. L. Pace
Manager, Site Licensing
and Industry Affairs

Enclosures
cc (Enclosures):

NRC Resident Inspector
Watts Bar Nuclear Plant
1260 Nuclear Plant Road
Spring City, Tennessee 37381

Mr. L. Mark Padovan, Senior Project Manager
U.S. Nuclear Regulatory Commission
MS 08G9
One White Flint North
11555 Rockville Pike
Rockville, Maryland 20852-2739

U.S. Nuclear Regulatory Commission
Region II
Sam Nunn Atlanta Federal Center
61 Forsyth St., SW, Suite 23T85
Atlanta, Georgia 30303

ENCLOSURE 1

WATTS BAR NUCLEAR PLANT UNIT 1
ANALYSIS OF CAPSULE W
REACTOR VESSEL MATERIAL SURVEILLANCE PROGRAM

BWXT Services, Inc.
Lynchburg Technology Center

Quality Assurance
Certification of Conformance

BWXS Contract Charge No. 1215-001-00-18-00-00-0000

Tennessee Valley Authorities Purchase Order 00N7D-264485-001

BWXT Services, Inc. hereby certifies that the item(s) or service(s) pertaining to analysis of temperature monitors, analysis of dosimetry, analysis of tensile specimens, and analysis of Charpy impact specimens provided on this order are in accordance with the requirements of the above-specified Tennessee Valley Authorities purchase order, dated 9/12/00, including Change Order No.1, dated 1/24/01.

This testing was conducted in accordance with the requirements of BWXT Services, Inc., Nuclear & Environmental Operations, Nuclear Materials Engineering Quality Assurance Plan 00001, Revision 00, dated 11/08/00, for the project titled " TVA-RVSP Capsule Evaluation from Watts Bar Nuclear Plant."

AUGUST 27, 2001
Date

Charlie C. Boyd, Jr.
Charlie C. Boyd, Jr.
Manager, BWXS QA

ANALYSIS OF CAPSULE W FROM THE TENNESSEE VALLEY AUTHORITY WATTS BAR UNIT 1 REACTOR VESSEL MATERIAL SURVEILLANCE PROGRAM

PREPARED BY
BWXT SERVICES, Inc.
2016 MT. ATHOS ROAD
LYNCHBURG, VIRGINIA 24504-5447

Prepared by: W. A. Pavinich 9/6/01
W. A. Pavinich

Reviewed by: Kevin Y. Hour 9/10/01
Kevin Y. Hour, NME Manager

Approved by: C. L. Clark 10 Sept 01
Chris L. Clark, N&EO Manager

TABLE OF CONTENTS

Section	Title	Page
1.0	SUMMARY OF RESULTS	1
2.0	INTRODUCTION	3
3.0	BACKGROUND	4
4.0	DESCRIPTION OF PROGRAM	5
5.0	PROCEDURES	10
	5.1 Visual Examination and Inventory	
	5.2 Thermal Monitors	
	5.3 Charpy Impact Testing	
	5.4 Tensile Testing	
	5.5 1/2T Compact Tension Specimen Tests	
6.0	MECHANICAL TESTING RESULTS	12
	6.1 Charpy V-Notch Impact Test Results	
	6.2 Tensile Test Results	
7.0	RADIATION ANALYSIS AND NEUTRON DOSIMETRY	31
	7.1 Introduction	
	7.2 Neutron Transport Calculation	
	7.3 Neutron Dosimetry	
	7.4 Projection of Vessel Exposure	
	7.5 Uncertainty Analysis	
	7.6 Conclusions	
8.0	SURVEILLANCE CAPSULE REMOVAL SCHEDULE	61
9.0	REFERENCES	62

APPENDIX A	RADIOGRAPHS OF THERMAL MONITORS WATTS BAR UNIT 1, CAPSULE W
APPENDIX B	CHARPY IMPACT TEST RESULTS WATTS BAR UNIT 1, CAPSULE W
APPENDIX C	FRACTURE SURFACES OF CHARPY IMPACT SPECIMENS WATTS BAR UNIT 1, CAPSULE W
APPENDIX D	INSTRUMENTED IMACT TEST RESULTS WATTS BAR UNIT 1, CAPSULE W
APPENDIX E	STRESS STRAIN CURVE WATTS BAR UNIT 1, CAPSULE W
APPENDIX F	PHOTOGRAPHS OF FRACTURED TENSILE SPECIMENS WATTS BAR UNIT 1, CAPSULE W

LIST OF TABLES

Table	Title	Page
4-1	Chemical Composition (wt%) of the Watts Bar Unit 1 Reactor Vessel Beltline Region Surveillance Material	6
4-2	Heat Treatment of the Watts Bar Unit 1 Reactor Vessel Surveillance Material	7
6-1	Charpy Impact Test Data for the Watts Bar Unit 1 Intermediate Shell Forging 05 Irradiated to a Fluence of 1.23x 10^{19} n/cm^2 (E > 1.0 MeV)	13
6-2	Charpy Impact Test Data for the Watts Bar Unit 1 Surveillance Weld Metal and HAZ Metal Irradiated to a Fluence of 1.23x 10^{19} n/cm^2 (E > 1.0 MeV)	14
6-3	Comparison of Watts Bar Unit 1 Surveillance Material 30 ft-lb Transition Temperature Shifts and Upper Shelf Energy Decreases with Regulatory Guide 1.99 Revision 2 Predictions	15
6-4	Tensile Properties of the Watts Bar Unit 1 Reactor Vessel Surveillance Materials Irradiated to 1.23x 10^{19} n/cm^2 (E > 1.0 MeV)	15
7-1	Calculated Exposure Rates at the Center of Surveillance Capsules	43
7-2	Calculated Exposure Rates at the Inner Radius of the Reactor Vessel (Clad-Base Metal Interface) at Several Azimuthal Angles at Axial Midplane	44
7-3	Radial Distribution of N (E > 1.0 MeV) within the Reactor Vessel Relative to Clad-Base Metal Interface at Axial Midplane	45
7-4	Radial Distribution of N (E > 1.0 MeV) within the Reactor Vessel Relative to Clad-Base Metal Interface	46
7-5	Radial Distribution of Iron dpa within the Reactor Vessel Relative to Clad-Base Metal Interface	47
7-6	Nuclear Parameters Used for Evaluation of Neutron Sensors	48
7-7	Monthly Thermal Generation Watts Bar Unit 1 Cycles 1 to 3	49
7-8	Measured Sensor Activities and Reaction Rates, Surveillance Capsule W	50
7-9	Comparison of Measured and Calculated Reaction Rates for Watts Bar Unit 1 Surveillance Capsules	51
7-10	Calculated Average Neutron Energy Spectrum at the Center of Surveillance Capsule W	52

LIST OF TABLES
(Cont'd)

Table	Title	Page
7-11	Calculated and Best-Estimate of Watts Bar Unit 1 Surveillance Capsules U and W	53
7-12	Best-Estimate Neutron Exposure Projections at the Vessel IR at the Axial Core Midplane	54
7-13	Best-Estimate Neutron Exposure Projections at the Vessel IR at the Maximum Axial Point	55
7-14	Best-Estimate Neutron Exposure Projections at the Vessel IR to the Circumferential Weld at 9.6 inches above the Axial Core Midplane	56
7-15	Best-Estimate Neutron Fluence (E > 1.0 MeV) Within the Watts Bar Unit 1 Reactor Vessel at the Maximum Axial Point (n/cm^2)	57
7-16	Updated Lead Factors for Watts Bar 1 Surveillance Capsules	59
7-17	Watts Bar Unit 1 Fluence Uncertainty	60
8-1	Watts Bar Unit 1 Reactor Vessel Surveillance Capsule Withdrawal Schedule	61

LIST OF FIGURES

Figure	Title	Page
4-1	Arrangement of Surveillance Capsules in the Watts Bar Unit 1 Reactor Vessel	8
4-2	Capsule W Diagram Showing the Location of Specimens, Thermal Monitors, and Dosimeters	9
6-1	Charpy Impact Energy vs. Temperature for Watts Bar Unit 1 Reactor Vessel Intermediate Shell Forging 05 (Tangential Orientation)	16
6-2	Lateral Expansion vs. Temperature for Watts Bar Unit 1 Reactor Vessel Intermediate Shell Forging 05 (Tangential Orientation)	17
6-3	Percent Shear vs. Temperature for Watts Bar Unit 1 Reactor Vessel Intermediate Shell Forging 05 (Tangential Orientation)	18
6-4	Charpy Impact Energy vs. Temperature for Watts Bar Unit 1 Reactor Vessel Intermediate Shell Forging 05 (Axial Orientation)	19
6-5	Lateral Expansion vs. Temperature for Watts Bar Unit 1 Reactor Vessel Intermediate Shell Forging 05 (Axial Orientation)	20
6-6	Percent Shear vs. Temperature for Watts Bar Unit 1 Reactor Vessel Intermediate Shell Forging 05 (Axial Orientation)	21
6-7	Charpy Impact Energy vs. Temperature for Watts Bar Unit 1 Reactor Vessel Weld Metal	22
6-8	Lateral Expansion vs. Temperature for Watts Bar Unit 1 Reactor Vessel Weld Metal	23
6-9	Percent Shear vs. Temperature for Watts Bar Unit 1 Reactor Vessel Weld Metal	24
6-10	Charpy Impact Energy vs. Temperature for Watts Bar Unit 1 Reactor Vessel Heat-Affected-Zone Material	25
6-11	Lateral Expansion vs. Temperature for Watts Bar Unit 1 Reactor Vessel Heat-Affected-Zone Material	26
6-12	Percent Shear vs. Temperature for Watts Bar Unit 1 Reactor Vessel Heat-Affected-Zone Material	27
6-13	Tensile Strength Properties for Watts Bar Unit 1 Reactor Vessel Intermediate Shell Forging 05 (Tangential Orientation)	28

LIST OF FIGURES
(Cont'd)

Figure	Title	Page
6-14	Ductility of Watts Bar Unit 1 Reactor Vessel Intermediate Shell Forging 05 (Tangential Orientation)	28
6-15	Tensile Strength Properties for Watts Bar Unit 1 Reactor Vessel Intermediate Shell Forging 05 (Axial Orientation)	29
6-16	Ductility of Watts Bar Unit 1 Reactor Vessel Intermediate Shell Forging 05 (Axial Orientation)	29
6-17	Tensile Strength Properties for Watts Bar Unit 1 Reactor Vessel Weld Metal	30
6-18	Ductility of Watts Bar Unit 1 Reactor Vessel Weld Metal	30
7-1	Location of Watts Bar Unit 1 Surveillance Capsules	39
7-2	Westinghouse Dual Surveillance Capsule Geometry	40
7-3	Fluence (E > 1.0 MeV) Relative to Core Axial Midplane at the Vessel Inner Radius at the End of Cycle 3 vs Height Within the Core Region	41
7-4	Fluence E > 1.0 MeV at Axial Mid plane at the Vessel Inner Radius at the End of Cycle 3 vs Azimuth	42

1.0 SUMMARY OF RESULTS

The analysis of the reactor vessel materials in Watts Bar Unit 1, capsule W, led to the following conclusions:

The capsule received an average fast neutron fluence (E> 1.0 MeV) of 1.23 x 10^{19} n/cm^2 after 3.81 effective full power years (EFPY) of plant operation.

Irradiation of the reactor vessel intermediate shell forging 05 Charpy specimens, oriented with the longitudinal axis of the specimen parallel to the major working direction (tangential orientation), to 1.23 x 10^{19} n/cm^2 (E > 1.0 MeV) resulted in a 30 ft-lb transition temperature increase of 111°F and an irradiated 30 ft-lb transition temperature of 54°F.

Irradiation of the reactor vessel intermediate shell forging 05 Charpy specimens, oriented with the longitudinal axis of the specimen perpendicular to the major working direction of the plate (axial orientation), 1.23 x 10^{19} n/cm^2 (E>1.0 MeV) resulted in a 30 ft-lb transition temperature increase of 124°F and an irradiated 30 ft-lb transition temperature of 79°F.

Irradiation of the weld metal Charpy specimens to 1.23 x 10^{19} n/cm^2 (E>1.0 MeV) resulted in a 30 ft-lb transition temperature increase of 31°F and an irradiated 30 ft-lb transition temperature of -1°F.

Irradiation of the weld Heat-Affected-Zone (HAZ) metal Charpy specimens to 1.23 x 10^{19} n/cm^2 (E>1.0 MeV) resulted in a 30 ft-lb transition temperature increase of 50°F and an irradiated 30 ft-lb transition temperature of -7°F.

The average upper shelf energy of the intermediate shell forging 05 (tangential orientation) resulted in an average energy decrease of 34 ft-lb after irradiation to 1.23 x 10^{19} n/cm^2 (E>1.0 MeV) and an average upper shelf energy of 98 ft-lb.

The average upper shelf energy of the intermediate shell forging 05 (axial orientation) resulted in an average energy decrease of 2 ft-lb after irradiation to 1.23 x 10^{19} n/cm^2 (E>1.0 MeV) and an average upper shelf energy of 60 ft-lb.

The average upper shelf energy of the weld metal Charpy specimens resulted in an average energy decrease of 19 ft-lb after irradiation to 1.23 x 10^{19} n/cm^2 (E>1.0 MeV) and an average upper shelf energy of 111 ft-lb.

The average upper shelf energy of the weld HAZ metal Charpy specimens resulted in an average energy decrease of 7 ft-lb after irradiation to 1.23 x 10^{19} n/cm^2 (E>1.0 MeV) and an average upper shelf energy of 82 ft.

A comparison of the Watts Bar Unit 1 reactor vessel beltline material test results with the Regulatory Guide 1.99, Revision 2[1], predictions led to the following conclusions:

- The measured 30 ft-lb shifts in transition temperature of all surveillance materials in capsule W are less than the Regulatory Guide 1.99, Revision 2, predictions.

- The measured decrease in USE of all surveillance materials in capsule W is less than the Regulatory Guide 1.99, Revision 2, predictions.

The best estimate end-of-license (32 EFPY) neutron fluence (E > 1.0 MeV) at the core midplane for the Watts Bar Unit 1 reactor vessel using the Regulatory Guide 1.99, Revision 2 attenuation equation is as follows:

Vessel inner radius*	=	1.844×10^{19} n/cm^2
Vessel 1/4 thickness	=	1.110×10^{19} n/cm^2
Vessel 3/4 thickness	=	4.021×10^{18} n/cm^2

*Clad/base metal interface

Based on capsule U and capsule W upper shelf energy (USE) values, all beltline materials are expected to have a USE greater than 50 ft-lb through end of license (EOL, 32 EFPY) as required by 10CFR50, Appendix G [2].

Based on an evaluation documented in WCAP-13587, Revision 1 [36], "Reactor Vessel Upper Shelf Energy Bounding Evaluation for Westinghouse Pressurized Water Reactors", the minimum acceptable USE for a four loop plant is 43 ft-lb. The projected minimum EOL USE for the Watts Bar Unit 1 intermediate shell forging 05 is greater than 43 ft-lb. Therefore, the bounding evaluation shows that the Watts Bar Unit 1 intermediate shell forging 05 will maintain an equivalent margin, with respect to USE through EOL. In addition, the results of capsule W and capsule U testing indicate that the measured EOL USE will be above 43 ft-lbs.

2.0 INTRODUCTION

A reactor vessel material surveillance program (RVSP) is required by the United States Nuclear Regulatory Commission (USNRC) to monitor neutron irradiation induced changes in Charpy impact and tensile properties for reactor vessel beltline materials. Description of the RVSP and the pre-irradiation mechanical properties of the reactor vessel materials for Watts Bar Unit 1 is presented in WCAP-9298, "Tennessee Valley Authority Watts Bar Unit No. 1 Reactor Vessel Radiation Surveillance Program" [3]. As a part of the RVSP for Watts Bars Unit 1, Capsule W was removed from the Watts Bar Unit 1 reactor after 3.81 EFPY of exposure and shipped to BWXT Hot Cell Facility, where the post-irradiation mechanical testing of the Charpy impact and tensile specimens was performed along with dosimeter counting and thermal monitor evaluation. This report presents the results of testing and the analysis of the data obtained from specimens of Watts Bar Unit 1, Capsule W.

3.0 BACKGROUND

The beltline region of the reactor pressure vessel is subjected to significant fast neutron fluence. Fast neutron irradiation causes an increase in hardness and yield strength and a decrease in ductility and toughness for low alloy, ferritic pressure vessel steels such as A508 Class 2 forgings (base material of the Watts Bar Unit 1 reactor pressure vessel beltline).

A method for ensuring the integrity of reactor pressure vessels has been presented in "Fracture Toughness Criteria for Protection Against Failure," Appendix G to Section XI of the ASME Boiler and Pressure Vessel Code [4]. The method uses fracture mechanics concepts and is based on the reference nil-ductility transition temperature (RT_{NDT}). RT_{NDT} is defined as the greater of either the drop weight nil-ductility transition temperature (NDTT per ASTM E-208 [5]) or the temperature 60°F less than the 50 ft-lb (and 35-mil lateral expansion) temperature as determined from Charpy specimens oriented perpendicular (Axial) to the major working direction of the forging. The RT_{NDT} of a given material is used to index that material to a reference stress intensity factor curve (K_{IR} curve) of Appendix G to the ASME Code [4]. When material is indexed to the K_{IR} curve, allowable stress intensity factors can be obtained for this material as a function of temperature. Allowable operating limits can then be determined using these allowable stress intensity factors.

RT_{NDT} values are adjusted to account for the effects of radiation on the reactor vessel material properties. The changes in mechanical properties of a given reactor pressure vessel steel are monitored by the RVSP. Surveillance capsules are periodically removed from the nuclear reactor and the encapsulated specimens tested. The increase in the average Charpy 30 ft-lb temperature (ΔRT_{NDT}) caused by irradiation is added to the initial RT_{NDT}, along with a margin (M) to adjust the RT_{NDT} (ART) to account for radiation embrittlement. The adjusted reference temperature (RT_{NDT} initial + M + ΔRT_{NDT}) is used to index the material to the K_{IR} curve and set operating limits to account for the effects of irradiation on the reactor vessel materials.

4.0 DESCRIPTION OF THE WATTS BAR UNIT 1 REACTOR VESSEL SURVEILLANCE PROGRAM

Prior to initial plant start-up, six surveillance capsules were inserted into the Watts Bar Unit 1 reactor vessel between the neutron pads and the vessel wall as shown in Figure 4-1. The capsules contain specimens made from intermediate shell forging 05 and weld metal fabricated with weld wire heat number 895075 with Grau L.O. (LW320) flux, lot P46. The weld used to fabricate the RVSP specimens is identical to submerged arc weld that joins forgings 04 and 05. Capsule W was removed after 3.81 effective full power years (EFPY) of plant operation. This capsule contained Charpy impact, tensile, and 1/2T-CT and bend bar fracture mechanics specimens made from intermediate shell forging 05, submerged arc weld metal, and heat-affected-zone (HAZ) metal of intermediate shell forging 05 identical to the reactor vessel beltline region welds. Test material obtained from intermediate shell forging 05 (after the thermal heat treatment and forming of the forging) was taken at least one thickness from the quenched ends of the forging. All test specimens were machined from the 1/4 thickness location of the forging after performing a simulated post-weld stress-relieving treatment on the test material. Specimens from weld metal and heat-affected-zone metal were machined from a stress-relieved weldment joining intermediate and lower shell forgings 05 and 04. All heat-affected-zone specimens were obtained from the weld heat-affected-zone of intermediate shell forging 05.

Charpy impact specimens from intermediate shell forging 05 were machined with some in the tangential orientation (longitudinal axis of the specimen parallel to the major working direction) and some in the axial orientation (longitudinal axis of the specimen perpendicular to the major working direction). The beltline region weld Charpy impact specimens were machined from the weldment such that the long dimension of each Charpy specimen was perpendicular to the weld direction. The notch of the weld metal Charpy specimens was machined such that the direction of crack propagation in the specimen was in the welding direction. Tensile specimens from intermediate shell forging 05 were machined in both the tangential and axial orientation. Tensile specimens from the weld metal were oriented with the long dimension of the specimen perpendicular to the weld direction.

Bend bar specimens were machined from forging 05 with the longitudinal axis of the specimen oriented in the rolling direction of the forging such that the simulated crack would propagate in a direction normal to the rolling direction of the forging. Compact tension test specimens from forging 05 were machined in both the axial and tangential orientations. Compact tension test specimens from the weld metal were machined normal to the weld direction with the notch oriented in the direction of the weld. All compact and bend bar specimens were fatigue precracked according to ASTM E399.

The chemical composition and heat treatment of the surveillance material is presented in Tables 4-1 and 4-2. The chemical analysis reported in Table 4-1 was obtained from unirradiated material used in the surveillance program [3].

Capsule W contained dosimeter wires of pure copper, iron, nickel, and aluminum-0.15 weight percent cobalt (cadmium-shielded and unshielded). In addition, cadmium shielded dosimeters of neptunium (Np^{237}) and uranium (U^{238}) were placed in the capsule to measure the integrated flux at specific neutron energy levels.

The arrangement of the various mechanical specimens, dosimeters and thermal monitors contained in Capsule W is shown in Figure 4-2.

TABLE 4-1				
Chemical Composition (wt%) of the Watts Bar Unit 1 Reactor Vessel Beltline Region Materials[3]				
Element	Intermediate Shell Forging 05[(a)]		Weld Metal[(b&c)]	
C	0.20	0.21	0.080	0.069
S	0.016	0.014	0.007	0.010
N	0.009	---	0.019	---
Co	<0.01	0.012	0.007	---
Cu	0.17	0.14	0.031	0.05
Si	0.25	0.25	0.27	0.22
Mo	0.57	0.61	0.54	0.56
Ni	0.80	0.79	0.75	0.70
Mn	0.73	0.68	1.94	1.97
Cr	0.32	0.34	0.023	0.05
V	<0.01	<0.02	0.001	---
P	0.012	0.013	0.015	0.010
Al	<0.019	0.049	0.019	---
Sn	0.010	---	0.003	---

Notes:

a. All analysis except for N and Sn were conducted by Rotterdam Dockyard Company/Krupp ladle analysis; N and Sn analysis were performed by Westinghouse.

b. The surveillance weldment is identical to the closing girth seam weldment between forging 04 and 05. The closing seam used weld wire heat number 895075 with Grau L.O. (LW320) flux, lot P46, except for the 1-inch root pass at the ID of the vessel. This root pass used weld wire heat number 899680 with type Grau L.O. (LW320) flux, lot P23, with as-deposited copper and phosphorus content of 0.03 and 0.009, respectively. The surveillance weldment specimens were not removed form this root area.

c. The left column results obtained from Westinghouse analyses, while the results in the right column were obtained from analyses conducted by Rotterdam Dockyard Company.

TABLE 4-2			
Heat Treatment of the Watts Bar Unit 1 Reactor Vessel Surveillance Material[3]			
Material	Temperature (°F)	Time (hrs.)	Coolant
Intermediate Shell Forging 05	1675 - 1700	3 1/2	Water-quenched
	1230 - 1240	6	Air Cooled
	1140 ± 25	21	Furnace Cooled
Weldment	1140 ± 25	14 hr., 56 min.	Furnace Cooled

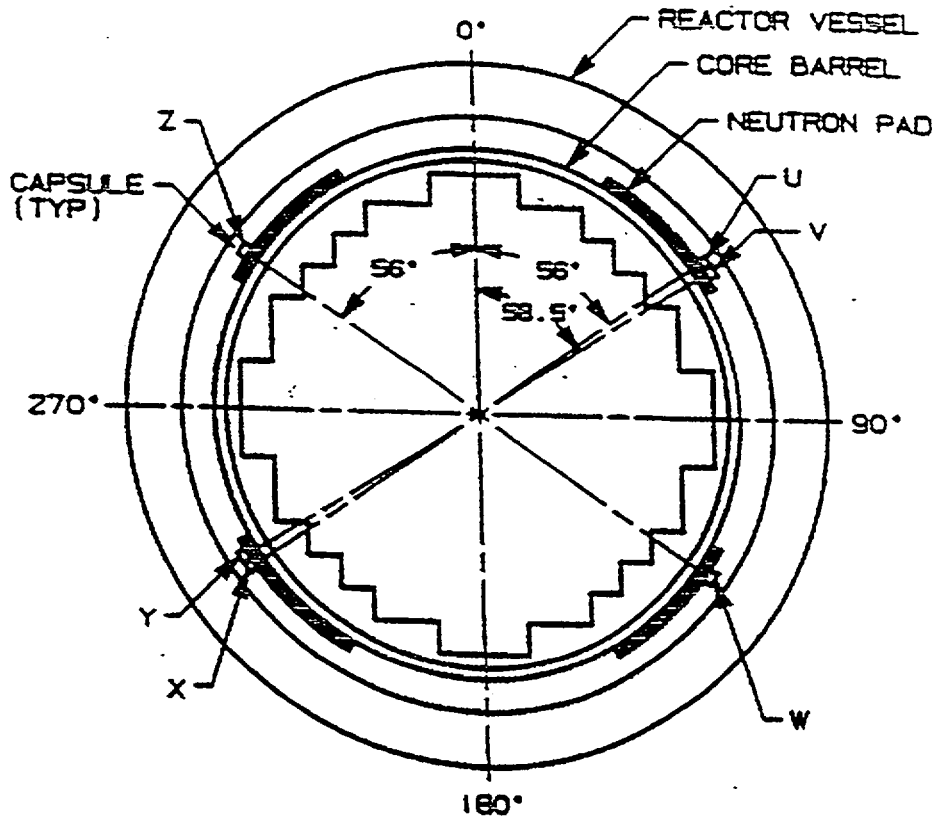

Figure 4-1. Arrangement of Surveillance Capsules in the Watts Bar Unit 1Reactor Vessel

Bend Bar	Tensile	Compact	Compact	Charpy	Charpy	Charpy	Compact	Compact	Charpy	Charpy
WL3	WW9	WW12	WW11	WW45 WH45	WW42 WH42	WW39 WH39	WL12	WL11	WW36 WH36	WW33 WH33
	WW8		WW10	WW44 WH44	WW41 WH41	WW38 WH38		WL10	WW35 WH35	WW32 WH32
	WW7		WW9	WW43 WH43	WW40 WH40	WW37 WH37		WL9	WW34 WH34	WW31 WH31

Dosimeter	Tensile	Charpy	Charpy	Charpy	Charpy	Charpy	Compact	Compact	Tensile
326	WL9	WT45 WL45	WT42 WL42	WT39 WL39	WT36 WL36	WT33 WL33	WT12	WT10	WT9
	WL8	WT44 WL44	WT41 WL41	WT38 WL38	WT35 WL35	WT32 WL32	WT11	WT9	WT8
	WL7	WT43 WL43	WT40 WL40	WT37 WL37	WT34 WL34	WT31 WL31			WT7

Legend:
- WL – Intermediate forging 05, Heat No. 527536, Tangential
- WT – Intermediate forging 05, Heat No. 527536, Axial
- WW – Weld metal
- WH – Heat affected zone material

Figure 4-2: Capsule W Diagram Showing the Location of Specimens, Thermal Monitors, and Dosimeters

Figure 4-2. Capsule W Diagram Showing the Location of Specimens, Thermal Monitors, and Dosimeters

5.0 PROCEDURES

5.1 Visual Examination and Inventory

All specimens were visually examined after the capsule was opened for indications of abnormalities. Contents of capsule W were inventoried and compared with the information of reference [3]. No discrepancies were found.

5.2 Thermal Monitors

Capsule W contained thermal monitors made from two low-melting-point eutectic alloys that were sealed in Pyrex tubes. The composition of the two eutectic alloys and their melting points are as follows:

2.5% Ag, 97.5% Pb	Melting Point: 579°F (304°C)
1.75% Ag, 0.75% Sn, 97.5% Pb	Melting Point: 590°F (310°C)

Thermal monitors were radiographed to detect evidence of melting (See Appendix A). No melting of the two low-melting point 579°F (304°C) and 590°F (310°C) eutectic alloys was observed, therefore the maximum temperature of test specimens of capsule W was less than 579°F (304°C).

5.3 Charpy Impact Testing

Charpy impact tests were conducted in accordance with 10CFR50, Appendices G and H [2], ASTM Specification E185-82 [6], LTC Technical Procedure TP-80. Four groups of Charpy specimens (longitudinally and transversely oriented base metal, weld metal, and weld metal HAZ) were impact tested between -50 °F and 350 °F. Absorbed energy, percent shear fracture, and lateral expansion values were determined in accordance with ASTM E23-93.

Load-time and energy-time signals were recorded in addition to the standard measurement of Charpy energy (E_D) using an instrumented tup in accordance with LTC Technical Procedure TP-412. From the load-time curves (Appendix D), the load of general yielding (P_{GY}), the time to general yielding (t_{GY}), the maximum load (P_M), the time to maximum load (t_M), the fast fracture load (P_F), the arrest load (P_A) were determined. The dynamic yield stress (σ_Y) was calculated using the following equation:

$$\sigma_Y = 33.33 * P_{GY} \qquad (1)$$

5.4 Tensile Testing

Tensile tests were conducted in accordance with 10CFR50, Appendices G and H [2], ASTM Specifications E8-94 [6] and E21-92 and LTC Technical Procedure TP-78. The tests were conducted at a strain rate of 0.0075 inch/inch/ until the 0.2% offset yield strength was achieved. The strain rate was then increased to 0.03 inch/inch/minute thereafter. The extensometer knife edges were spring-loaded to the specimen and operated through specimen failure. The extensometer gage length was 1.00 inch. The extensometer is rated as Class B-2 in accordance with ASTM E83-93 [11].

The yield load, ultimate load, fracture load, total elongation, and uniform elongation were determined directly from the load-extension curve. The yield strength, ultimate strength, and fracture strength were calculated using the original cross-sectional area. The final diameter and final gage length were determined from post-fracture photographs. The fracture area used to calculate the fracture stress (true stress at fracture) and percent reduction in area was computed using the final diameter measurement.

5.5 1/2T Compact Tension and Bend Bar Specimen Tests

The 1/2T compact tension specimens and the bend bar were not tested at the date of this report and are presently being stored at the BWXT Hot Cell facility. The axial 1/2T-CT specimens will be tested in the future to determine J-R curves for the intermediate forging. The bend bar and tangential 1/2T-CT will remain in storage and not tested. The results of this testing will reported elsewhere.

6.0 MECHANICAL TEST RESULTS

6.1 Charpy Impact Test Results

The results of the Charpy impact tests performed on the various materials of Capsule W, which received a fluence of 1.23 x 10^{19} n/cm^2 (E > 1.0 MeV) in 3.81 EFPY of operation, are presented in Tables 6-1 and 6-2 and Appendix B and are compared with baseline results [3] and results of Capsule U [12] as shown in Figures 6-1 through 6-12. The transition temperature increases and upper shelf energy decreases for Capsule W materials are summarized in Table 6-3. A comparison of the Watts Bar Unit 1 reactor vessel beltline material test results with the Regulatory Guide 1.99, Revision 2 [1] predictions is given in Table 6-3. The measured 30 ft-lb shift in transition temperature and measured decrease in USE of all surveillance materials contained in Capsule W are less than the Regulatory Guide 1.99, Revision 2 predictions.

The fracture surfaces of the Charpy specimens of the various surveillance Capsule W materials are shown in Appendix C. An increasingly ductile or tougher appearance with increasing test temperature can be observed.

All beltline materials, with exception to the intermediate shell forging 05, are expected to have an upper shelf energy (USE) greater than 50 ft-lb through end of license (EOL, 32 EFPY) as required by 10CFR50, Appendix G [2]. In September of 1993, Westinghouse completed an evaluation to demonstrate that all Westinghouse Owners Group (WOG) Plant reactor vessels have a margin of safety, relative to USE, equivalent to that required by Appendix G of the ASME Code. This was accomplished by performing generic bounding evaluations per the proposed ASME Section XI, Appendix X. This evaluation is documented in WCAP-13587, Rev. 1 [42] provides the minimum USE, 43 ft-lb, for a four loop Westinghouse NSSS plant. The projected minimum EOL USE for the Watts Bar Unit 1 intermediate shell forging 05 is greater than 43 ft-lb. Therefore, the bounding WOG evaluation shows that the Watts Bar Unit 1 intermediate shell forging 05 will maintain an equivalent margin through EOL, with respect to USE in accordance with the requirements of 10 CFR Part 50, Appendix G.

The load-time records for individual instrumented Charpy specimen tests are shown in Appendix D. The results presented in this report are based on a regression of all capsule data using a hyperbolic tangent curve-fitting program. Appendix B presents Charpy plots and the program input data.

6.2 Tensile Test Results

All tensile tests were performed in accordance with Technical Procedure TP-78. ASTM Specification E8-94 [9] and E21-92 [10]. All tensile tests data including engineering and true stress strain plots can be found in Appendix E.

The results of the tensile tests performed on the various materials contained in Capsule W irradiated to 1.23 x 10^{19} n/cm^2 (E>1.0 MeV) are presented in Table 6-4 and are compared with unirradiated results [3] as shown in Figures 6-13 through 6-18. In general, strength increased and ductility decreased with increasing neutron fluence.

The fractured tensile specimens for the intermediate shell forging 05 material are shown in Appendix F.

Table 6-1. Charpy Impact Data for the Watts Bar Unit 1, SA 508 Class 2 Forging, Heat Number 527536(R 05), Fluence 1.23 x 10^{19} n/cm^2 (E > 1.0 MeV)

Specimen Number	Temperature, °F	Impact Energy, ft-lb	Lateral Expansion, mils	Shear Fracture, %
		Tangential		
WL35	40	15.0	13	10
WL42	50	22.0	17	20
WL41	60	37.5	30	25
WL39	60	49.5	37	40
WL38	70	39.5	32	30
WL36	100	47.5	36	40
WL45	125	57.0	48	60
WL32	140	70.5	53	70
WL37	150	76.5	65	85
WL40	200	97.0	76	100
WL34	250	102.5	82	100
WL43	350	93.5	78	100
		Axial		
WT38	40	10.0	10	0
WT43	70	18.5	20	15
WT34	70	20.5	19	15
WT32	100	23.5	25	25
WT39	125	30.5	30	35
WT36	150	29.5	32	40
WT33	165	39	41	55
WT40	175	39.5	42	55
WT41	185	48.5	49	85
WT45	200	54.5	53	100
WT44	250	63.5	64	100
WT37	350	62.5	55	100

Table 6-2. Charpy Impact Data for the Watts Bar Unit 1 Reactor Vessel, Weld Metal and HAZ Metal Fluence 1.23×10^{19} n/cm^2 (E > 1.0 MeV)

Specimen Number	Temperature, °F	Impact Energy, ft-lb	Lateral Expansion, mils	Shear Fracture, %
		Weld Metal		
WW37	-50	13.0	10	0
WW31	-20	20.0	19	30
WW42	10	32.0	27	55
WW43	25	41.5	35	60
WW44	40	56.0	49	65
WW36	55	61.5	54	65
WW34	70	71.5	55	70
WW38	100	75	64	75
WW35	125	87.5	74	90
WW33	150	98.5	82	100
WW45	200	113.0	90	100
WW41	350	123.5	87	100
		HAZ Metal		
WH33	-50	15.0	9	0
WH36	-30	37.5	22	25
WH37	-20	26.5	17	30
WH41	10	33.0	25	45
WH44	40	37.0	29	50
WH31	70	57.0	40	50
WH40	85	44.5	34	60
WH43	100	69.0	52	90
WH45	150	86.5	70	100
WH39	200	79.5	63	100
WH38	300	81.0	63	100
WH34	350	60.5	55	100

Table 6-3. Comparison of Watts Bar Unit 1 Surveillance Material 30 ft-lb Transition Temperature Shifts and Upper Shelf Energy Decreases with Regulatory Guide 1.99 Revision 2 Predictions

Material	Unirradiated 30 ft-lb Temp. (°F)	Capsule W 30 ft-lb Temp. (°F)	Measured 30 ft-lb Temp. Shift (°F)	Predicted 30 ft-lb Temp. Shift (°F)	Unirradiated USE (ft-lb)	Capsule W USE (ft-lb)	Measured USE Decrease (ft-lb)	Predicted USE Decrease (ft-lb)
Forging Tangential	-57	54	111	---	132	98	34	---
Forging Axial	45	124	79	---	62	60	2	---
Weld Metal	-32	-1	31	---	131	112	19	---
HAZ Metal	-57	-7	50	---	89	82	7	---

Table 6-4. Tensile Properties of the Watts Bar Unit 1 Reactor Vessel Surveillance Materials Irradiated to 1.233×10^{19} n/cm^2 (E > 1.0 MeV)

Material	Specimen Number	Test Temp. (°F)	0.2% Yield Strength (Ksi)	Ultimate Strength (Ksi)	Fracture Load (Kip)	Fracture Stress (Ksi)	Fracture Strength (Ksi)	Uniform Elongation (%)	Total Elongation (%)	Reduction in Area (%)
Intermediate Forging 05 (Tangential)	WL8	70	86.7	106.7	3.61	192.6	73.6	9.9	23.9	61.8
	WL7	175	83.1	101.3	3.29	191.5	67.1	9.3	21.7	65.0
	WL9	550	77.2	101.0	3.74	166.6	76.1	8.9	19.1	54.3
Intermediate Forging 05 (Axial)	WT9	70	85.7	105.3	4.11	179.9	83.7	10.5	20.7	53.5
	WT8	200	81.8	99.9	3.75	159.7	76.5	9.4	19.4	52.1
	WT7	550	76.4	99.9	4.08	150.9	83.1	9.8	18.2	44.9
Weld Metal	WW8	70	76.7	89.7	3.11	208.9	63.4	12.8	28.0	69.6
	WW9	150	72.5	85.5	25.2	180.3	51.4	11.7	27.7	71.5
	WW7	550	67.2	86.1	26.7	173.4	54.4	10.8	24.1	68.6

SHELL FORGING 05 TANGENTIAL

CVGRAPH 5.0 Hyperbolic Tangent Curve Printed on 09/10/2001 09:41 AM
Data Set(s) Plotted

Curve	Plant	Capsule	Material	Ori.	Heat #
1	Watts Bar 1	UNIRR	SA508CL2	LT	527536(R 05)
2	Watts Bar 1	U	SA508CL2	LT	527536(R 05)
3	Watts Bar 1	W	SA508CL2	LT	527536(R 05)

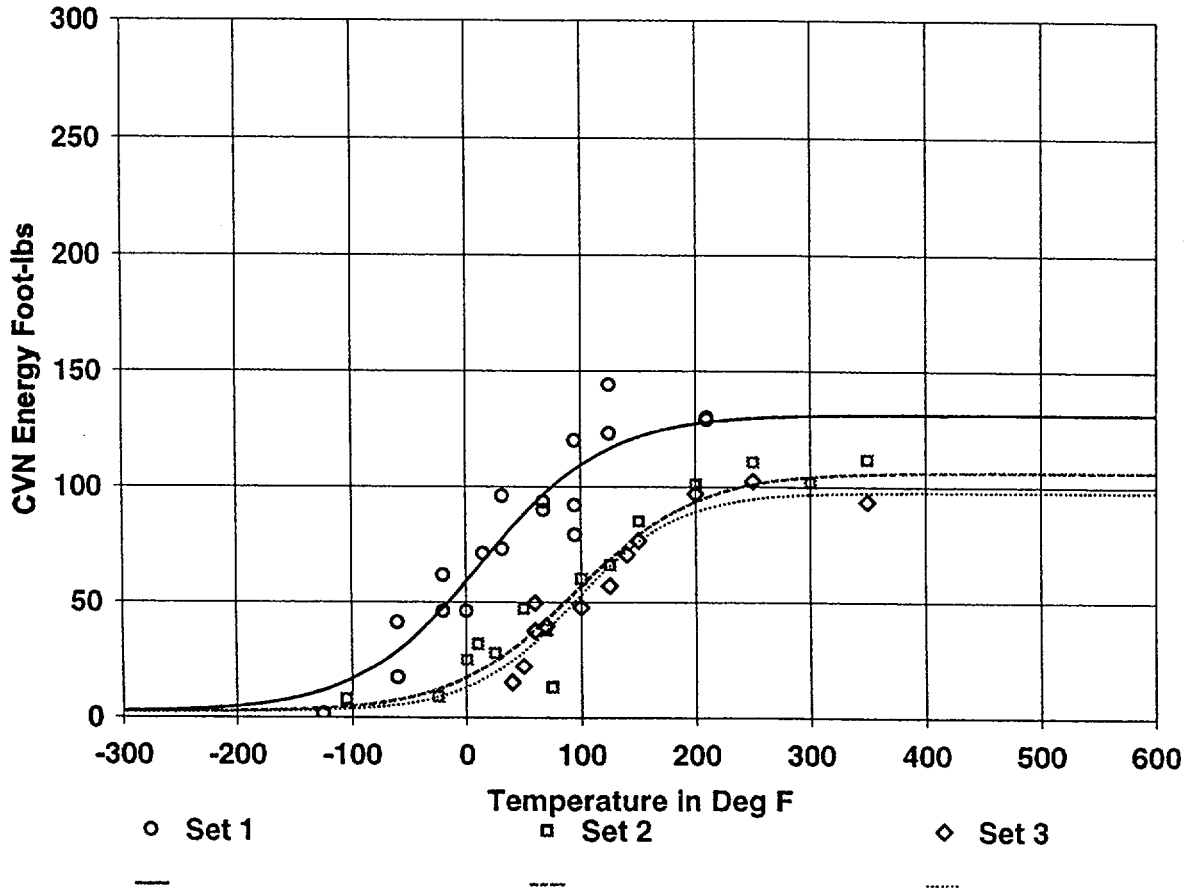

Results

Curve	Fluence	LSE	USE	d-USE	T @30	d-T @30	T @50	d-T @50
1	0	2.2	131.5	.0	-57.0	.0	-15.5	.0
2	5.05E+18	2.2	106.5	-25.0	41.2	98.2	86.3	101.7
3	1.23E+19	2.2	97.7	-33.8	54.3	111.3	94.9	110.3

Figure 6-1. Charpy Impact Energy vs. Temperature for Watts Bar Unit 1 Reactor Vessel Intermediate Shell Forging 05 (Tangential Orientation)

SHELL FORGING 05 TANGENTIAL

CVGRAPH 5.0 Hyperbolic Tangent Curve Printed on 09/10/2001 09:44 AM
Data Set(s) Plotted

Curve	Plant	Capsule	Material	Ori.	Heat #
1	Watts Bar 1	UNIRR	SA508CL2	LT	527536(R 05)
2	Watts Bar 1	U	SA508CL2	LT	527536(R 05)
3	Watts Bar 1	W	SA508CL2	LT	527536(R 05)

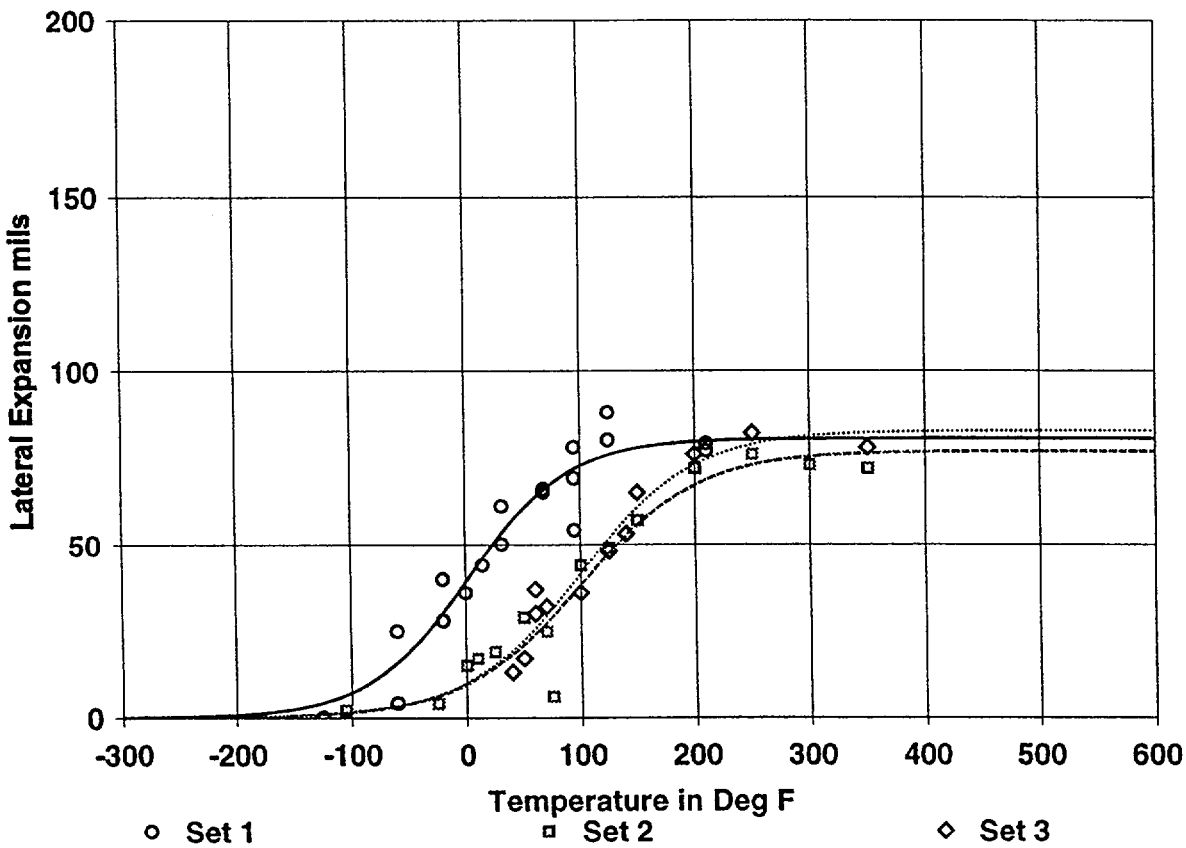

Results

Curve	Fluence	LSE	USE	d-USE	T @35	d-T @35
1	0	.0	80.5	.0	-9.5	.0
2	5.05E+18	.0	76.9	-3.6	91.0	100.5
3	1.23E+19	.0	82.6	2.1	84.3	93.8

Figure 6-2. Lateral Expansion vs. Temperature for Watts Bar Unit 1 Reactor Vessel Intermediate Shell Forging 05 (Tangential Orientation)

SHELL FORGING 05 TANGENTIAL

CVGRAPH 5.0 Hyperbolic Tangent Curve Printed on 09/10/2001 09:41 AM
Data Set(s) Plotted

Curve	Plant	Capsule	Material	Ori.	Heat #
1	Watts Bar 1	UNIRR	SA508CL2	LT	527536(R 05)
2	Watts Bar 1	U	SA508CL2	LT	527536(R 05)
3	Watts Bar 1	W	SA508CL2	LT	527536(R 05)

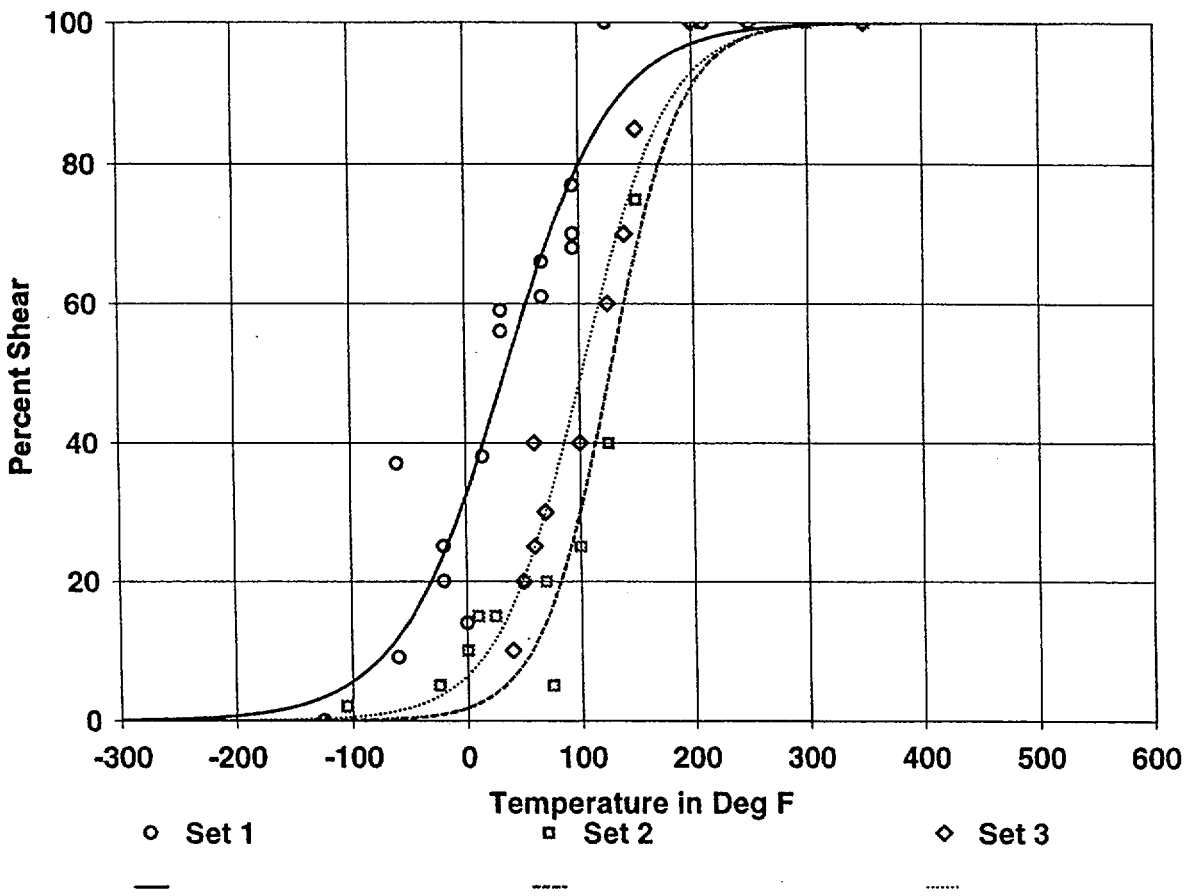

Results

Curve	Fluence	LSE	USE	d-USE	T @50	d-T @50
1	0	.0	100.0	.0	34.8	.0
2	5.05E+18	.0	100.0	.0	126.6	91.8
3	1.23E+19	.0	100.0	.0	102.2	67.5

Figure 6-3. Percent Shear vs. Temperature for Watts Bar Unit 1 Reactor Vessel Intermediate Shell Forging 05 (Tangential Orientation)

SHELL FORGING 05 AXIAL

CVGRAPH 5.0 Hyperbolic Tangent Curve Printed on 09/10/2001 09:32 AM
Data Set(s) Plotted

Curve	Plant	Capsule	Material	Ori.	Heat #
1	Watts Bar 1	UNIRR	SA508CL2	TL	527536(R 05)
2	Watts Bar 1	U	SA508CL2	TL	527536(R 05)
3	Watts Bar 1	W	SA508CL2	TL	527536(R 05)

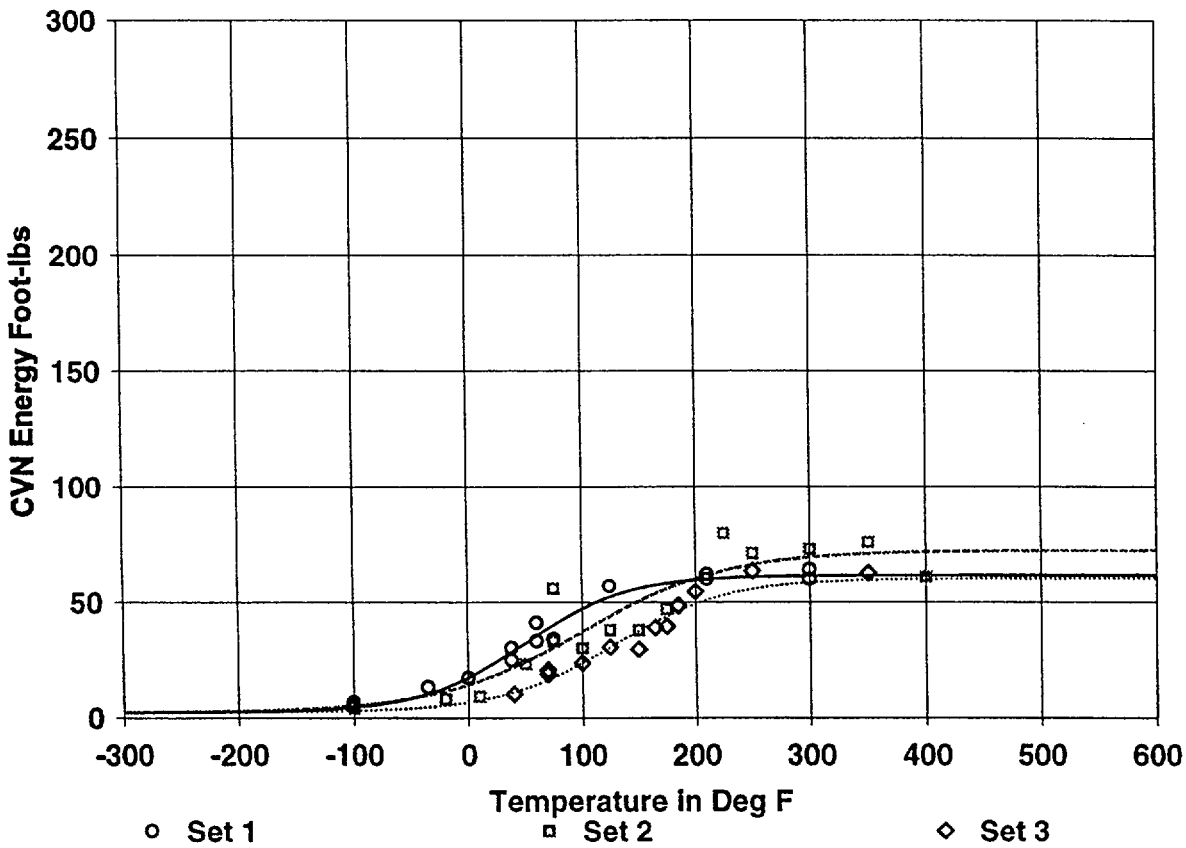

Results

Curve	Fluence	LSE	USE	d-USE	T @30	d-T @30	T @50	d-T @50
1	0	2.2	61.6	.0	43.4	.0	113.3	.0
2	5.05E+18	2.2	72.2	10.6	73.9	30.5	148.7	35.5
3	1.23E+19	2.2	60.2	-1.4	124.2	80.8	205.9	92.6

Figure 6-4. Charpy Impact Energy vs. Temperature for Watts Bar Unit 1 Reactor Vessel Intermediate Shell Forging 05 (Axial Orientation)

SHELL FORGING 05 AXIAL

CVGRAPH 5.0 Hyperbolic Tangent Curve Printed on 09/10/2001 09:38 AM
Data Set(s) Plotted

Curve	Plant	Capsule	Material	Ori.	Heat #
1	Watts Bar 1	UNIRR	SA508CL2	TL	527536(R 05)
2	Watts Bar 1	U	SA508CL2	TL	527536(R 05)
3	Watts Bar 1	W	SA508CL2	TL	527536(R 05)

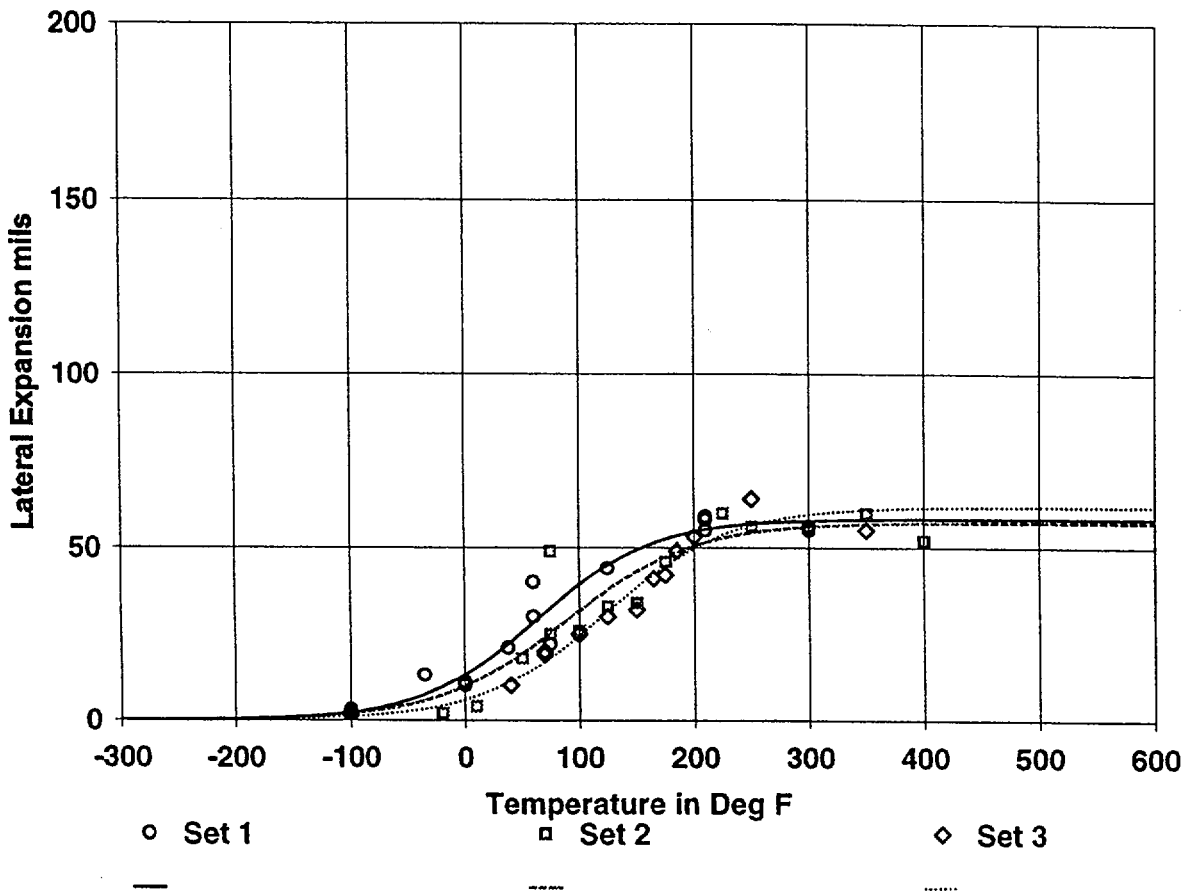

Results

Curve	Fluence	LSE	USE	d-USE	T @35	d-T @35
1	0	.0	58.3	.0	83.8	.0
2	5.05E+18	.0	57.3	-1.0	113.3	29.5
3	1.23E+19	.0	61.8	3.5	138.0	54.3

Figure 6-5. Lateral Expansion vs. Temperature for Watts Bar Unit 1 Reactor Vessel Intermediate Shell Forging 05 (Axial Orientation)

SHELL FORGING 05 AXIAL

CVGRAPH 5.0 Hyperbolic Tangent Curve Printed on 09/10/2001 09:37 AM
Data Set(s) Plotted

Curve	Plant	Capsule	Material	Ori.	Heat #
1	Watts Bar 1	UNIRR	SA508CL2	TL	527536(R 05)
2	Watts Bar 1	U	SA508CL2	TL	527536(R 05)
3	Watts Bar 1	W	SA508CL2	TL	527536(R 05)

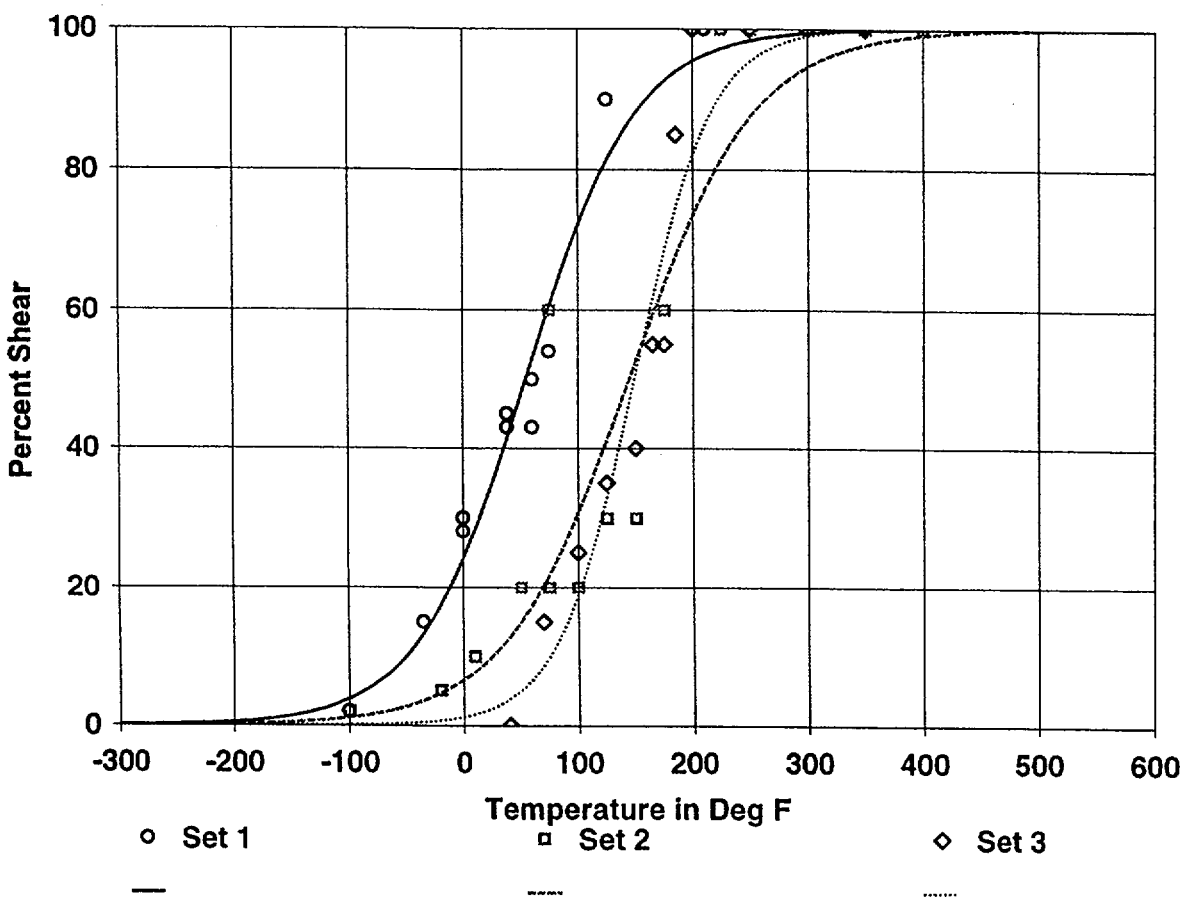

Results

Curve	Fluence	LSE	USE	d-USE	T @50	d-T @50
1	0	.0	100.0	.0	54.5	.0
2	5.05E+18	.0	100.0	.0	144.3	89.7
3	1.23E+19	.0	100.0	.0	149.1	94.5

Figure 6-6. Percent Shear vs. Temperature for Watts Bar Unit 1 Reactor Vessel Intermediate Shell Forging 05 (Axial Orientation)

WELD

CVGRAPH 5.0 Hyperbolic Tangent Curve Printed on 09/10/2001 09:45 AM
Data Set(s) Plotted

Curve	Plant	Capsule	Material	Ori.	Heat #
1	Watts Bar 1	UNIRR	SA508CL2	NA	895075(W H)
2	Watts Bar 1	U	SA508CL2	NA	895075(W H)
3	Watts Bar 1	W	SA508CL2	NA	895075(W H)

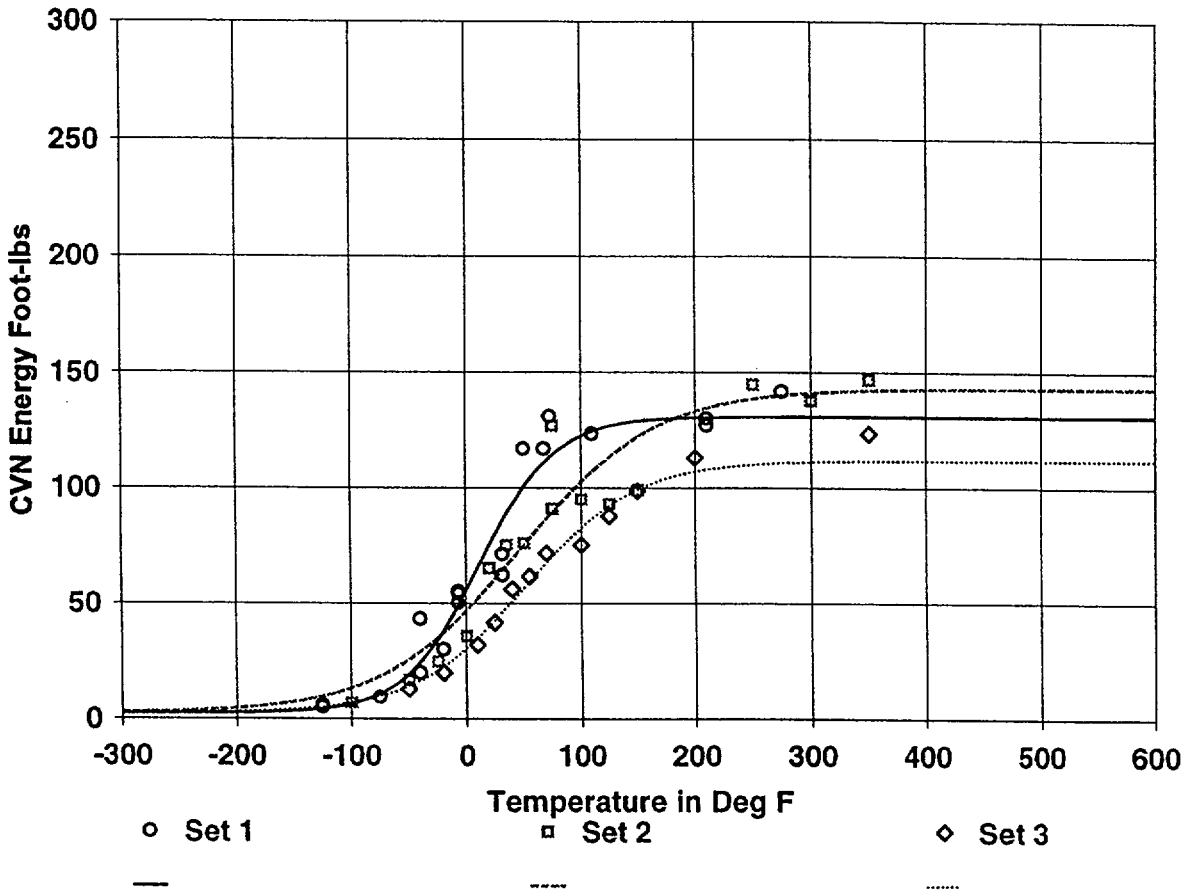

Results

Curve	Fluence	LSE	USE	d-USE	T @30	d-T @30	T @50	d-T @50
1	0	2.2	130.8	.0	-31.2	.0	-6.0	.0
2	5.05E+18	2.2	143.3	12.5	-37.9	-6.7	6.2	12.2
3	1.23E+19	2.2	111.7	-19.1	-.6	30.6	39.3	45.2

Figure 6-7. Charpy Impact Energy vs. Temperature for Watts Bar Unit 1 Reactor Vessel Weld Metal

WELD

CVGRAPH 5.0 Hyperbolic Tangent Curve Printed on 09/10/2001 09:48 AM
Data Set(s) Plotted

Curve	Plant	Capsule	Material	Ori.	Heat #
1	Watts Bar 1	UNIRR	SA508CL2	NA	895075(W H)
2	Watts Bar 1	U	SA508CL2	NA	895075(W H)
3	Watts Bar 1	W	SA508CL2	NA	895075(W H)

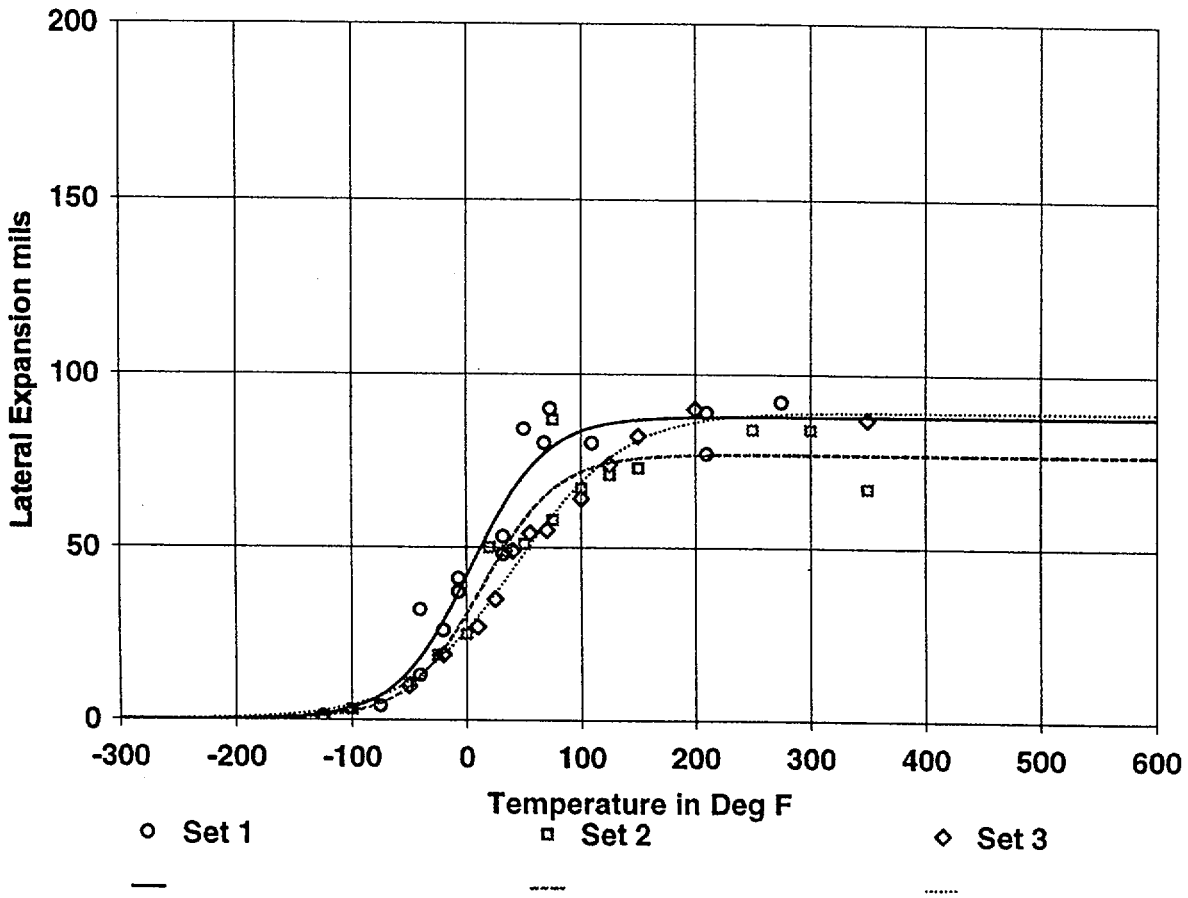

Results

Curve	Fluence	LSE	USE	d-USE	T @35	d-T @35
1	0	.0	87.8	.0	-10.0	.0
2	5.05E+18	.0	76.9	-10.9	7.4	17.3
3	1.23E+19	.0	89.2	1.4	21.9	31.9

Figure 6-8. Lateral Expansion vs. Temperature for Watts Bar Unit 1 Reactor Vessel Weld Metal

WELD

CVGRAPH 5.0 Hyperbolic Tangent Curve Printed on 09/10/2001 09:47 AM
Data Set(s) Plotted

Curve	Plant	Capsule	Material	Ori.	Heat #
1	Watts Bar 1	UNIRR	SA508CL2	NA	895075(W H)
2	Watts Bar 1	U	SA508CL2	NA	895075(W H)
3	Watts Bar 1	W	SA508CL2	NA	895075(W H)

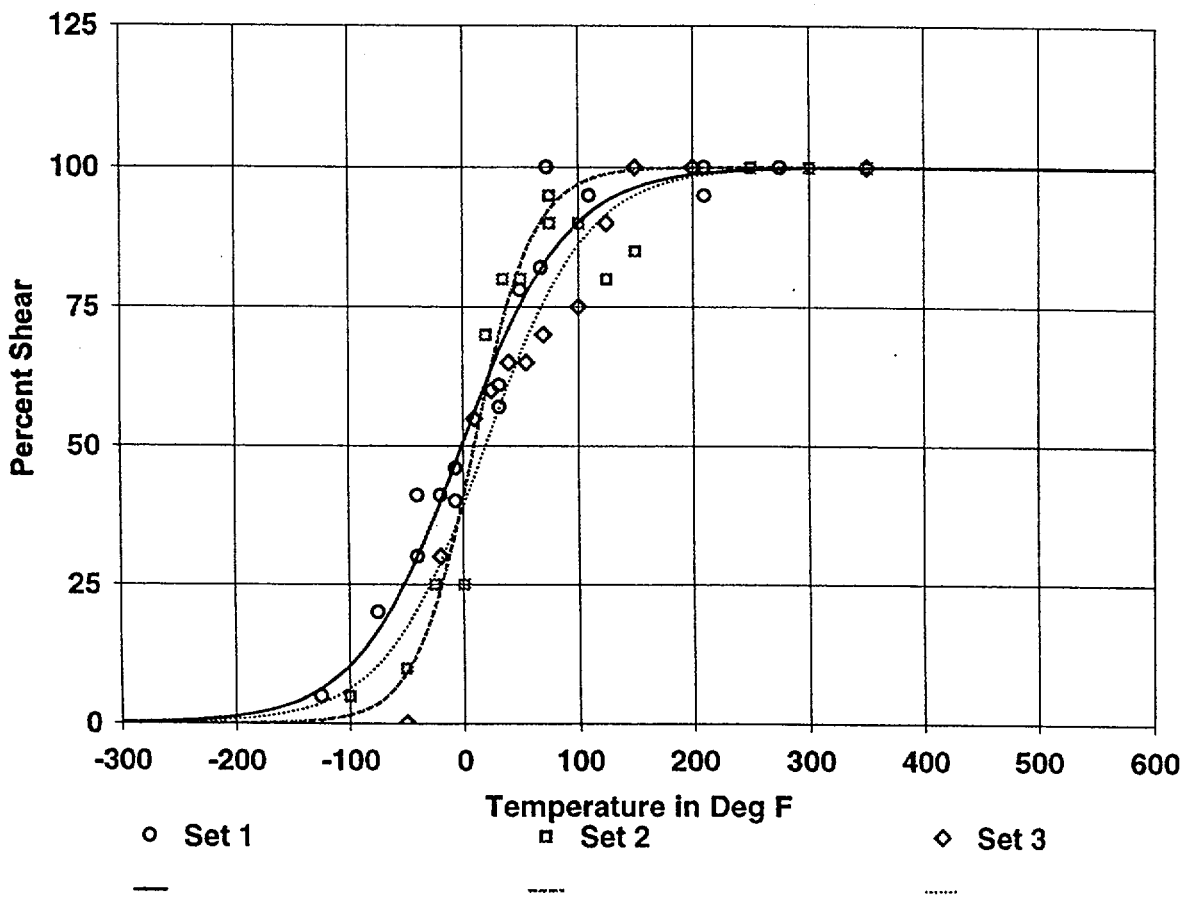

Results

Curve	Fluence	LSE	USE	d-USE	T @50	d-T @50
1	0	.0	100.0	.0	-1.3	.0
2	5.05E+18	.0	100.0	.0	9.6	10.9
3	1.23E+19	.0	100.0	.0	19.8	21.1

Figure 6-9. Percent Shear vs. Temperature for Watts Bar Unit 1 Reactor Vessel Weld Metal

HEAT-AFFECTED-ZONE

CVGRAPH 5.0 Hyperbolic Tangent Curve Printed on 09/10/2001 09:49 AM
Data Set(s) Plotted

Curve	Plant	Capsule	Material	Ori.	Heat #
1	Watts Bar 1	UNIRR	SA508CL2	NA	895075(W H)
2	Watts Bar 1	U	SA508CL2	NA	895075(W H)
3	Watts Bar 1	W	SA508CL2	NA	895075(W H)

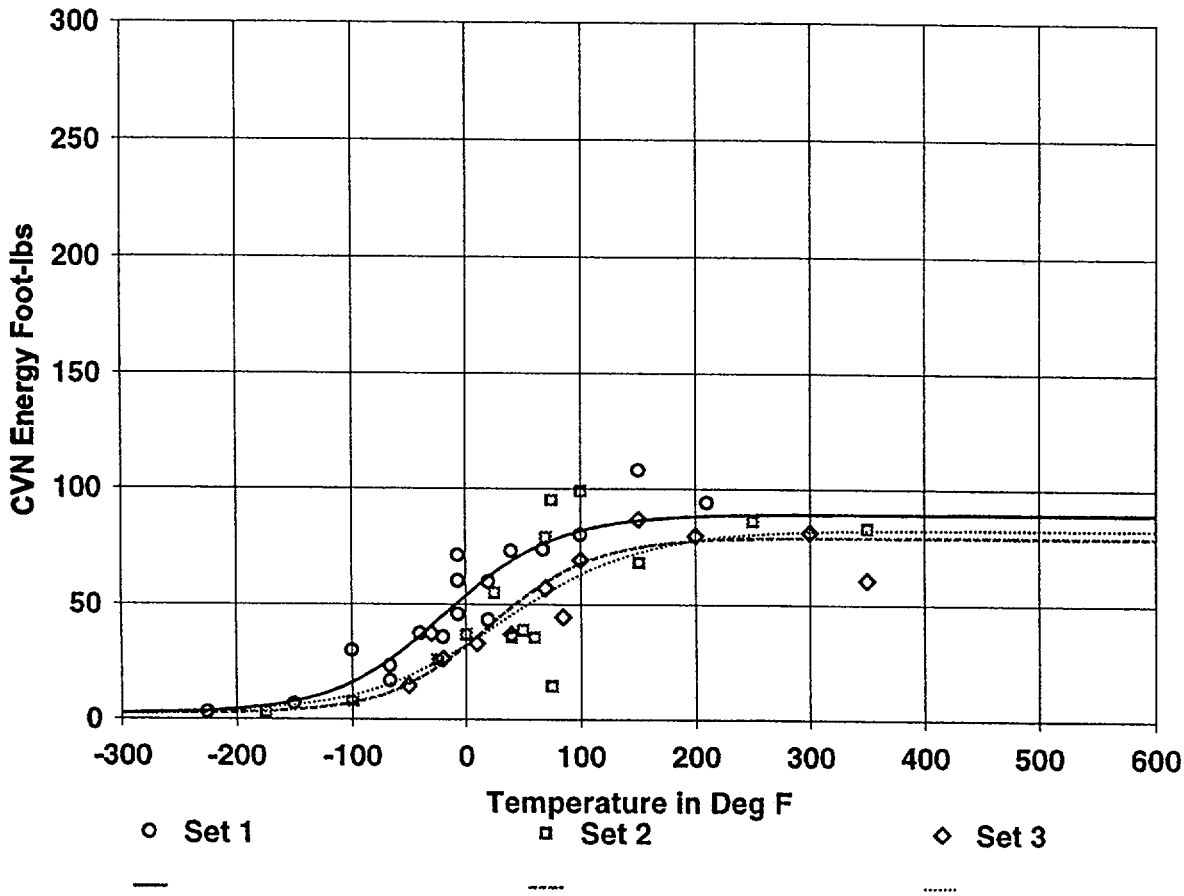

Results

Curve	Fluence	LSE	USE	d-USE	T @30	d-T @30	T @50	d-T @50
1	0	2.2	89.0	.0	-56.3	.0	-8.7	.0
2	5.05E+18	2.2	79.0	-10.0	-5.4	50.9	43.6	52.3
3	1.23E+19	2.2	82.3	-6.7	-7.3	49.0	55.7	64.4

Figure 6-10. Charpy Impact Energy vs. Temperature for Watts Bar Unit 1 Reactor Vessel Heat-Affected-Zone Material

HEAT-AFFECTED-ZONE

CVGRAPH 5.0 Hyperbolic Tangent Curve Printed on 09/10/2001 09:50 AM
Data Set(s) Plotted

Curve	Plant	Capsule	Material	Ori.	Heat #
1	Watts Bar 1	UNIRR	SA508CL2	NA	895075(W H)
2	Watts Bar 1	U	SA508CL2	NA	895075(W H)
3	Watts Bar 1	W	SA508CL2	NA	895075(W H)

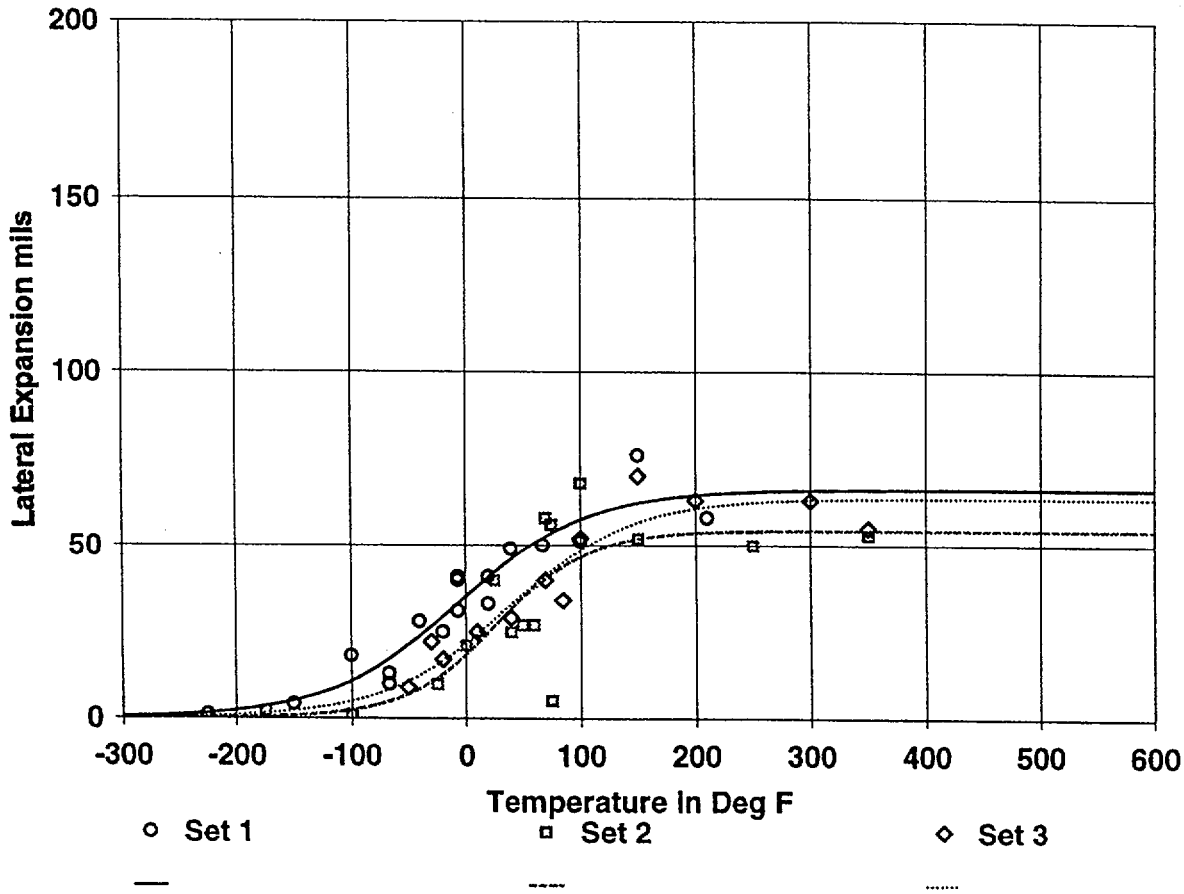

Results

Curve	Fluence	LSE	USE	d-USE	T @35	d-T @35
1	0	.0	66.3	.0	-.7	.0
2	5.05E+18	.0	54.4	-11.9	51.1	51.8
3	1.23E+19	.0	63.6	-2.7	47.9	48.6

Figure 6-11. Lateral Expansion vs. Temperature for Watts Bar Unit 1 Reactor Vessel Heat-Affected-Zone Material

HEAT-AFFECTED-ZONE

CVGRAPH 5.0 Hyperbolic Tangent Curve Printed on 09/10/2001 09:50 AM
Data Set(s) Plotted

Curve	Plant	Capsule	Material	Ori.	Heat #
1	Watts Bar 1	UNIRR	SA508CL2	NA	895075(W H)
2	Watts Bar 1	U	SA508CL2	NA	895075(W H)
3	Watts Bar 1	W	SA508CL2	NA	895075(W H)

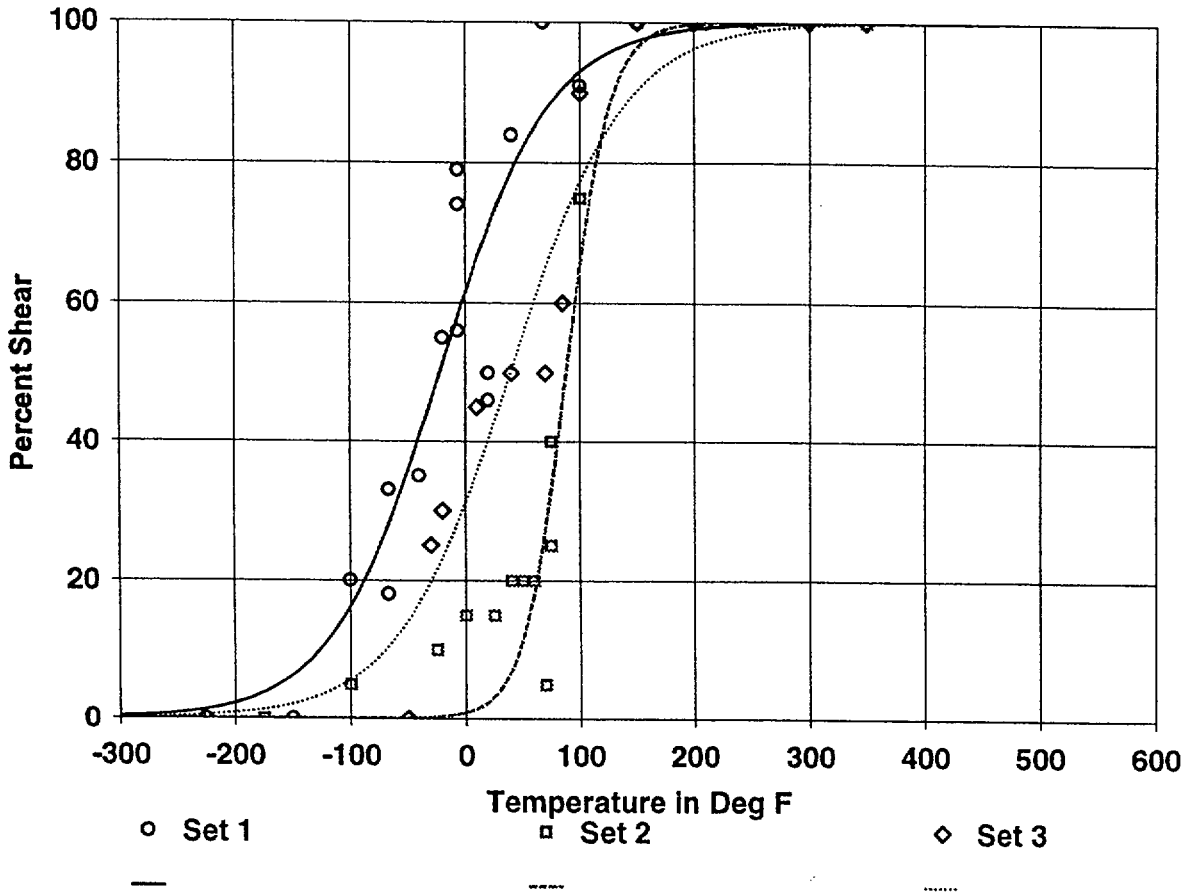

Results

Curve	Fluence	LSE	USE	d-USE	T @50	d-T @50
1	0	.0	100.0	.0	-22.3	.0
2	5.05E+18	.0	100.0	.0	88.1	110.4
3	1.23E+19	.0	100.0	.0	39.6	61.8

Figure 6-12. Percent Shear vs. Temperature for Watts Bar Unit 1 Reactor Vessel Heat-Affected-Zone Material

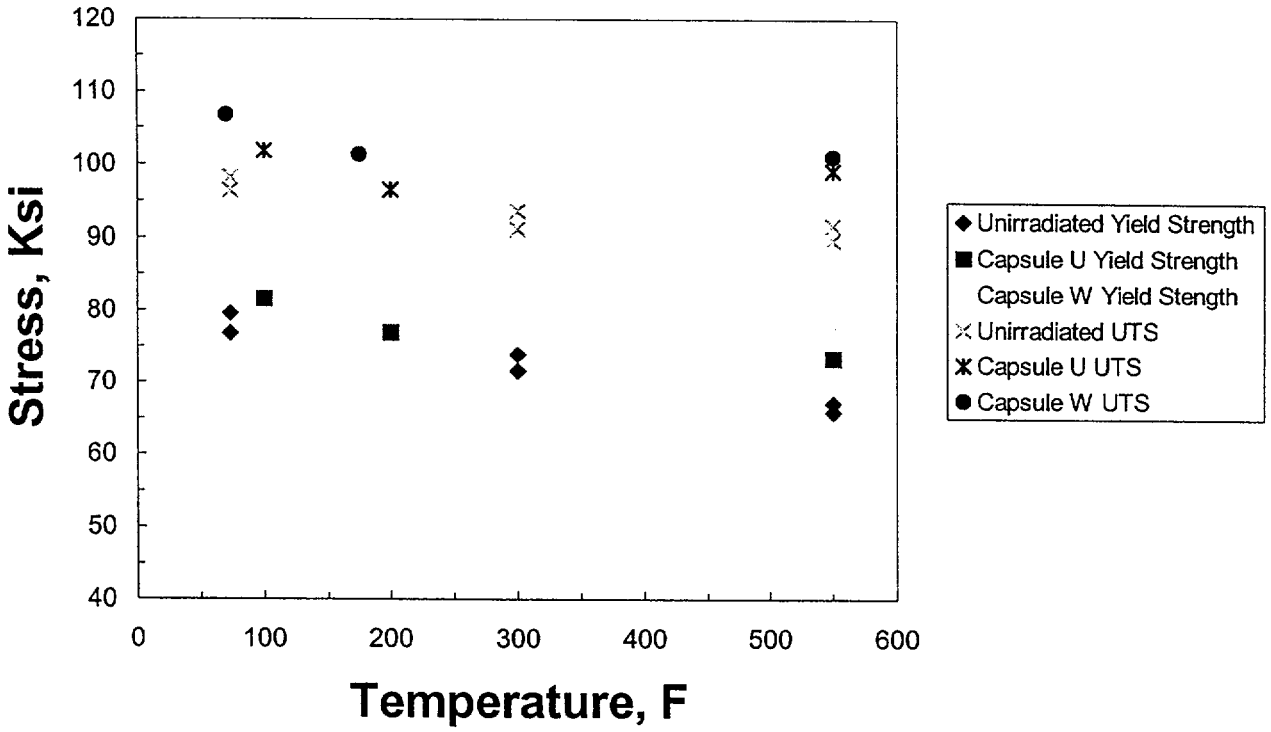

Figure 6-13. Tensile Strength Properties for Watts Bar Unit 1 Reactor Vessel Intermediate Shell Forging 05 (Tangential Orientation)

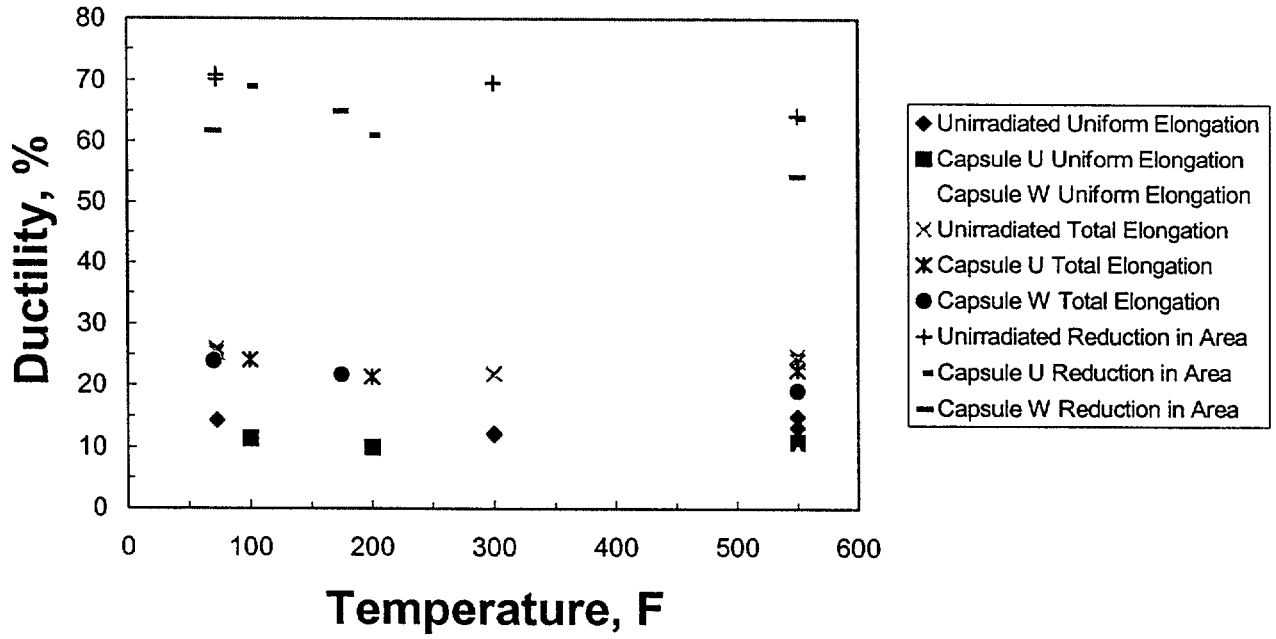

Figure 6-14. Ductility of Watts Bar Unit 1 Reactor Vessel Intermediate Shell Forging 05 (Tangential Orientation)

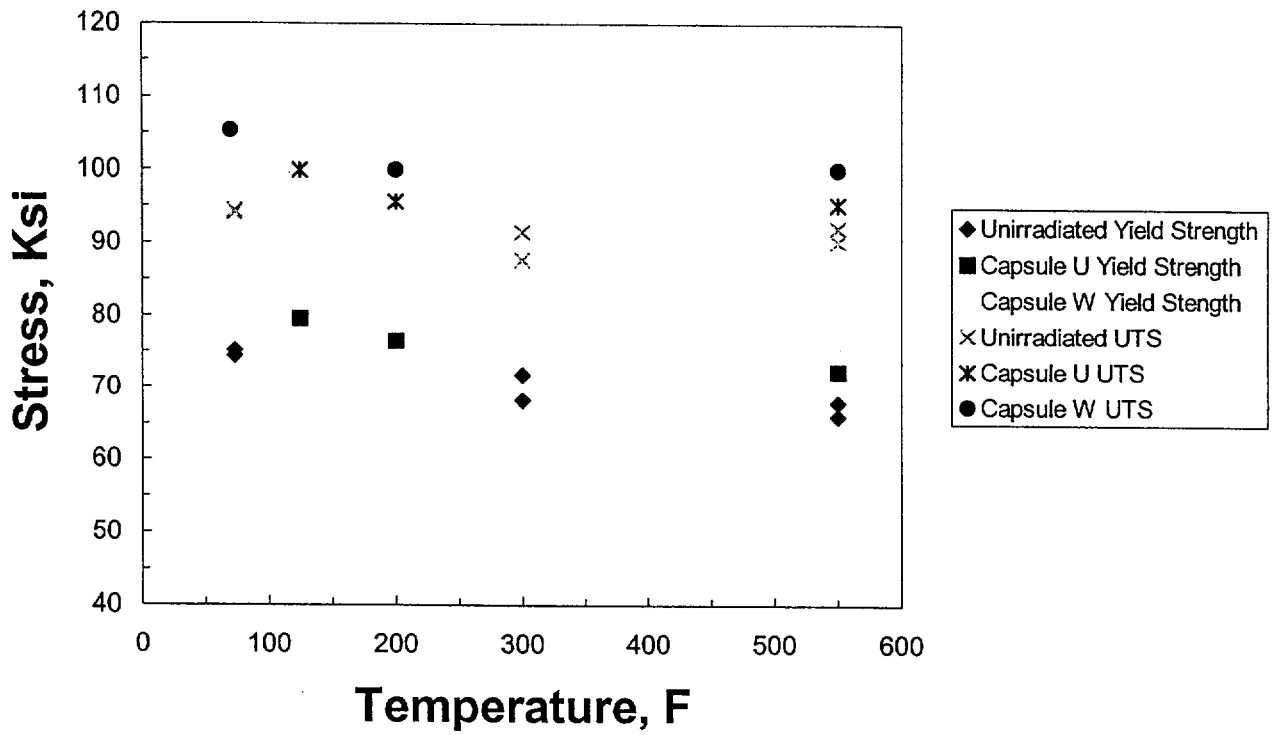

Figure 6-15. Tensile Strength Properties for Watts Bar Unit 1 Reactor Vessel Intermediate Shell Forging 05 (Axial Orientation)

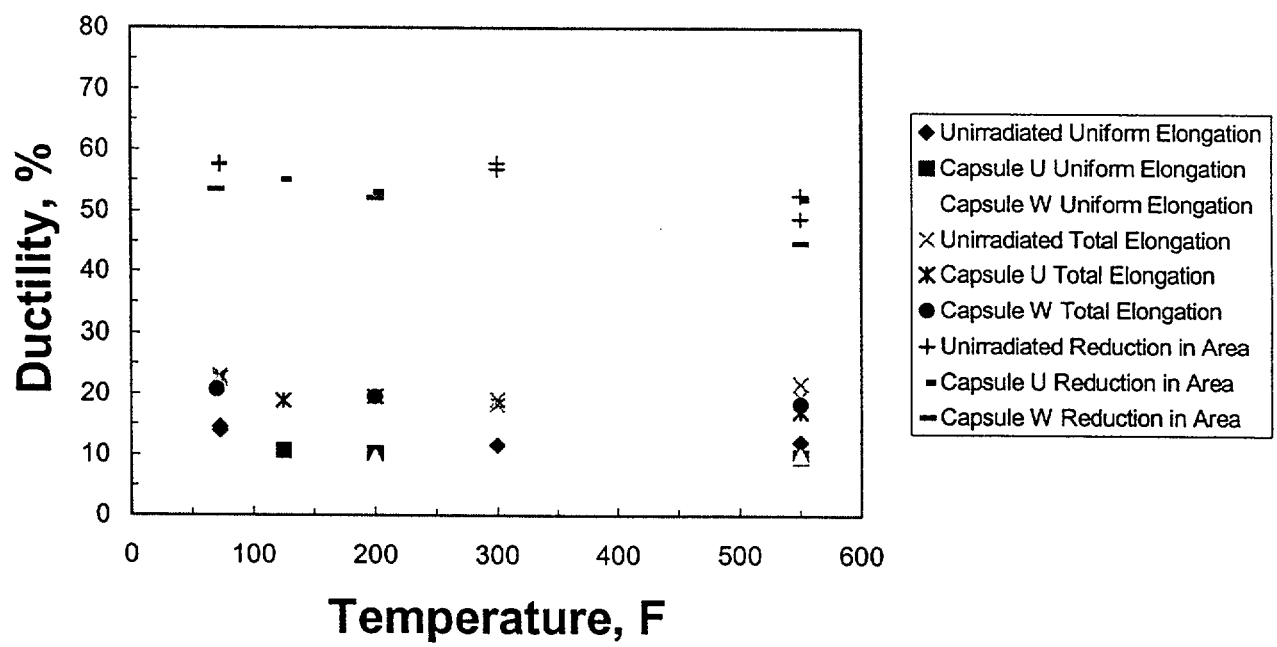

Figure 6-16. Ductility of Watts Bar Unit 1 Reactor Vessel Intermediate Shell Forging 05 (Axial Orientation)

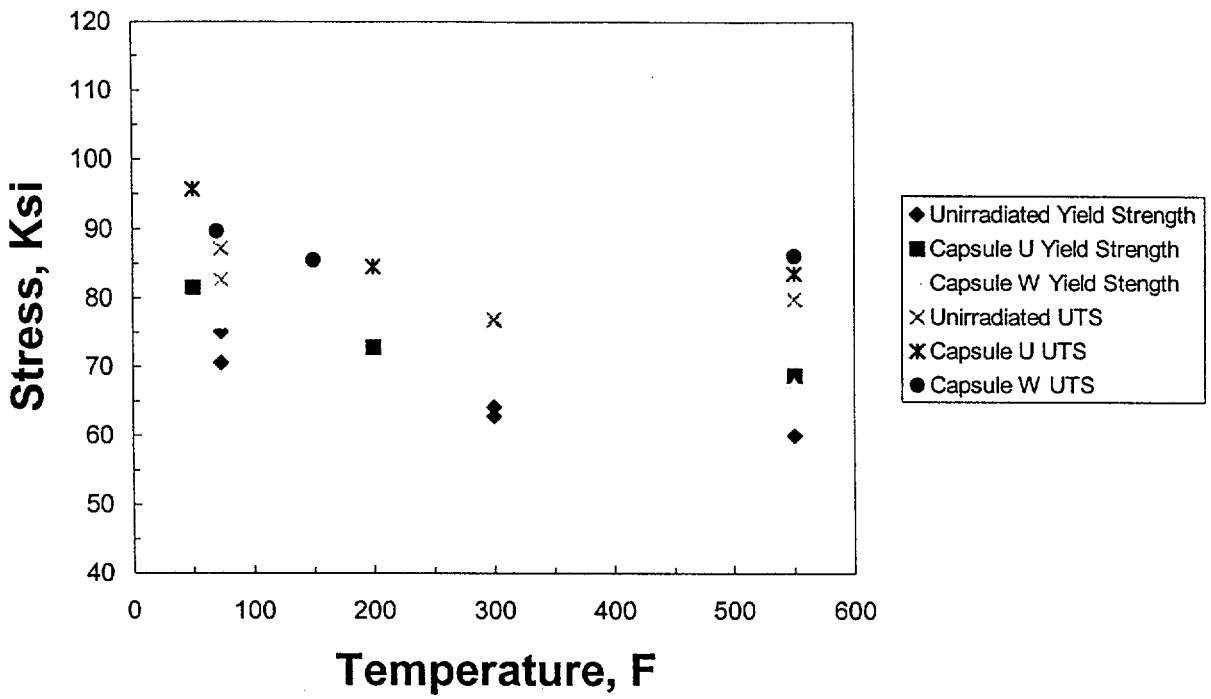

Figure 6-17. Tensile Strength Properties for Watts Bar Unit 1 Reactor Vessel Weld Metal

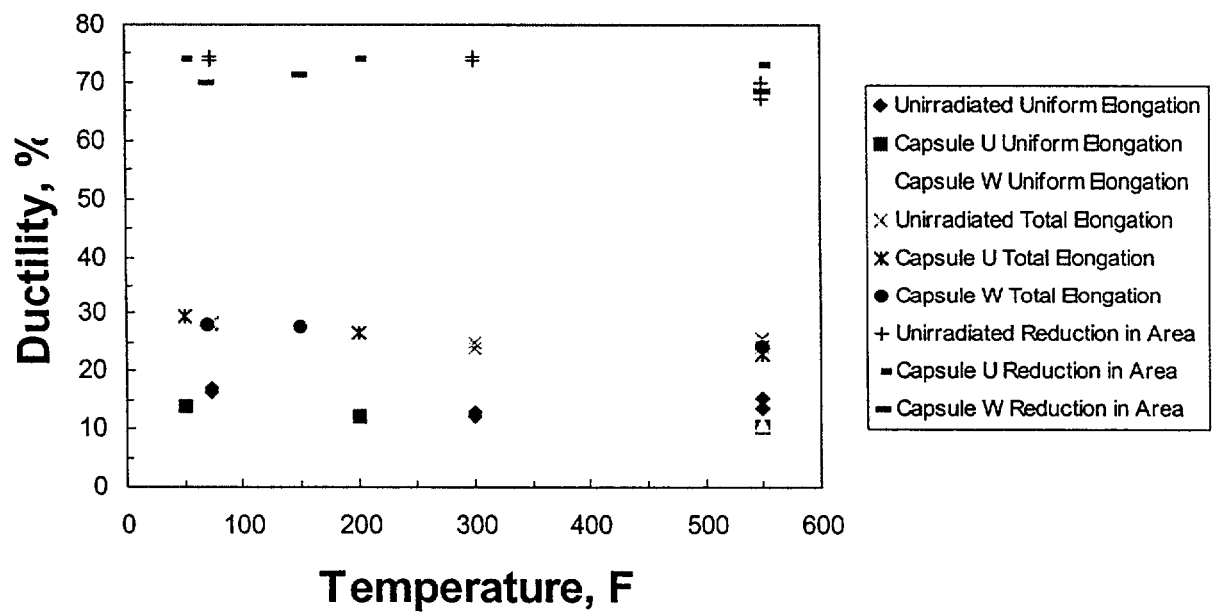

Figure 6-18. Ductility of Watts Bar Unit 1 Reactor Vessel Weld Metal

SECTION 7.0

NEUTRON TRANSPORT AND DOSIMETRY ANALYSIS

7.1 Introduction

This section contains the results of the analysis of the neutron dosimetry contained in the Watts Bar Unit 1 surveillance capsule W. Recommended values for the surveillance capsule fluence and for the reactor vessel exposure are provided. The analysis is based on current state-of-the-art methodology and follows the guidelines given in the recently issued Regulatory Guide 1.190, "Calculational and Dosimetry Methods for Determining Pressure Vessel Neutron Fluence" [13].

The evaluation of the surveillance capsule fluence is used to interpret the neutron radiation induced property changes in the test specimens and to relate these property changes to correlations derived from evaluations of other irradiated specimens. These correlations are based on fast neutron fluence (neutrons above 1 MeV) and are used to evaluate the extent of vessel embrittlement. The evaluation of the fluence to the surveillance capsule specimens is carried out by a combination of an analytical calculation to determine the neutron environment in the capsule and the measurements on the dosimetry specimens. The analytical calculation is also used to determine the neutron exposure at various positions in the reactor vessel. The capsule measurements provide a validation of this determination and relate the capsule measurements to the present and future condition of the reactor vessel.

Although the fast neutron fluence ($E > 1$ MeV) is used to correlate the material property changes, neutrons of all energies will make some contribution to the vessel embrittlement. Correlations have also been developed using fast neutron fluence ($E > 0.1$ MeV) and iron displacements per atom (dpa). The dpa parameter is defined by ASTM Standard E693 [14] and this parameter is recommended in Regulatory Guide 1.99, Revision 2 [15] for assessment of embrittlement gradients within the reactor vessel wall. Accordingly, all exposure results are reported in terms of dpa and fluence ($E > 0.1$ MeV) in addition to fluence ($E > 1$ MeV).

7.2 Neutron Transport Calculation

The neutron exposure of reactor structures is determined by a neutron transport calculation, or a combination of neutron transport calculations, to represent the distribution of neutron flux in three dimensions. The calculation determines the distribution of neutrons of all energies from their source from fission in the core region to their eventual absorption or leakage from the system. The calculation uses a model of the reactor geometry that includes the significant structures and geometrical details necessary to define the neutron environment at locations of interest. The detailed plant specific dimensions were taken from Reference [16]. In particular, the detailed geometry of the surveillance capsules must be included in the model. A cross section of the reactor geometry at axial midplane is shown in Figure 7-1 (taken from Reference [17]). This figure shows the six irradiation capsules which are located at azimuthal angles of 56°, 58.5°, 124°, 236°, 238.5°, and 304°. These capsules are located at angles symmetrical to 31.5° or 34°.

The transport calculations for Watts Bar Unit 1 were carried out in R-2 and R-Z geometry using the DORT two-dimensional discrete ordinates code [18] and the BUGLE-96 cross-section library [19]. The DORT code is an update of the DOT code which has been in use for this type of problem for

many years. The BUGLE-96 library is a 47 energy group ENDF/B-VI based data set produced specifically for light water reactor applications (an update of the earlier SAILOR library). This library contains cross-sections collapsed using a PWR core spectrum which were used for the core region. Outside the core region, cross sections collapsed using PWR downcomer and PWR vessel spectra were used. In these analyses, anisotropic scattering was treated with a P_3 expansion of the scattering cross-sections, and the angular discretization was modeled with an S_8 order of angular quadrature. These procedures are in accordance with ASTM Standard E-482 [20].

The computer codes were obtained from the Radiation Safety Information Computational Center (RSICC) at Oak Ridge National Laboratory. Each code was then compiled on the computer used for the calculations and a series of test cases were run to verify the code performance. The test cases all agreed within allowable tolerance with established results. The calculational procedures meet standards specified by the NRC and ASTM as appropriate. In particular, the analysis (including all modeling details and cross-sections) is consistent with Regulatory Guide 1.190 [13].

R-2 Calculations

The R-2 model included 170 mesh points in the radial direction covering the range from the center of the core to about 16 inches into the biological shield. This large number of mesh points was used to accurately calculate the neutron flux transport from the core edge to the outside of the vessel. In the azimuthal direction, 60 mesh points were used to model a single octant of the reactor. Inspection of the fuel loading patterns indicated that only minor deviations from octantal symmetry were present and these were ignored. The octant selected for the fuel power distribution was that containing surveillance capsule W. The 60 points provided good definition of the variation of the core edge with angle and defined the azimuthal flux variation in the vessel. In the discussion below, all angles are referred to in the first octant (i.e. relative to the nearest cardinal axis). It should be noted that the azimuthal flux shape between 45° and 90° is the mirror image of that between 0° and 45° (i.e. an angle of 50° corresponds to 40° in the first octant).

The core region used a homogenized material distribution which includes the fuel, fuel cladding, and the water. While the water temperature increases as the water passes through the fuel, it was deemed adequate to use the average core water temperature to define the water density throughout the entire core region. Water temperature in the bypass region (between the core baffle and barrel) was assumed to be halfway between the core average temperature and the downcomer temperature.

The neutron source was determined from assembly power burnups and axial power profiles for each cycle using data supplied in Reference [21]. The DOTSOR code (available as part of the LEPRICON code package [22]), was used to convert the cycle power distributions from x,y to R,2 coordinates and place the source in each mesh cell. The source per group was defined by an average fission spectrum calculated for a fission breakdown by isotope determined for the average burnup of the outer fuel assemblies for each case. The main isotopes that contribute to the fission spectrum are U-235 and Pu-239, but contributions from U-238, Pu-240, and Pu-241 were also included. Almost all of the neutrons that reach the capsule and vessel originate in the outer rows of fuel assemblies. The source calculations used the appropriate power distribution for all the fuel assemblies together with estimated pin power distributions to obtain the spatial source variation within the fuel assemblies. Plant specific pin power distributions were not available, so the pin power distributions were estimated based on calculations for another Westinghouse PWR [23].

The calculations of the fuel fission parameters for each cycle were made using the ORIGEN 2.1 code [24]. This code calculates the effects of burnup on the neutron source in order to obtain appropriate values for the fission contribution from each fissionable nuclide. This was carried out using an ORIGEN PWR cross section library appropriate for high burnup fuel.

To obtain the neutron flux distributions, three R-2 calculations were performed for each cycle to represent the neutron pad and capsule geometry. As shown in Figure 7-1, two octants have two capsules, two octants have a single capsule, and the remaining octants have no capsules attached to the neutron pad. A plan view of a double capsule geometry is shown in Figure 7-2 (taken from Reference [17]). The different amounts of steel around the capsule between the single capsule and double capsule geometry will affect the capsule flux and thus calculations were done for both geometries. In addition, although all the neutron pads are 35° in extent, they are not located symmetrically (due to the capsules) and thus different octants have different length pads. In two of the octants with no capsule, the pad only extends between 30° and 45°. These octants will have the maximum vessel fluence at angles near 30°, and this calculation geometry was therefore used to obtain vessel neutron exposure.

R-Z Calculations

A second set of transport calculations was performed for each case in R-Z geometry. The R-Z model used the same radial mesh as the R-2 model and represented the axial geometry with 70 mesh points. Regions above and below the core were modeled based on data from [25]. Inspection of the detailed axial power distributions for each assembly indicated that variation from an average power shape was small. Therefore, a single axial power shape was used for each fuel cycle calculation. The radial power shape was determined by integration of the azimuthal distribution used for the R-2 calculation. Source in the bypass region was set to zero. For the R-Z model, the core radius was taken to be that which gave the equivalent core volume. In the model, the neutron pad and surveillance capsules were not included. The model also did not include the former plates.

Flux Synthesis

As indicated above, the calculations were carried out in 2 dimensions. In order to estimate the fluence rate in the 3 dimensional geometry, the following equation was used to evaluate the flux N for each cycle case:

$$N(R,2,Z) = N(R,2) * N(R,Z) / N(R)$$

In this equation, N(R,2) is taken from the DORT R,2 calculation (normalized to the power at midplane in the model region), and N(R,Z) is from the R,Z calculation normalized to the power in the entire core. A third calculation determined N(R) using a one-dimensional cylindrical model normalized at core midplane. The model for the one-dimensional calculation used the same radial geometry and neutron source as the R,Z calculation.

Calculated exposure rate results from the neutron transport analysis are given in Tables 7-1 through 7-5 for the first three fuel cycles. In Table 7-1, the fluence rate (E > 1 MeV), fluence rate (E > 0.1 MeV), and dpa/s are given for the capsule positions. This includes capsules at 34° in the two geometries: double capsule (e.g. capsule U); and single capsule (e.g. capsule W).

In Table 7-2, the exposure rate results are given for the pressure vessel inner radius (defined as the boundary between the stainless steel clad and the base metal) calculated at the axial midplane. The midplane location is given here rather than the maximum fluence location since the axial flux peak exhibits some variation between cycles, depending on the fuel management scheme. Later in this report, fluences will be evaluated for the maximum point on the reactor vessel. The axial variation of fluence at the vessel inner radius is shown in Figure 7-3. This figure is for the fluence integrated over the first three fuel cycles. The azimuthal fluence variation is shown in Figure 7-4.

Radial gradient data for fluence (E > 1 MeV), fluence (E > 0.1 MeV), and dpa are given in tables 7-3, 7-4, and 7-5, respectively. These data are for the fluence for the first three cycles and are evaluated at axial midplane. These ratios vary slightly depending on fuel management and also vary with axial location. To a good approximation, however, these ratios can be used to estimate neutron exposure within the vessel given the exposure at the vessel inner radius.

Comparison of the calculated results for cycle 1 in Tables 7-1 and 7-2 indicates that the present results for flux level (E > 1.0 MeV) fall below given those in Reference [17]. The capsule results are about 4% below and the vessel results are 12-18% lower. The present calculation differs from that in Reference [17] in several respects. The two most important are the treatment of the pin power distributions in the assemblies on the core periphery and in the modeling of the surveillance capsule geometry. The difference in pin power distributions affects the neutron leakage from the core and introduces a flux magnitude bias. This bias varies slightly with azimuthal angle because the effect of the edge pins varies depending on whether the angle is near a flat fuel assembly surface or near an assembly corner. The modeling details of the capsule geometries can affect both the magnitude of the flux and the spectrum in the capsule. Other differences between the calculations also exist, including vessel dimensions used in the model, the number of mesh points in the model, the method used to convert the power distributions from X,Y coordinates to R-2 , and reactor operating temperatures. In addition, the synthesis technique gives a slightly lower fluence since the calculation takes into account axial streaming. Discussion of the uncertainties associated with each of these effects is given in Section 7.5.

7.3 Neutron Dosimetry

The neutron dosimetry monitors included in the Watts Bar Unit 1 surveillance program are listed in Table 7-6. Also given in Table 7-6 are the nuclear reactions and associated nuclear constants that were used to relate the measured product activities to reaction rates at the measurement location. The dosimeters were all located at the radial center of the capsule and were placed at three axial locations designated top, middle, and bottom. The iron, nickel, copper, and cobalt-aluminum monitors, in wire form, were placed in holes drilled in spacers at each of these axial levels within the capsules. The uranium and neptunium fission monitors were shielded by cadmium covers to minimize fission contributions from impurities and were located at only the dosimeter block located near the axial center of the capsule. The cobalt-aluminum monitors were irradiated both bare and cadmium shielded.

The radiometric dosimetry monitors each respond to neutrons according to their unique reaction cross section. Each monitor responds to neutrons over an energy range as indicated approximately in Table 7-6. The reactions occur over the course of the irradiation producing radioactive products that, with appropriate corrections for decay, provide an integral measure of the exposure. From the measured

reactions then, the neutron fluence can be deduced using the reaction cross section together with the calculated neutron flux spectrum at the dosimeter location.

The specific activity of each of the dosimeters was determined using established ASTM procedures [26 through 34]. Samples were prepared and weighed and the activity of each monitor was determined by means of a lithium-drifted germanium, Ge(Li), gamma spectrometer. The irradiation history of the Watts Bar Unit 1 reactor during cycles one through three is given in Table 7-7. Using this history, the activation of each detector was calculated using the calculated reaction rate at full power for each cycle. Comparison of the calculated disintegration rate at the shutdown time for the third cycle with the reaction rate gives the saturation factor which relates measured disintegrations per second (dps) to reactions per second (rps).

Measured dosimeter results corrected to the end of irradiation (September 10, 2000) are given in Table 7-8. This table also gives the measurement error including both random and systematic error. The reaction rates derived from the measurements are given in the last column of this table. These reaction rates are normalized to full reactor power at the calculated flux level in the capsule for cycle 3.

Comparisons of calculated and measured results for both capsule U and capsule W are made in Table 7-9. In this table, the results for the dosimeters of the same type have been averaged with no axial correction. Since the height of the surveillance capsule is small relative to the total height of the core, the axial difference may be neglected within the accuracy of the measurements. The capsule U results are taken directly from Reference [17] and indicate that the fast reaction measurement results are consistent and that the calculation falls below the measurements by an average of 15%. The results for capsule W are very similar with an average bias of 12.8%. Combining these results indicates that the calculations are biased low by a factor of 0.861. The consistency of the data indicates that the calculated spectrum in the fast region is accurate enough to predict relative reaction rates. The cobalt data indicates that the thermal part of the spectrum is not as accurate. The calculated neutron spectrum (average flux for the first three cycles of operation) is given in Table 7-10.

In Table 7-11, exposure parameters for the center of the surveillance capsules are given. The table contains the calculated values integrated using the flux values in Table 7-1, and best- estimate values which are obtained by using the capsule specific fast neutron average bias values from Table 7-9. The best-estimate values are recommended for use in correlating the metallurgical specimen measurements.

7.4 Projections of Vessel Exposure

Regulatory Guide 1.190 [13] states that an absolute calculation should be used for vessel fluence calculations, but a bias factor may be applied if justified. This is consistent with ASTM standards [26, 35]. In the case of the data for Watts Bar Unit 1, the bias indicated by the dosimetry falls within an allowable limit of 20% and so is acceptable for use with no correction. However, the consistency of the data, together with the limitations of the calculational model as discussed above, indicate that the bias is likely to be real. Moreover, use of a bias correction will result in a more conservative vessel fluence estimate. Therefore, the recommended vessel fluence values are the calculated values times a factor of 1/0.861 (or 1.162).
The neutron exposure at the vessel inner radius at the end of cycle 3 (3.81 efpy), and at future times of 16 efpy and 32 efpy, is given for several axial points in Tables 7-12 through 7-14. In Table 7-12,

the exposure is evaluated at core axial midplane. The maximum fluence, however, is calculated to lie about 36 inches below midplane at the end of cycle 3, and the fluence at this point is given in Table 7-13. The exact location of the maximum fluence rate will vary by cycle, so at future times, the maximum may move to a different axial point. Another axial point of interest is the circumferential weld in the beltline region which is located at 9.6 inches above midplane. Results for this location are given in Table 7-14.

Projections to 16 efpy and 32 efpy were made using the average fluence rate calculated for cycles 2 and 3. These two cycles are similar in neutron leakage from the core and differ from cycle 1 which started with all fresh fuel. Therefore, it is reasonable to not use the initial cycle in fluence projections. Although cycles 2 and 3 are not equilibrium cycles, the neutronic design is likely to be similar to upcoming fuel cycles in terms of vessel and capsule exposure rates.

Table 7-15 presents data on fluence E > 1.0 MeV at the maximum axial point at the surface and at the 1/4T and 3/4T positions within the vessel. These data are provided at 16 and 32 efpy to allow for calculation of heatup and cooldown curves. Data within the vessel are provided as determined by three different methods. The first set of data uses the calculated fluence attenuation within the vessel to get results at the interior positions. The other two methods are based on dpa attenuation.

Radiation embrittlement effects are usually correlated with fluence E > 1 MeV. However, it is generally thought that dpa might be a better correlation parameter and, if this is correct, the use of the fluence E > 1 MeV values within the vessel are non-conservative. Accordingly, a dpa attenuation factor is used for fluence through the vessel. Table 7-15 also provides results with the dpa attenuation calculated using a formulation specified in the NRC Regulatory Guide 1.99 (Revision 2) [15].

The dpa values in this report are calculated from the ASTM E693-94 Standard dpa cross-section [14]. This evaluation of the dpa cross section is based on the ENDF-IV cross-section file. A new dpa cross-section evaluation based on ENDF-VI (consistent with the cross-sections in BUGLE-96) is expected to be used as the standard in the future. This change is not expected to have any significant impact on the results.

It should be noted that the fluence projections made in this evaluation fall far below those made in the surveillance capsule U report [17]. The primary reason for this difference is that the previous projections of fluence were made on the basis of the cycle 1 results and the present projections are based on the flux levels calculated for cycles 2 and 3. Inspection of the relative power generated in the outer assemblies indicates that cycles 2 and 3 fall about 40% below cycle 1. The new projections are consistent with this difference.

Updated lead factors for the Watts Bar Unit 1 surveillance capsules are given in Table 7-16. The lead factors for the capsules still being irradiated are evaluated as of the end of cycle 3, but lead factor changes with fuel loading are expected to be small.

7.5 Uncertainty Analysis

To conform to the procedures in Regulatory Guide 1.190, a detailed analytic uncertainty analysis was performed. Each contributor to the uncertainty was investigated individually by performing a set of transport calculations to determine the magnitude of effect on the fluence of each perturbation from the reference configuration. A summary of the uncertainty contributions from each source is summarized in

Table 7-17. Each independent uncertainty contribution is summed in quadrature to give the total uncertainty in fluence in the capsule and at vessel locations. The uncertainties considered include those in nuclear data, source normalization, reactor geometry, material densities, source distribution, transport calculation methodology, and time history uncertainties.

Nuclear data input to the transport calculations includes the multigroup cross sections and neutron spectrum. Uncertainties in the cross sections are complicated because of the large number of cross section values and the correlations between these values. Although the uncertainties in individual cross section values may be relatively large, the total effect of cross section uncertainties is limited by adjustments made by cross section evaluators to agree with benchmark data. The approach taken here is to limit the cross section uncertainty effects to just the total cross section and to evaluate this by varying the material densities (see below).

Uncertainty in the multigroup fission source arises from uncertainty in the fission spectra for each fissioning isotope, the distribution of fission among the fissioning isotopes, the energy release per fission (6), and the number of neutrons produced per fission (Λ). Uncertainty in the fission spectrum is mainly at the higher energies, which may affect the copper reaction rate but has little effect on the fluence above 1 MeV except for very deep penetrations. The uncertainty was represented as an uncertainty in fuel burnup, which was assumed to be 5000 MWd/MTU (megawatt days per metric ton of uranium). The source normalization is proportional to the ratio Λ / 6 which both increase with burnup and thus have a small effect on the source normalization. In addition to the normalization uncertainty due to Λ / 6, there is an overall normalization uncertainty in reactor power as measured by the heat balance. This uncertainty was taken to be a typical plant value of 2%.

Geometry uncertainties were estimated using typical plant tolerances. The uncertainties in Table 7-17 are based on assumed uncertainties of 0.031 inches in barrel thickness, 0.062 inches in the capsule radial centerline, and 0.125 inches in vessel inner radius. In addition, an uncertainty in the capsule model was included. The major source in modeling uncertainty is existence of a water gap (see Figure 7-2) between the capsule and barrel, since no print was available to define this gap. The effect of this gap on the calculated fluence above 1 MeV was determined to be 4.6%. This gap will change the neutron spectrum in the capsule and probably largely explains the difference in capsule lead factors between the current calculation and that reported in [17].

Water density uncertainties were based on assumed temperature uncertainties of 5° F in the downcomer and bypass regions, and 10° F in the core. Material densities for the structural components and the vessel are well known, but, as discussed above, the cross section uncertainty was included as a density variation. An estimate for this uncertainty was derived by considering vessel mockup benchmark results [36], comparisons of reactor cavity and surveillance capsule measurements [37 to 40], and comparisons of cross section evaluations [41]. It was concluded that uncertainties due to the iron cross section contribute a 10% effect on fluence through a reactor vessel. This translates into a cross section uncertainty of 3.5%. This value was adopted as the density variation and uncertainties were calculated based on this uncertainty estimate. In addition, the core cross sections for the fuel and cladding were also assumed to have this uncertainty. This estimate includes effects due to the core homogenization.

Source uncertainties were estimated for both the assembly power distributions and the pin power distributions. It is assumed that the relative assembly power values are known to about 0.01. For outer assemblies, which can have a relative power below 0.4, this uncertainty can be as large as 3%.

This upper limit value was assumed. Plant specific pin power distributions were not available for Watts Bar Unit 1, so estimates of the pin power distributions were made based on other PWR plants. This is considered to be the major source of the observed bias in the results. A calculation was made using a flat source shape within the assemblies. This resulted in a flux level increase at the vessel averaging 30%. To obtain a 1σ uncertainty estimate, this 30% range was divided by 4, resulting in a 7.5% estimate. To get this value, it was assumed that the bias in the calculation was largely removed by using the measured bias defined above.

The neutron transport was calculated using a model of the reactor and S_N code. This is only an approximation to the solution of the Boltzmann transport equation and thus also contributes uncertainty. Two components of this uncertainty were considered. First, the uncertainty of the core model was considered. From the VENUS benchmark measurements, it was found that a typical range of C/E results was about 10%. Thus the standard deviation was about 5% and this value was used here. The second component was the adequacy of the S_8 calculation. To test this, S_{16} calculations were performed for a previous case to compare to the S_8. Differences ranged to as high as 3% at the outside of the vessel. The upper limit difference was added in quadrature to the 5% from the first modeling effect.

Flux history effects are included here to represent the deviation of a true fluence integral over the cycle from the single calculation performed for the midplane fuel source. A value of 4% uncertainty was estimated based on typical axial source variations during a cycle.

Uncertainty values were obtained by combining all the identified contributors to produce a total uncertainty in the capsule, and at the vessel IR. 1/4T, and 3/4T position. The uncertainties vary from 13-14% for the capsule and vessel IR, to about 19% at the 3/4T position. All the uncertainties are estimated to be less than 20%.

An uncertainty evaluation was also performed to evaluate the uncertainty in the best-estimate value for the capsule fluence. This value has much less dependence on the calculation because the fluence is evaluated at the exact position where the dosimeter monitors are located. The value thus depends on the accuracy of the measurements (5-6%), the flux history (4%), and the calculated spectral shape (4.3%). Combining these uncertainties, the uncertainty in the capsule fluence value was found to be 8%.

7.6 Conclusions

Calculations of neutron fluence for the first 3 cycles of Watts Bar Unit 1 have been completed. Evaluations were performed of the measured dosimetry from capsule W and comparisons were made with previous measurements made on capsule U. These comparisons indicated a bias in the calculations, and the recommended vessel fluence values are obtained by increasing the calculated values by a factor of 1.162. Uncertainties in the fluence at the vessel IR and ¼ T were estimated to be about 13-15%. The analysis was carried out to meet all the criteria set forth in Regulatory Guide 1.190.

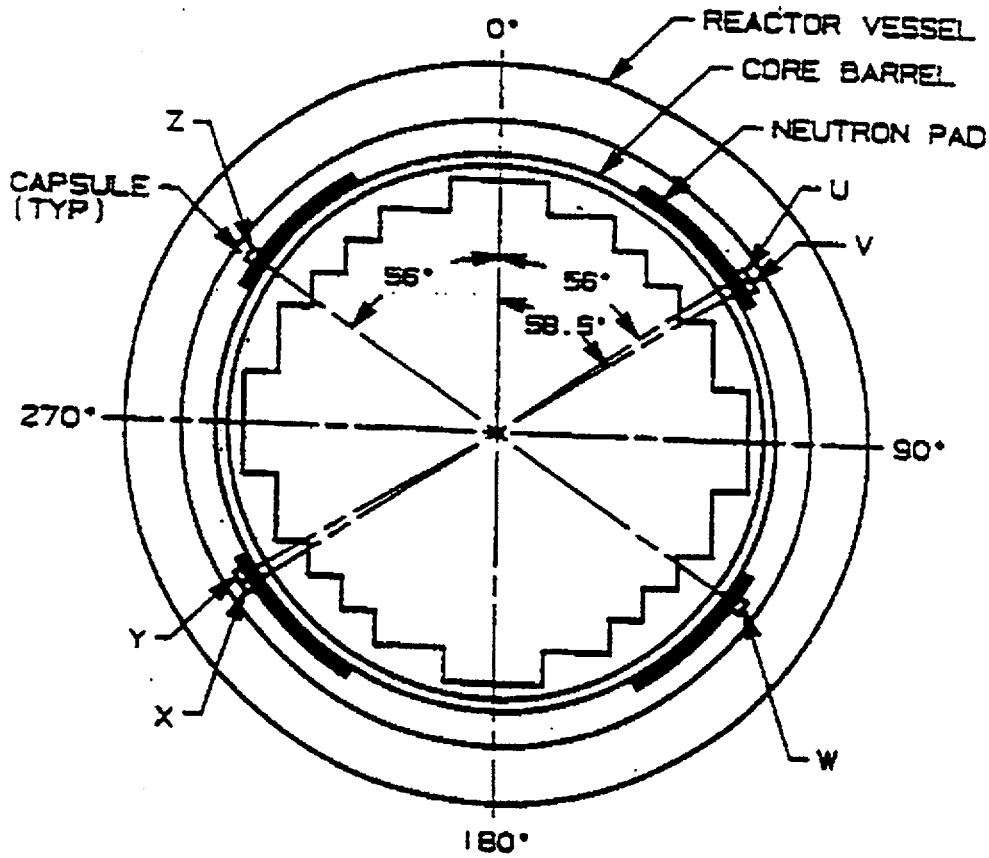

Figure 7-1 Locations of Watts Bar Unit 1 Surveillance Capsules

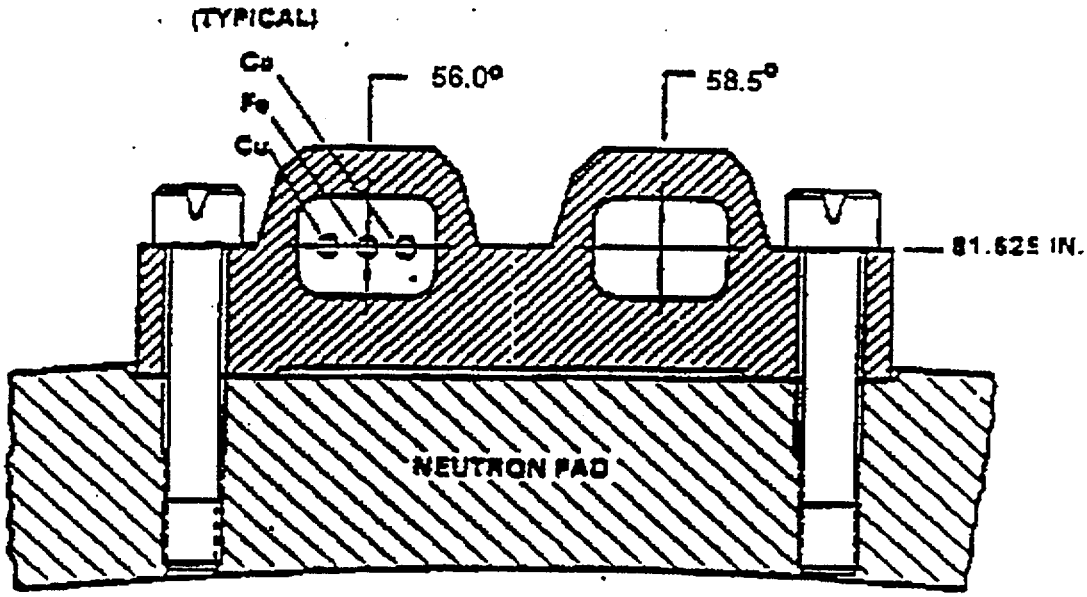

Figure 7-2 Westinghouse Dual Surveillance Capsule Geometry

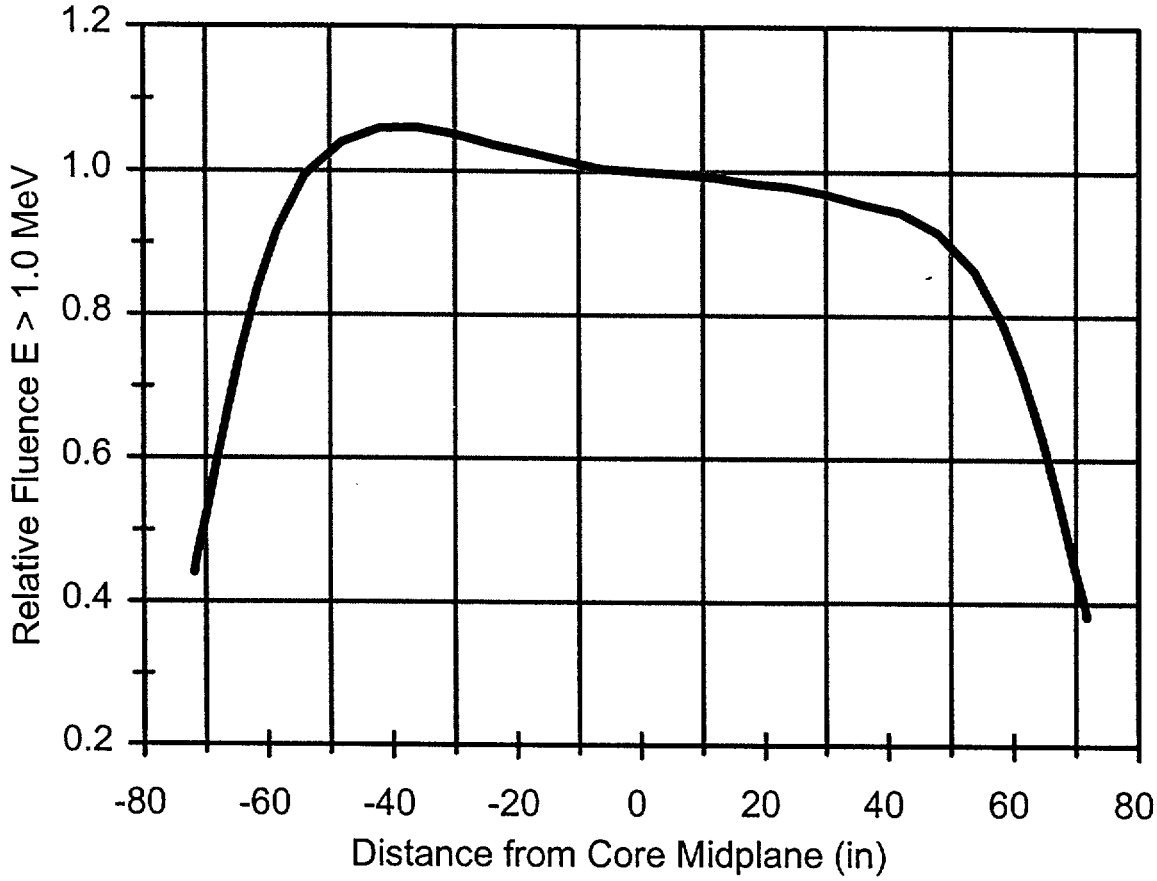

Figure 7-3 Fluence (E > 1.0 MeV) Relative to Core Axial Midplane at the Vessel Inner Radius at the End of Cycle 3 vs Height Within the Core Region

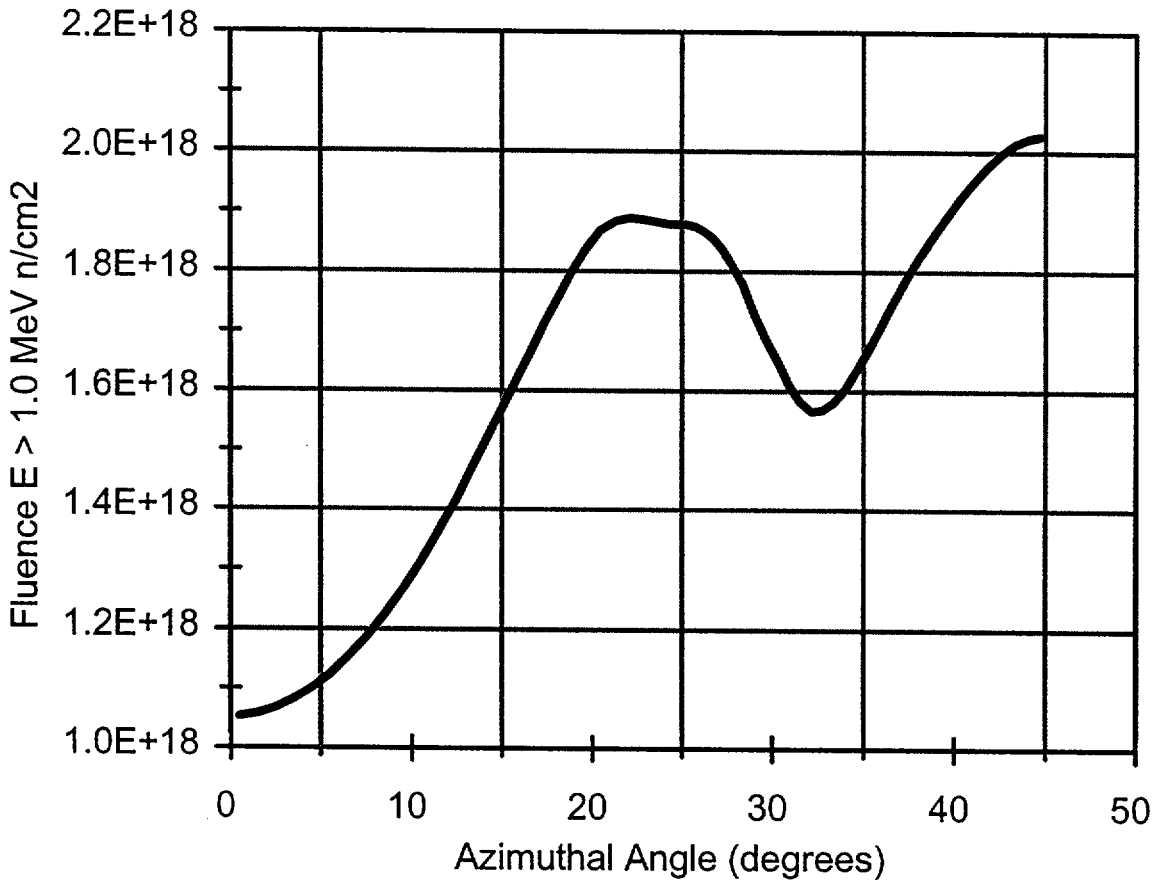

Figure 7-4 Fluence E > 1.0 MeV at Axial Midplane at the Vessel Inner Radius at the End of Cycle 3 vs Azimuth

Table 7-1

Calculated Exposure Rates at the Center of Surveillance Capsules

N (E > 1.0 MeV) n/cm^2-s			
Cycle	31.5° double capsule	34° double capsule	34° single capsule
1	1.00E+11	1.18E+11	1.13E+11
2	7.15E+10	8.15E+10	7.84E+10
3	7.05E+10	8.10E+10	7.80E+10
N (E > 0.1 MeV) n/cm^2-s			
Cycle	31.5° double capsule	34° double capsule	34° single capsule
1	5.24E+11	6.16E+11	5.59E+11
2	3.66E+11	4.19E+11	3.79E+11
3	3.60E+11	4.16E+11	3.77E+11
Iron Displacement Rate (dpa/s)			
Cycle	31.5° double capsule	34° double capsule	34° single capsule
1	2.15E-10	2.53E-10	2.35E-10
2	1.52E-10	1.73E-10	1.61E-10
3	1.50E-10	1.72E-10	1.60E-10

Table 7-2

Calculated Exposure Rates at the Inner Radius of the Reactor Vessel (Clad-Base Metal Interface) at Several Azimuthal Angles at Axial Midplane

N (E > 1.0 MeV) n/cm^2-s				
Cycle	0°	15°	30°	45°
1	1.075E+10	1.643E+10	1.710E+10	2.163E+10
2	7.400E+09	1.153E+10	1.254E+10	1.466E+10
3	8.290E+09	1.151E+10	1.227E+10	1.472E+10
N (E > 0.1 MeV) n/cm^2-s				
Cycle	0°	15°	30°	45°
1	2.256E+10	3.465E+10	3.914E+10	5.476E+10
2	1.549E+10	2.424E+10	2.840E+10	3.675E+10
3	1.729E+10	2.417E+10	2.779E+10	3.688E+10
Iron Displacement Rate (dpa/s)				
Cycle	0°	15°	30°	45°
1	1.668E-11	2.521E-11	2.663E-11	3.424E-11
2	1.152E-11	1.775E-11	1.954E-11	2.321E-11
3	1.288E-11	1.773E-11	1.912E-11	2.331E-11

Table 7-3

Radial Distribution of N (E > 1.0 MeV) within the Reactor Vessel Relative to Clad-Base Metal Interface at Axial Midplane

Radius	Azimuthal Angle			
(cm)	0°	15°	30°	45°
220.091[a]	1.0000	1.0000	1.0000	1.0000
220.282	0.9908	0.9907	0.9908	0.9905
220.770	0.9583	0.9581	0.9583	0.9566
221.556	0.8963	0.8956	0.8959	0.8924
222.533	0.8133	0.8119	0.8119	0.8060
223.510	0.7300	0.7279	0.7278	0.7202
224.486	0.6510	0.6483	0.6483	0.6392
225.463[b]	0.5781	0.5750	0.5749	0.5650
226.440	0.5118	0.5083	0.5084	0.4978
227.417	0.4520	0.4483	0.4484	0.4376
228.393	0.3985	0.3946	0.3948	0.3840
229.370	0.3507	0.3468	0.3470	0.3365
230.347	0.3083	0.3043	0.3047	0.2944
231.324	0.2707	0.2667	0.2672	0.2573
232.300	0.2375	0.2335	0.2340	0.2247
233.277	0.2081	0.2042	0.2047	0.1960
234.254	0.1822	0.1784	0.1789	0.1707
235.231	0.1594	0.1556	0.1562	0.1486
236.207[c]	0.1393	0.1356	0.1362	0.1291
237.184	0.1217	0.1179	0.1185	0.1120
238.161	0.1061	0.1023	0.1030	0.0969
239.138	0.0924	0.0885	0.0892	0.0835
240.114	0.0804	0.0761	0.0768	0.0716
241.091	0.0699	0.0648	0.0656	0.0606
241.579[d]	0.0594	0.0534	0.0544	0.0496

a. Vessel inner radius (clad-base metal interface)
b. Vessel ¼ T
c. Vessel ¾ T
d. Vessel outer radius

Table 7-4

Radial Distribution of N (E > 0.1 MeV) within the Reactor Vessel Relative to Clad-Base Metal Interface

Radius	Azimuthal Angle			
(cm)	0°	15°	30°	45°
220.091[a]	1.0000	1.0000	1.0000	1.0000
220.282	1.0079	1.0075	1.0074	1.0061
220.770	1.0136	1.0112	1.0126	1.0075
221.556	1.0091	1.0042	1.0070	0.9975
222.533	0.9907	0.9825	0.9870	0.9716
223.510	0.9625	0.9512	0.9573	0.9373
224.486	0.9290	0.9148	0.9227	0.8983
225.463[b]	0.8927	0.8760	0.8850	0.8572
226.440	0.8550	0.8358	0.8463	0.8154
227.417	0.8167	0.7954	0.8068	0.7736
228.393	0.7783	0.7551	0.7673	0.7321
229.370	0.7401	0.7152	0.7280	0.6915
230.347	0.7024	0.6760	0.6892	0.6515
231.324	0.6652	0.6374	0.6510	0.6127
232.300	0.6287	0.5998	0.6134	0.5746
233.277	0.5929	0.5628	0.5766	0.5377
234.254	0.5579	0.5269	0.5405	0.5016
235.231	0.5235	0.4916	0.5050	0.4665
236.207[c]	0.4899	0.4572	0.4702	0.4321
237.184	0.4570	0.4234	0.4360	0.3986
238.161	0.4248	0.3901	0.4023	0.3654
239.138	0.3933	0.3572	0.3688	0.3326
240.114	0.3624	0.3243	0.3351	0.2994
241.091	0.3322	0.2906	0.3007	0.2651
241.579[d]	0.3020	0.2570	0.2663	0.2308

a. Vessel inner radius (clad-base metal interface)
b. Vessel ¼ T
c. Vessel ¾ T
d. Vessel outer radius

Table 7-5

Radial Distribution of Iron dpa within the Reactor Vessel
Relative to Clad-Base Metal Interface

Radius	Azimuthal Angle			
(cm)	0°	15°	30°	45°
220.091[a]	1.0000	1.0000	1.0000	1.0000
220.282	0.9918	0.9918	0.9924	0.9921
220.770	0.9639	0.9636	0.9658	0.9648
221.556	0.9121	0.9113	0.9157	0.9145
222.533	0.8438	0.8422	0.8490	0.8470
223.510	0.7757	0.7731	0.7822	0.7798
224.486	0.7109	0.7074	0.7184	0.7156
225.463[b]	0.6507	0.6463	0.6588	0.6558
226.440	0.5954	0.5900	0.6039	0.6005
227.417	0.5447	0.5385	0.5534	0.5497
228.393	0.4985	0.4916	0.5071	0.5031
229.370	0.4564	0.4488	0.4648	0.4606
230.347	0.4181	0.4099	0.4261	0.4216
231.324	0.3831	0.3743	0.3906	0.3859
232.300	0.3511	0.3418	0.3580	0.3530
233.277	0.3219	0.3120	0.3280	0.3228
234.254	0.2950	0.2847	0.3003	0.2948
235.231	0.2703	0.2596	0.2747	0.2690
236.207[c]	0.2474	0.2363	0.2508	0.2448
237.184	0.2263	0.2146	0.2285	0.2223
238.161	0.2067	0.1944	0.2076	0.2010
239.138	0.1884	0.1754	0.1878	0.1808
240.114	0.1714	0.1572	0.1688	0.1613
241.091	0.1558	0.1396	0.1504	0.1420
241.579[d]	0.1401	0.1220	0.1320	0.1227

a. Vessel inner radius (clad-base metal interface)
b. Vessel ¼ T
c. Vessel ¾ T
d. Vessel outer radius

Table 7-6

Nuclear Parameters Used for Evaluation of Neutron Sensors

Monitor Material	Reaction	Atom Fraction of Target	Approximate Response Range	Product Half-Life	Fission Yield %
Copper	$^{63}Cu(n,\alpha)^{60}Co$	0.6917	E > 5 MeV	1925.5 d	
Iron	$^{54}Fe(n,p)^{54}Mn$	0.05845	E > 2 MeV	312.12 d	
Nickel	$^{58}Ni(n,p)^{58}Co$	.6827	E > 2 MeV	70.82 d	
U-238	$^{238}U(n,f)^{137}Cs$	1.0	E > 1 MeV	30.0 y	6.021
Np-237	$^{237}Np(n,f)^{137}Cs$	1.0	E > 0.1 MeV	30.0 y	6.170
Cobalt-Al	$^{59}Co(n,\gamma)^{60}Co$	0.0015	Thermal and Resonance	1925.5 d	

Table 7-7

Monthly Thermal Power Generation for Watts Bar Unit 1
Cycles 1 to 3

Cycle 1		Cycle 2		Cycle 3	
Month	Thermal Generation MW-hr	Month	Thermal Generation MW-hr	Month	Thermal Generation MW-hr
Jan-96	9519	Oct-97	709914	Apr-99	1068631
Feb-96	49773	Nov-97	2449654	May-99	2454763
Mar-96	475248	Dec-97	2527971	Jun-99	2454685
Apr-96	999029	Jan-98	2523492	Jul-99	2536887
May-96	1713718	Feb-98	2142012	Aug-99	2526645
Jun-96	2348718	Mar-98	2180599	Sep-99	2455157
Jul-96	2523691	Apr-98	2370444	Oct-99	2540350
Aug-96	2525629	May-98	2535488	Nov-99	2454874
Sep-96	2184725	Jun-98	2445551	Dec-99	2536956
Oct-96	1114619	Jul-98	2531951	Jan-00	2536601
Nov-96	2202224	Aug-98	2486237	Feb-00	2373327
Dec-96	2523130	Sep-98	2429447	Mar-00	2536915
Jan-97	1956638	Oct-98	2470835	Apr-00	2451520
Feb-97	2147746	Nov-98	2452741	May-00	2536436
Mar-97	1645462	Dec-98	2535907	Jun-00	2455171
Apr-97	2236507	Jan-99	2280206	Jul-00	2534880
May-97	2519097	Feb-99	1519605	Aug-00	2279989
Jun-97	2237128	Mar-99	0	Sep-00	570521
Jul-97	2399891				
Aug-97	1934439				
Sep-97	262258				

Table 7-8

Measured Sensor Activities and Reaction Rates
Surveillance Capsule W

Reaction	Capsule Location	Measured Activity[a] μCi/g	Measurement Uncertainty %	Reaction Rate[b] Rps/atom
$^{63}Cu(n,\alpha)^{60}Co$	top	4.975	5.3	4.641E-17
	middle	5.265	5.3	4.912E-17
	bottom	5.223	5.3	4.872E-17
$^{54}Fe(n,p)^{54}Mn$	top	1251	5.3	4.587E-15
	middle	1308	5.3	4.797E-15
	bottom	1269	5.3	4.653E-15
$^{58}Ni(n,p)^{58}Co$	top	1664	5.3	6.320E-15
	middle	1713	5.3	6.506E-15
	bottom	1665	5.3	6.324E-15
$^{238}U(n,f)^{137}Cs$	middle	9.130	6.8	2.341E-14
$^{237}Np(n,f)^{137}Cs$	middle	124.8	5.6	3.084E-13
$^{59}Co(n,\gamma)^{60}Co$ (Cd)	top	2.740E+05	6.9	2.291E-12
	middle	2.616E+05	6.6	2.188E-12
	bottom	2.690E+05	7.2	2.249E-12
$^{59}Co(n,\gamma)^{60}Co$	top	5.483E+05	6.8	4.584E-12
	middle	5.070E+05	6.8	4.239E-12
	bottom	5.247E+05	6.7	4.387E-12
$^{59}Co(n,\gamma)^{60}Co$ ref.	top	4.803E+05	6.6	4.015E-12
	middle	4.191E+05	6.5	3.504E-12
	bottom	4.432E+05	6.3	3.705E-12

a. Units are μCi of product nuclide per gram of target nuclide. The U-238(n,f)Cs-137 measurement has been corrected to account for an estimated 0.15 fraction of the activity from U-235 and built-in Pu-239 fission.

b. The reaction rates are normalized to flux levels for Cycle 3.

Table 7-9

Comparison of Measured and Calculated Reaction Rates for Watts Bar Unit 1 Surveillance Capsules

Surveillance Capsule U

Reaction	Calculated Rps/atom	Measured Rps/atom[a]	Calc/Meas
$^{63}Cu(n,\alpha)^{60}Co$	4.75E-17	5.80E-17	0.819
$^{54}Fe(n,p)^{54}Mn$	5.73E-15	6.34E-15	0.903
$^{58}Ni(n,p)^{58}Co$	8.23E-15	8.79E-15	0.937
$^{238}U(n,f)^{137}Cs$	3.44E-14	4.75E-14	0.725
$^{237}Np(n,f)^{137}Cs$	3.93E-13	4.53E-13	0.868
Average C/M for above fast reactions:			0.850
$^{59}Co(n,\gamma)^{60}Co$ (Cd)	2.42E-12	3.45E-12	0.700
$^{59}Co(n,\gamma)^{60}Co$	3.08E-12	6.41E-12	0.481

a. Data from Reference [17]. Surveillance capsule U was withdrawn at the end of cycle 1.

Surveillance Capsule W

Reaction	Calculated Rps/atom	Measured Rps/atom	Calc/Meas
$^{63}Cu(n,\alpha)^{60}Co$	3.62E-17	4.81E-17	0.752
$^{54}Fe(n,p)^{54}Mn$	4.10E-15	4.68E-15	0.876
$^{58}Ni(n,p)^{58}Co$	5.83E-15	6.38E-15	0.913
$^{238}U(n,f)^{137}Cs$	2.35E-14	2.34E-14	1.003
$^{237}Np(n,f)^{137}Cs$	2.51E-13	3.08E-13	0.815
Average C/M for above fast reactions:			0.872
$^{59}Co(n,\gamma)^{60}Co$ (Cd)	1.49E-12	2.24E-12	0.665
$^{59}Co(n,\gamma)^{60}Co$	1.94E-12	4.07E-12	0.476

Table 7-10

Calculated Average Neutron Energy Spectrum at the Center of Surveillance Capsule W

Energy Group	Upper Group Energy (MeV)	Neutron Flux (n/cm^2-s)	Energy Group	Upper Group Energy (MeV)	Neutron Flux (n/cm^2-s)
1	1.733E+01	9.110E+06	25	2.972E-01	5.215E+10
2	1.419E+01	2.910E+07	26	1.832E-01	5.562E+10
3	1.221E+01	1.287E+08	27	1.111E-01	4.134E+10
4	1.000E+01	2.570E+08	28	6.738E-02	2.708E+10
5	8.607E+00	4.549E+08	29	4.087E-02	8.054E+09
6	7.408E+00	1.096E+09	30	3.183E-02	4.448E+09
7	6.065E+00	1.712E+09	31	2.606E-02	9.936E+09
8	4.966E+00	3.680E+09	32	2.418E-02	8.448E+09
9	3.679E+00	3.215E+09	33	2.188E-02	9.194E+09
10	3.012E+00	2.630E+09	34	1.503E-02	1.555E+10
11	2.725E+00	3.189E+09	35	7.102E-03	2.440E+10
12	2.466E+00	1.610E+09	36	3.355E-03	2.444E+10
13	2.365E+00	4.506E+08	37	1.585E-03	3.398E+10
14	2.346E+00	2.367E+09	38	4.540E-04	1.726E+10
15	2.231E+00	7.117E+09	39	2.145E-04	1.870E+10
16	1.921E+00	9.165E+09	40	1.013E-04	2.447E+10
17	1.653E+00	1.521E+10	41	3.727E-05	2.734E+10
18	1.353E+00	3.722E+10	42	1.068E-05	1.504E+10
19	1.003E+00	2.681E+10	43	5.044E-06	1.603E+10
20	8.209E-01	1.352E+10	44	1.855E-06	9.612E+09
21	7.427E-01	4.988E+10	45	8.764E-07	5.464E+09
22	6.081E-01	3.991E+10	46	4.140E-07	5.486E+09
23	4.979E-01	5.142E+10	47	1.000E-07	1.737E+10
24	3.688E-01	5.059E+10			

Table 7-11

Calculated and Best-Estimate Exposure of Watts Bar Unit 1 Surveillance Capsules U and W

Capsule U

Parameter	Calculated Value	Best-Estimate Value
N (E > 1.0 MeV) n/cm^2	4.393E+18	5.167E+18
N (E > 0.1 MeV) n/cm^2	2.301E+19	2.706E+19
Iron dpa	9.446E-03	1.111E-02

Capsule W

Parameter	Calculated Value	Best-Estimate Value
N (E > 1.0 MeV) n/cm^2	1.072E+19	1.230E+19
N (E > 0.1 MeV) n/cm^2	5.224E+19	5.993E+19
Iron dpa	2.205E-02	2.529E-02

Table 7-12

Best-Estimate Neutron Exposure Projections at the Vessel IR at the Axial Core Midplane

Exposure at 3.81 EFPY[a] (End of Cycle 3)				
angle	0°	15°	30°	45°
N (E > 1.0 MeV) n/cm^2	1.224E+18	1.822E+18	1.937E+18	2.354E+18
N (E > 0.1 MeV) n/cm^2	2.561E+18	3.835E+18	4.404E+18	5.924E+18
Iron dpa	1.902E-03	2.803E-03	3.017E-03	3.726E-03

a. Effective full-power years at 3459 MWth.

Exposure projected to 16 EFPY				
angle	0°	15°	30°	45°
N (E > 1.0 MeV) n/cm^2	4.732E+18	6.965E+18	7.473E+18	8.912E+18
N (E > 0.1 MeV) n/cm^2	9.890E+18	1.464E+19	1.694E+19	2.236E+19
Iron dpa	7.359E-03	1.072E-02	1.164E-02	1.411E-02

Exposure at 32 EFPY				
angle	0°	15°	30°	45°
N (E > 1.0 MeV) n/cm^2	9.339E+18	1.372E+19	1.474E+19	1.752E+19
N (E > 0.1 MeV) n/cm^2	1.951E+19	2.882E+19	3.340E+19	4.394E+19
Iron dpa	1.452E-02	2.112E-02	2.297E-02	2.774E-02

Table 7-13

Best-Estimate Neutron Exposure Projections at the Vessel IR
at the Maximum Axial Point

Exposure at 3.81 EFPY[a] (End of Cycle 3)				
angle	0°	15°	30°	45°
N (E > 1.0 MeV) n/cm^2	1.254E+18	1.866E+18	1.985E+18	2.409E+18
N (E > 0.1 MeV) n/cm^2	2.616E+18	3.914E+18	4.497E+18	6.041E+18
Iron dpa	1.946E-03	2.866E-03	3.087E-03	3.808E-03

a. Effective full-power years at 3459 MWth.

Exposure projected to 16 EFPY				
angle	0°	15°	30°	45°
N (E > 1.0 MeV) n/cm^2	4.962E+18	7.300E+18	7.833E+18	9.338E+18
N (E > 0.1 MeV) n/cm^2	1.034E+19	1.529E+19	1.770E+19	2.335E+19
Iron dpa	7.704E-03	1.122E-02	1.219E-02	1.476E-02

Exposure at 32 EFPY				
angle	0°	15°	30°	45°
N (E > 1.0 MeV) n/cm^2	9.831E+18	1.443E+19	1.551E+19	1.844E+19
N (E > 0.1 MeV) n/cm^2	2.047E+19	3.022E+19	3.502E+19	4.607E+19
Iron dpa	1.526E-02	2.219E-02	2.413E-02	2.914E-02

Table 7-14

Best-Estimate Neutron Exposure Projections at the Vessel IR to the Circumferential Weld at 9.6 inches above Axial Core Midplane

Exposure at 3.81 EFPY[a] (End of Cycle 3)				
angle	0°	15°	30°	45°
N (E > 1.0 MeV) n/cm^2	1.212E+18	1.805E+18	1.918E+18	2.331E+18
N (E > 0.1 MeV) n/cm^2	2.535E+18	3.796E+18	4.359E+18	5.863E+18
Iron dpa	1.883E-03	2.775E-03	2.987E-03	3.689E-03

a. Effective full-power years at 3459 MWth.

Exposure projected to 16 EFPY				
angle	0°	15°	30°	45°
N (E > 1.0 MeV) n/cm^2	4.698E+18	6.913E+18	7.418E+18	8.846E+18
N (E > 0.1 MeV) n/cm^2	9.813E+18	1.452E+19	1.681E+19	2.218E+19
Iron dpa	7.304E-03	1.064E-02	1.155E-02	1.400E-02

Exposure at 32 EFPY				
angle	0°	15°	30°	45°
N (E > 1.0 MeV) n/cm^2	9.275E+18	1.362E+19	1.464E+19	1.740E+19
N (E > 0.1 MeV) n/cm^2	1.937E+19	2.861E+19	3.315E+19	4.361E+19
Iron dpa	1.442E-02	2.097E-02	2.280E-02	2.754E-02

Table 7-15

Best-Estimate Projected Neutron Fluence (E > 1.0 MeV) Within the Watts Bar Unit 1 Reactor Vessel at the Maximum Axial Point (n/cm^2)

Fluence Based on E > 1.0 MeV Slope

Fluence Projected to 16 EFPY				
angle	0°	15°	30°	45°
Surface (Vessel IR)	4.962E+18	7.300E+18	7.833E+18	9.338E+18
¼ T	2.865E+18	4.193E+18	4.495E+18	5.270E+18
¾ T	6.870E+17	9.845E+17	1.058E+18	1.199E+18

Fluence Projected to 32 EFPY				
angle	0°	15°	30°	45°
Surface (Vessel IR)	9.831E+18	1.443E+19	1.551E+19	1.844E+19
¼ T	5.677E+18	8.292E+18	8.902E+18	1.041E+19
¾ T	1.361E+18	1.947E+18	2.096E+18	2.368E+18

Fluence Based on Calculated dpa Slope[a]

Fluence Projected to 16 EFPY				
angle	0°	15°	30°	45°
Surface (Vessel IR)	4.962E+18	7.300E+18	7.833E+18	9.338E+18
¼ T	3.216E+18	4.701E+18	5.134E+18	6.100E+18
¾ T	1.204E+18	1.695E+18	1.921E+18	2.246E+18

Fluence Projected to 32 EFPY				
angle	0°	15°	30°	45°
Surface (Vessel IR)	9.831E+18	1.443E+19	1.551E+19	1.844E+19
¼ T	6.372E+18	9.295E+18	1.017E+19	1.204E+19
¾ T	2.385E+18	3.352E+18	3.803E+18	4.436E+18

a. Best-estimate fluence at the vessel inner radius times the ratio of dpa at the vessel interior points to the dpa at the vessel inner radius.

Table 7-15 Continued

Best-Estimate Projected Neutron Fluence (E > 1.0 MeV) Within the Watts Bar Unit 1 Reactor Vessel at the Maximum Axial Point (n/cm^2)

Fluence Based on RG1.99(Rev 2) Slope Formula[a]

Fluence Projected to 16 EFPY				
angle	0°	15°	30°	45°
Surface (Vessel IR)	4.962E+18	7.300E+18	7.833E+18	9.338E+18
¼ T	2.987E+18	4.394E+18	4.715E+18	5.621E+18
¾ T	1.082E+18	1.592E+18	1.708E+18	2.037E+18

Fluence Projected to 32 EFPY				
angle	0°	15°	30°	45°
Surface (Vessel IR)	9.831E+18	1.443E+19	1.551E+19	1.844E+19
¼ T	5.918E+18	8.688E+18	9.338E+18	1.110E+19
¾ T	2.144E+18	3.148E+18	3.383E+18	4.021E+18

a. Best-estimate fluence at the vessel inner radius times exp(-0.24*x) where x is the distance into the vessel in inches.

Table 7-16

Updated Lead Factors for Watts Bar Unit 1 Surveillance Capsules

Capsule	Status	Lead Factor
U	Withdrawn after cycle 1	5.39
V	Irradiation continuing	4.64
W	Withdrawn after cycle 3	5.21
X	Irradiation continuing	5.37
Y	Irradiation continuing	4.64
Z	Irradiation continuing	5.21

Table 7-17

Watts Bar Unit 1 Fluence Uncertainty[a]

Uncertainty Contributor	Capsule percent	Vessel IR percent	Vessel 1/4T percent	Vessel 3/4T percent
Source normalization and spectrum	1.5	1.5	1.5	1.5
Heat Balance	2.0	2.0	2.0	2.0
Steel cross section, density	5.6	5.9	8.3	14.3
Core density	2.0	2.1	2.1	2.1
Core water density	1.3	1.2	1.2	1.2
Barrel thickness	0.4	0.6	0.6	0.6
Downcomer water	1.0	2.1	2.1	2.1
Bypass water	1.4	1.2	1.2	1.2
Radial source	3.0	3.0	3.0	3.0
Pin power shape	7.5	7.5	7.5	7.5
Flux history	4.0	4.0	4.0	4.0
Methods	5.8	5.8	5.8	5.8
Capsule location	1.8	0.0	0.0	0.0
Capsule model	4.6	0.0	0.0	0.0
Vessel IR	0.0	3.5	3.5	3.4
TOTAL	13.6	13.4	14.6	18.7

a. Uncertainty in fluence E > 1.0 MeV at the end of cycle 3 (5.81 efpy)

8.0 SURVEILLANCE CAPSULE REMOVAL SCHEDULE

The following surveillance capsule removal schedule meets the requirements of ASTM E185-82 and is recommended for future capsules to be removed from the Watts Bar Unit 1 reactor vessel. This recommended removal schedule is applicable to 32 EFPY of operation.

TABLE 8-1

Watts Bar Unit 1 Reactor Vessel Surveillance Capsule Withdrawal Schedule

Capsule	Location	Lead Factor[a]	Removal Time (EFPY)[b]	Fluence (n/cm^2, E > 1.0 MeV)[a]
U	56°	5.39	1.20	5.167×10^{18} (c)
W	124°	5.21	3.80	1.230×10^{19} (d)
X	236°	5.37	5.98	1.844×10^{19} (e)
Z	304°	5.21	9.25	2.766×10^{19} (f)
V[g]	58.5°	4.64	Standby	---
Y[g]	238.5°	4.64	Standby	---

Notes:

a. Updated in Capsule W dosimetry analysis, See Section 7 of this report.

b. Effective Full Power Years (EFPY) from plant startup.

c. Plant specific evaluation

d. This fluence is the plant specific evaluation and is the approximate fluence at 1/4T at end of license (32 EFPY).

e. This fluence is equal to the calculated peak reactor vessel surface fluence at EOL (32 EFPY).

f. This fluence is not less than once or greater than twice the peak EOL fluence, and is approximately equal to the peak vessel fluence at 48 EFPY.

g. These capsules will reach a fluence of approximately 2.8×10^{19} (48 EFPY Peak Fluence) at approximately 10.7 EFPY.

9.0 REFERENCES

1. Regulatory Guide 1.99, Revision 2, Radiation Embrittlement of Reactor Vessel Materials, U.S. Nuclear Regulatory Commission, May 1988.

2. Code of Federal Regulations, 10CFR50, Appendix G, Fracture Toughness Requirements, and Appendix H, Reactor Vessel Material Surveillance Program Requirements, U.S. Nuclear Regulatory Commission, Washington, D.C.

3. WCAP-9298, "Tennessee Valley Authority Watts Bar Unit 1 Reactor Vessel Radiation Surveillance Program", P.A. Peter, August 1995.

4. Section XI of the ASME Boiler and Pressure Vessel Code, Appendix G, Fracture Toughness Criteria for Protection Against Failure.

5. ASTM E208, Standard Test Method for Conducting Drop-Weight Test to Determine Nil-Ductility Transition Temperature of Ferritic Steels, in ASTM Standards, Section 3, American Society for Testing and Materials, Philadelphia, PA.

6. ASTM E185-82, Standard Practice for Conducting Surveillance Tests for Light-Water Cooled Nuclear Power Reactor Vessels, E706 (IF), in ASTM Standards, Section 3, American Society for Testing and Materials, Philadelphia, PA, 1993.

7. ASTM E23-93, Standard Test Methods for Notched Bar Impact Testing of Metallic Materials, in ASTM Standards, Section 3, American Society for Testing and Materials, Philadelphia, PA, 1993.

8. ASTM A370-92, Standard Test Methods and Definitions for Mechanical Testing of Steel Products, in ASTM Standards, Section 3, American Society for Testing and Materials, Philadelphia, PA 1993.

9. ASTM E8-94, Standard Test Methods for Tension Testing of Metallic Materials, in ASTM Standards, Section 3, American Society for Testing and Materials, Philadelphia, PA 1994.

10. ASTM E21-92, Standard Test Methods for Elevated Temperature Tension Tests of Metallic Materials, in ASTM Standards, Section 3, American Society for Testing and Materials, Philadelphia, PA 1993.

11. ASTM E83-93, Standard Practice for Verification and Classification of Extensometers, in ASTM Standards, Section 3, American Society for Testing and Materials, Philadelphia, PA 1993.

12. WCAP-15046, "Analysis of Capsule U from the Tennessee Valley Authority Watts Bar Unit 1 Reactor Vessel Radiation Surveillance Program", T. J. Laubham, G. K. Roberts, J. F. Williams, June 1998.

13. Regulatory Guide 1.190, Calculational and Dosimetry Methods for Determining Pressure Vessel Neutron Fluence, U. S. Nuclear Regulatory Commission, March 2001.

14. ASTM Designation E693-94, Standard Practice for Characterizing Neutron Exposures in Iron and Low Alloy Steels in Terms of Displacements per Atom (dpa), in ASTM Standards, Section 12, American Society for Testing and Materials, Philadelphia, PA, 2000.

15. Regulatory Guide 1.99, Revision 2, Radiation Embrittlement of Reactor Vessel Materials, U. S. Nuclear Regulatory Commission, May 1988.

16. FAX from D. Briggs (TVA) to M. P. Manahan, Sr. (MPM Technologies, Inc.), "Neutron Transport Data for Watts Bar Unit 1 Transport Calculations," June 27, 2001.

17. Laubham, T. J., Roberts, G. K., and Williams, J. F., WCAP-15046, "Analysis of Capsule U from the Tennessee Valley Authority Watts Bar Unit 1 Reactor Vessel Radiation Surveillance Program," Westinghouse Electric Company, P. O. Box 355, Pittsburgh, PA 15230, June 1998.

18. RSICC Computer Code Collection, CCC-543, TORT-DORT-PC, Two- and Three-Dimensional Discrete Ordinates Transport Version 2.7.3, available from the Radiation Safety Information Computational Center, Oak Ridge National Laboratory, Oak Ridge, TN, June 1996.

19. RSICC Data Library Collection, DLC-185, BUGLE-96, Coupled 47 Neutron, 20 Gamma Ray Group Cross Section Library Derived from ENDF/B-VI for LWR Shielding and Pressure Vessel Dosimetry Applications, available from the Radiation Safety Information Computational Center, Oak Ridge National Laboratory, Oak Ridge, TN, March 1996.

20. ASTM Designation E482-89, *Standard Guide for Application of Neutron Transport Methods for Reactor Vessel Surveillance*, in ASTM Standards, Section 12, American Society for Testing and Materials, Philadelphia, PA, 2000.

21. Letter L36 010514 800, J. F. Burrow(TVA) to R. D. Briggs(TVA), "Neutron Transport Data for Analysis of Surveillance Capsule Fluence," May 11, 2001.

22. RSICC Peripheral Shielding Routine Code Collection, PSR-277, LEPRICON, PWR Pressure Vessel Surveillance Dosimetry Analysis System, available from the Radiation Safety Information Computational Center, Oak Ridge National Laboratory, Oak Ridge, TN, June 1995.

23. Letter, J. B. Sun to M. P. Manahan, Sr., "Physics Data for Analysis of Cavity Dosimetry from Turkey Point Unit 3", NF-97-336, August 26, 1997.

24. RSICC Computer Code Collection, CCC-371, "ORIGEN 2.1, Isotope Generation and Depletion Code Matrix Exponential Method," available from the Radiation Safety Information Computational Center, Oak Ridge National Laboratory, Oak Ridge, TN, May 1999.

25. Remec, I. and Kam, F. B. K., "H. B. Robinson-2 Pressure Vessel Benchmark," NUREG/CR-6453, Oak Ridge National Laboratory, Oak Ridge, TN, February 1998.

26. ASTM Designation E853-87, *Standard Practice for Analysis and Interpretation of Light-Water Reactor Surveillance Results*, in ASTM Standards, Section 12, American Society for Testing and Materials, Philadelphia, PA, 2000.

27. ASTM Designation E1005-97, *Standard Test Method for Application and Analysis of Radiometric Monitors for Reactor Vessel Surveillance*, in ASTM Standards, Section 12, American Society for Testing and Materials, Philadelphia, PA, 2000.

28. ASTM Designation E261-98, *Standard Practice for Determining Neutron Fluence, Fluence Rate, and Spectra by Radioactivation Techniques*, in ASTM Standards, Section 12, American Society for Testing and Materials, Philadelphia, PA, 2000.

29. ASTM Designation E262-97, *Standard Test Method for Determining Thermal Neutron Reaction and Fluence Rates by Radioactivation Techniques*, in ASTM Standards, Section 12, American Society for Testing and Materials, Philadelphia, PA, 2000.

30. ASTM Designation E263-00, *Standard Test Method for Determining Fast-Neutron Reaction Rates by Radioactivation of Iron*, in ASTM Standards, Section 12, American Society for Testing and Materials, Philadelphia, PA, 2000.

31. ASTM Designation E264-92, *Standard Test Method for Determining Fast-Neutron Reaction Rates by Radioactivation of Nickel*, in ASTM Standards, Section 12, American Society for Testing and Materials, Philadelphia, PA, 2000.

32. ASTM Designation E523-92, *Standard Test Method for Determining Fast-Neutron Reaction Rates by Radioactivation of Copper*, in ASTM Standards, Section 12, American Society for Testing and Materials, Philadelphia, PA, 2000.

33. ASTM Designation E704-96, *Standard Test Method for Measuring Reaction Rates by Radioactivation of Uranium-238*, in ASTM Standards, Section 12, American Society for Testing and Materials, Philadelphia, PA, 2000.

34. ASTM Designation E705-96, *Standard Test Method for Measuring Reaction Rates by Radioactivation of Neptunium-237*, in ASTM Standards, Section 12, American Society for Testing and Materials, Philadelphia, PA, 2000.

35. ASTM Designation E560-84, *Standard Practice for Extrapolating Reactor Vessel Surveillance Dosimetry Results*, in ASTM Standards, Section 12, American Society for Testing and Materials, Philadelphia, PA, 2000.

36. McElroy, W.N., Ed., "LWR-PV-SDIP: PCA Experiments and Blind Test", NUREG/CR-1861, 1981.

37. Lippincott, E.P., "Consumers Power Company Palisades Nuclear Plant Reactor Vessel Fluence Analysis", WCAP-13348, May 1992.

38. Maerker, R.E., et.al., "Application of LEPRICON Methodology to LWR Pressure Vessel Dosimetry", *Reactor Dosimetry: Methods, Applications, and Standardization, ASTM STP 1001*, 1989, pp 405-414.

39. Anderson, S.L., "Westinghouse Fast Neutron Exposure Methodology for Pressure Vessel Fluence Determination and Dosimetry Evaluation", WCAP-13362, May 1992.

40. Lippincott, E.P., et.al., "Evaluation of Surveillance Capsule and Reactor Cavity Dosimetry from H. B. Robinson Unit 2, Cycle 9", WCAP-11104, NUREG/CR-4576, February 1987.

41. Haghighat, A. and Veerasingam, "Comparison of the Different Cross Section Libraries used for Reactor Pressure Vessel Fluence Calculations", *Trans. Amer. Nuclear Society*, 64, p. 357, 1991.

42. WCAP-13587, Rev. 1, "Reactor Vessel Upper Shelf Energy Bounding Evaluation for Westinghouse Pressurized Water Reactors", M.J. Malone, et al., September 1993.

APPENDIX A

RADIOGRAPH OF THERMAL MONITORS
WATTS BAR UNIT 1, CAPSULE W

BABCOCK · WILCOX
LYNCHBURG RESEARCH CENTER
RA11 1032601

TVA

TOP

BOT

MID

APPENDIX B

CHARPY IMPACT TEST RESULTS
WATTS BAR UNIT 1, CAPSULE W

CAPSULE-W TANGENTIAL

CVGRAPH 5.0 Hyperbolic Tangent Curve Printed on 09/10/2001 09:06 AM
Page 1
Coefficients of Curve 1
A = 49.95 B = 47.75 C = 91. T0 = 94.8 D = 0.00E+00
Equation is A + B * [Tanh((T-To)/(C+DT))]
Upper Shelf Energy=97.7(Fixed) Lower Shelf Energy=2.2(Fixed)
Temp@30 ft-lbs=54.4 Deg F Temp@50 ft-lbs=94.9 Deg F
Plant: Watts Bar 1 Material: SA508CL2 Heat: 527536(R 05)
Orientation: LT Capsule: W Fluence: 1.23E+19 n/cm^2

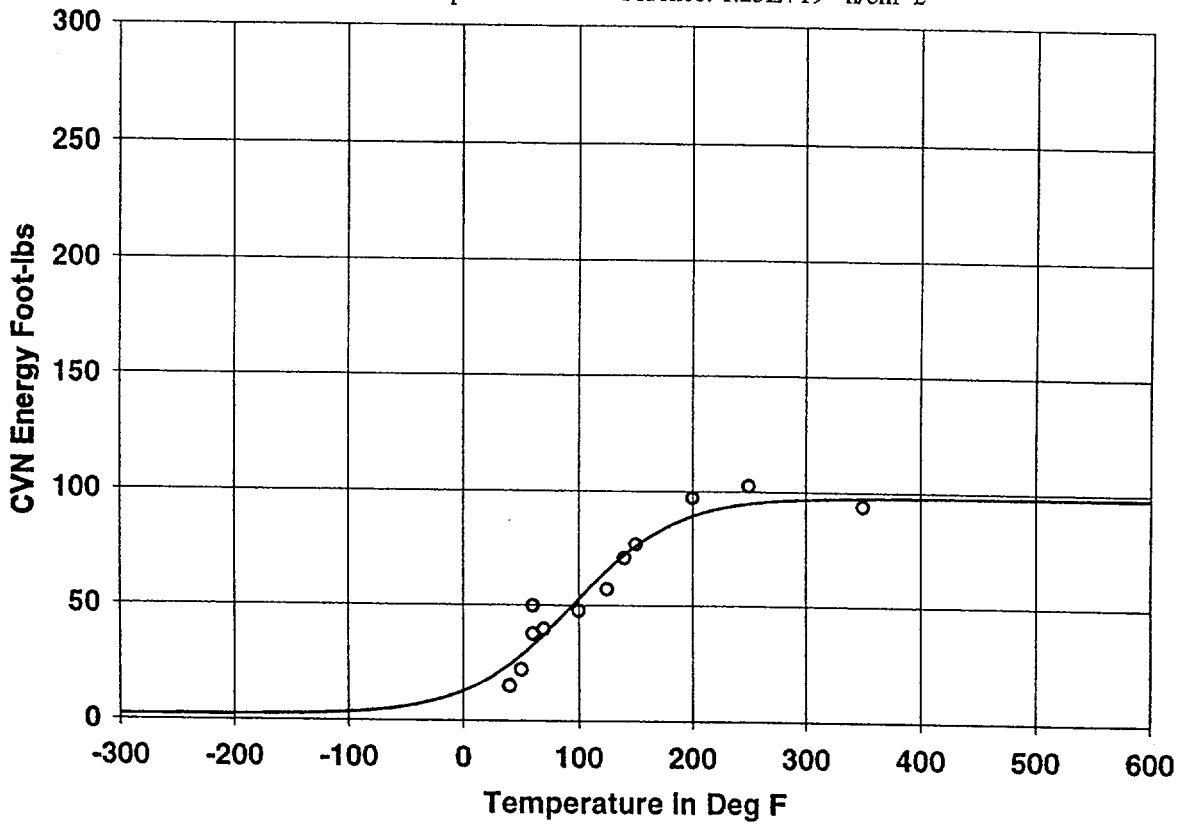

Charpy V-Notch Data

Temperature	Input CVN	Computed CVN	Differential
40.00	15.00	24.23	-9.23
50.00	22.00	28.17	-6.17
60.00	37.50	32.53	4.97
60.00	49.50	32.53	16.97
70.00	39.50	37.25	2.25
100.00	47.50	52.68	-5.18
125.00	57.00	65.24	-8.24
140.00	70.50	71.89	-1.39
150.00	76.50	75.82	.68

CAPSULE-W TANGENTIAL

Page 2
Plant: Watts Bar 1 Material: SA508CL2 Heat: 527536(R 05)
Orientation: LT Capsule: W Fluence: 1.23E+19 n/cm^2

Charpy V-Notch Data

Temperature	Input CVN	Computed CVN	Differential
200.00	97.00	89.09	7.91
250.00	102.50	94.65	7.85
350.00	93.50	97.35	-3.85

Correlation Coefficient = .964

CAPSULE-W TANGENTIAL

CVGRAPH 5.0 Hyperbolic Tangent Curve Printed on 09/10/2001 09:08 AM
Page 1
Coefficients of Curve 1
A = 50. B = 50. C = 75.89 T0 = 102.25 D = 0.00E+00
Equation is A + B * [Tanh((T-To)/(C+DT))]
Temperature at 50% Shear = 102.2
Plant: Watts Bar 1 Material: SA508CL2 Heat: 527536(R 05)
Orientation: LT Capsule: W Fluence: 1.23E+19 n/cm^2

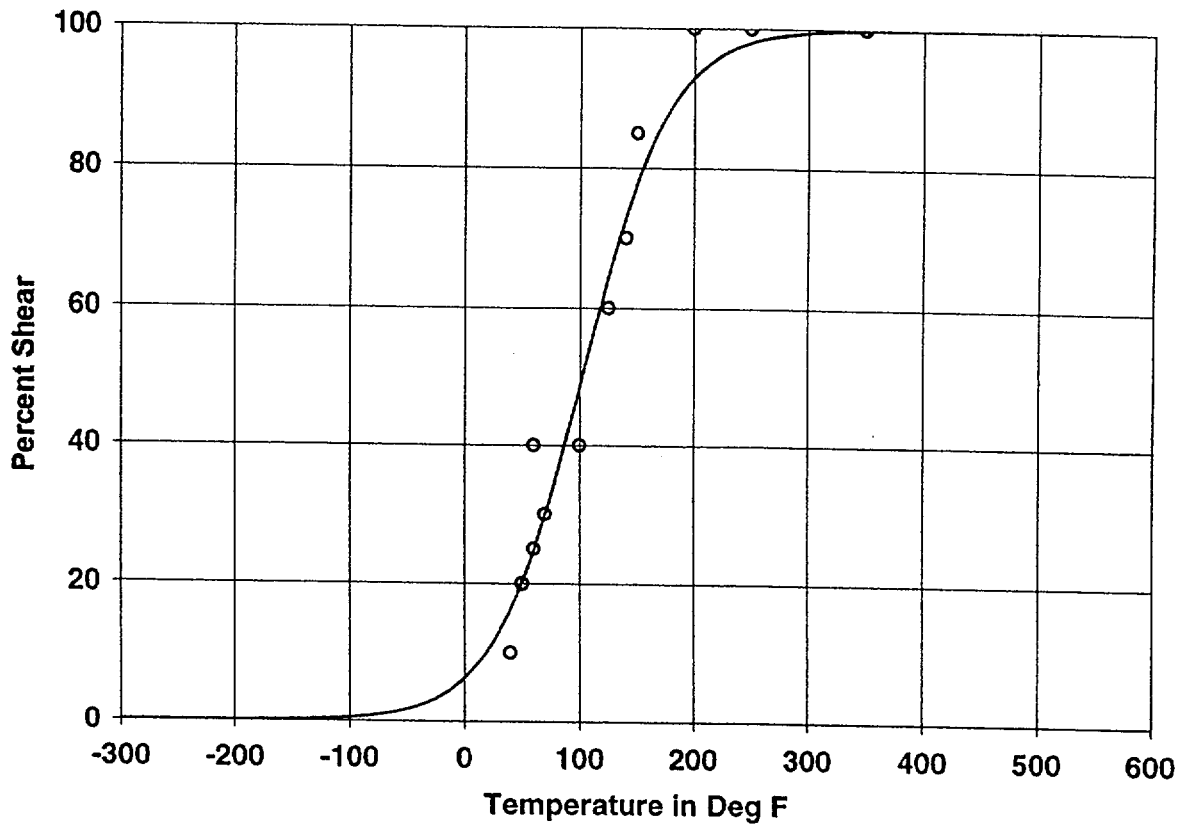

Charpy V-Notch Data

Temperature	Input Percent Shear	Computed Percent Shear	Differential
40.00	10.00	16.24	-6.24
50.00	20.00	20.15	-.15
60.00	25.00	24.73	.27
60.00	40.00	24.73	15.27
70.00	30.00	29.95	.05
100.00	40.00	48.52	-8.52
125.00	60.00	64.56	-4.56
140.00	70.00	73.01	-3.01
150.00	85.00	77.88	7.12

CAPSULE-W TANGENTIAL

Page 2
Plant: Watts Bar 1 Material: SA508CL2 Heat: 527536(R 05)
Orientation: LT Capsule: W Fluence: 1.23E+19 n/cm^2

Charpy V-Notch Data

Temperature	Input Percent Shear	Computed Percent Shear	Differential
200.00	100.00	92.93	7.07
250.00	100.00	98.00	2.00
350.00	100.00	99.85	.15

Correlation Coefficient = .981

CAPSULE-W TANGENTIAL

CVGRAPH 5.0 Hyperbolic Tangent Curve Printed on 09/10/2001 09:12 AM
Page 1
Coefficients of Curve 1
A = 41.32 B = 41.32 C = 99.72 T0 = 99.66 D = 0.00E+00
Equation is A + B * [Tanh((T-To)/(C+DT))]
Upper Shelf L.E.=82.6 Lower Shelf L.E.=.0(Fixed)
Temp.@L.E. 35 mils=84.3 Deg F
Plant: Watts Bar 1 Material: SA508CL2 Heat: 527536(R 05)
Orientation: LT Capsule: W Fluence: 1.23E+19 n/cm^2

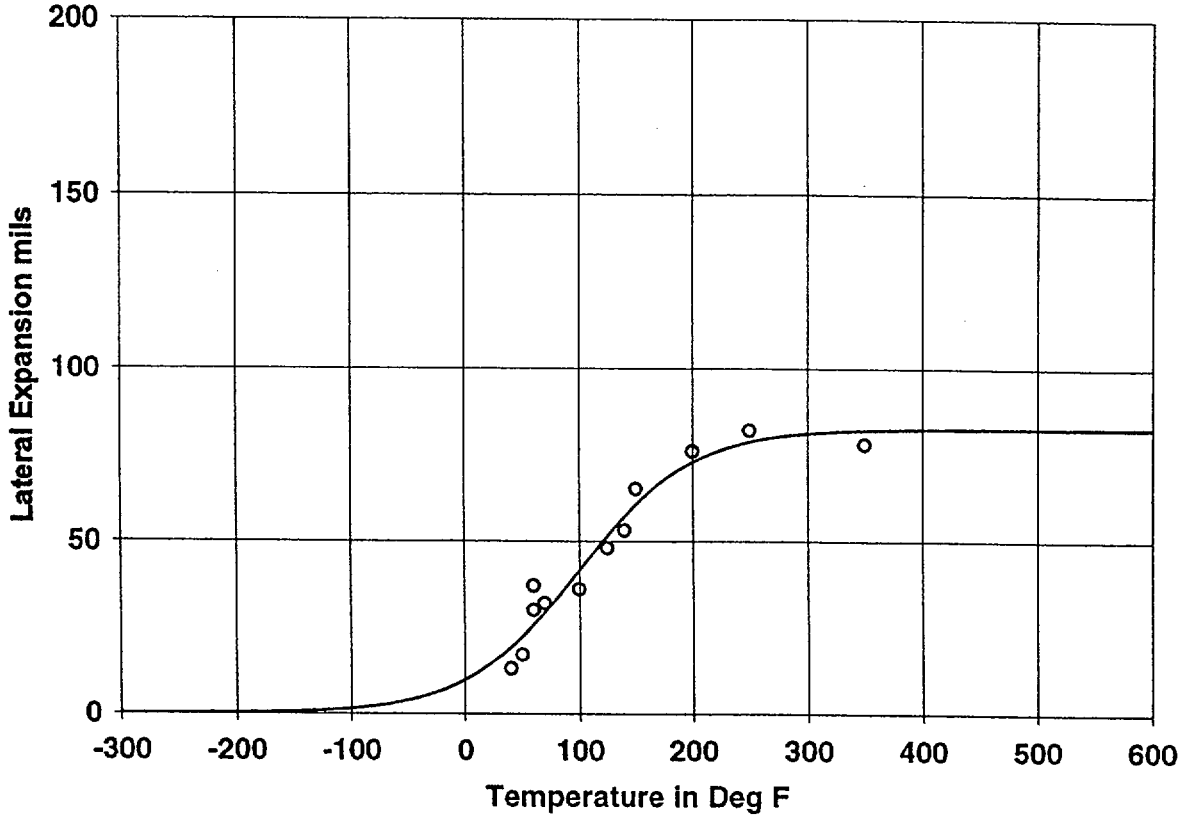

Charpy V-Notch Data

Temperature	Input L.E.	Computed L.E.	Differential
40.00	13.00	19.18	-6.18
50.00	17.00	22.29	-5.29
60.00	30.00	25.70	4.30
60.00	37.00	25.70	11.30
70.00	32.00	29.38	2.62
100.00	36.00	41.46	-5.46
125.00	48.00	51.60	-3.60
140.00	53.00	57.18	-4.18
150.00	65.00	60.58	4.42

CAPSULE-W TANGENTIAL

Page 2
Plant: Watts Bar 1 Material: SA508CL2 Heat: 527536(R 05)
Orientation: LT Capsule: W Fluence: 1.23E+19 n/cm^2

Charpy V-Notch Data

Temperature	Input L.E.	Computed L.E.	Differential
200.00	76.00	72.90	3.10
250.00	82.00	78.78	3.22
350.00	78.00	82.11	-4.11

Correlation Coefficient = .972

CAPSULE-W AXIAL

CVGRAPH 5.0 Hyperbolic Tangent Curve Printed on 09/10/2001 08:59 AM
Page 1
Coefficients of Curve 1
A = 31.2 B = 29. C = 100.35 T0 = 128.35 D = 0.00E+00
Equation is A + B * [Tanh((T-To)/(C+DT))]
Upper Shelf Energy=60.2(Fixed) Lower Shelf Energy=2.2(Fixed)
Temp@30 ft-lbs=124.2 Deg F Temp@50 ft-lbs=205.9 Deg F
Plant: Watts Bar 1 Material: SA508CL2 Heat: 527536(R 05)
Orientation: TL Capsule: W Fluence: 1.23E+19 n/cm^2

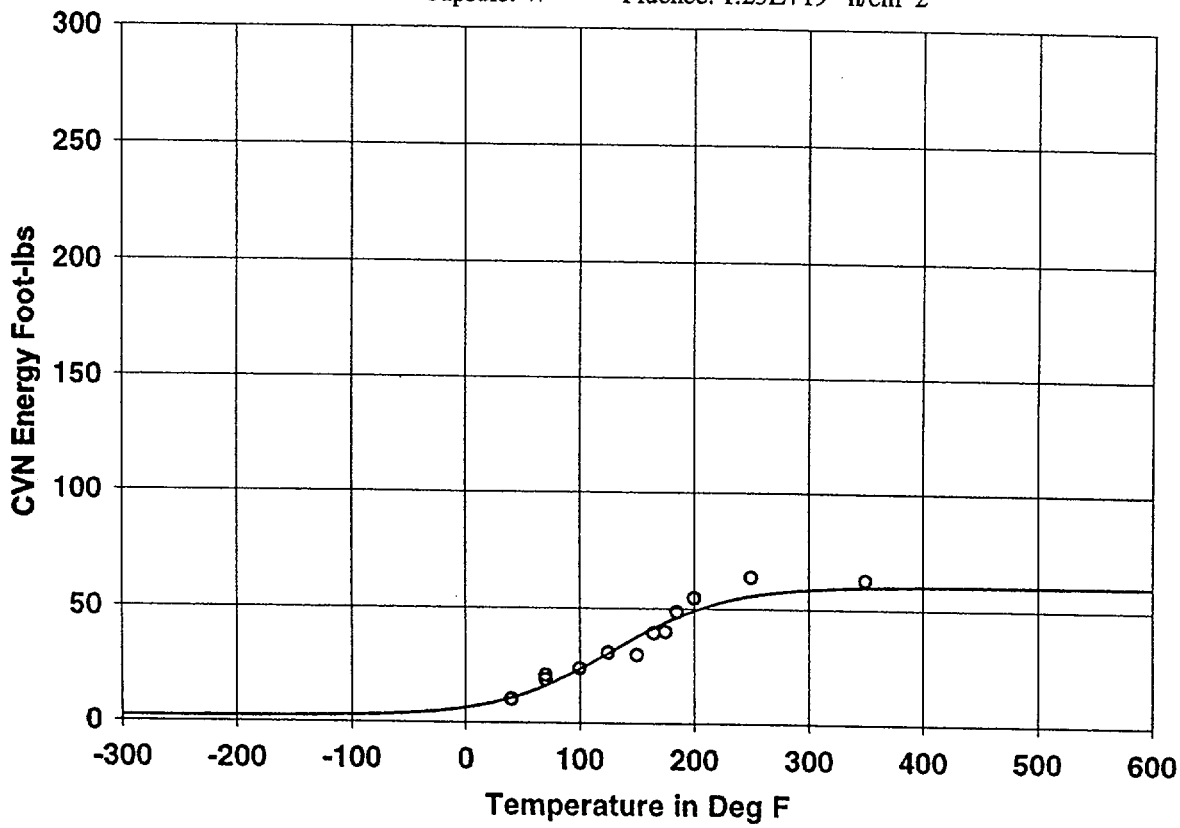

Charpy V-Notch Data

Temperature	Input CVN	Computed CVN	Differential
40.00	10.00	10.71	-.71
70.00	18.50	16.01	2.49
70.00	20.50	16.01	4.49
100.00	23.50	23.22	.28
125.00	30.50	30.23	.27
150.00	29.50	37.36	-7.86
165.00	39.00	41.34	-2.34
175.00	39.50	43.79	-4.29
185.00	48.50	46.03	2.47

CAPSULE-W AXIAL

Page 2
Plant: Watts Bar 1 Material: SA508CL2 Heat: 527536(R 05)
Orientation: TL Capsule: W Fluence: 1.23E+19 n/cm^2

Charpy V-Notch Data

Temperature	Input CVN	Computed CVN	Differential
200.00	54.50	48.98	5.52
250.00	63.50	55.48	8.02
350.00	62.50	59.51	2.99

Correlation Coefficient = .970

CAPSULE-W AXIAL

CVGRAPH 5.0 Hyperbolic Tangent Curve Printed on 09/10/2001 08:58 AM
Page 1
Coefficients of Curve 1
A = 50. B = 50. C = 66.93 T0 = 149.08 D = 0.00E+00
Equation is A + B * [Tanh((T-To)/(C+DT))]
Temperature at 50% Shear = 149.1
Plant: Watts Bar 1 Material: SA508CL2 Heat: 527536(R 05)
Orientation: TL Capsule: W Fluence: 1.23E+19 n/cm^2

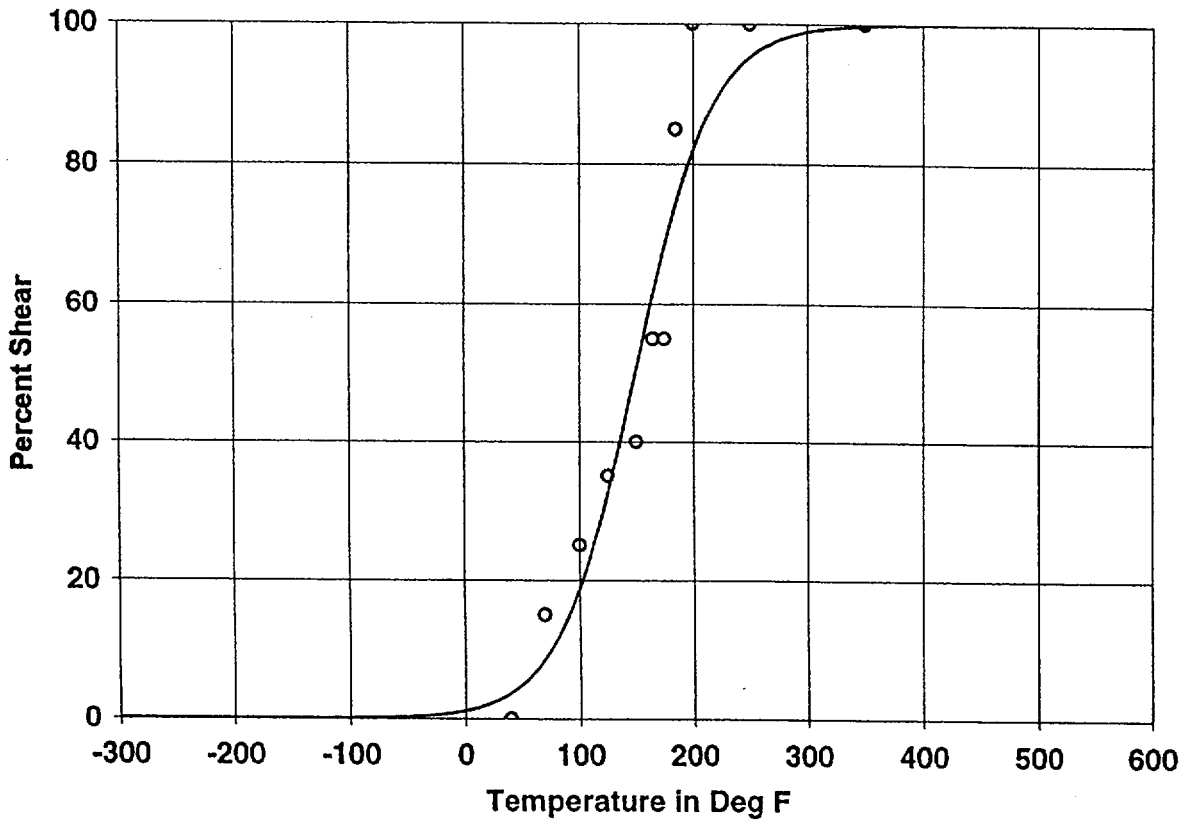

Charpy V-Notch Data

Temperature	Input Percent Shear	Computed Percent Shear	Differential
40.00	.00	3.70	-3.70
70.00	15.00	8.60	6.40
70.00	15.00	8.60	6.40
100.00	25.00	18.75	6.25
125.00	35.00	32.75	2.25
150.00	40.00	50.69	-10.69
165.00	55.00	61.68	-6.68
175.00	55.00	68.45	-13.45
185.00	85.00	74.53	10.47

CAPSULE-W AXIAL

Page 2
Plant: Watts Bar 1 Material: SA508CL2 Heat: 527536(R 05)
Orientation: TL Capsule: W Fluence: 1.23E+19 n/cm^2

Charpy V-Notch Data

Temperature	Input Percent Shear	Computed Percent Shear	Differential
200.00	100.00	82.08	17.92
250.00	100.00	95.33	4.67
350.00	100.00	99.75	.25

Correlation Coefficient = .969

CAPSULE-W AXIAL

CVGRAPH 5.0 Hyperbolic Tangent Curve Printed on 09/10/2001 08:57 AM
Page 1
Coefficients of Curve 1
A = 30.92 B = 30.92 C = 108.87 T0 = 123.59 D = 0.00E+00
Equation is A + B * [Tanh((T-To)/(C+DT))]
Upper Shelf L.E.=61.8 Lower Shelf L.E.=.0(Fixed)
Temp.@L.E. 35 mils=138.0 Deg F
Plant: Watts Bar 1 Material: SA508CL2 Heat: 527536(R 05)
Orientation: TL Capsule: W Fluence: 1.23E+19 n/cm^2

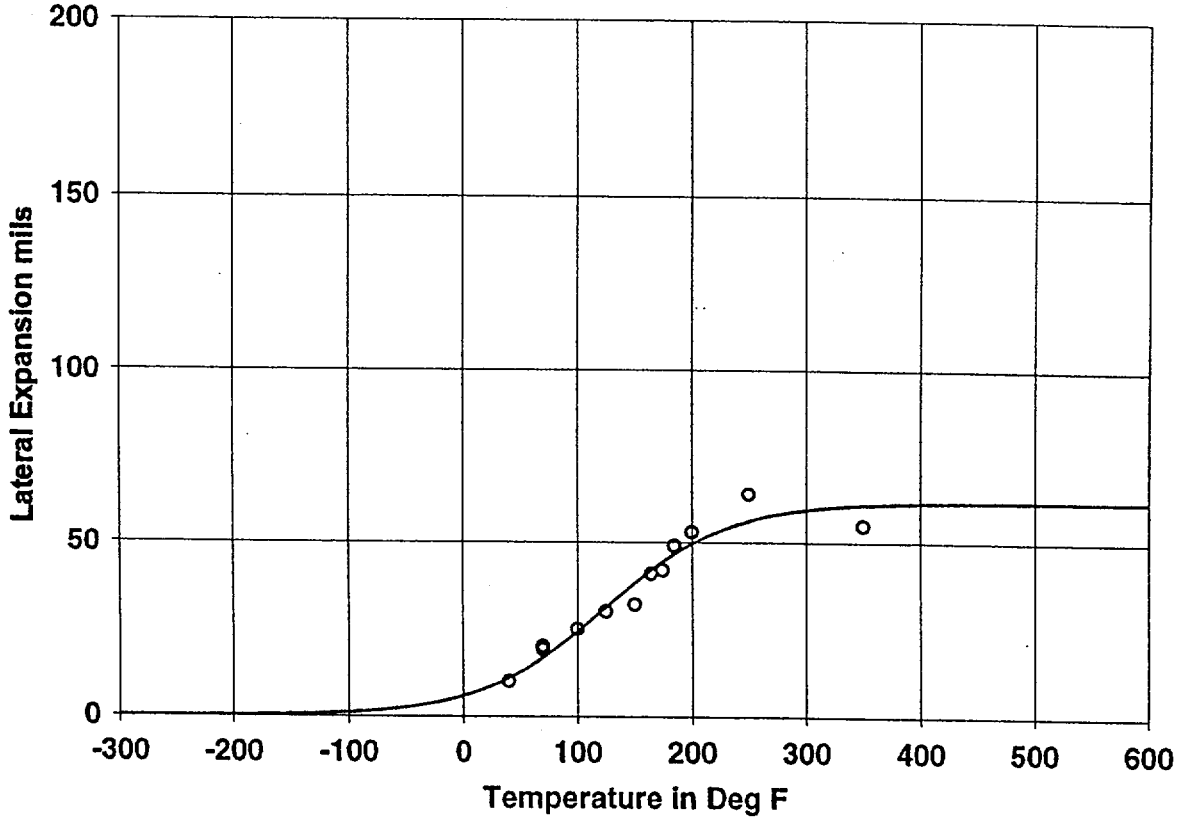

Charpy V-Notch Data

Temperature	Input L.E.	Computed L.E.	Differential
40.00	10.00	10.96	-.96
70.00	20.00	16.82	3.18
70.00	19.00	16.82	2.18
100.00	25.00	24.32	.68
125.00	30.00	31.32	-1.32
150.00	32.00	38.28	-6.28
165.00	41.00	42.15	-1.15
175.00	42.00	44.53	-2.53
185.00	49.00	46.72	2.28

CAPSULE-W AXIAL

Page 2
Plant: Watts Bar 1 Material: SA508CL2 Heat: 527536(R 05)
Orientation: TL Capsule: W Fluence: 1.23E+19 n/cm^2

Charpy V-Notch Data

Temperature	Input L.E.	Computed L.E.	Differential
200.00	53.00	49.65	3.35
250.00	64.00	56.32	7.68
350.00	55.00	60.89	-5.89

Correlation Coefficient = .971

CAPSULE-W WELD

CVGRAPH 5.0 Hyperbolic Tangent Curve Printed on 09/10/2001 09:25 AM
Page 1
Coefficients of Curve 1
A = 56.95 B = 54.75 C = 97.02 T0 = 51.66 D = 0.00E+00
Equation is A + B * [Tanh((T-To)/(C+DT))]
Upper Shelf Energy=111.7(Fixed) Lower Shelf Energy=2.2(Fixed)
Temp@30 ft-lbs=-.6 Deg F Temp@50 ft-lbs=39.3 Deg F
Plant: Watts Bar 1 Material: SA508CL2 Heat: 895075(W H)
Orientation: NA Capsule: W Fluence: 1.23E+19 n/cm^2

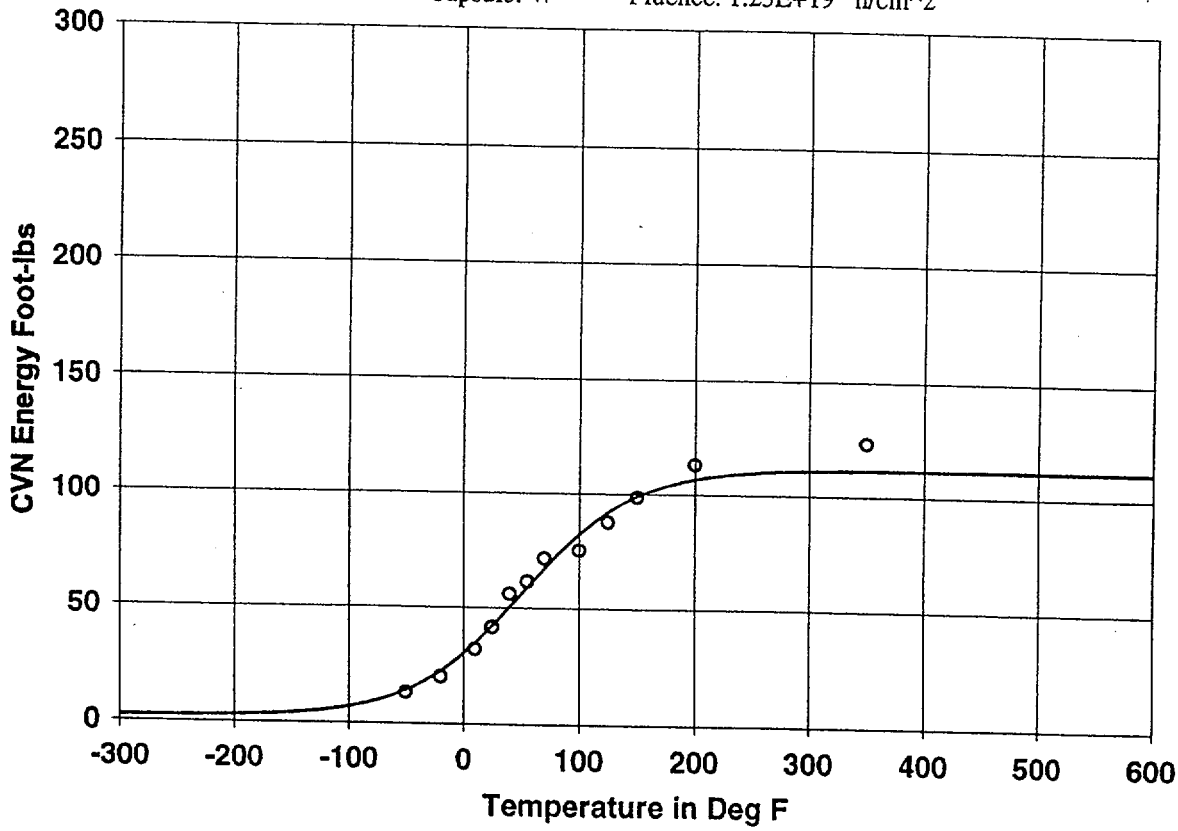

Charpy V-Notch Data

Temperature	Input CVN	Computed CVN	Differential
-50.00	13.00	14.19	-1.19
-20.00	20.00	22.55	-2.55
10.00	32.00	34.79	-2.79
25.00	41.50	42.27	-.77
40.00	56.00	50.40	5.60
55.00	61.50	58.84	2.66
70.00	71.50	67.18	4.32
100.00	75.00	82.18	-7.18
125.00	87.50	91.92	-4.42

CAPSULE-W WELD

Page 2
Plant: Watts Bar 1 Material: SA508CL2 Heat: 895075(W H)
Orientation: NA Capsule: W Fluence: 1.23E+19 n/cm^2

Charpy V-Notch Data

Temperature	Input CVN	Computed CVN	Differential
150.00	98.50	98.96	-.46
200.00	113.00	106.79	6.21
350.00	123.50	111.47	12.03

Correlation Coefficient = .990

CAPSULE-W WELD

CVGRAPH 5.0 Hyperbolic Tangent Curve Printed on 09/10/2001 09:28 AM
Page 1
Coefficients of Curve 1
A = 50. B = 50. C = 88.62 T0 = 19.8 D = 0.00E+00
Equation is A + B * [Tanh((T-To)/(C+DT))]
Temperature at 50% Shear = 19.8
Plant: Watts Bar 1 Material: SA508CL2 Heat: 895075(W H)
Orientation: NA Capsule: W Fluence: 1.23E+19 n/cm^2

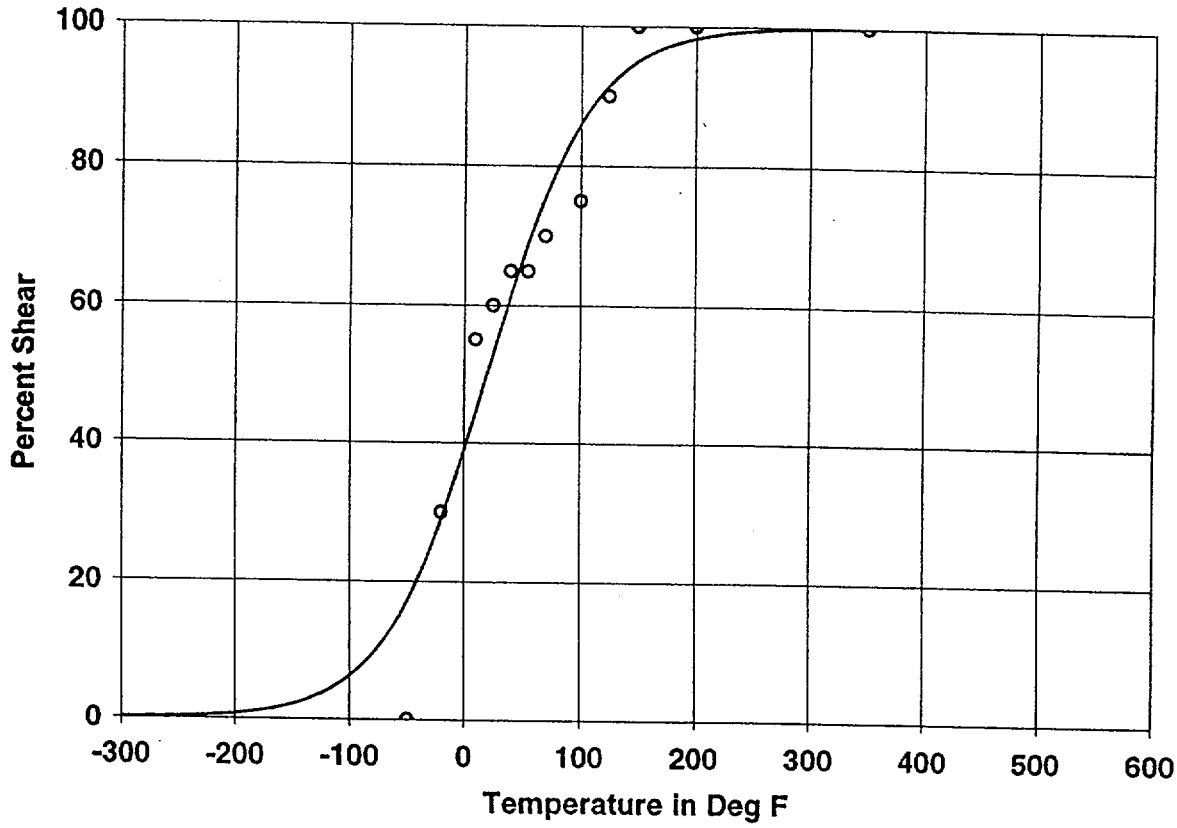

Charpy V-Notch Data

Temperature	Input Percent Shear	Computed Percent Shear	Differential
-50.00	.00	17.15	-17.15
-20.00	30.00	28.94	1.06
10.00	55.00	44.49	10.51
25.00	60.00	52.93	7.07
40.00	65.00	61.20	3.80
55.00	65.00	68.88	-3.88
70.00	70.00	75.64	-5.64
100.00	75.00	85.94	-10.94
125.00	90.00	91.48	-1.48

CAPSULE-W WELD

Page 2
Plant: Watts Bar 1 Material: SA508CL2 Heat: 895075(W H)
Orientation: NA Capsule: W Fluence: 1.23E+19 n/cm^2

Charpy V-Notch Data

Temperature	Input Percent Shear	Computed Percent Shear	Differential
150.00	100.00	94.97	5.03
200.00	100.00	98.32	1.68
350.00	100.00	99.94	.06

Correlation Coefficient = .967

CAPSULE-W WELD

CVGRAPH 5.0 Hyperbolic Tangent Curve Printed on 09/10/2001 09:27 AM
Page 1
Coefficients of Curve 1
A = 44.58 B = 44.58 C = 95.28 T0 = 42.68 D = 0.00E+00
Equation is A + B * [Tanh((T-To)/(C+DT))]
Upper Shelf L.E.=89.2 Lower Shelf L.E.=.0(Fixed)
Temp.@L.E. 35 mils=21.9 Deg F
Plant: Watts Bar 1 Material: SA508CL2 Heat: 895075(W H)
Orientation: NA Capsule: W Fluence: 1.23E+19 n/cm^2

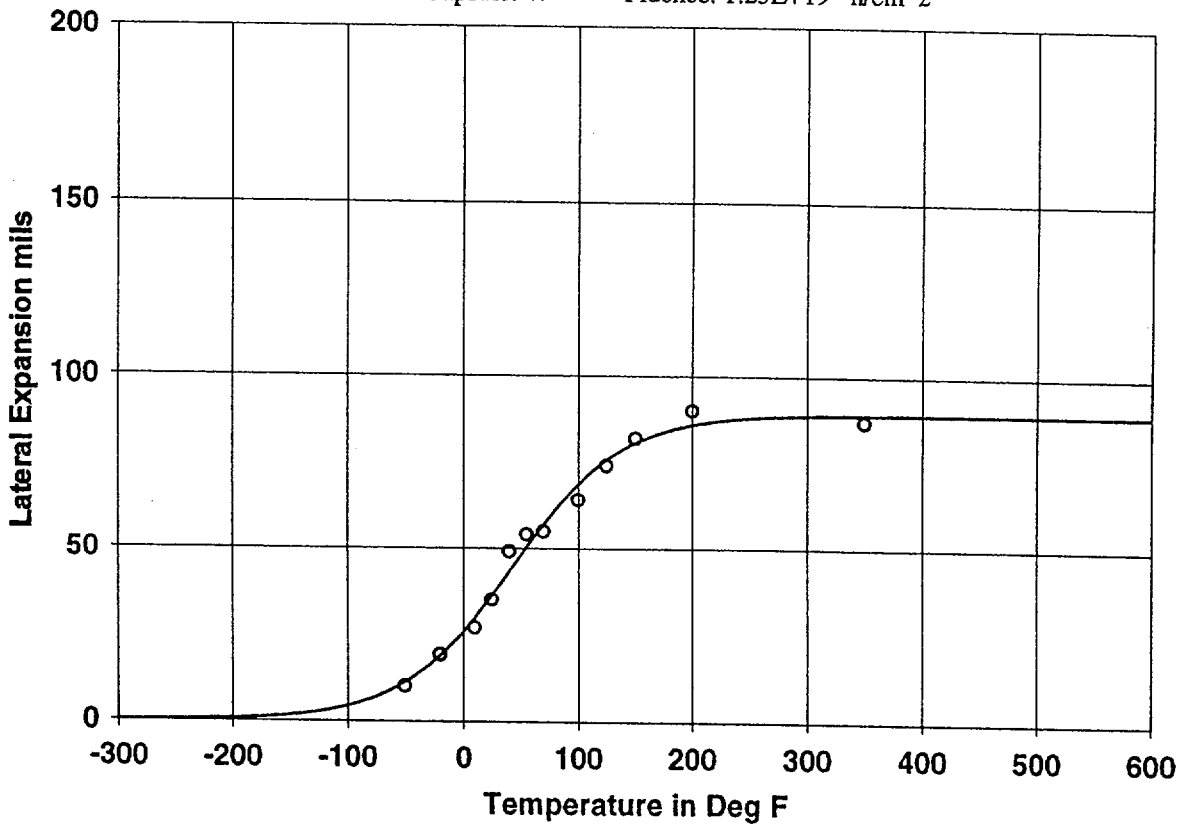

Charpy V-Notch Data

Temperature	Input L.E.	Computed L.E.	Differential
-50.00	10.00	11.15	-1.15
-20.00	19.00	18.86	.14
10.00	27.00	29.86	-2.86
25.00	35.00	36.40	-1.40
40.00	49.00	43.32	5.68
55.00	54.00	50.31	3.69
70.00	55.00	57.02	-2.02
100.00	64.00	68.57	-4.57
125.00	74.00	75.71	-1.71

CAPSULE-W WELD

Page 2
Plant: Watts Bar 1 Material: SA508CL2 Heat: 895075(W H)
Orientation: NA Capsule: W Fluence: 1.23E+19 n/cm^2

Charpy V-Notch Data

Temperature	Input L.E.	Computed L.E.	Differential
150.00	82.00	80.67	1.33
200.00	90.00	85.99	4.01
350.00	87.00	89.01	-2.01

Correlation Coefficient = .993

CAPSULE-W HEAT-AFFECTED-ZONE

CVGRAPH 5.0 Hyperbolic Tangent Curve Printed on 09/10/2001 09:16 AM
Page 1
Coefficients of Curve 1
A = 42.25 B = 40.05 C = 122.96 T0 = 31.6 D = 0.00E+00
Equation is A + B * [Tanh((T-To)/(C+DT))]
Upper Shelf Energy=82.3(Fixed) Lower Shelf Energy=2.2(Fixed)
Temp@30 ft-lbs=-7.2 Deg F Temp@50 ft-lbs=55.8 Deg F
Plant: Watts Bar 1 Material: SA508CL2 Heat: 895075(W H)
Orientation: NA Capsule: W Fluence: 1.23E+19 n/cm^2

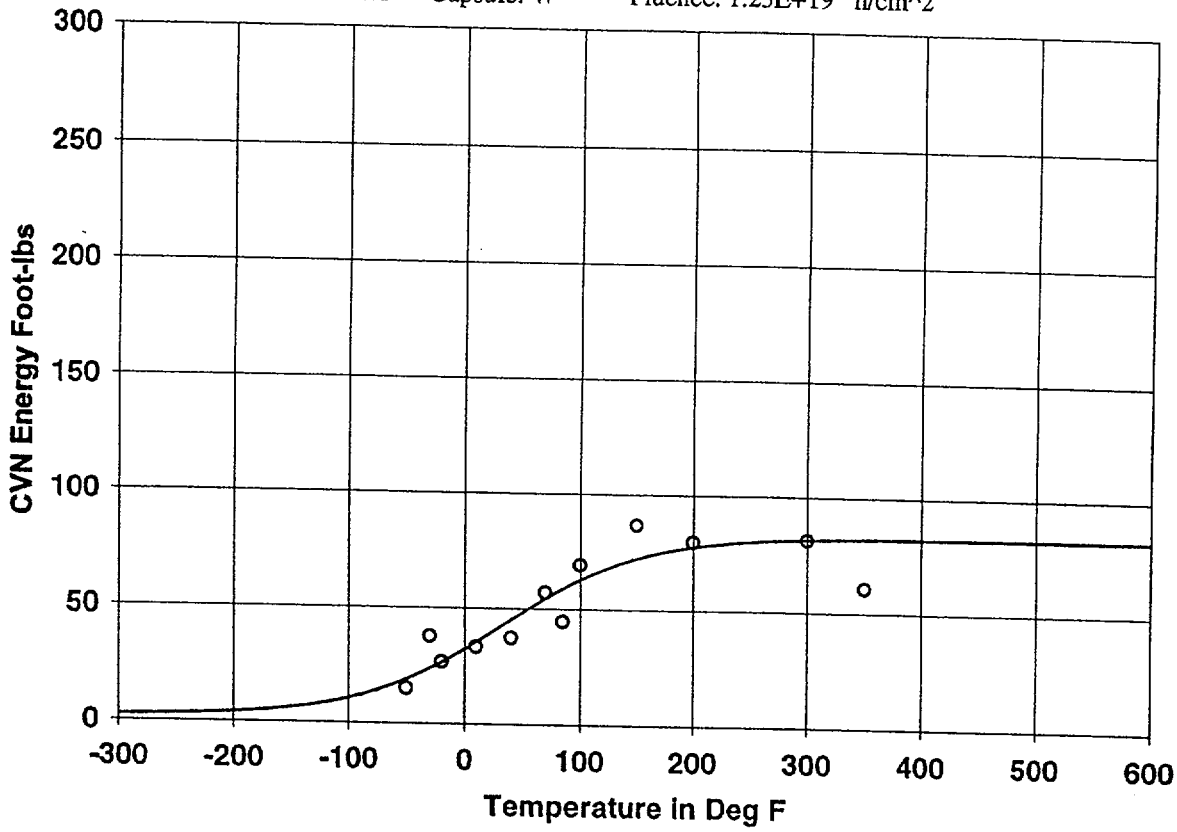

Charpy V-Notch Data

Temperature	Input CVN	Computed CVN	Differential
-50.00	15.00	18.99	-3.99
-30.00	37.50	23.71	13.79
-20.00	26.50	26.36	.14
10.00	33.00	35.29	-2.29
40.00	37.00	44.98	-7.98
70.00	57.00	54.36	2.64
85.00	44.50	58.63	-14.13
100.00	69.00	62.48	6.52
150.00	86.50	72.11	14.39

CAPSULE-W HEAT-AFFECTED-ZONE

Page 2

Plant: Watts Bar 1 Material: SA508CL2 Heat: 895075(W H)
Orientation: NA Capsule: W Fluence: 1.23E+19 n/cm^2

Charpy V-Notch Data

Temperature	Input CVN	Computed CVN	Differential
200.00	79.50	77.44	2.06
300.00	81.00	81.29	-.29
350.00	60.50	81.85	-21.35

Correlation Coefficient = .901

CAPSULE-W HEAT-AFFECTED-ZONE

CVGRAPH 5.0 Hyperbolic Tangent Curve Printed on 09/10/2001 09:18 AM
Page 1
Coefficients of Curve 1
A = 50. B = 50. C = 99.03 T0 = 39.58 D = 0.00E+00
Equation is A + B * [Tanh((T-To)/(C+DT))]
Temperature at 50% Shear = 39.6
Plant: Watts Bar 1 Material: SA508CL2 Heat: 895075(W H)
Orientation: NA Capsule: W Fluence: 1.23E+19 n/cm^2

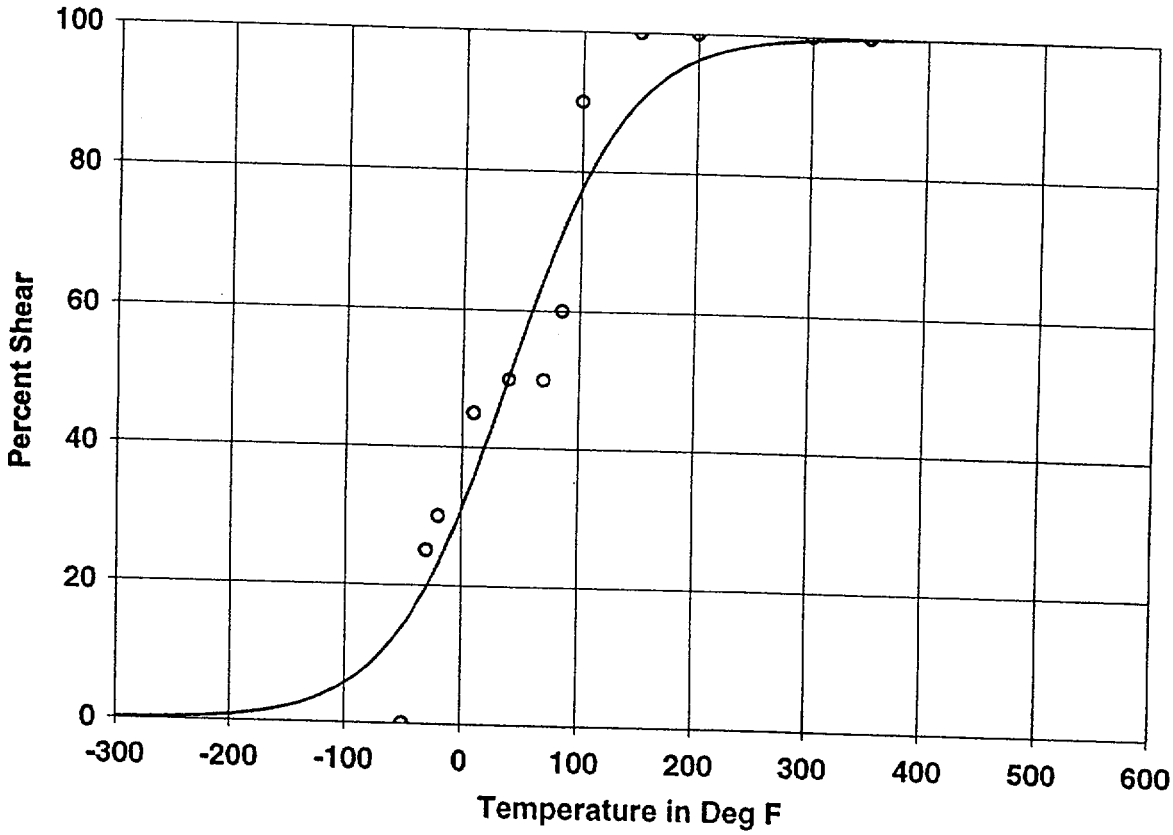

Charpy V-Notch Data

Temperature	Input Percent Shear	Computed Percent Shear	Differential
-50.00	.00	14.07	-14.07
-30.00	25.00	19.70	5.30
-20.00	30.00	23.09	6.91
10.00	45.00	35.49	9.51
40.00	50.00	50.21	-.21
70.00	50.00	64.89	-14.89
85.00	60.00	71.45	-11.45
100.00	90.00	77.21	12.79
150.00	100.00	90.29	9.71

CAPSULE-W HEAT-AFFECTED-ZONE

Page 2
Plant: Watts Bar 1 Material: SA508CL2 Heat: 895075(W H)
Orientation: NA Capsule: W Fluence: 1.23E+19 n/cm^2

Charpy V-Notch Data

Temperature	Input Percent Shear	Computed Percent Shear	Differential
200.00	100.00	96.23	3.77
300.00	100.00	99.48	.52
350.00	100.00	99.81	.19

Correlation Coefficient = .963

CAPSULE-W HEAT-AFFECTED-ZONE

CVGRAPH 5.0 Hyperbolic Tangent Curve Printed on 09/10/2001 09:23 AM
Page 1
Coefficients of Curve 1
A = 31.8 B = 31.8 C = 108.76 T0 = 36.94 D = 0.00E+00
Equation is A + B * [Tanh((T-To)/(C+DT))]
Upper Shelf L.E.=63.6 Lower Shelf L.E.=.0(Fixed)
Temp.@L.E. 35 mils=47.9 Deg F
Plant: Watts Bar 1 Material: SA508CL2 Heat: 895075(W H)
Orientation: NA Capsule: W Fluence: 1.23E+19 n/cm^2

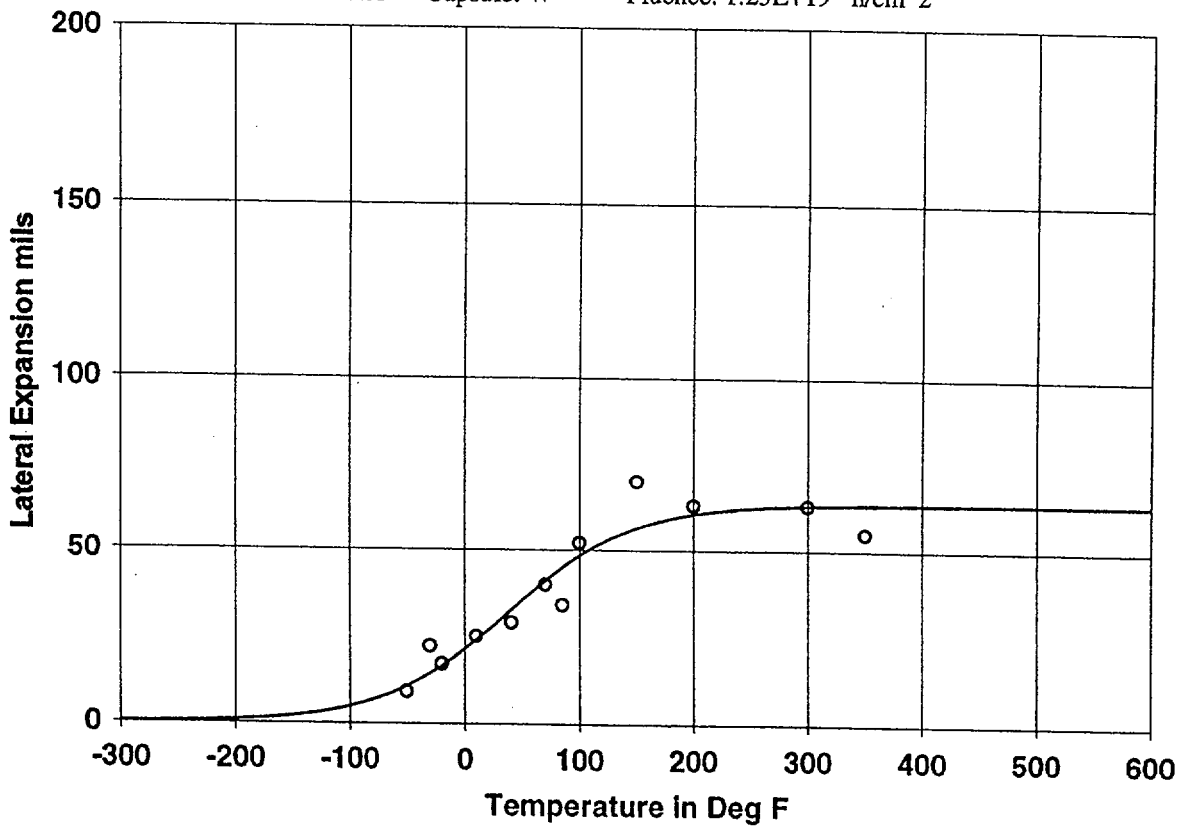

Charpy V-Notch Data

Temperature	Input L.E.	Computed L.E.	Differential
-50.00	9.00	10.70	-1.70
-30.00	22.00	14.37	7.63
-20.00	17.00	16.52	.48
10.00	25.00	24.08	.92
40.00	29.00	32.70	-3.70
70.00	40.00	41.18	-1.18
85.00	34.00	45.00	-11.00
100.00	52.00	48.42	3.58
150.00	70.00	56.53	13.47

CAPSULE-W HEAT-AFFECTED-ZONE

Page 2

Plant: Watts Bar 1 Material: SA508CL2 Heat: 895075(W H)
Orientation: NA Capsule: W Fluence: 1.23E+19 n/cm^2

Charpy V-Notch Data

Temperature	Input L.E.	Computed L.E.	Differential
200.00	63.00	60.58	2.42
300.00	63.00	63.10	-.10
350.00	55.00	63.40	-8.40

Correlation Coefficient = .947

APPENDIX C

FRACTURE SURFACES OF CHARPY IMPACT SPECIMENS WATTS BAR UNIT 1, CAPSULE W

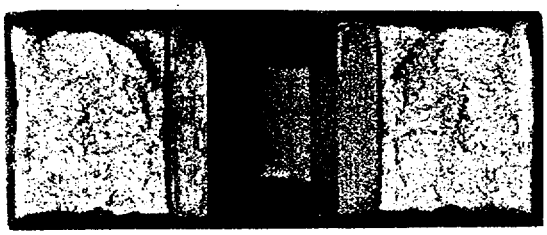

Specimen No. WL35, Test Temperature 40°F

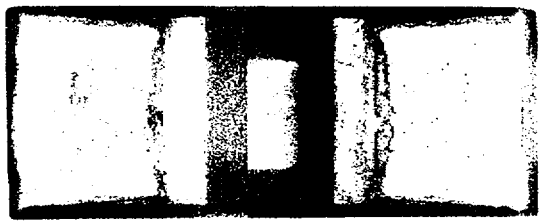

Specimen No. WL38, Test Temperature 70°F

Specimen No. WL42, Test Temperature 50°F

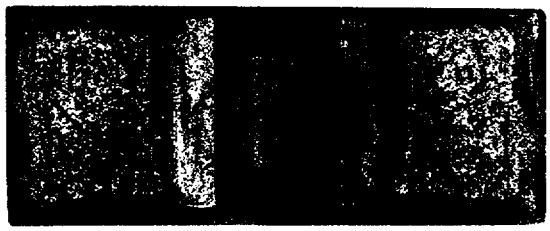

Specimen No. WL36, Test Temperature 100°F

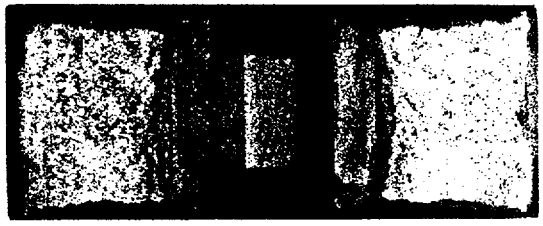

Specimen No. WL41, Test Temperature 60°F

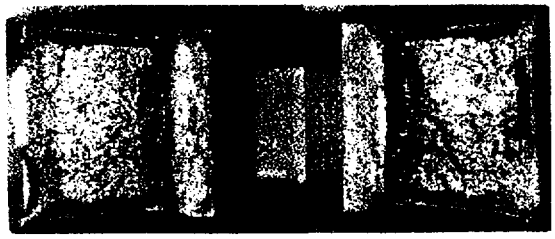

Specimen No. WL45, Test Temperature 125°F

Specimen No. WL39, Test Temperature 60°F

Specimen No. WL32, Test Temperature 140°F

Specimen No. WL37, Test Temperature 150°F

Specimen No. WL34, Test Temperature 250°F

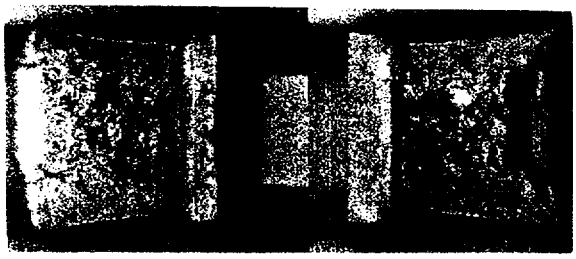

Specimen No. WL40, Test Temperature 200°F

Specimen No. WL43, Test Temperature 300°F

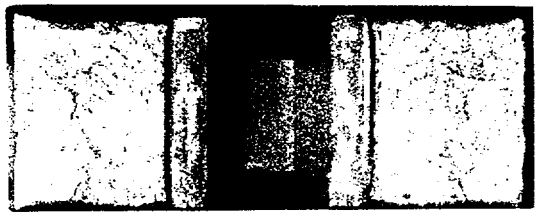

Specimen No. WW37, Test Temperature -50°F

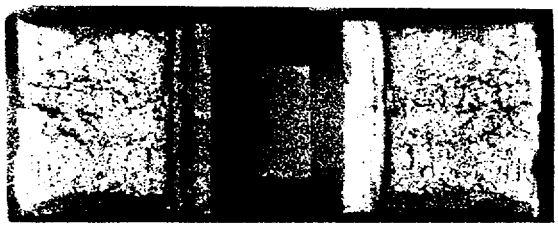

Specimen No. WW31, Test Temperature -20°F

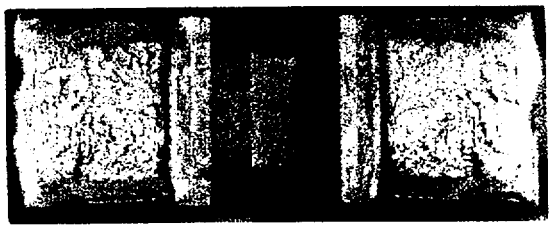

Specimen No. WW42, Test Temperature 10°F

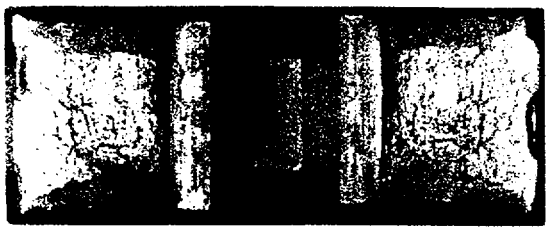

Specimen No. WW43, Test Temperature 25°F

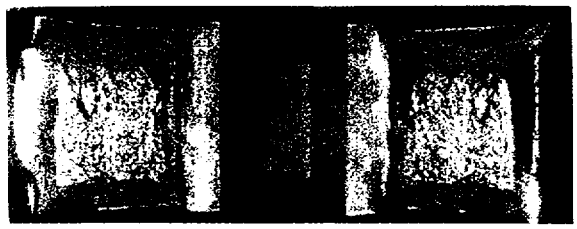

Specimen No. WW44, Test Temperature 40°F

Specimen No. WW36, Test Temperature 55°F

Specimen No. WW34, Test Temperature 70°F

Specimen No. WW38, Test Temperature 100°F

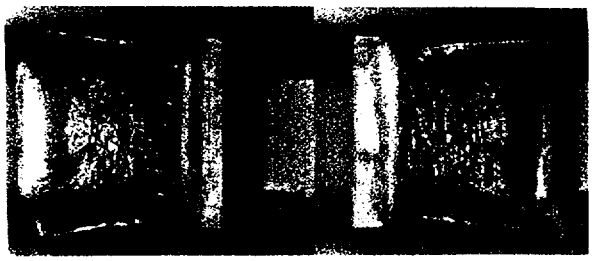

Specimen No. WW35, Test Temperature 125°F

Specimen No. WW45, Test Temperature 200°F

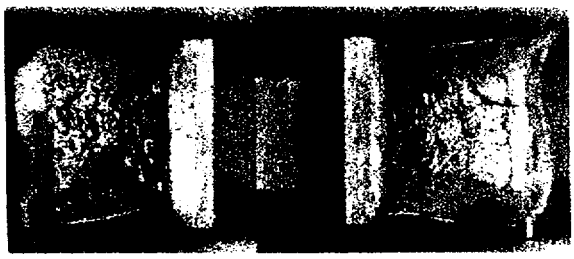

Specimen No. WW33, Test Temperature 150°F

Specimen No. WW41, Test Temperature 350°F

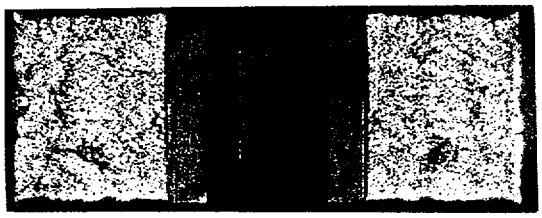

Specimen No. WT38, Test Temperature 40°F

Specimen No. WT39, Test Temperature 125°F

Specimen No. WT34, Test Temperature 70°F

Specimen No. WT36, Test Temperature 150°F

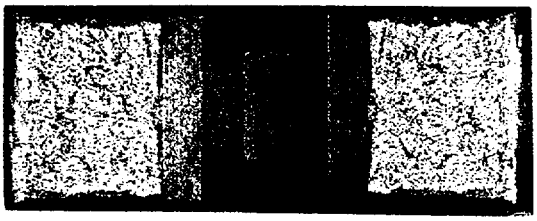

Specimen No. WT43, Test Temperature 70°F

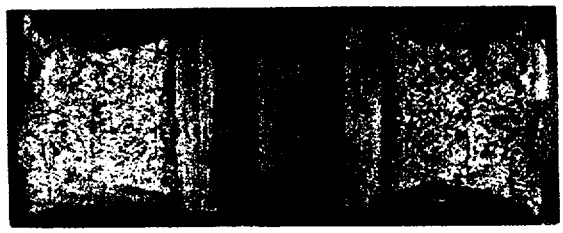

Specimen No. WT40, Test Temperature 175°F

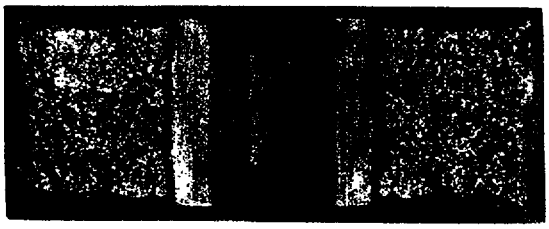

Specimen No. WT32, Test Temperature 100°F

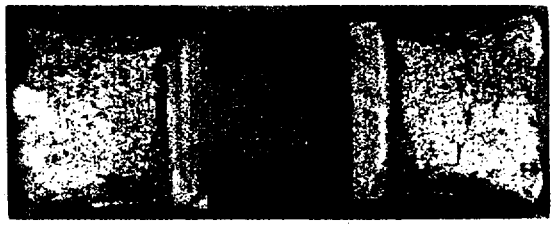

Specimen No. WT33, Test Temperature 165°F

Specimen No. WT41, Test Temperature 185°F

Specimen No. WT44, Test Temperature 250°F

Specimen No. WT45, Test Temperature 200°F

Specimen No. WT37, Test Temperature 350°F

Specimen No. WH33, Test Temperature -50°F

Specimen No. WH44, Test Temperature 40°F

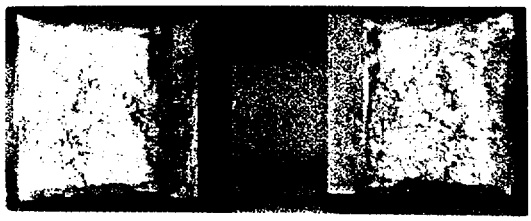

Specimen No. WH36, Test Temperature -30°F

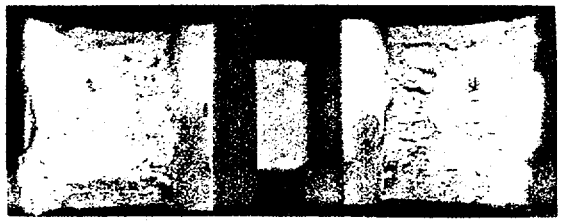

Specimen No. WH31, Test Temperature 70°F

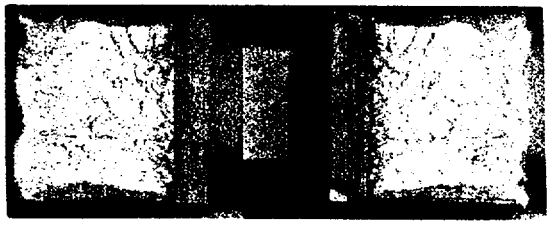

Specimen No. WH37, Test Temperature -20°F

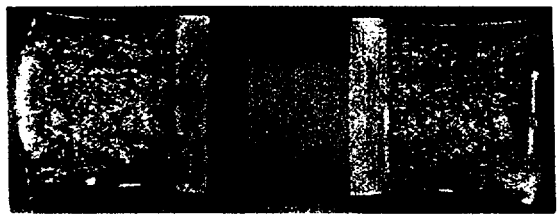

Specimen No. WH40, Test Temperature 85°F

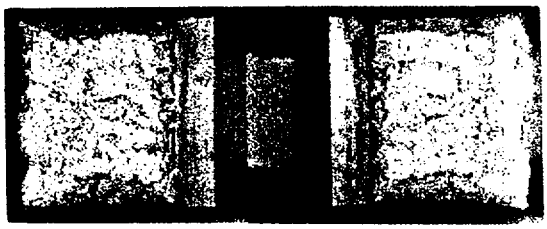

Specimen No. WH41, Test Temperature 10°F

Specimen No. WH43, Test Temperature 100°F

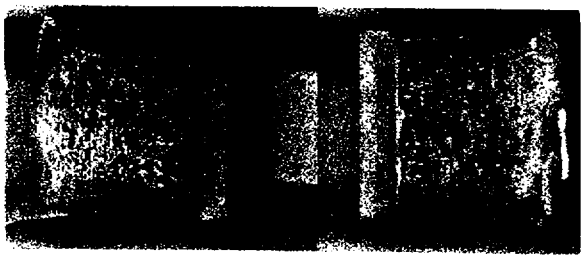

Specimen No. WH45, Test Temperature 150°F

Specimen No. WH38, Test Temperature 300°F

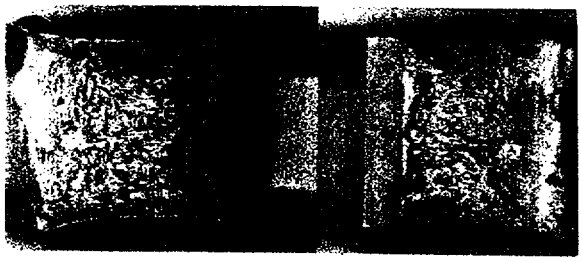

Specimen No. WH39, Test Temperature 200°F

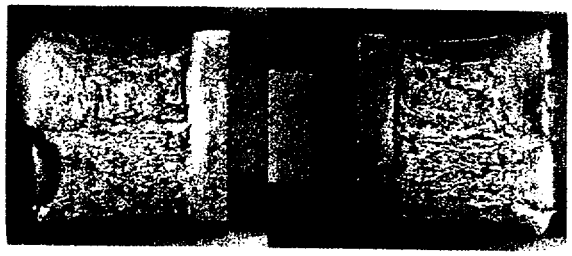

Specimen No. WH34, Test Temperature 350°F

APPENDIX D

INSTRUMENTED CHARPY IMPACT TEST RESULTS
WATTS BAR UNIT 1, CAPSULE W

Specimen	Yield Properties			Maximum Load Properties			Fast Fracture Properties			Crack Arrest Properties			Propagation Load Properties		Total Energy Properties		Shear Lip Properties	Dynamic Yield Strength
ID	Time (µs)	Load (lbf)	Energy (ft-lbf)	Time (µs)	Load (lbf)	Energy (ft-lbf)	Time (µs)	Load (lbf)	Energy (ft-lbf)	Time (µs)	Load (lbf)	Energy (ft-lbf)	Load (lbf)	Energy (ft-lbf)	Time (µs)	Energy (ft-lbf)	Energy (ft-lbf)	(ksi)
WH33	146	3878	5.03	239	4165	11.23	250	4138	12.00	306	0	14.23	4161	2.99	306	14.23	2.22	129
WH36	148	3770	5.04	525	4529	31.84	525	4529	31.84	607	0	35.45	4540	3.61	607	35.45	3.61	126
WH37	152	3763	5.12	327	4204	16.83	357	4145	18.96	475	794	22.10	3351	7.35	1008	24.18	5.22	125
WH41	148	3641	4.96	407	4170	22.22	407	4170	22.22	523	1451	26.54	2719	9.26	1322	31.46	9.26	121
WH44	149	3556	4.84	413	4119	22.12	413	4119	22.12	524	2226	27.00	1893	13.73	1614	35.85	13.73	119
WH31	148	3422	4.83	420	4034	22.11	686	3669	39.68	798	2268	45.02	1401	33.81	2634	55.92	16.24	114
WH40	156	3303	4.77	340	3724	15.78	394	3685	19.16	476	3103	23.80	582	27.08	2620	42.86	23.69	110
WH43	154	3264	4.50	532	4106	28.97	772	3379	44.49	858	2854	48.93	524	41.40	2766	70.37	25.88	109
WH39	158	2967	4.83	606	4020	32.50	NA	NA	NA	NA	NA	NA	0	46.89	3170	79.39	NA	99
WH38	152	2783	3.93	526	3636	25.03	NA	NA	NA	NA	NA	NA	0	55.78	3558	80.80	NA	93
WH34	164	2790	4.68	524	3487	24.58	NA	NA	NA	NA	NA	NA	0	34.80	3022	59.38	NA	93
WL35	146	3535	4.81	226	3807	9.70	226	3807	9.70	291	0	11.73	3813	2.03	290	11.73	2.03	118
WL42	146	3498	4.68	323	4004	15.90	327	3997	16.17	391	0	18.39	3991	2.49	391	18.39	2.21	117
WL41	143	3473	4.59	522	4361	30.11	562	4287	33.06	624	0	35.39	4299	5.28	624	35.39	2.33	116
WL39	146	3512	4.66	609	4359	36.37	737	4225	45.73	802	0	48.09	4225	11.72	802	48.09	2.36	117
WL38	154	3508	5.16	528	4384	30.53	580	4329	34.36	644	0	36.88	4361	6.35	644	36.88	2.52	117
WL36	160	3206	3.82	630	4278	34.82	718	4264	41.18	840	782	44.40	3482	12.23	1930	47.06	5.88	107
WL45	154	3218	4.69	612	4237	34.64	782	4020	46.52	900	1175	50.32	2845	22.30	3062	56.94	10.42	107
WL32	162	3096	5.02	700	4119	39.94	1044	3282	61.78	1154	1104	64.85	2178	30.86	2934	70.80	9.02	103
WL37	174	3172	4.97	550	4168	28.98	1096	3034	63.74	1204	1451	67.09	1582	49.35	3060	78.33	14.59	106
WL40	180	3043	5.09	544	4048	27.62	NA	NA	NA	NA	NA	NA	0	72.48	3362	100.10	NA	101
WL34	160	2910	4.75	702	4034	38.62	NA	NA	NA	NA	NA	NA	0	68.47	4124	107.09	NA	97
WL43	138	2677	3.30	620	3751	30.91	NA	NA	NA	NA	NA	NA	0	64.29	3710	95.20	NA	89
WT38	149	3439	4.74	149	3439	4.74	149	3439	4.74	228	0	7.81	3452	3.07	228	7.81	3.07	115
WT43	146	3301	4.22	292	3590	12.70	292	3590	12.70	404	656	15.11	2935	3.43	660	16.14	3.43	110
WT34	136	3229	4.16	302	3715	13.87	302	3715	13.87	367	0	15.94	3719	2.07	367	15.94	2.07	108
WT32	160	3172	4.78	340	3749	15.35	340	3749	15.35	460	745	18.30	3004	6.37	1552	21.71	6.37	106
WT39	160	3041	4.75	418	3765	19.89	418	3765	19.89	536	1348	23.44	2417	8.79	1622	28.68	8.79	101
WT36	174	2939	4.68	354	3508	14.60	354	3508	14.60	474	1525	18.56	1983	13.00	3046	27.59	13.00	98
WT33	170	2914	5.08	438	3606	20.31	438	3606	20.31	552	2151	25.03	1456	17.38	2778	37.69	17.38	97
WT40	152	2884	3.73	474	3758	22.30	474	3758	22.30	588	1941	26.74	1817	16.67	3040	38.97	16.67	96
WT41	150	2783	3.77	448	3629	20.26	576	3234	27.93	658	2590	31.76	644	27.36	3034	47.62	19.70	93
WT45	160	2824	4.50	526	3717	25.46	NA	NA	NA	NA	NA	NA	0	28.34	3024	53.80	NA	94
WT44	162	2737	4.38	530	3613	24.86	NA	NA	NA	NA	NA	NA	0	38.85	2930	63.71	NA	91
WT37	146	2553	3.55	534	3542	24.20	NA	NA	NA	NA	NA	NA	0	37.55	2926	61.75	NA	85
WW37	157	3547	4.59	237	3715	9.40	237	3715	9.40	290	0	11.22	3749	1.82	290	11.22	1.82	118
WW31	142	3388	4.33	280	3636	12.51	280	3636	12.51	397	1113	15.72	2523	5.89	826	18.40	5.89	113
WW42	146	3321	4.38	396	3823	19.45	396	3823	19.45	510	1944	23.83	1879	11.79	1498	31.24	11.79	111
WW43	148	3222	4.54	438	3873	21.96	470	3850	24.06	582	2548	29.40	1302	18.99	2102	40.95	16.89	107
WW44	146	3179	4.44	604	4052	33.03	612	4050	33.58	738	2562	40.26	1488	24.18	2742	57.21	23.63	106
WW36	142	3151	4.22	700	4030	38.96	906	3889	52.81	1020	1658	57.47	2231	23.48	2012	62.44	9.63	105
WW34	142	3105	4.03	702	3986	38.32	1036	3712	60.27	1152	1693	64.84	2019	33.26	2570	71.58	11.31	103
WW38	162	2953	4.63	708	4014	38.28	1052	3735	61.09	1256	1318	68.36	2417	38.98	3016	77.27	16.18	98
WW35	152	2875	4.17	706	3894	37.31	NA	NA	NA	NA	NA	NA	0	54.03	3194	91.35	NA	96
WW33	144	2760	3.74	708	3839	36.69	NA	NA	NA	NA	NA	NA	0	63.56	3708	100.26	NA	92
WW45	160	2677	4.24	802	3698	40.79	NA	NA	NA	NA	NA	NA	0	77.81	3760	118.59	NA	89
WW41	138	2473	3.48	806	3457	39.13	NA	NA	NA	NA	NA	NA	0	89.08	4364	128.21	NA	82

PROJ. NO. 1215-001 QA NO. 00001

ENERGY - TIME TRACE FOR SPECIMEN WT41

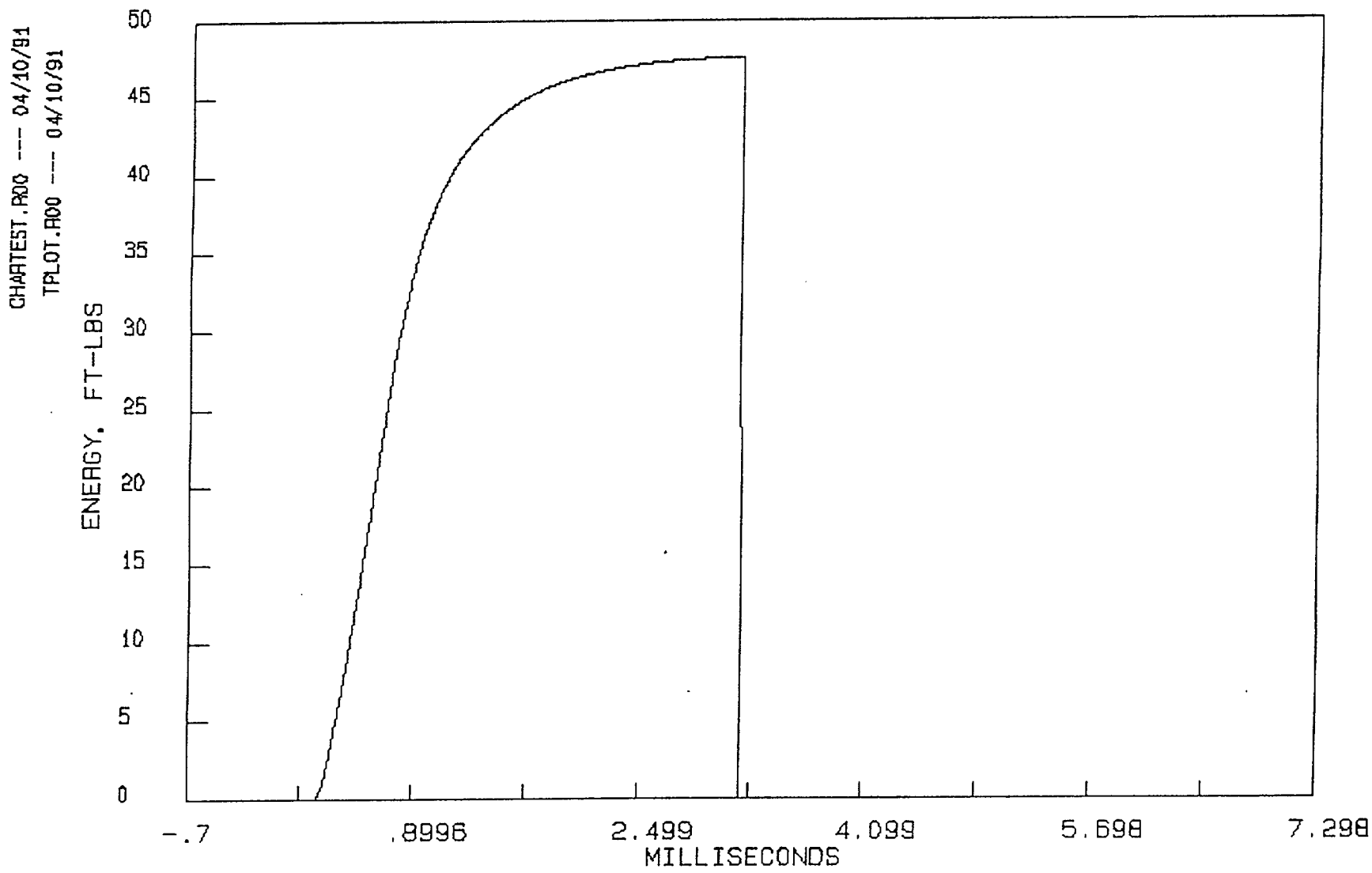

PROJ. NO. 1215-001 QA NO. 00001

LOAD - TIME TRACE FOR SPECIMEN WT33

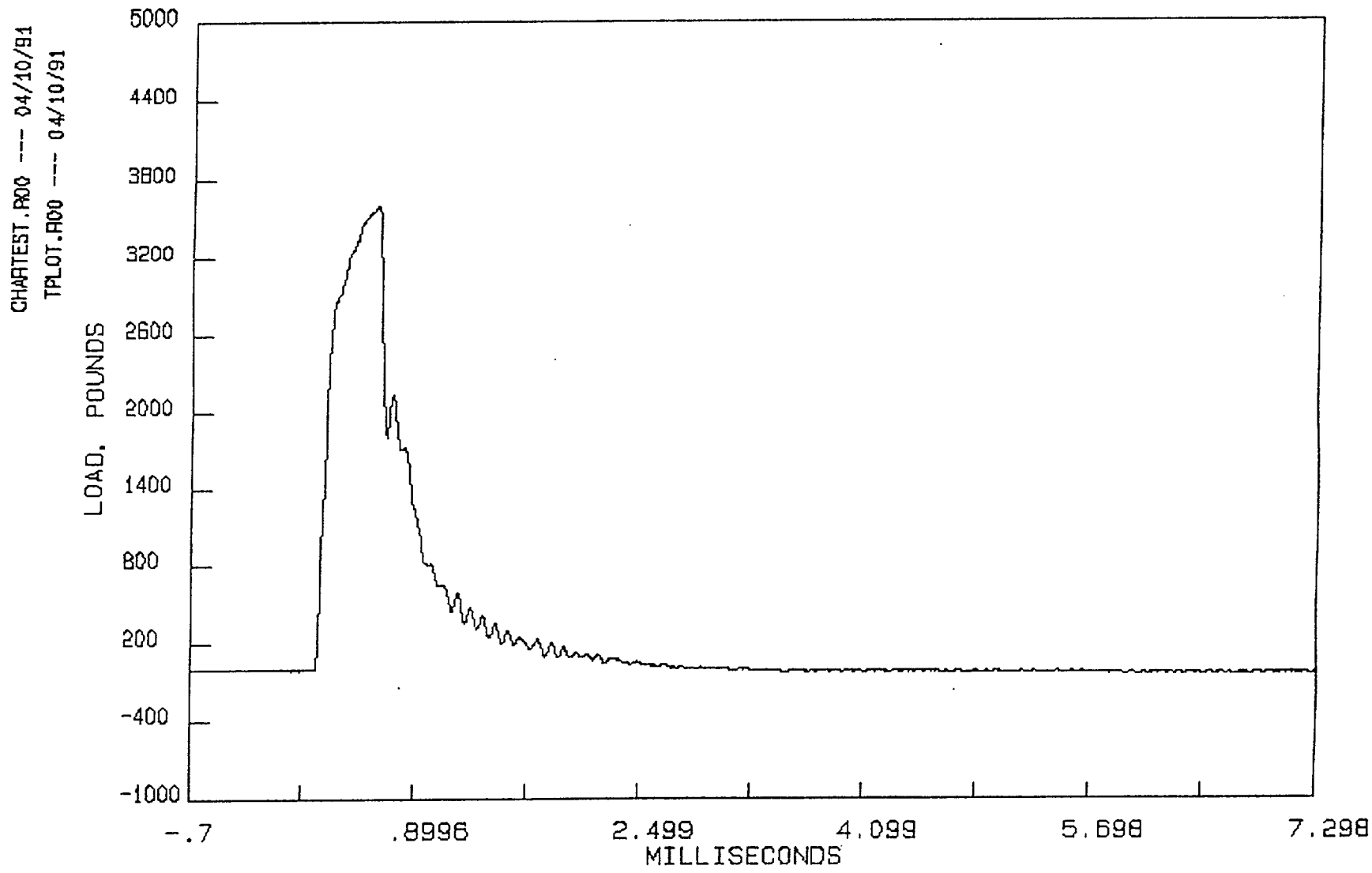

PROJ. NO. 1215-001 QA NO. 00001

ENERGY - TIME TRACE FOR SPECIMEN WT33

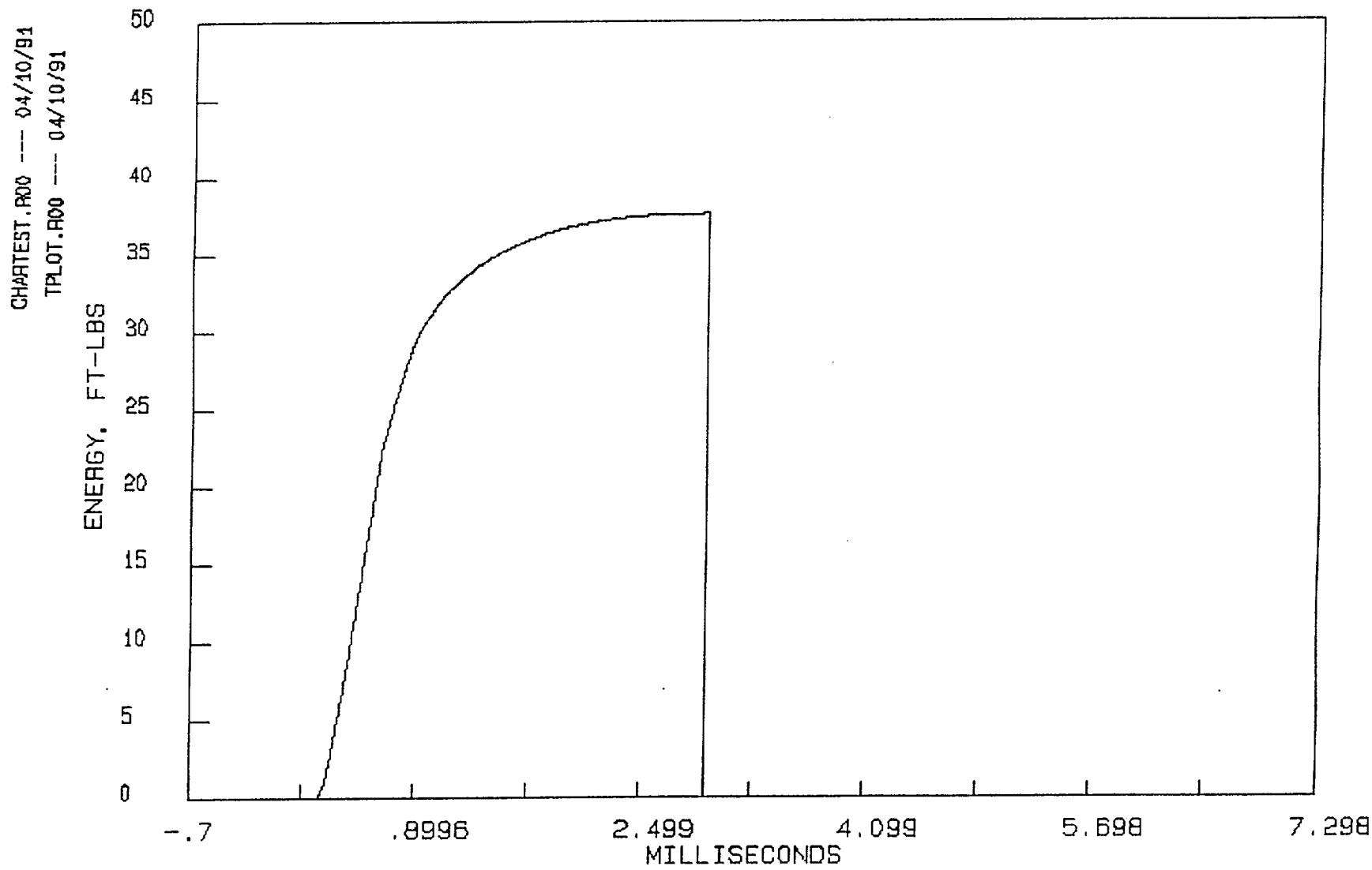

PROJ. NO. 1215-001 QA NO. 00001

LOAD - TIME TRACE FOR SPECIMEN WT34

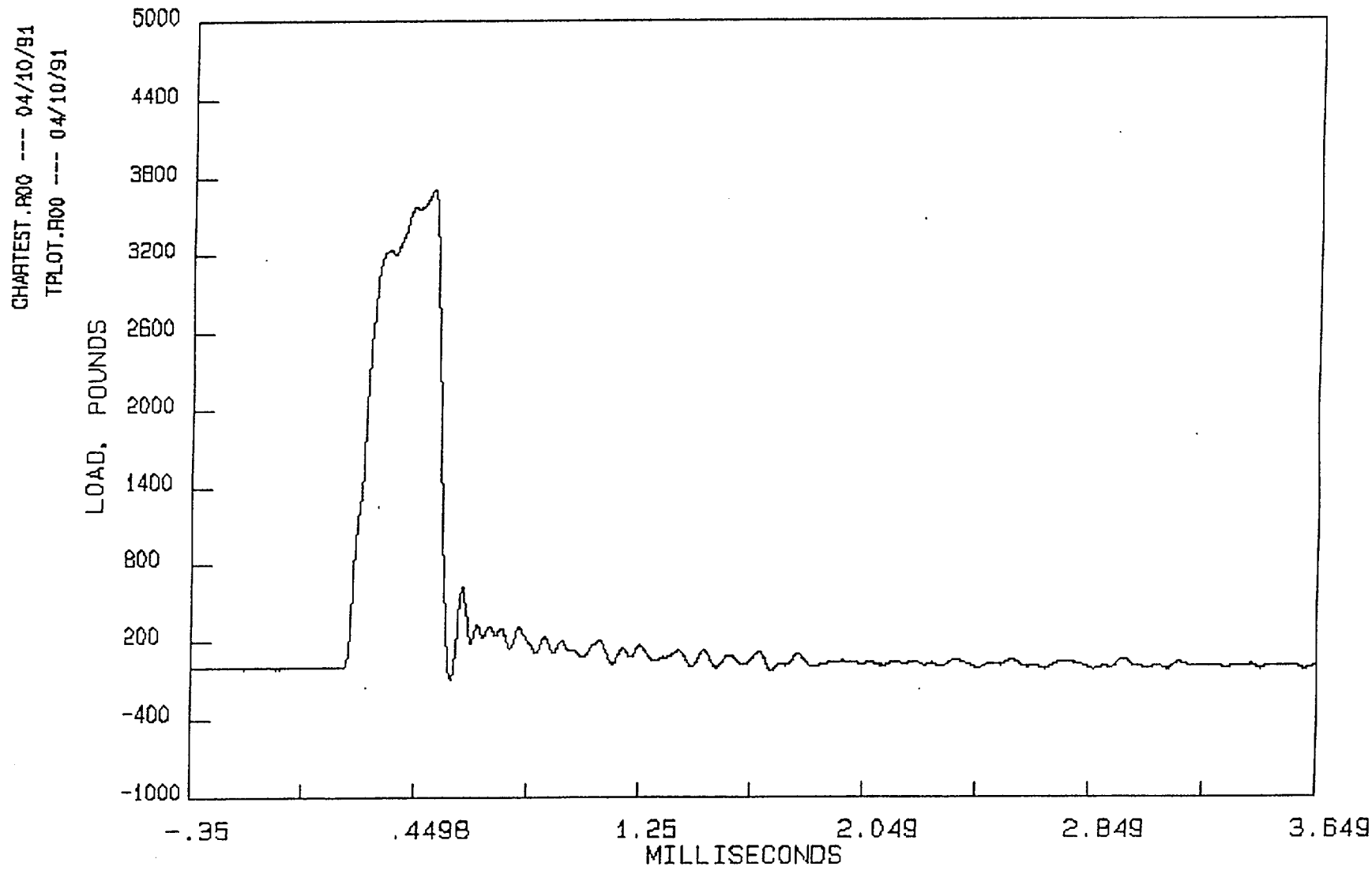

PROJ. NO. 1215-001 QA NO. 00001

ENERGY - TIME TRACE FOR SPECIMEN WT34

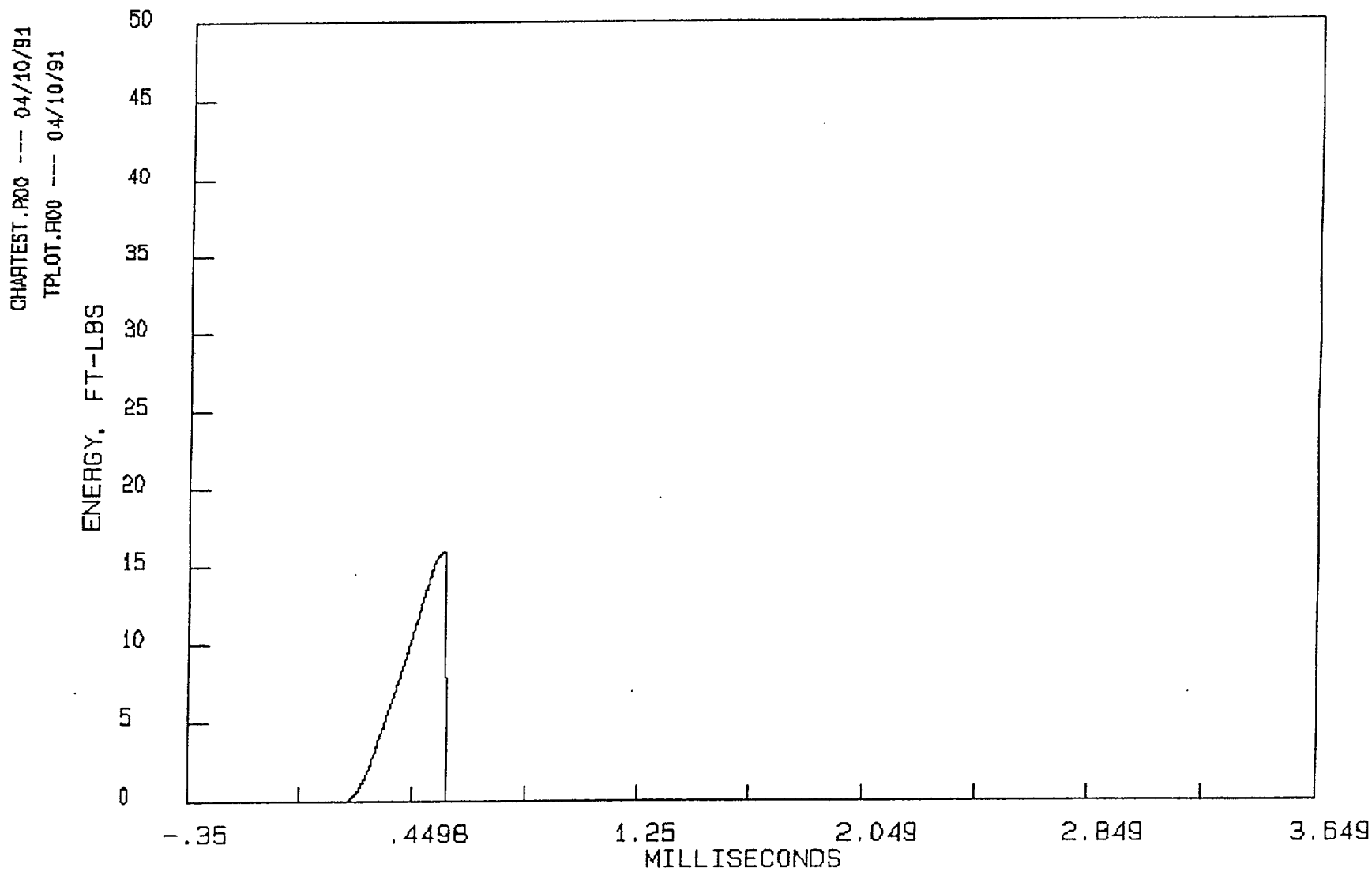

PROJ. NO. 1215-001 QA NO. 00001

LOAD - TIME TRACE FOR SPECIMEN WT44

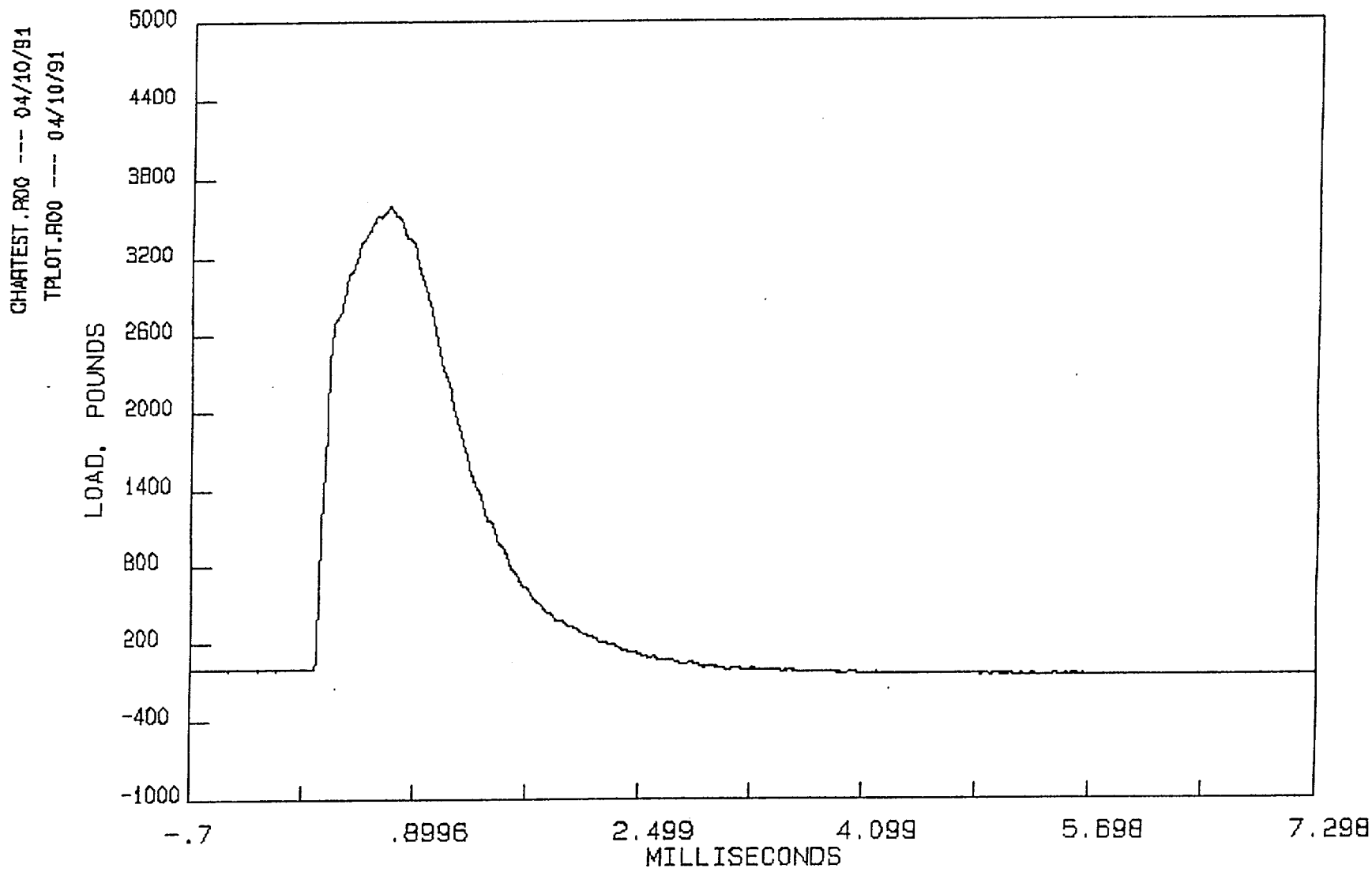

PROJ. NO. 1215-001 QA NO. 00001

ENERGY - TIME TRACE FOR SPECIMEN WT44

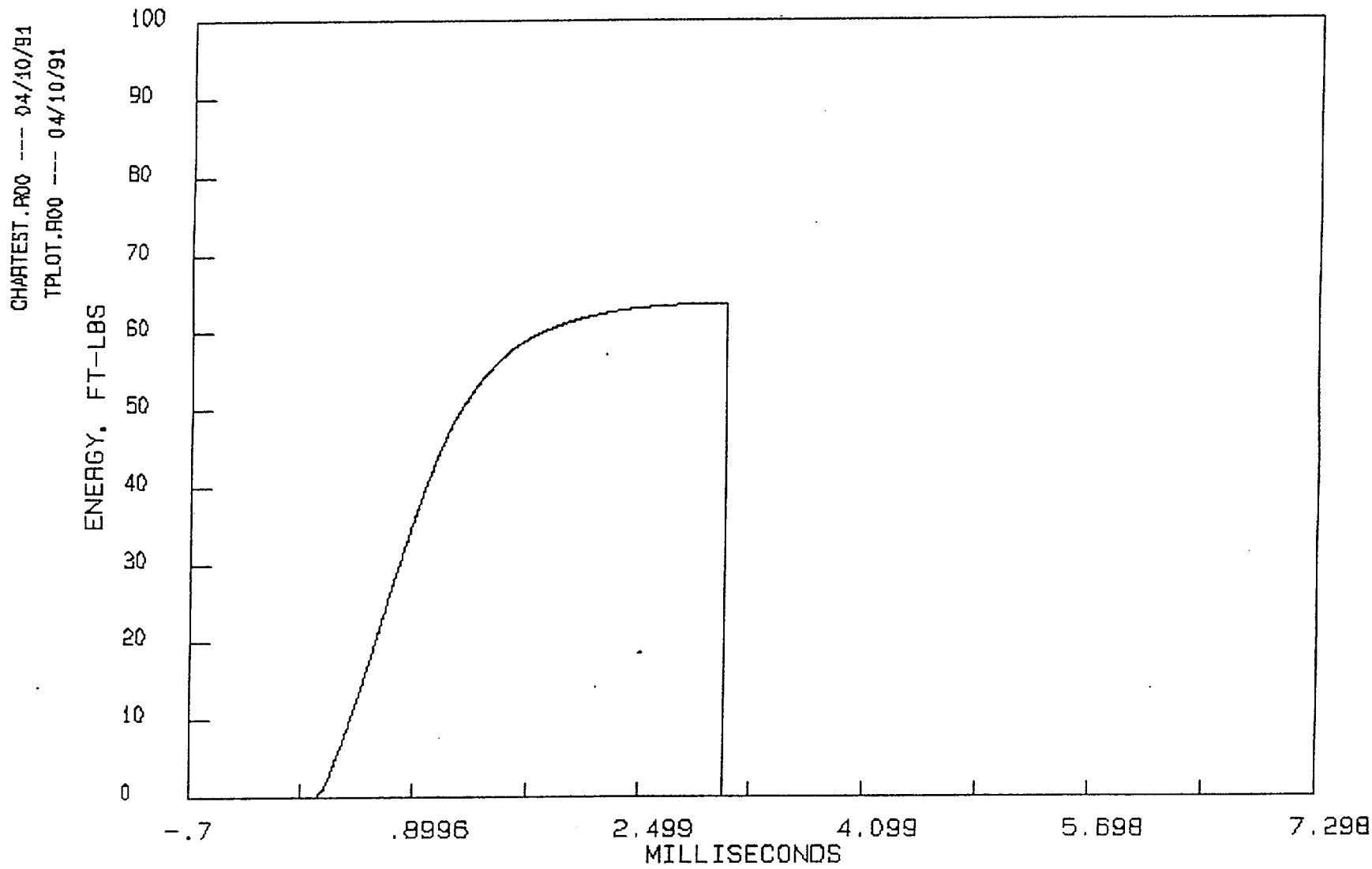

PROJ. NO. 1215-001 QA NO. 00001

LOAD - TIME TRACE FOR SPECIMEN WT39

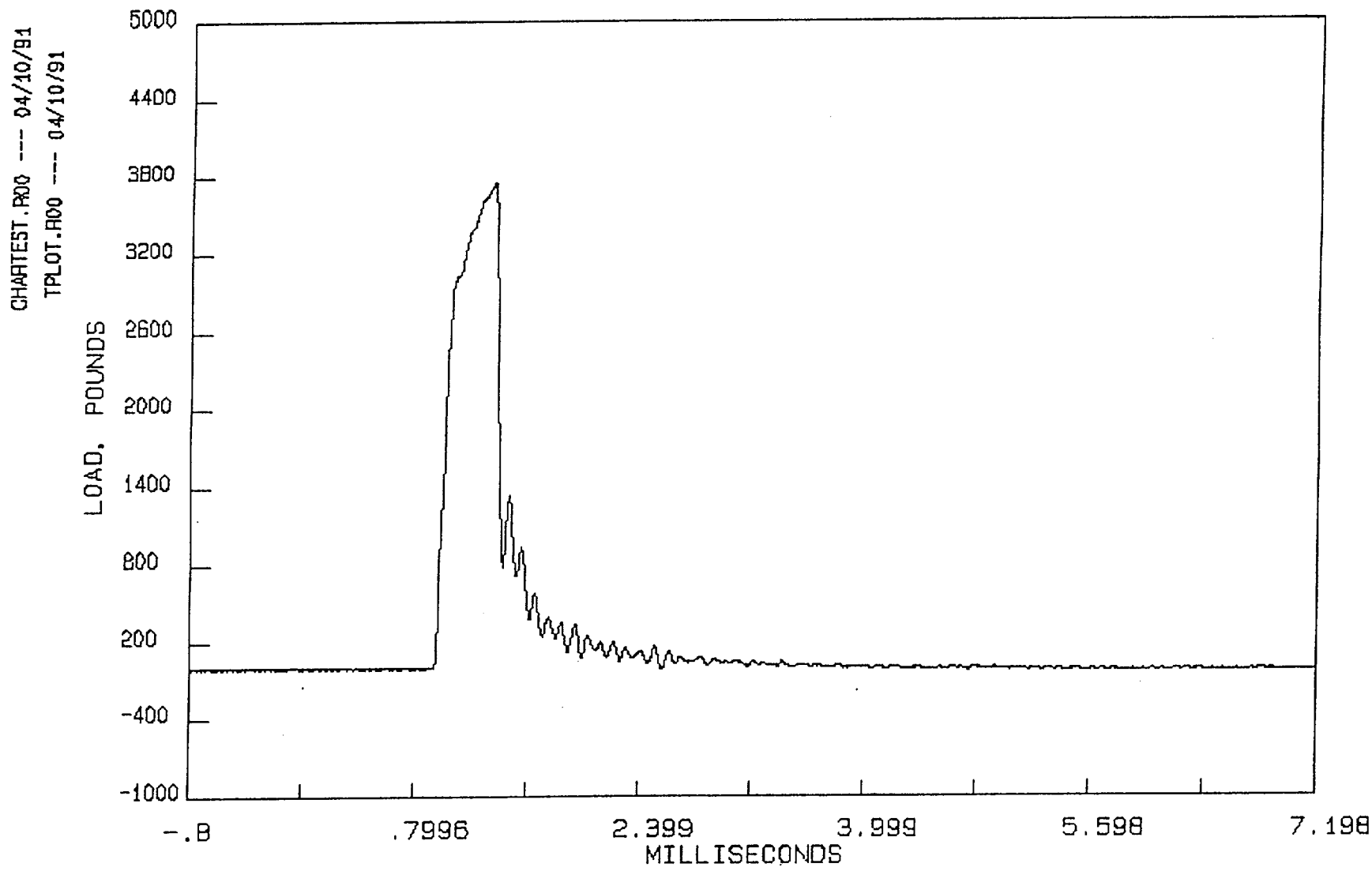

PROJ. NO. 1215-001 QA NO. 00001

ENERGY - TIME TRACE FOR SPECIMEN WT39

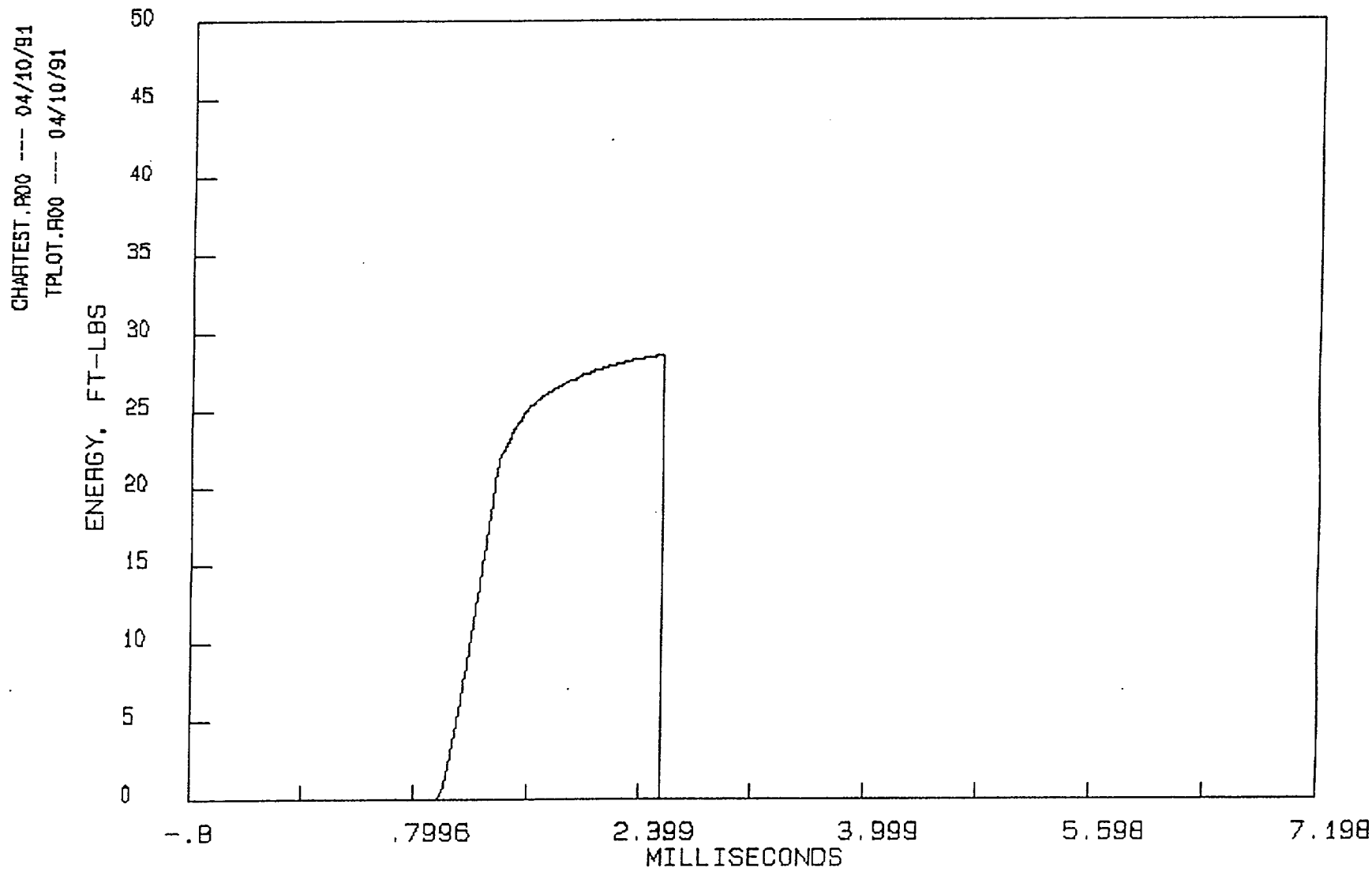

PROJ. NO. 1215-001 QA NO. 00001

LOAD - TIME TRACE FOR SPECIMEN WT38

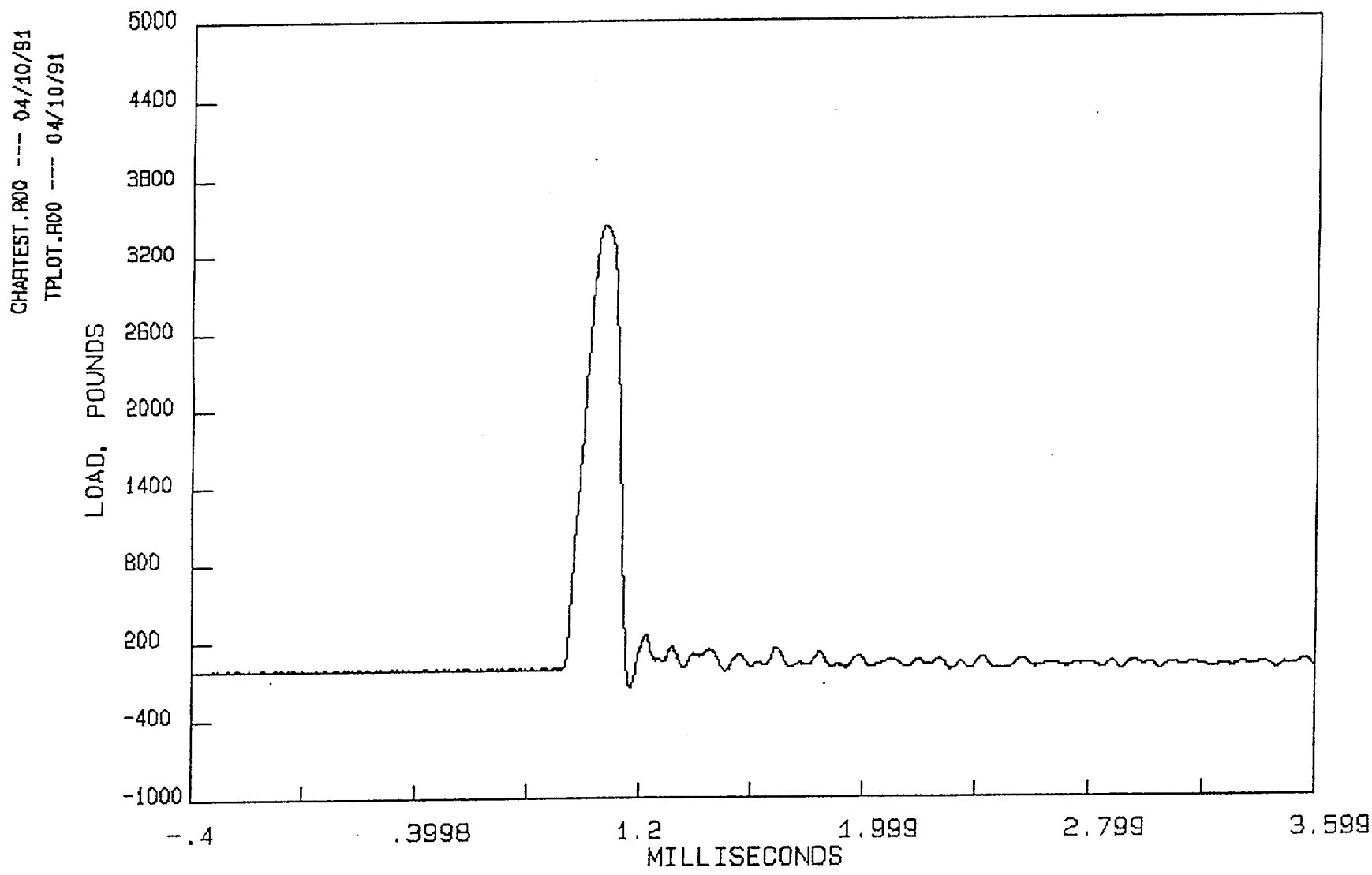

PROJ. NO. 1215-001 QA NO. 00001

ENERGY - TIME TRACE FOR SPECIMEN WT38

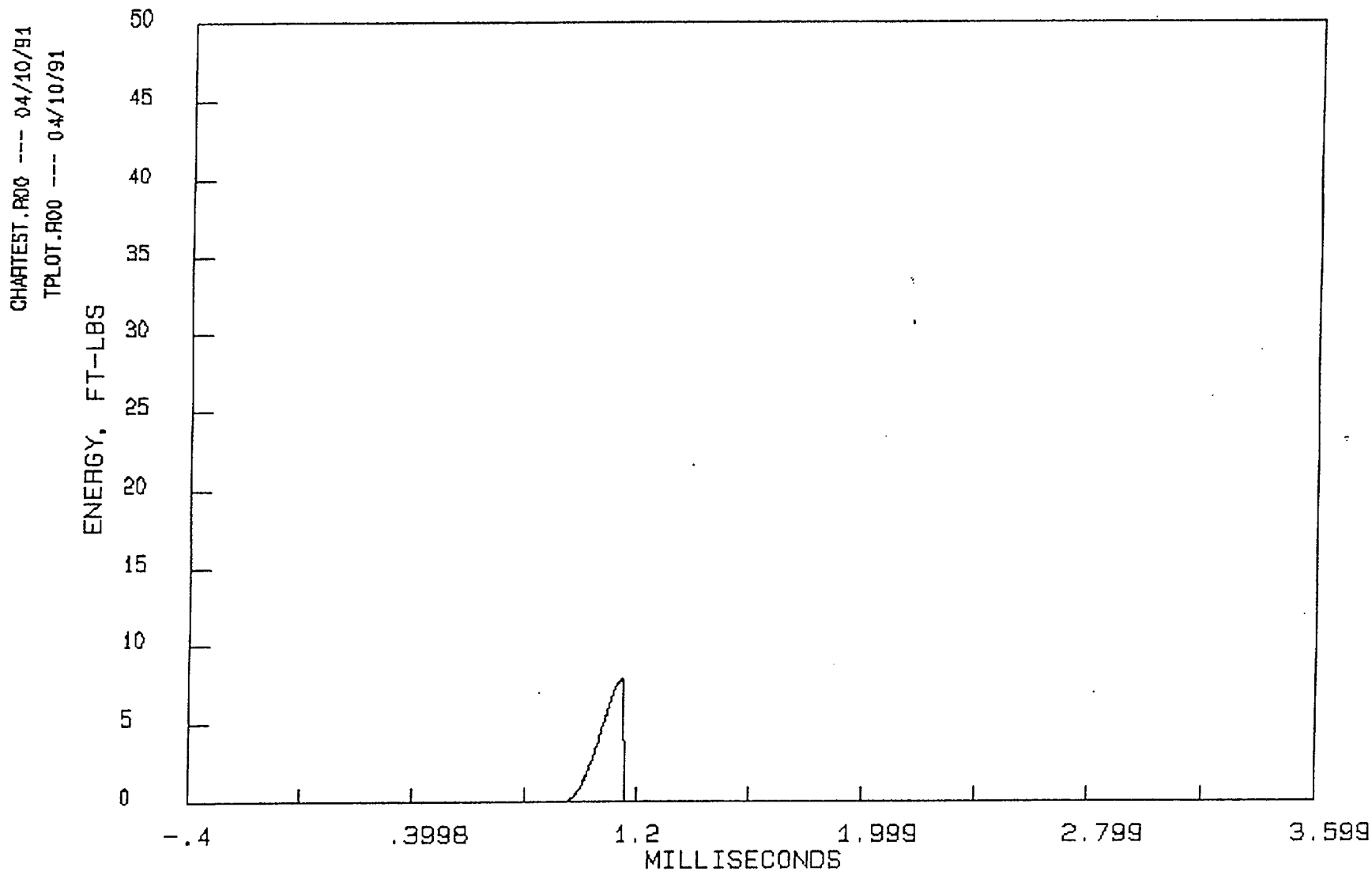

PROJ. NO. 1215-001 QA NO. 00001

LOAD - TIME TRACE FOR SPECIMEN WT40

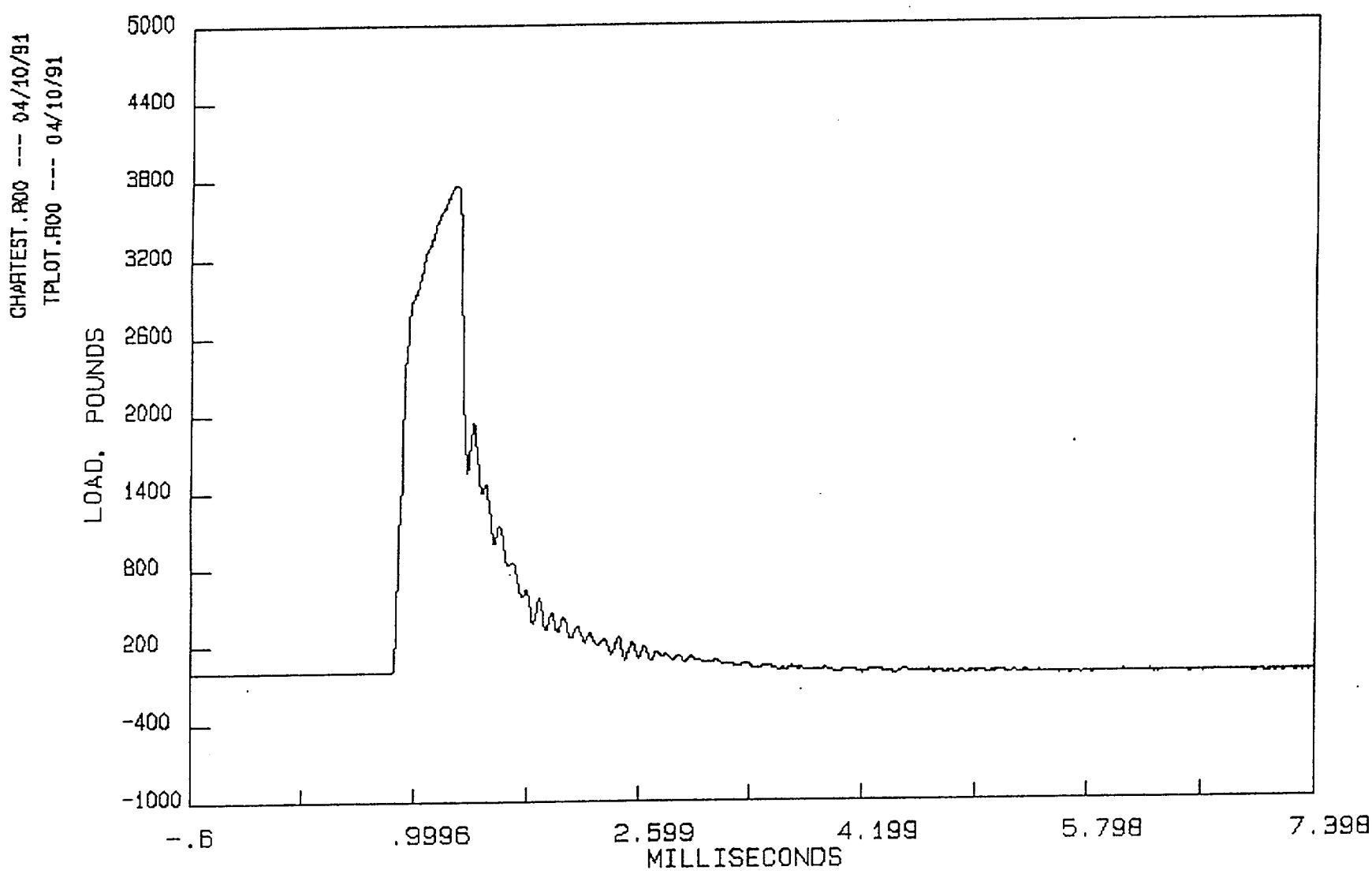

PROJ. NO. 1215-001 QA NO. 00001

ENERGY - TIME TRACE FOR SPECIMEN WT40

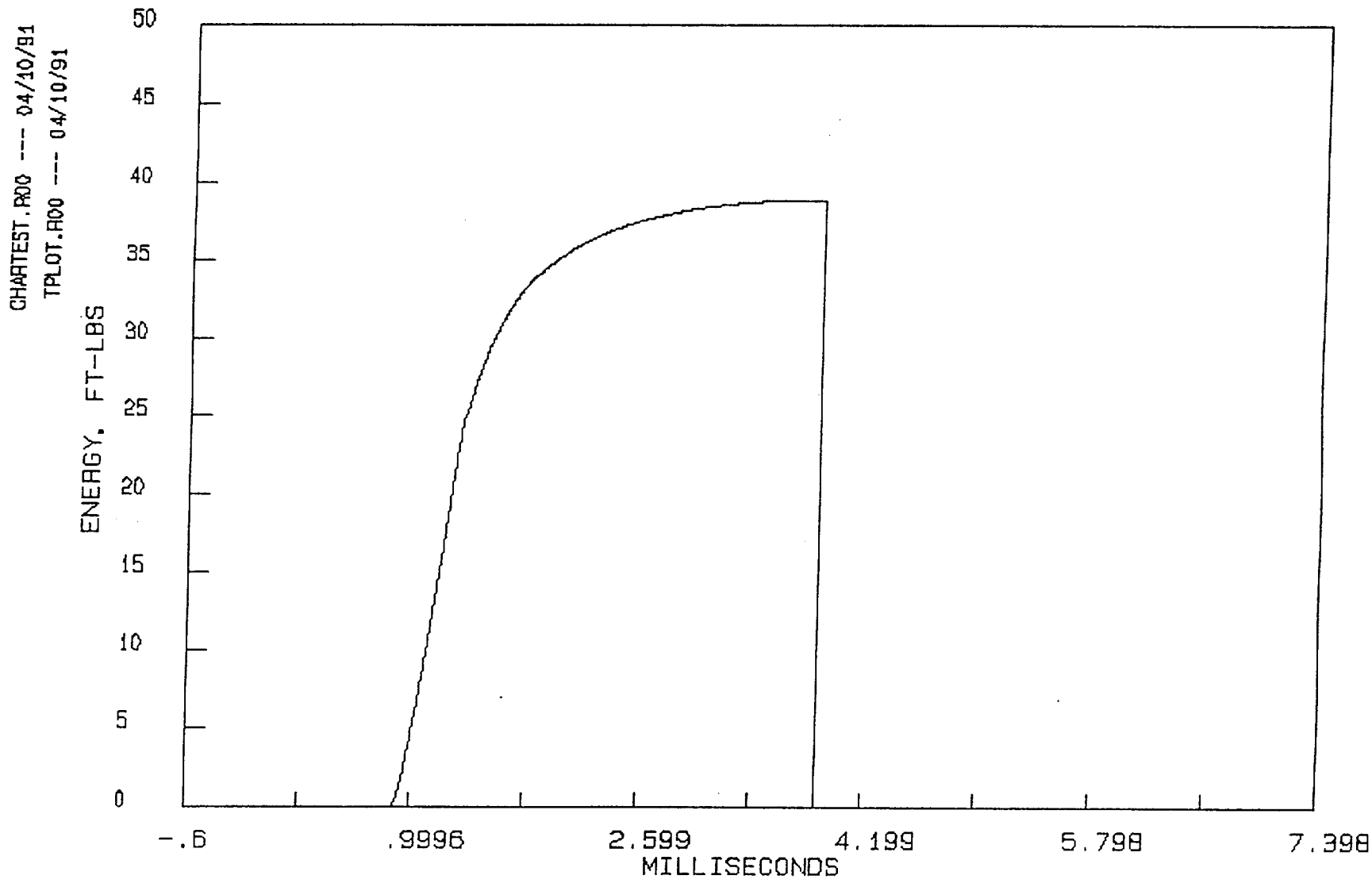

PROJ. NO. 1215-001 QA NO. 00001

LOAD - TIME TRACE FOR SPECIMEN WT32

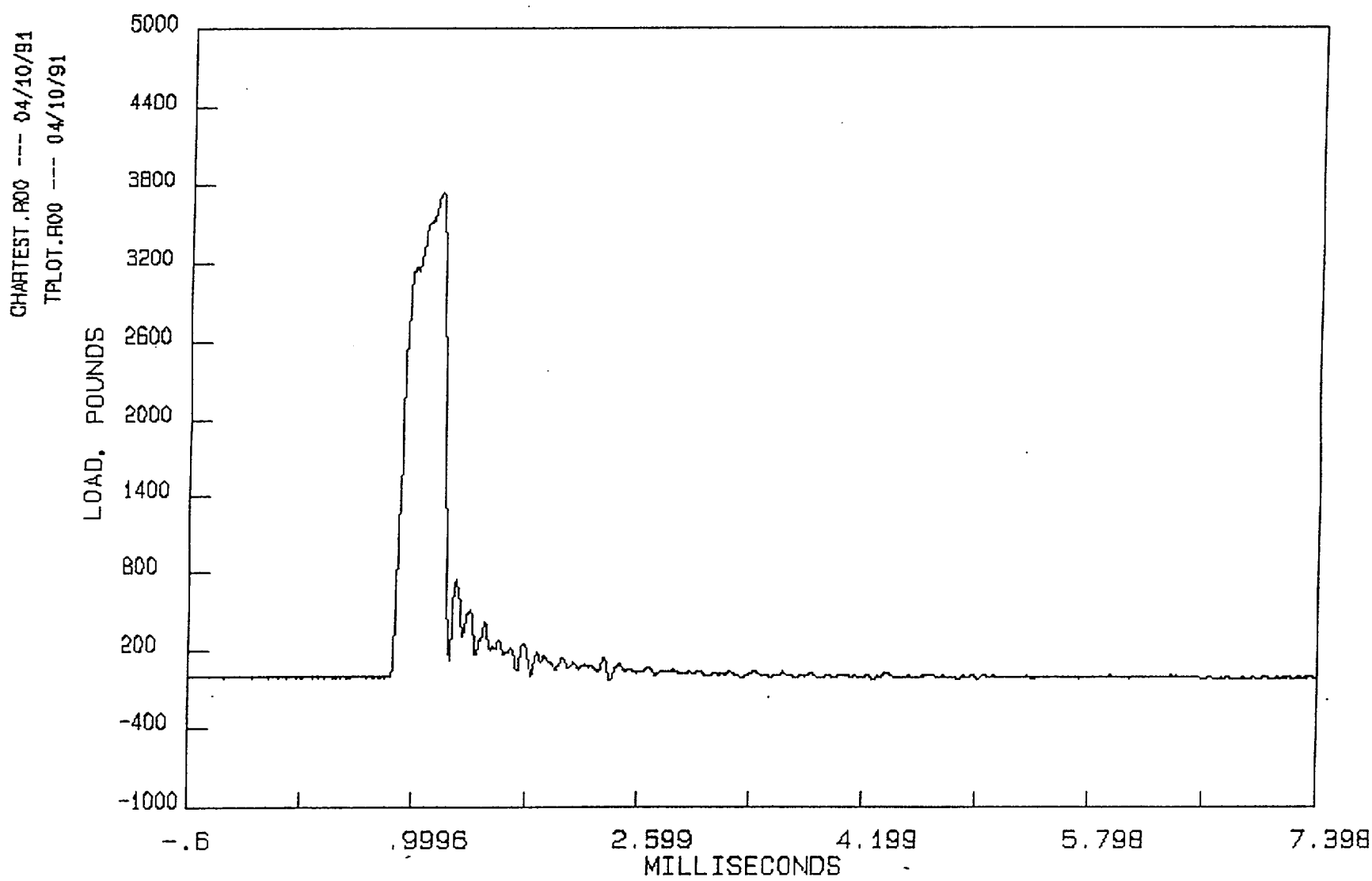

PROJ. NO. 1215-001 QA NO. 00001

ENERGY - TIME TRACE FOR SPECIMEN WT32

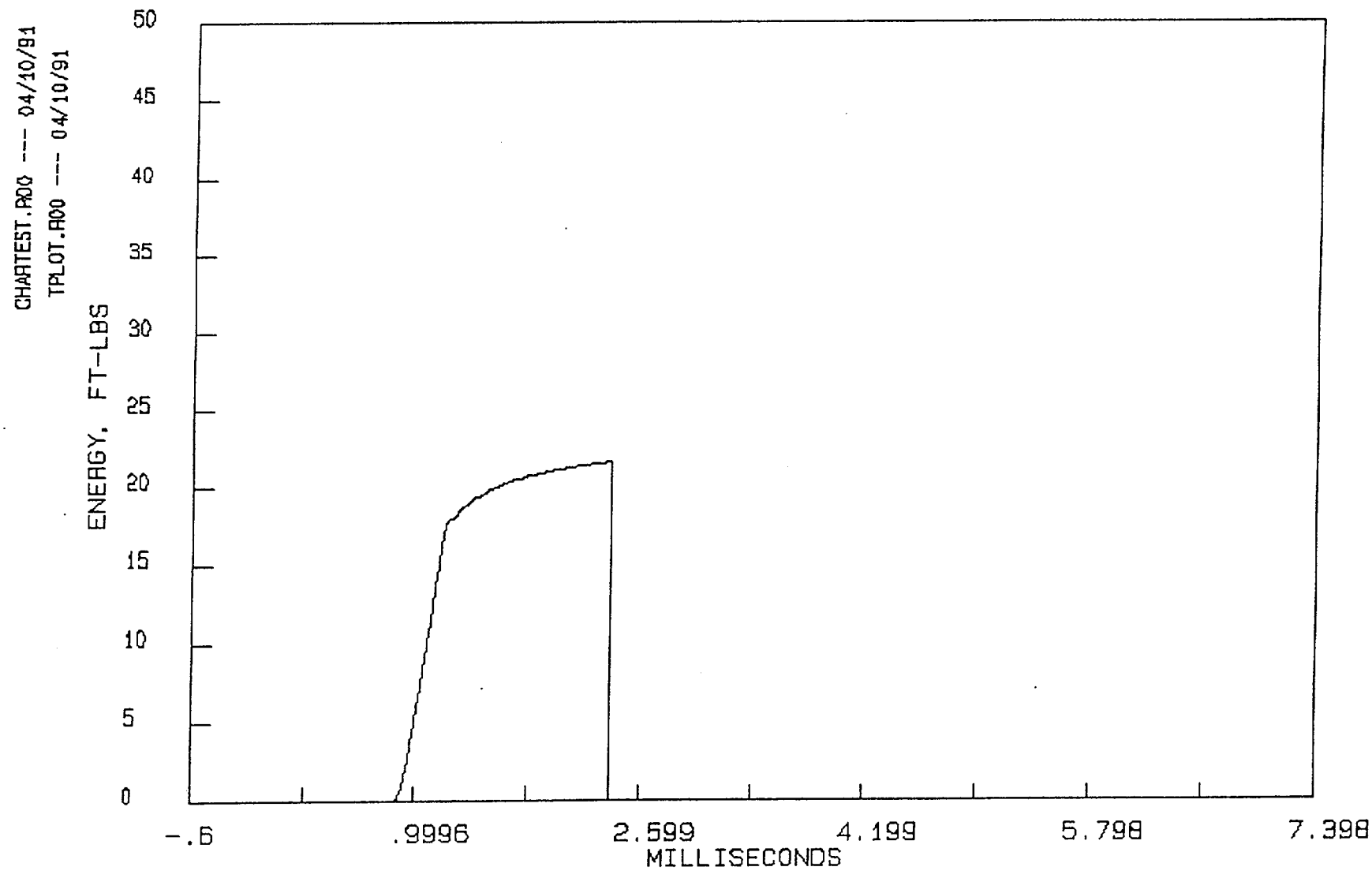

PROJ. NO. 1215-001 QA NO. 00001

LOAD - TIME TRACE FOR SPECIMEN WT37

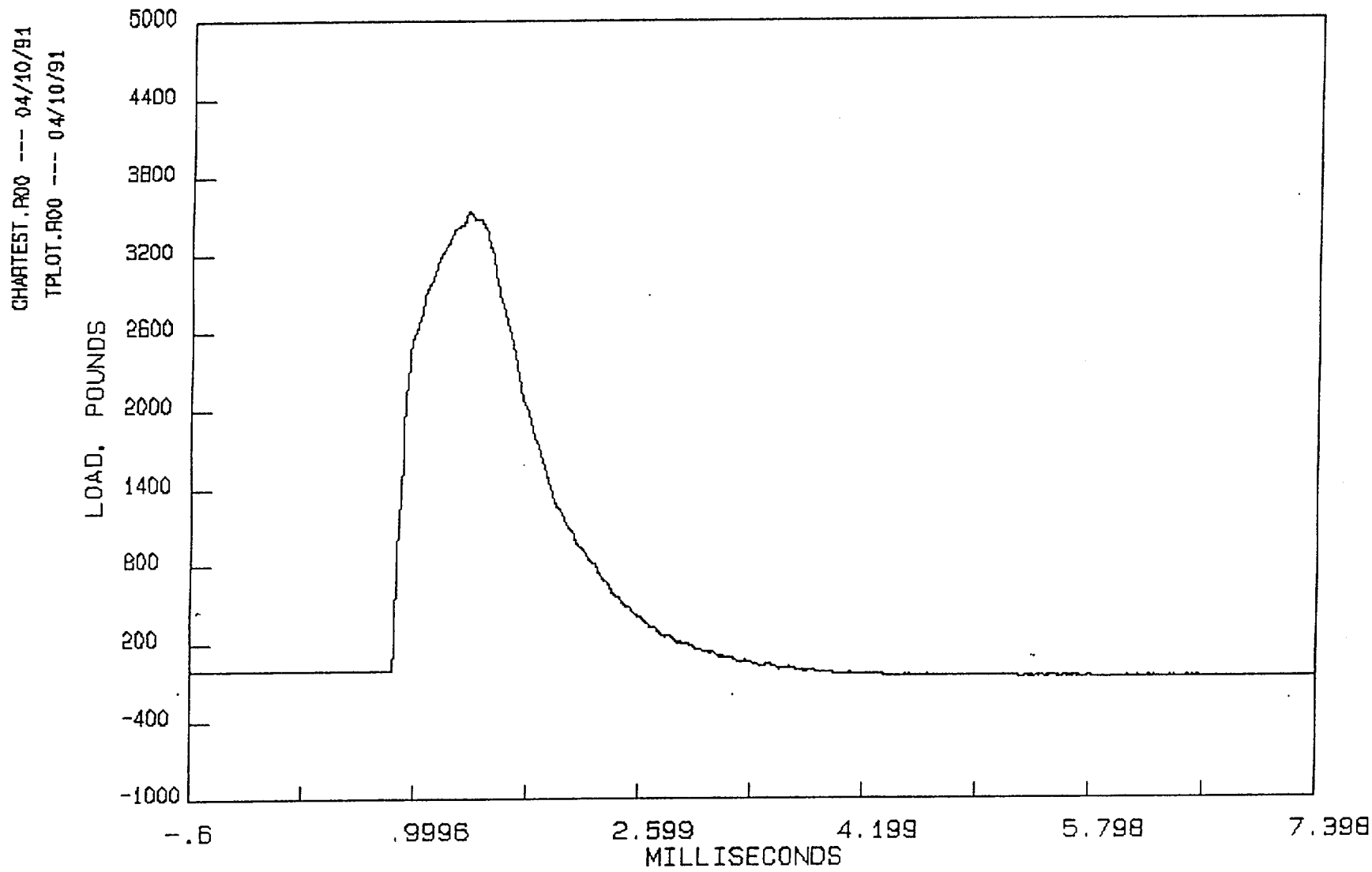

PROJ. NO. 1215-001 QA NO. 00001

ENERGY - TIME TRACE FOR SPECIMEN WT37

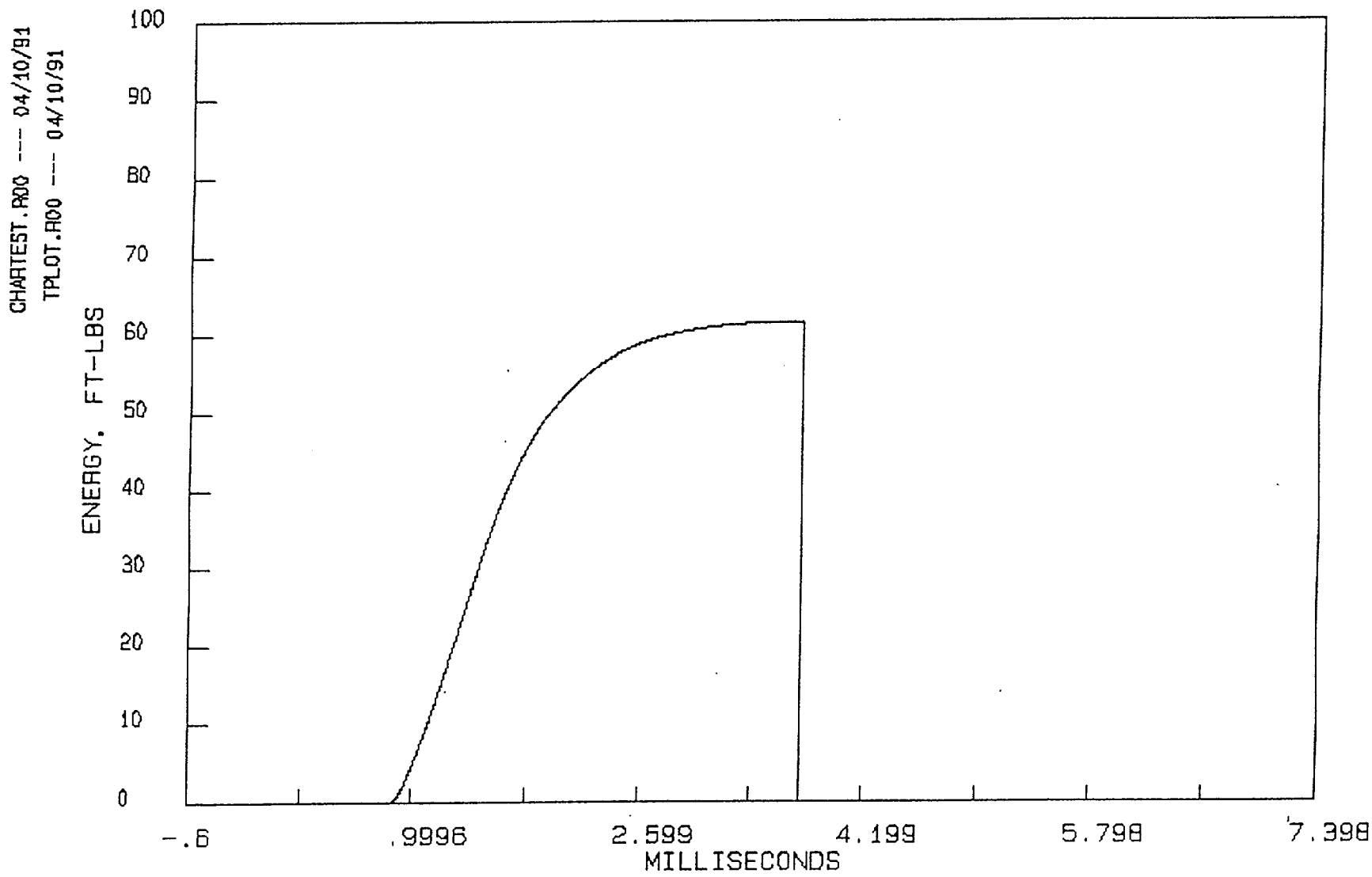

PROJ. NO. 1215-001 QA NO. 00001

LOAD - TIME TRACE FOR SPECIMEN WT36

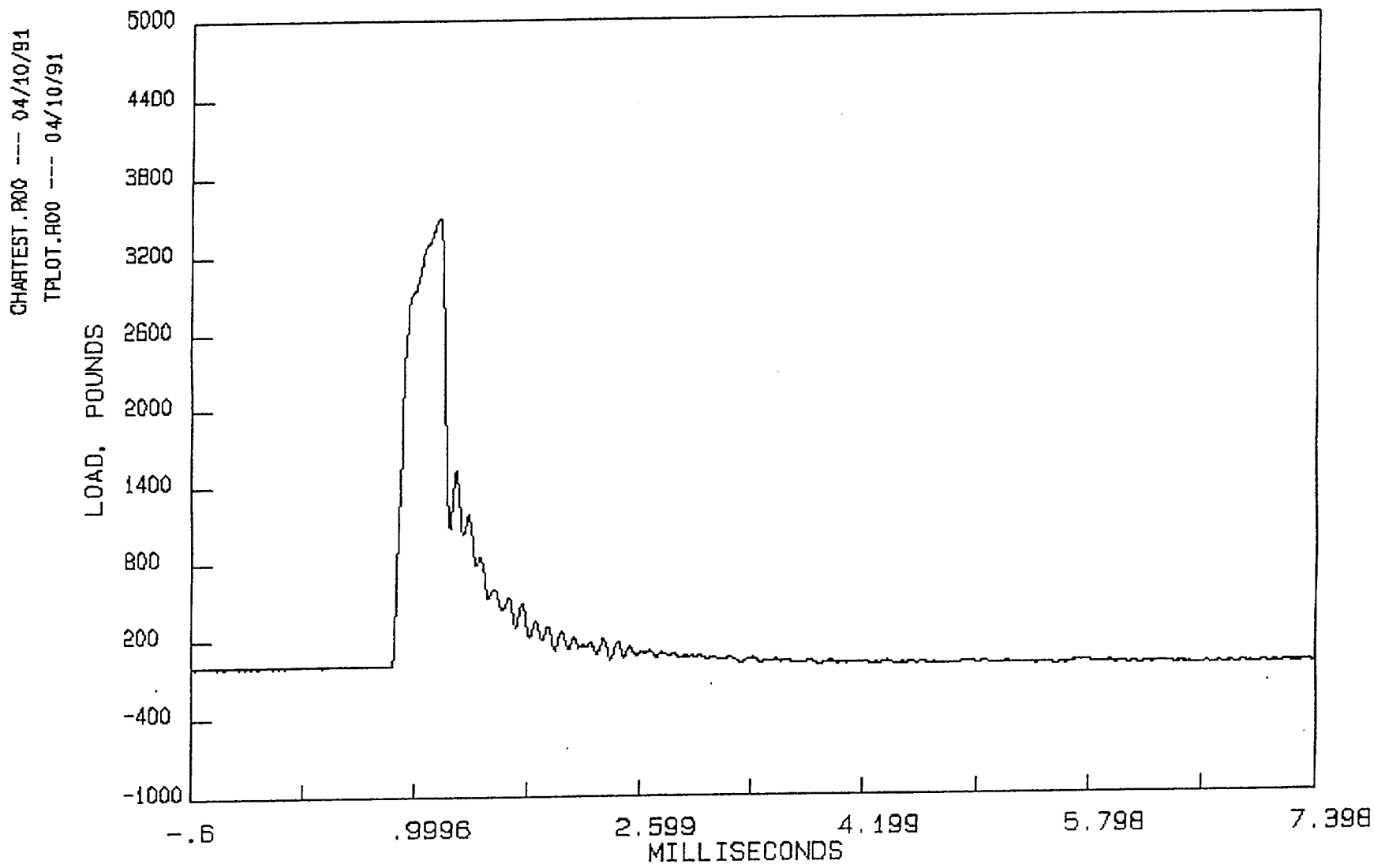

PROJ. NO. 1215-001 QA NO. 00001

ENERGY - TIME TRACE FOR SPECIMEN WT36

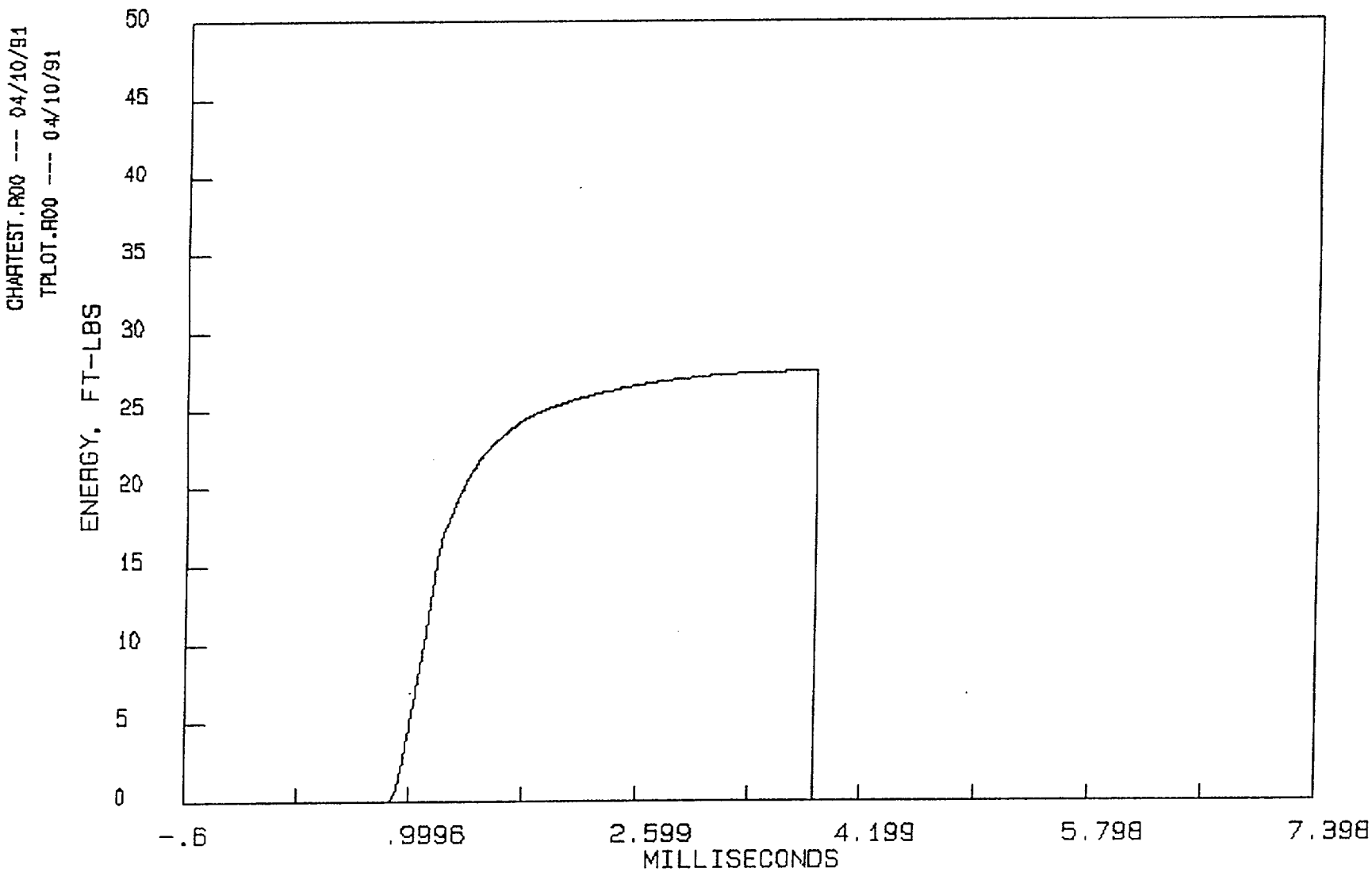

PROJ. NO. 1215-001 QA NO. 00001

LOAD - TIME TRACE FOR SPECIMEN WT43

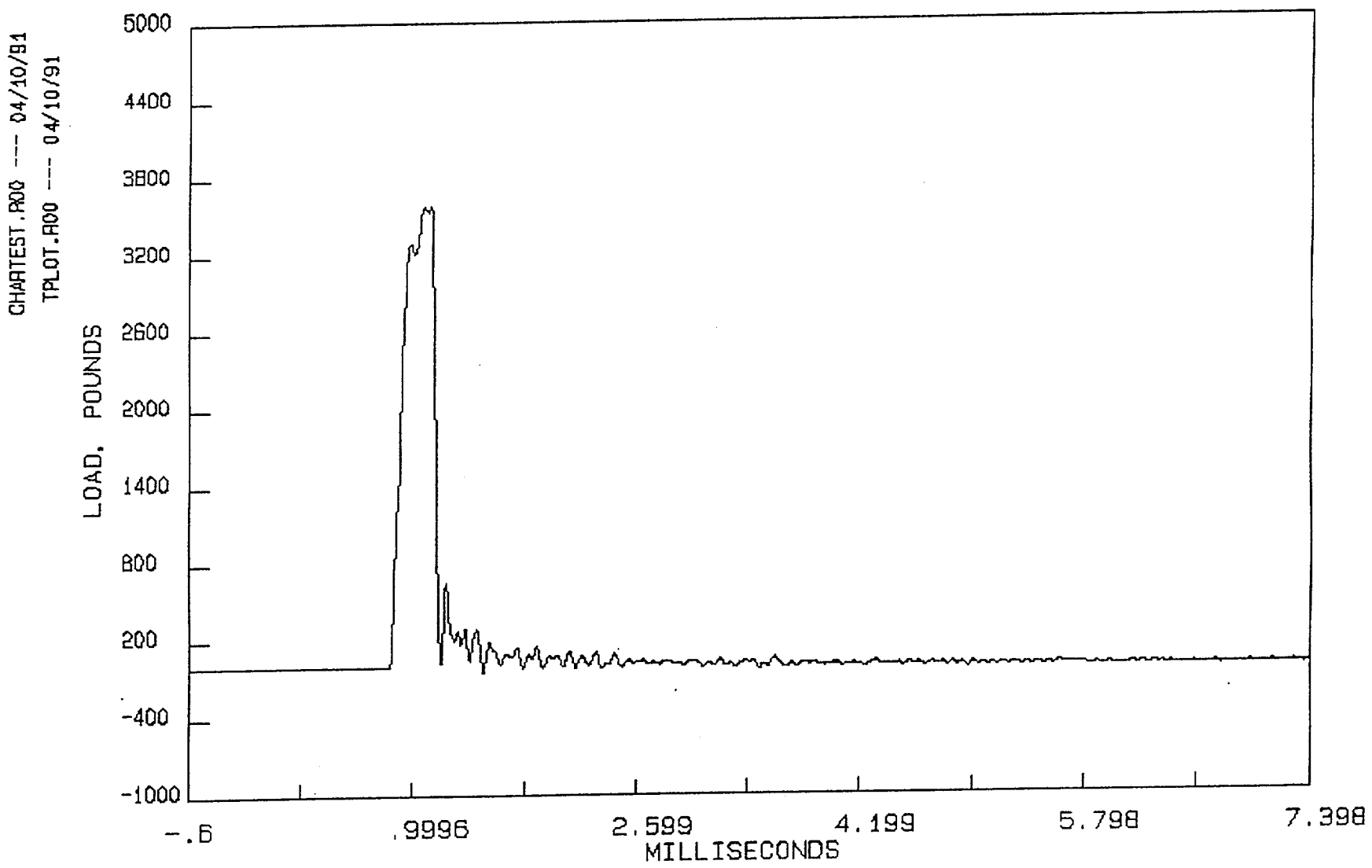

PROJ. NO. 1215-001 QA NO. 00001

ENERGY - TIME TRACE FOR SPECIMEN WT43

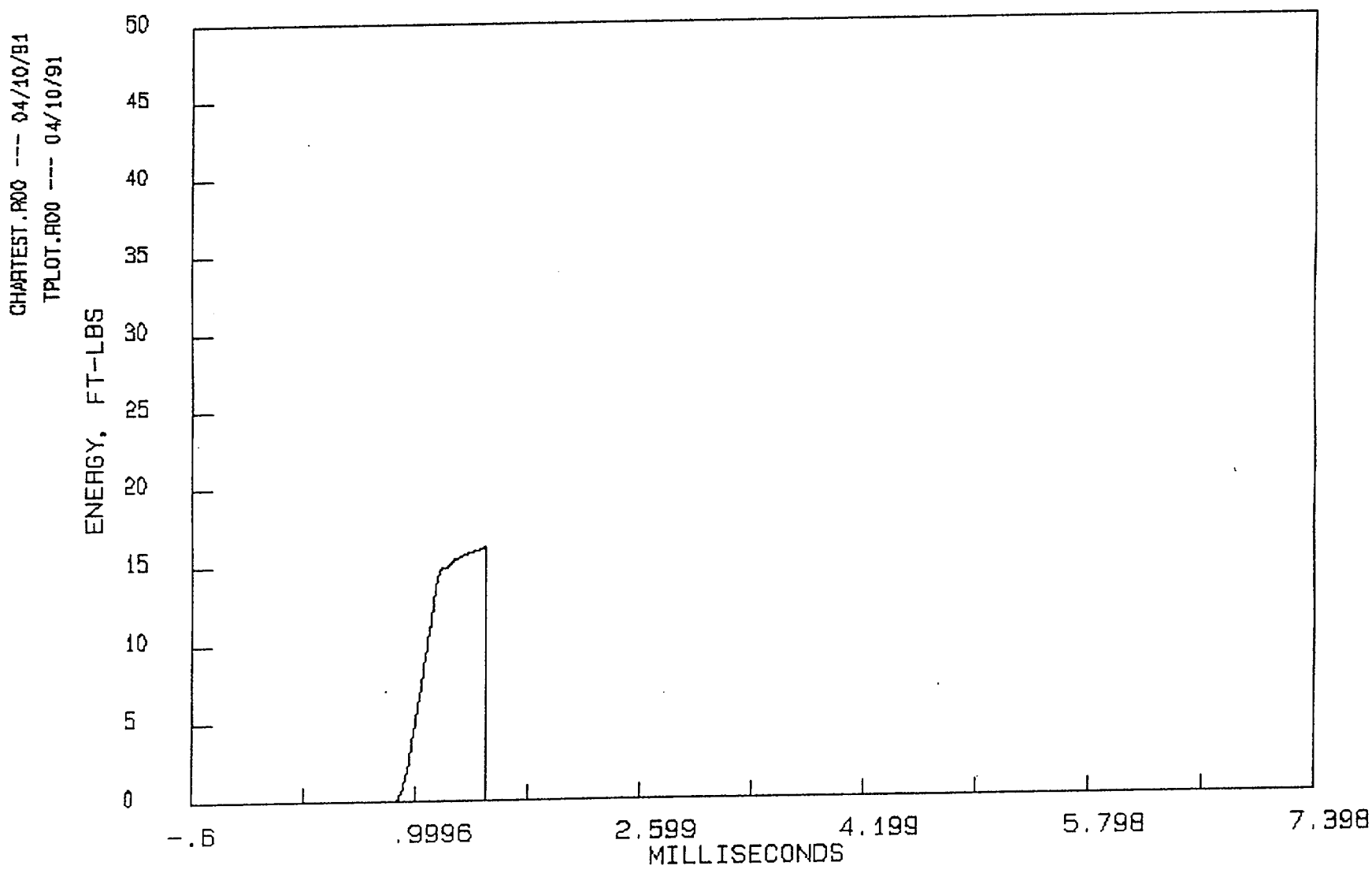

PROJ. NO. 1215-001 QA NO. 00001

LOAD - TIME TRACE FOR SPECIMEN WW43

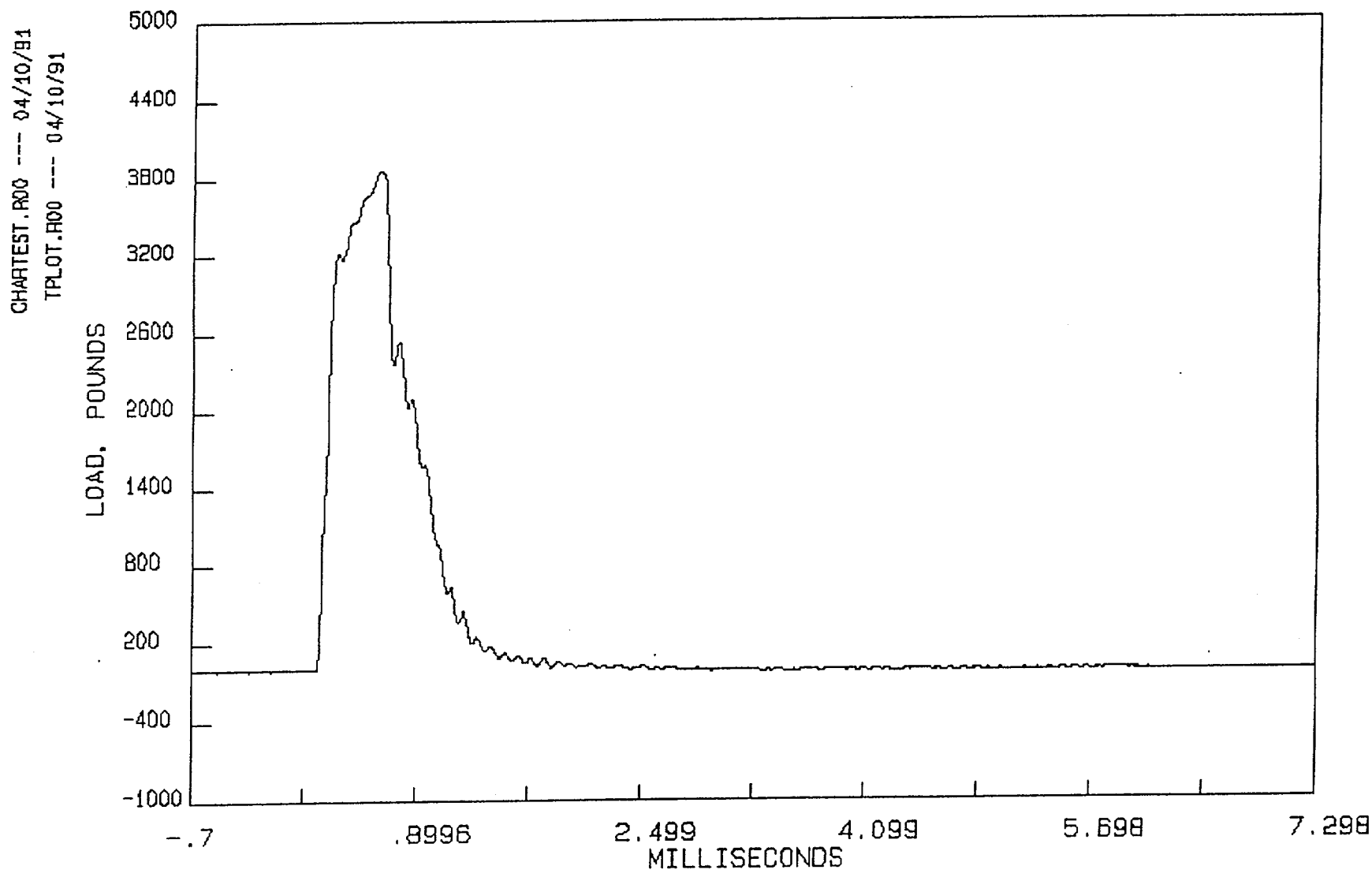

PROJ. NO. 1215-001 QA NO. 00001

ENERGY - TIME TRACE FOR SPECIMEN WW43

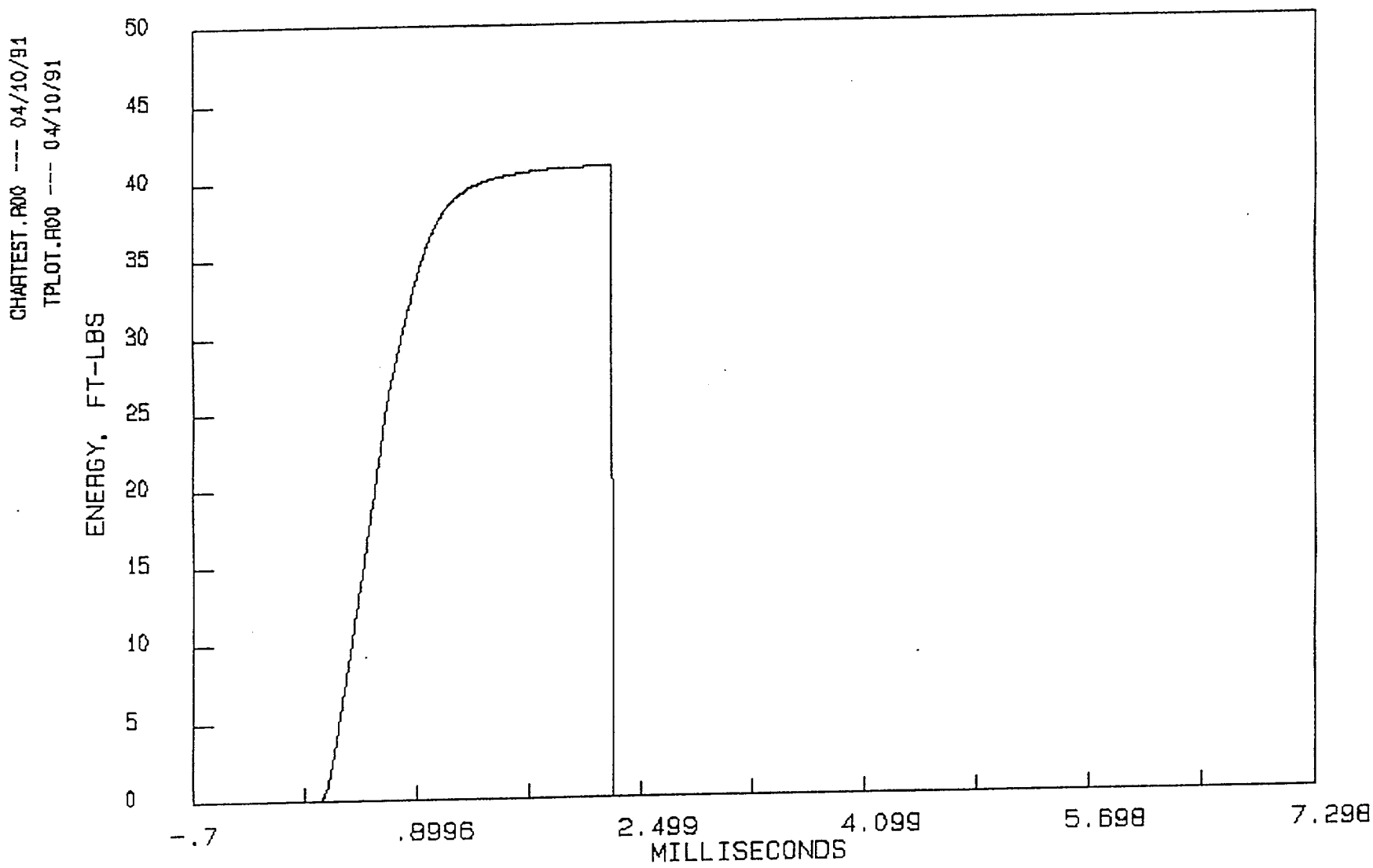

PROJ. NO. 1215-001 QA NO. 00001

LOAD - TIME TRACE FOR SPECIMEN WW36

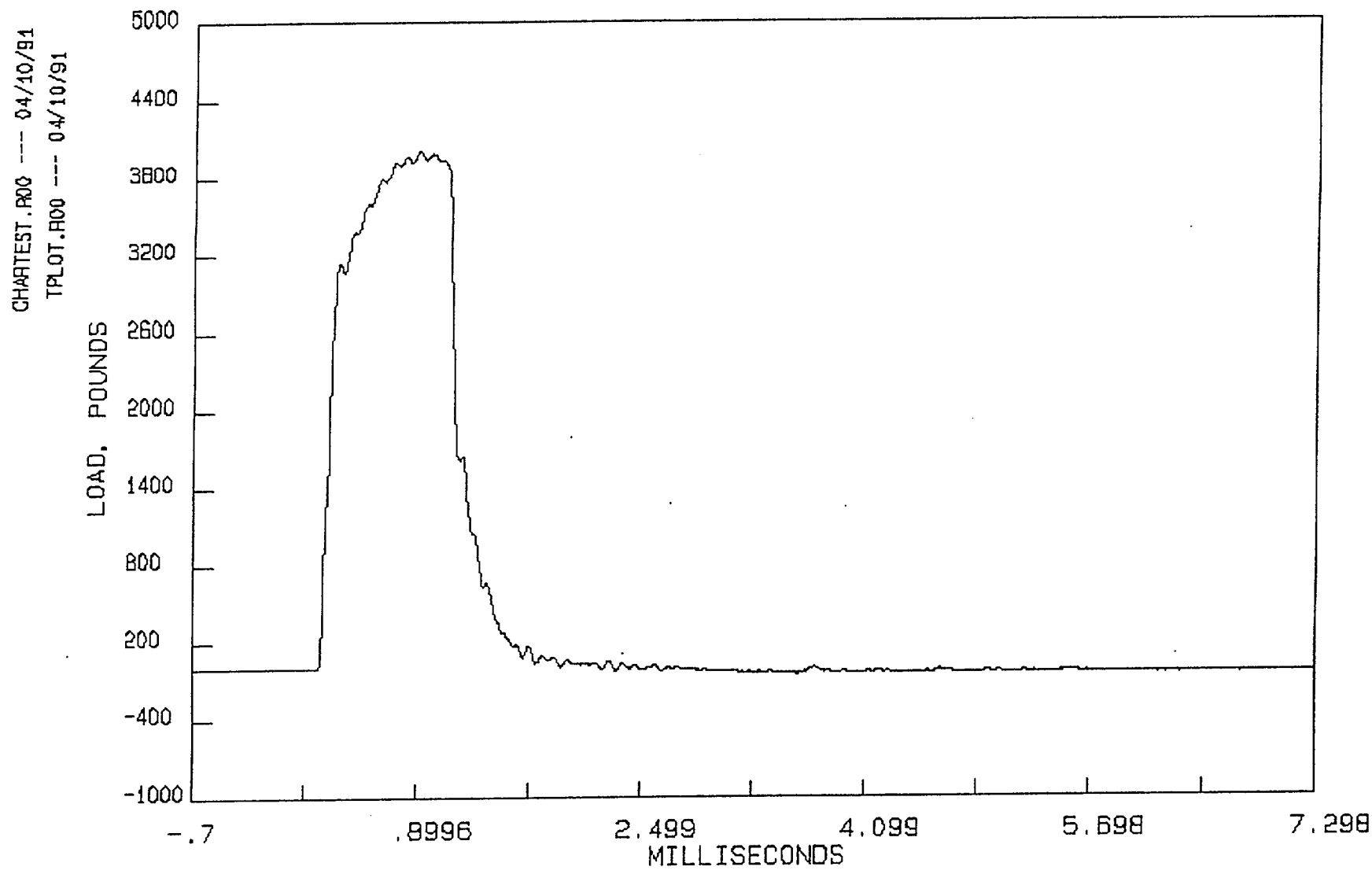

PROJ. NO. 1215-001 QA NO. 00001

ENERGY - TIME TRACE FOR SPECIMEN WW36

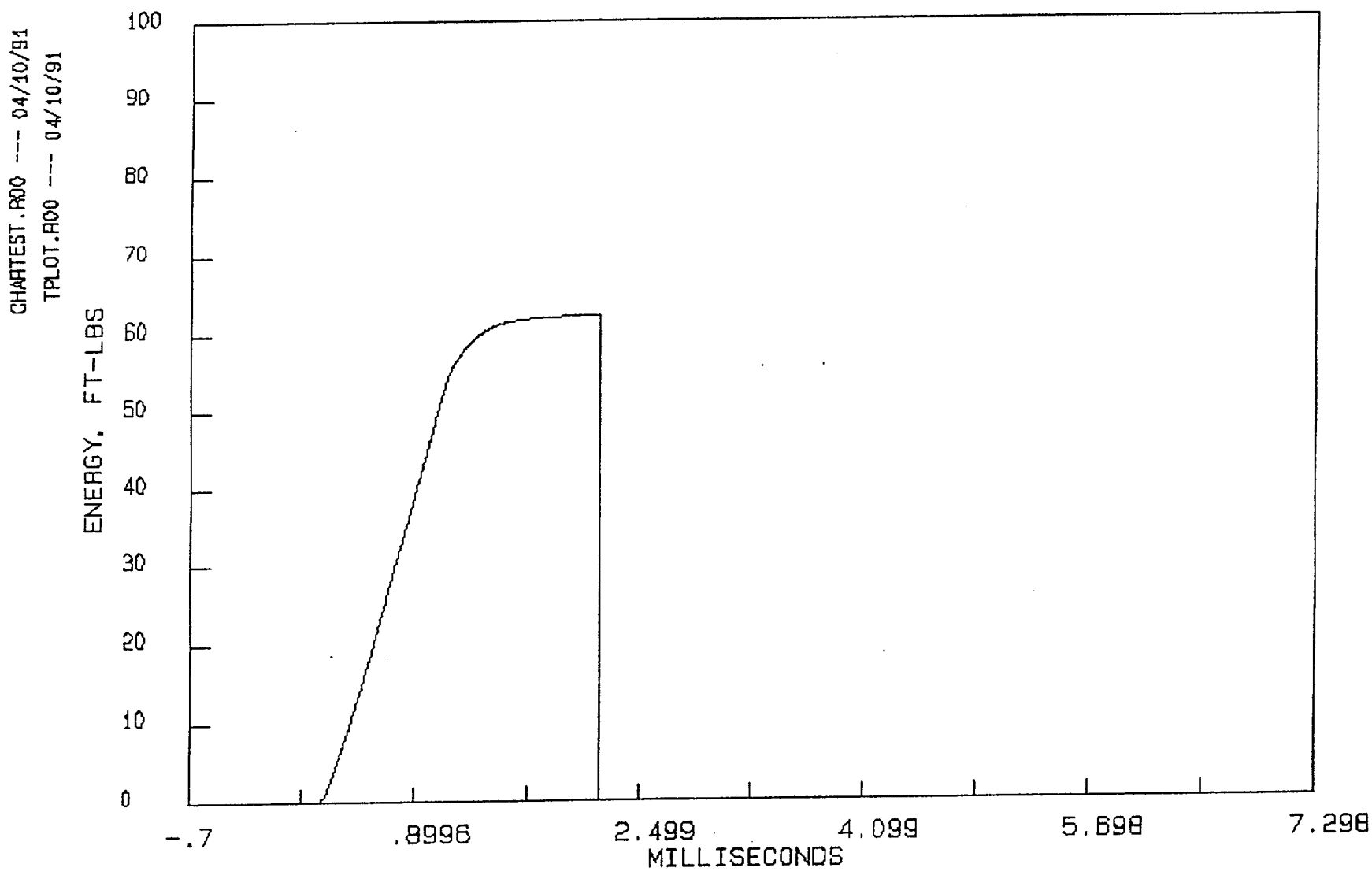

PROJ. NO. 1215-001 QA NO. 00001

LOAD - TIME TRACE FOR SPECIMEN WW37

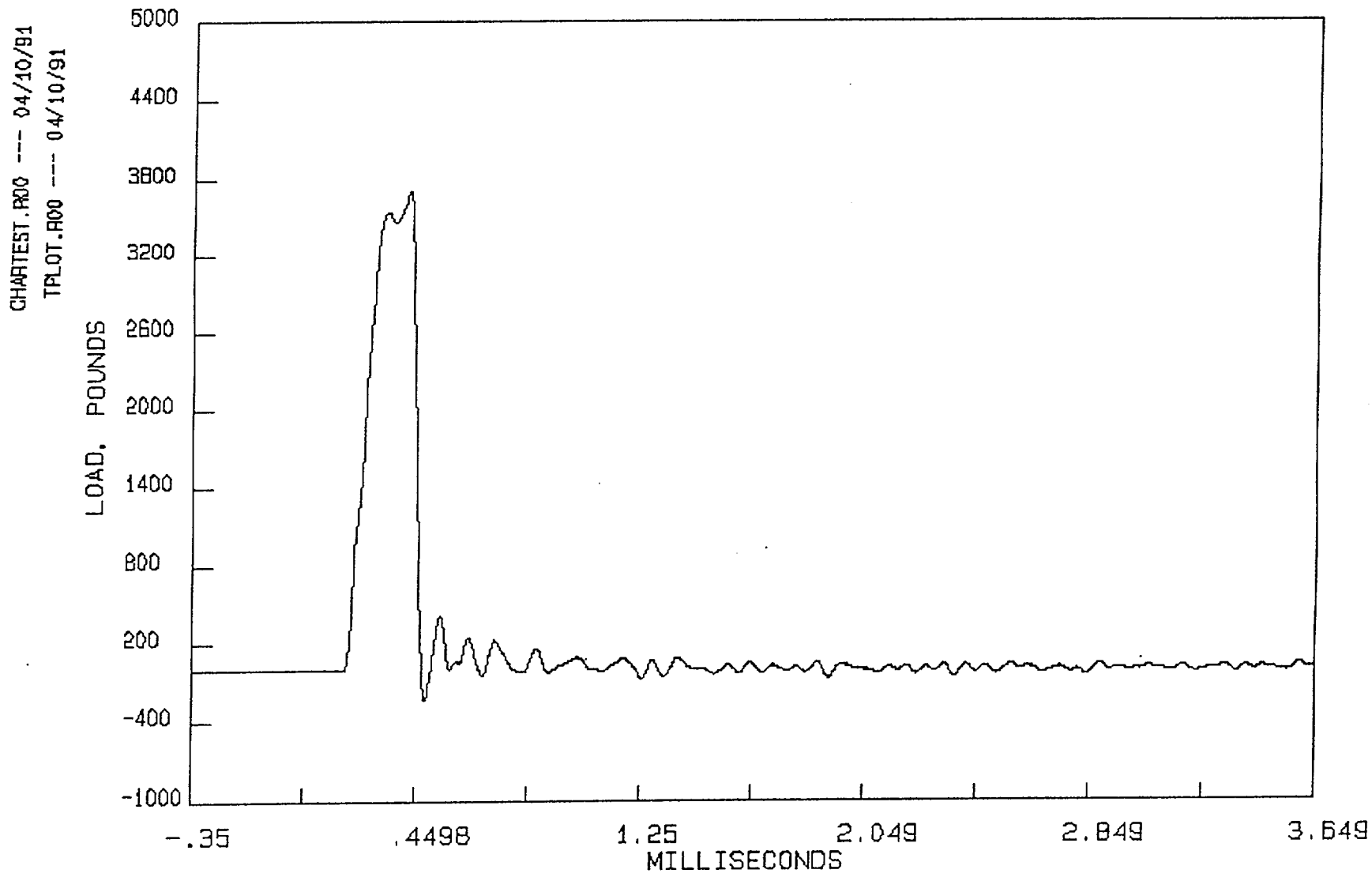

PROJ. NO. 1215-001 QA NO. 00001

ENERGY - TIME TRACE FOR SPECIMEN WW37

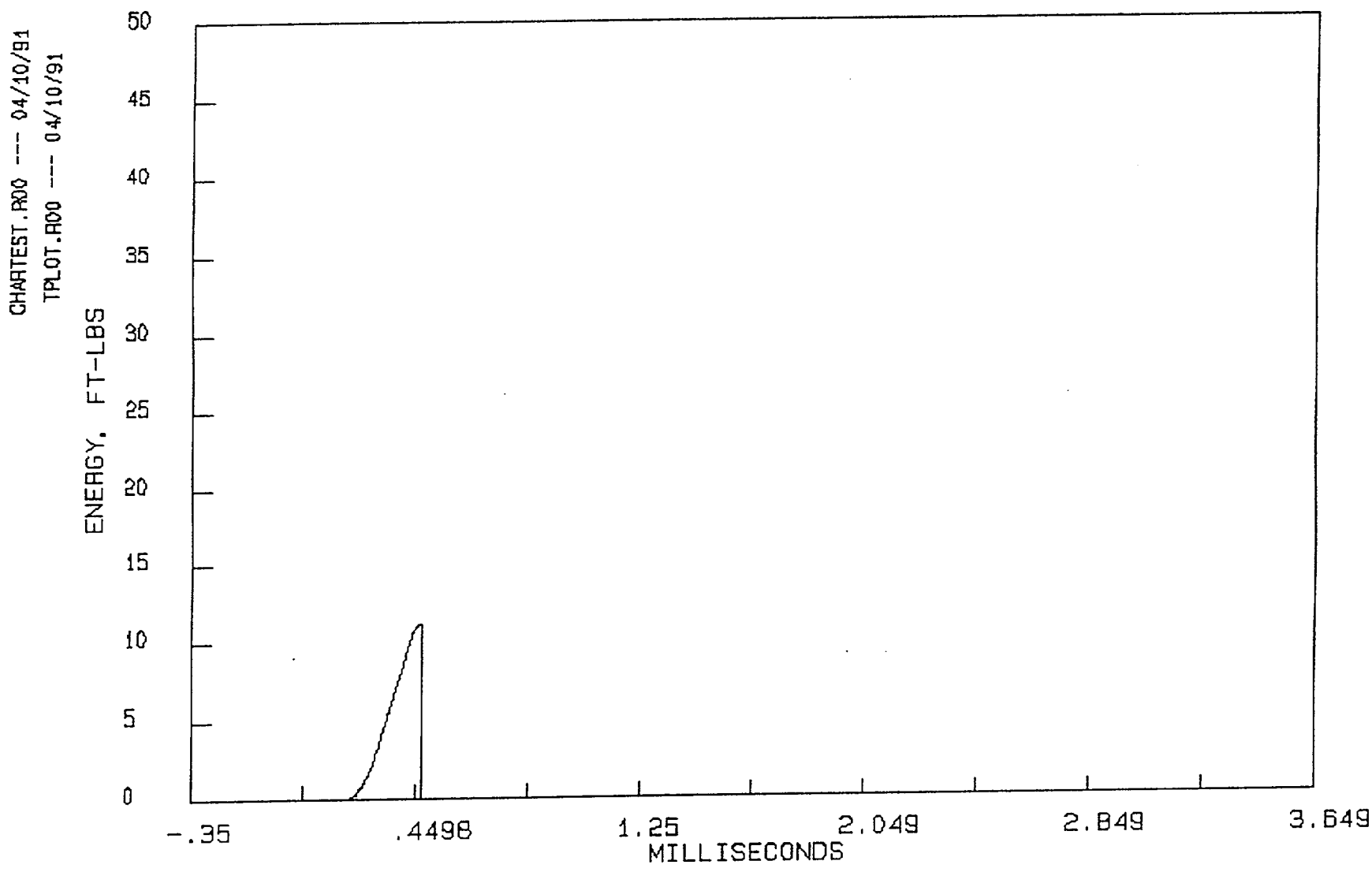

PROJ. NO. 1215-001 QA NO. 99001

LOAD - TIME TRACE FOR SPECIMEN WW31

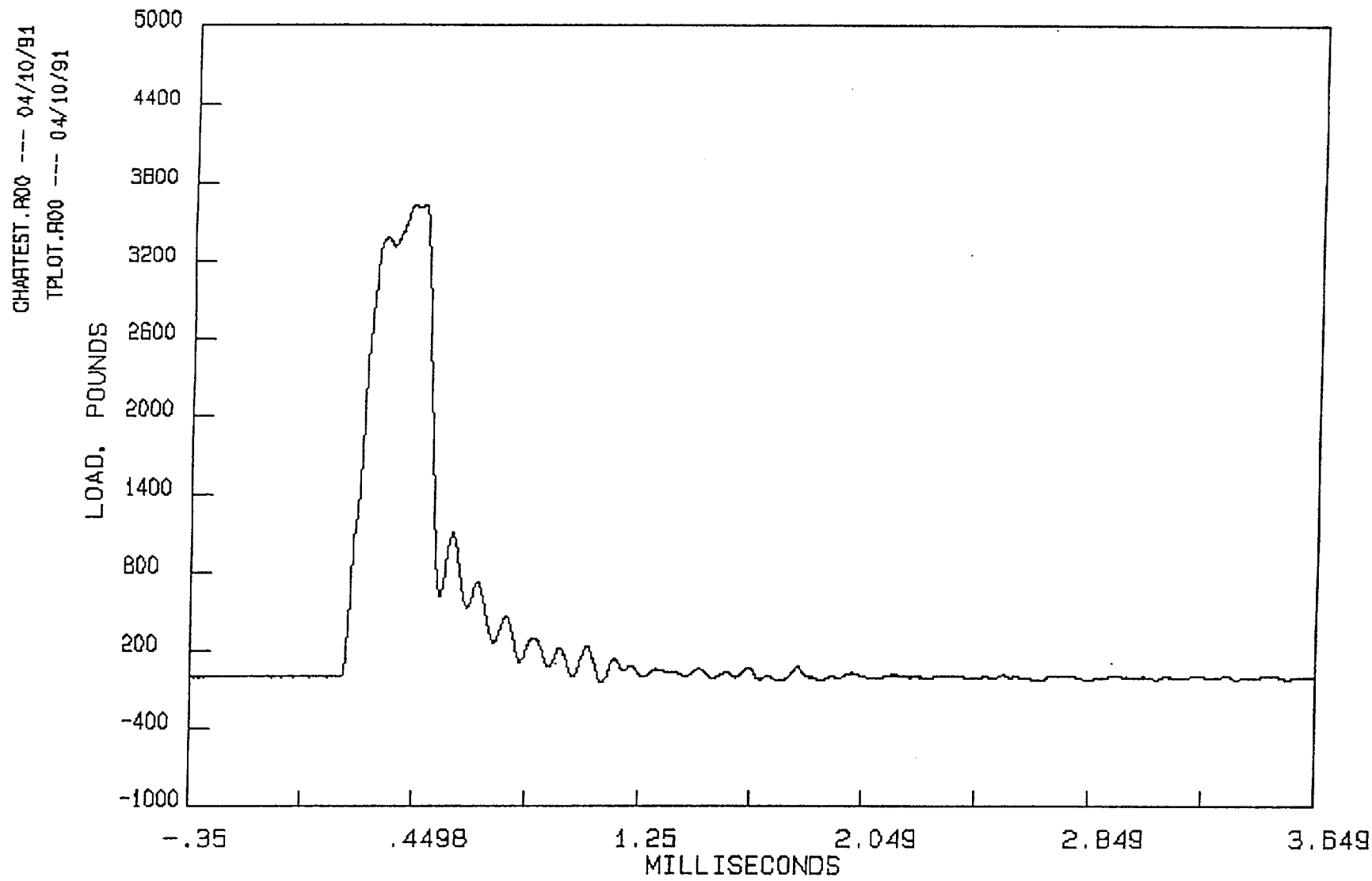

PROJ. NO. 1215-001 QA NO. 99001

ENERGY - TIME TRACE FOR SPECIMEN WW31

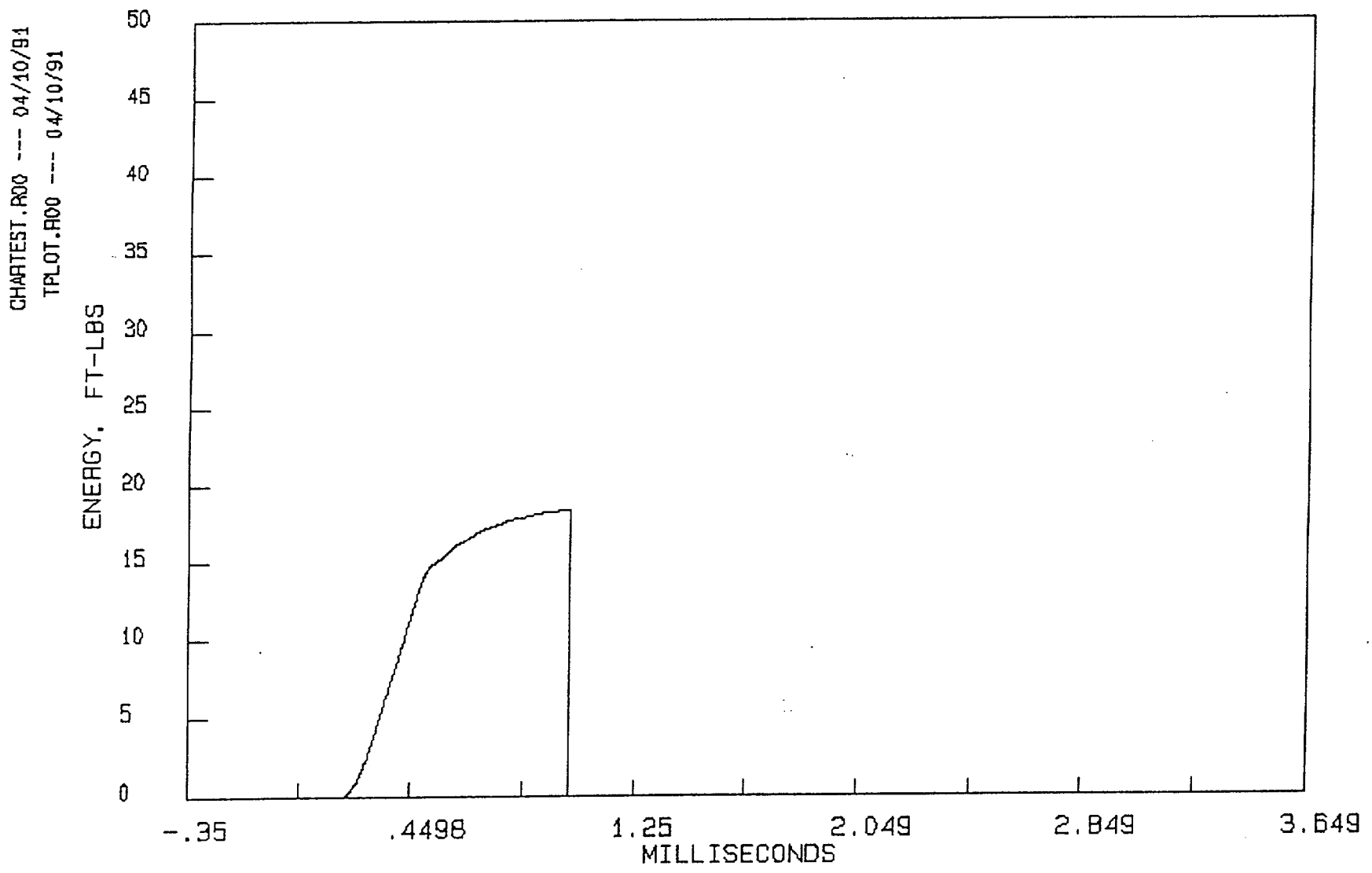

PROJ. NO. 1215-001 QA NO. 99001

LOAD - TIME TRACE FOR SPECIMEN WW35

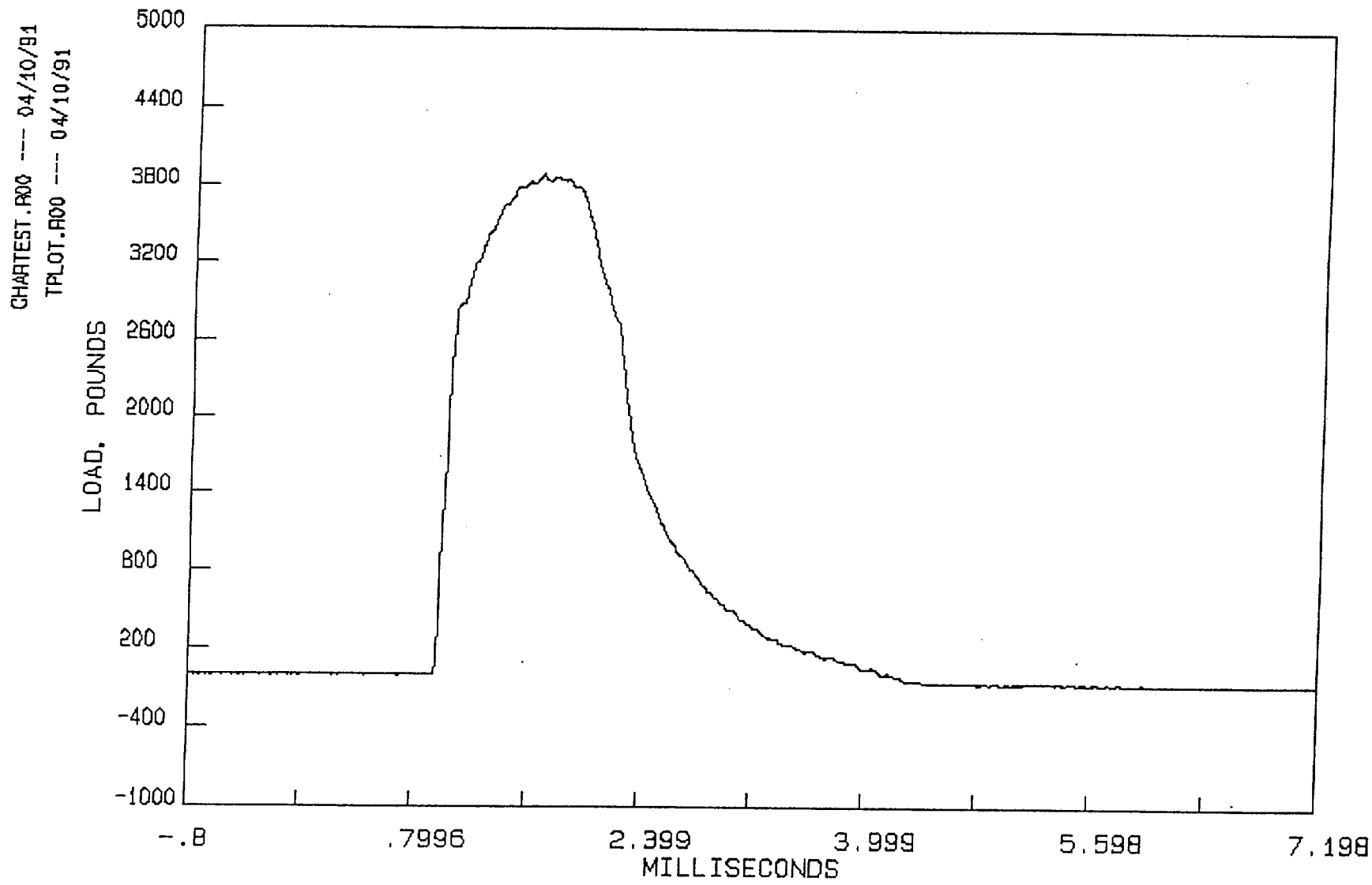

PROJ. NO. 1215-001 QA NO. 99001

ENERGY - TIME TRACE FOR SPECIMEN WW35

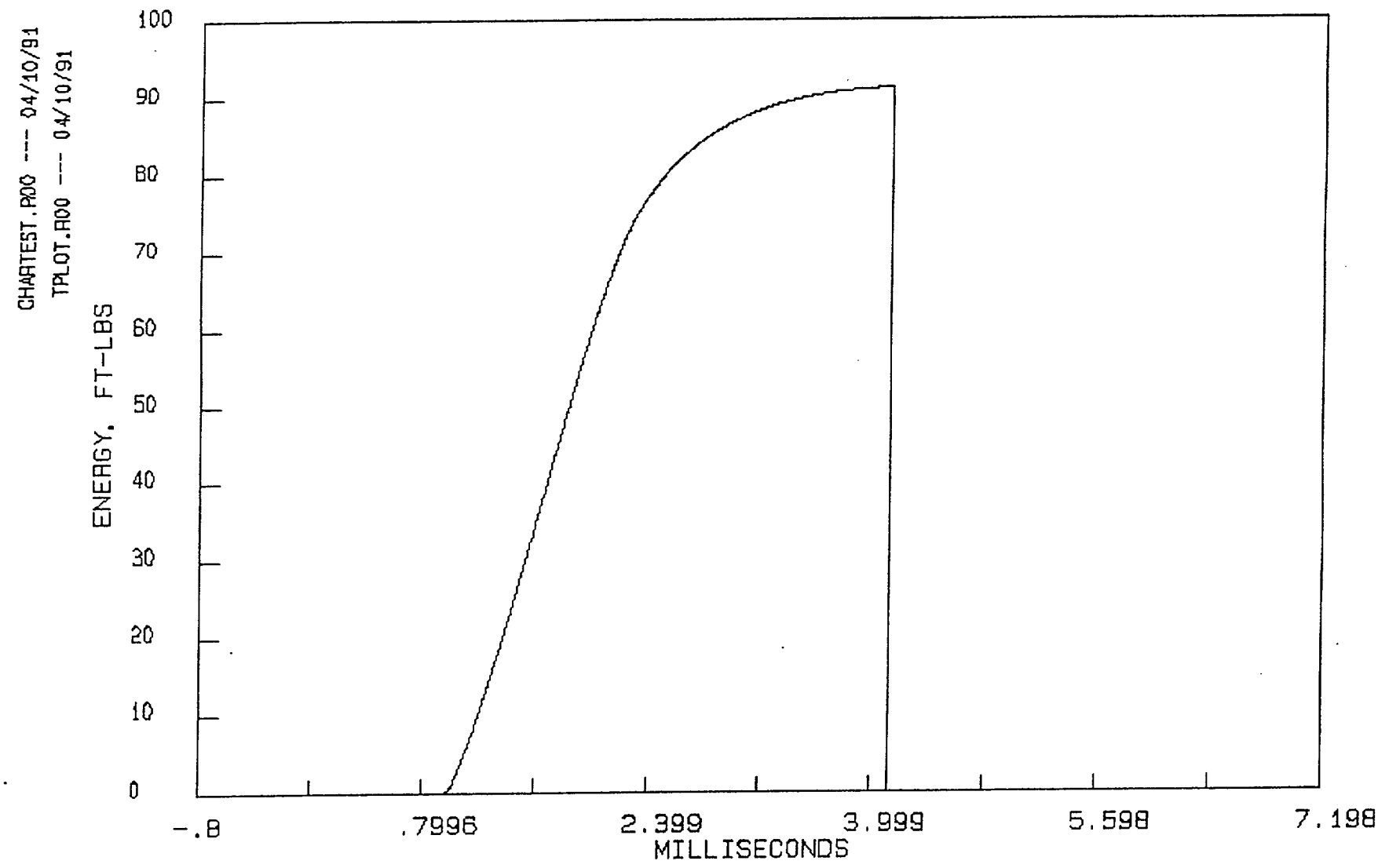

PROJ. NO. 1215-001 QA NO. 99001

LOAD - TIME TRACE FOR SPECIMEN WW42

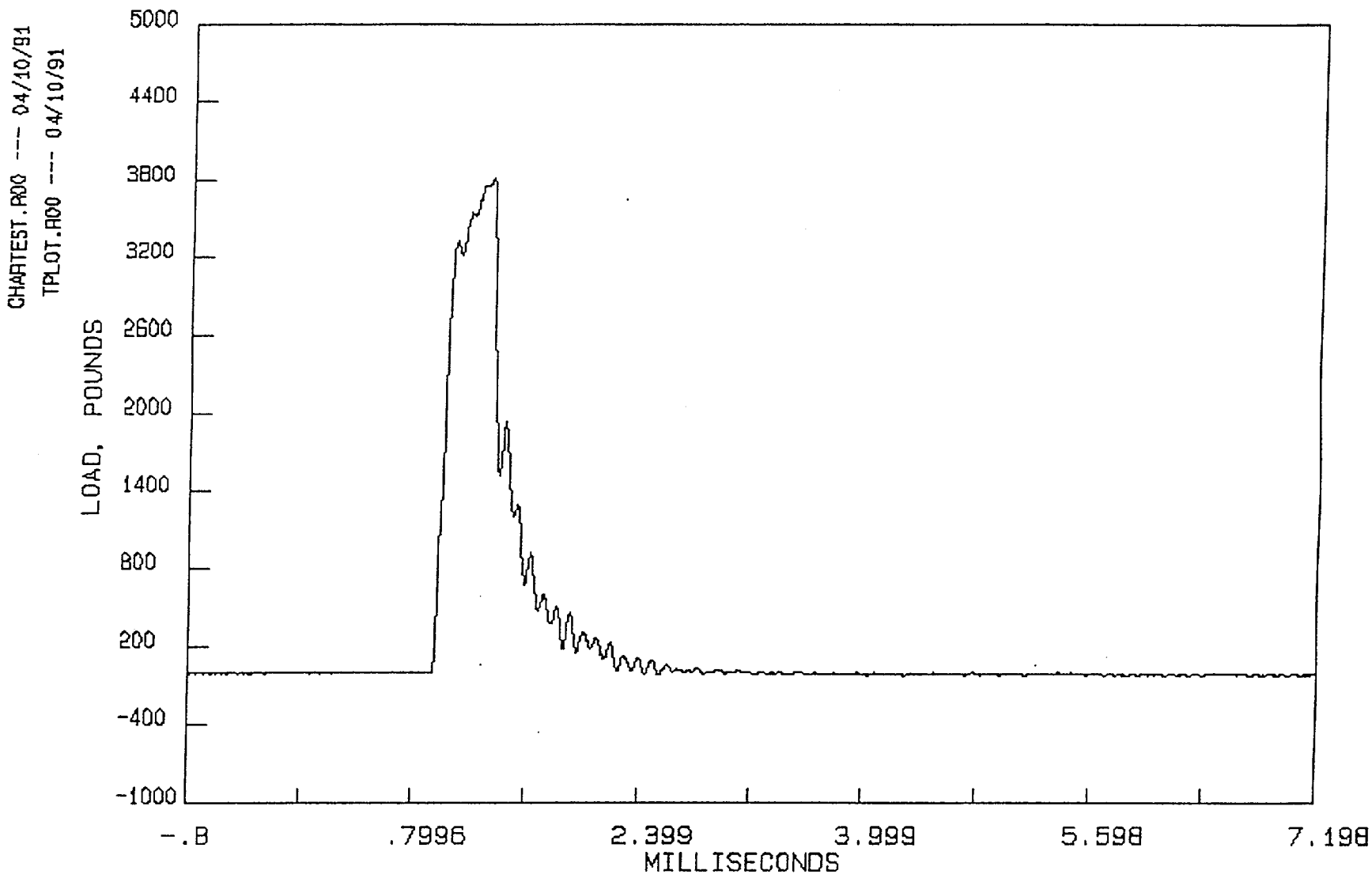

PROJ. NO. 1215-001 QA NO. 00001

LOAD - TIME TRACE FOR SPECIMEN WT45

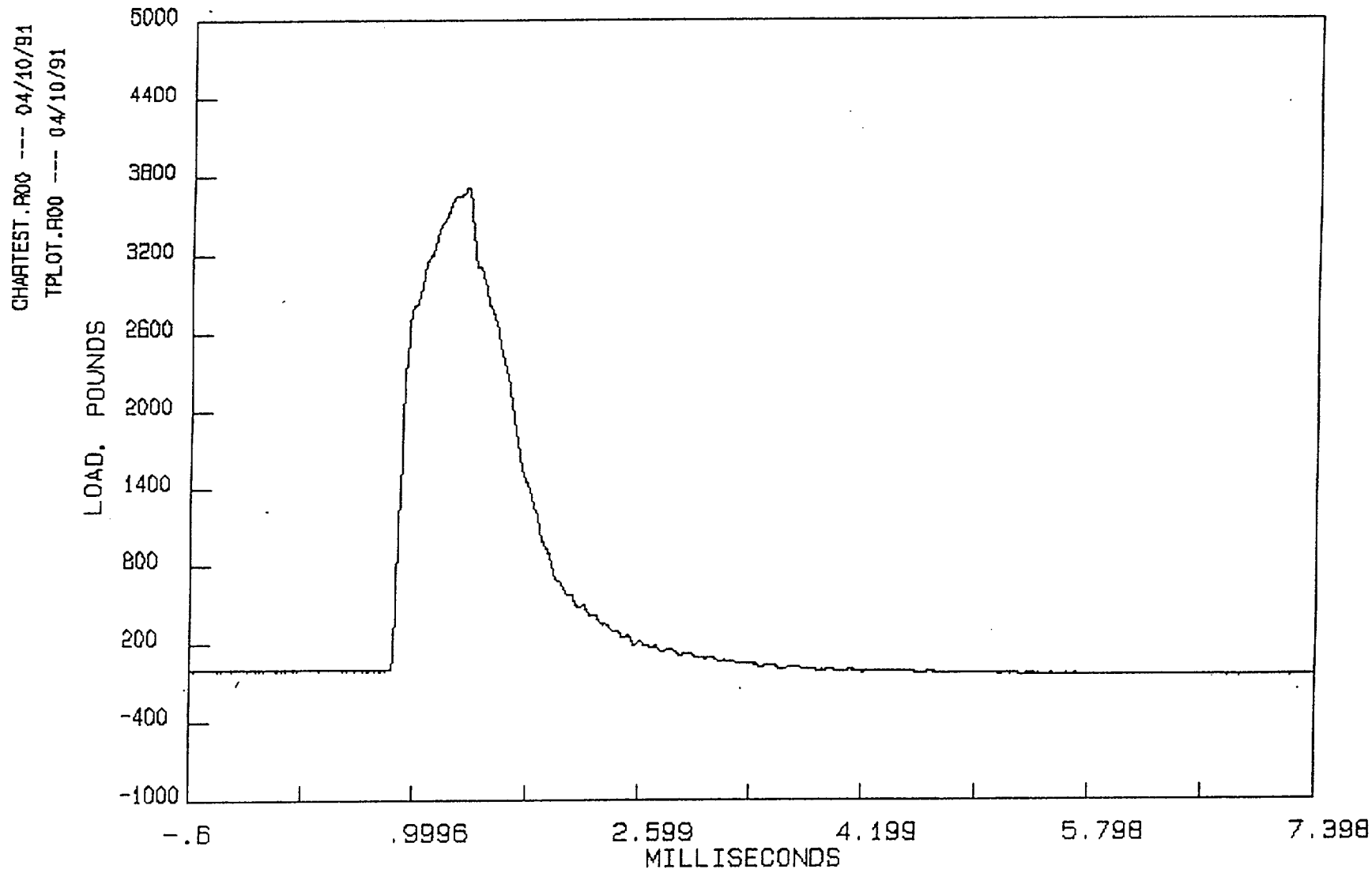

PROJ. NO. 1215-001 QA NO. 00001

ENERGY - TIME TRACE FOR SPECIMEN WT45

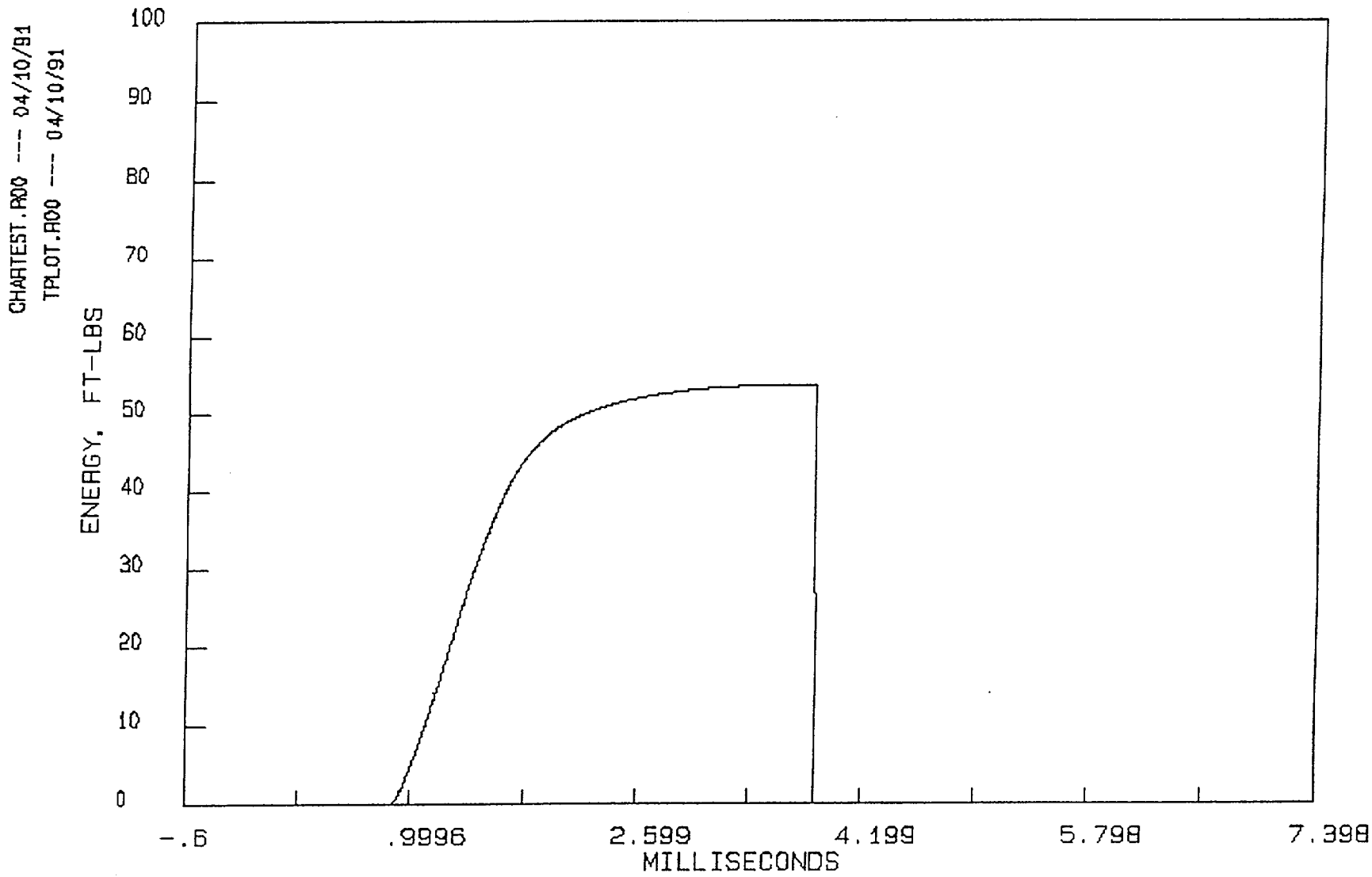

PROJ. NO. 1215-001 QA NO. 99001

ENERGY - TIME TRACE FOR SPECIMEN WW42

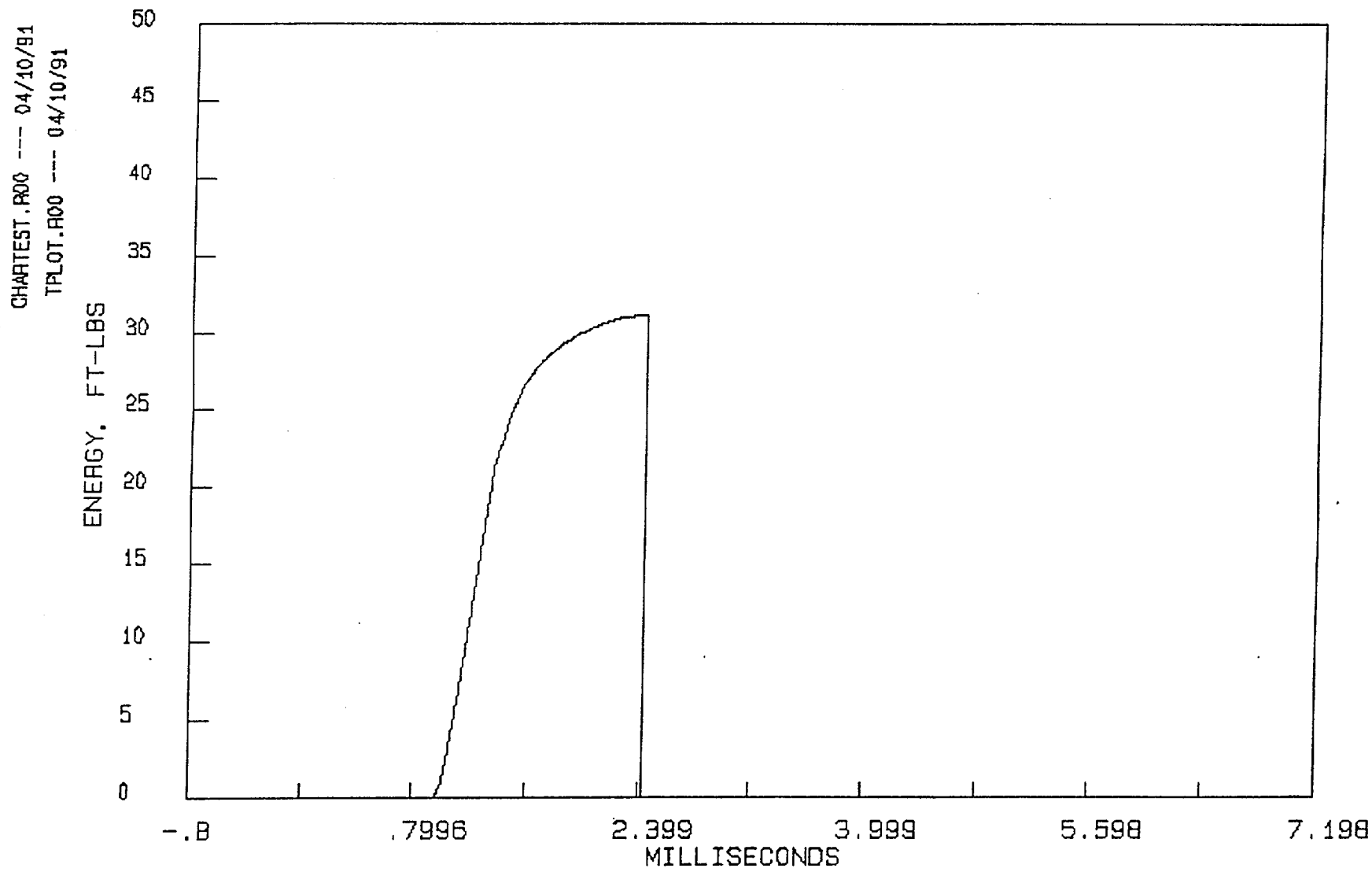

PROJ. NO. 1215-001 QA NO. 99001

LOAD - TIME TRACE FOR SPECIMEN WW44

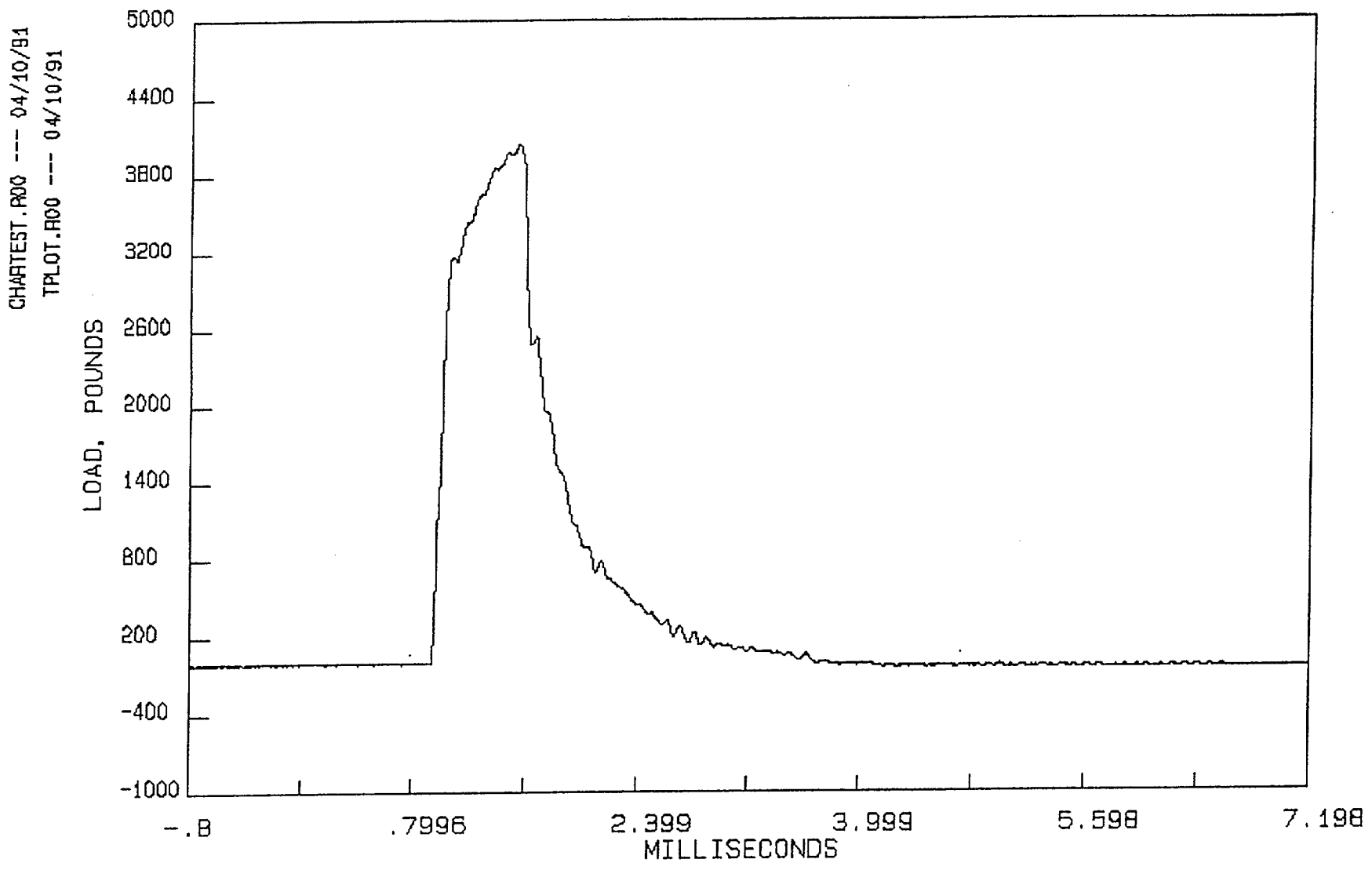

PROJ. NO. 1215-001 QA NO. 99001

ENERGY - TIME TRACE FOR SPECIMEN WW44

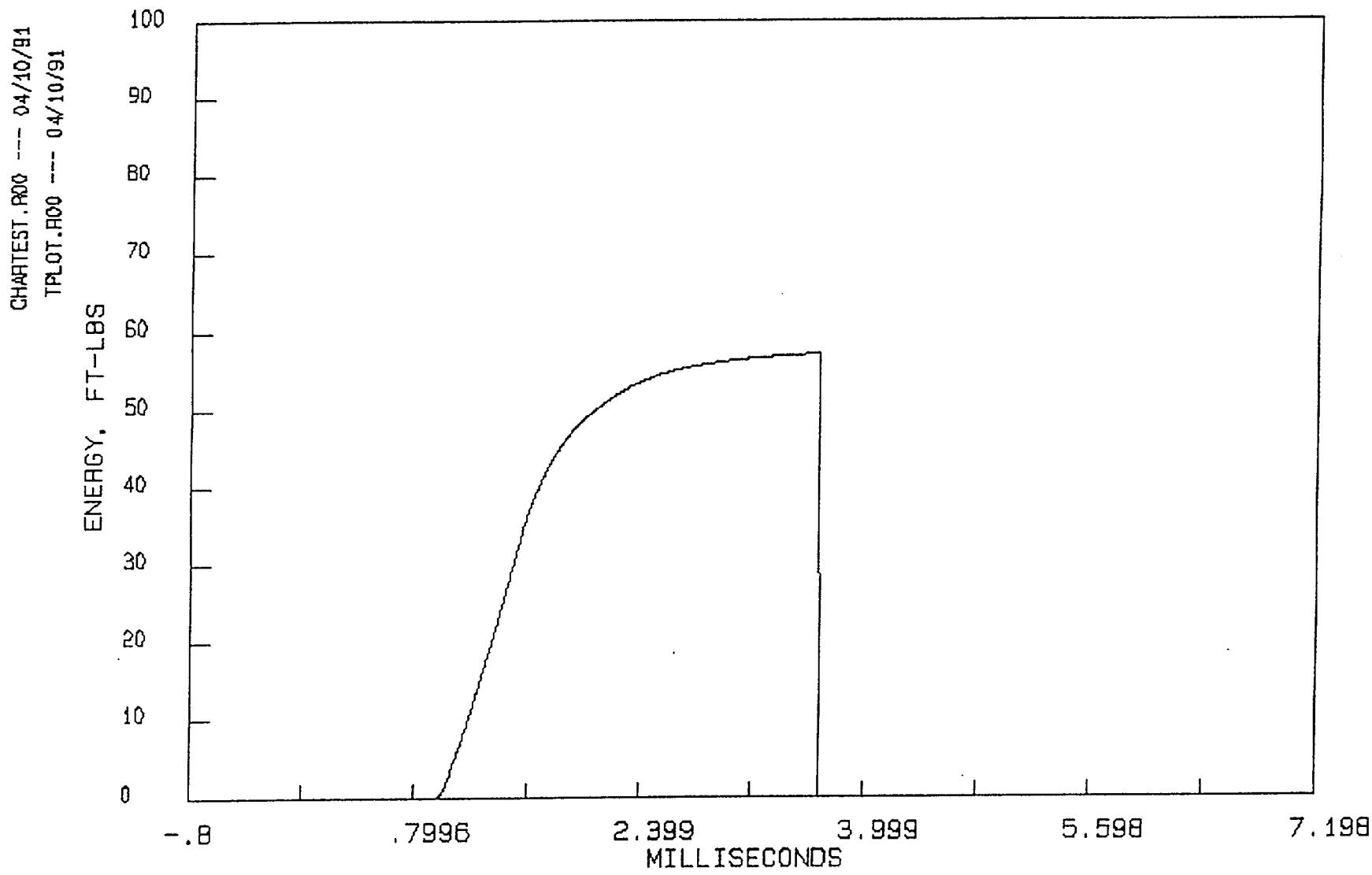

PROJ. NO. 1215-001 QA NO. 99001

LOAD - TIME TRACE FOR SPECIMEN WW38

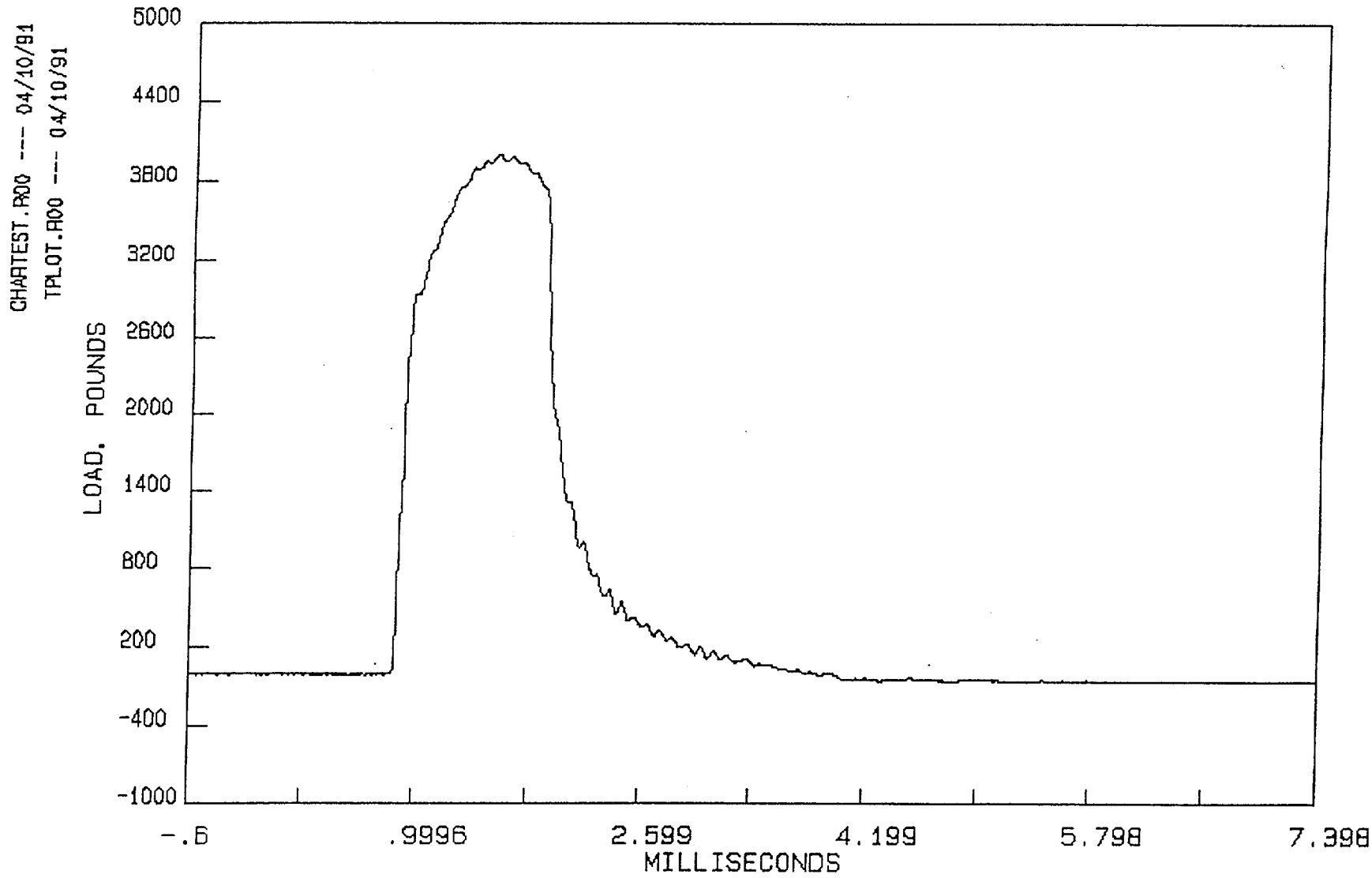

PROJ. NO. 1215-001 QA NO. 99001

ENERGY - TIME TRACE FOR SPECIMEN WW38

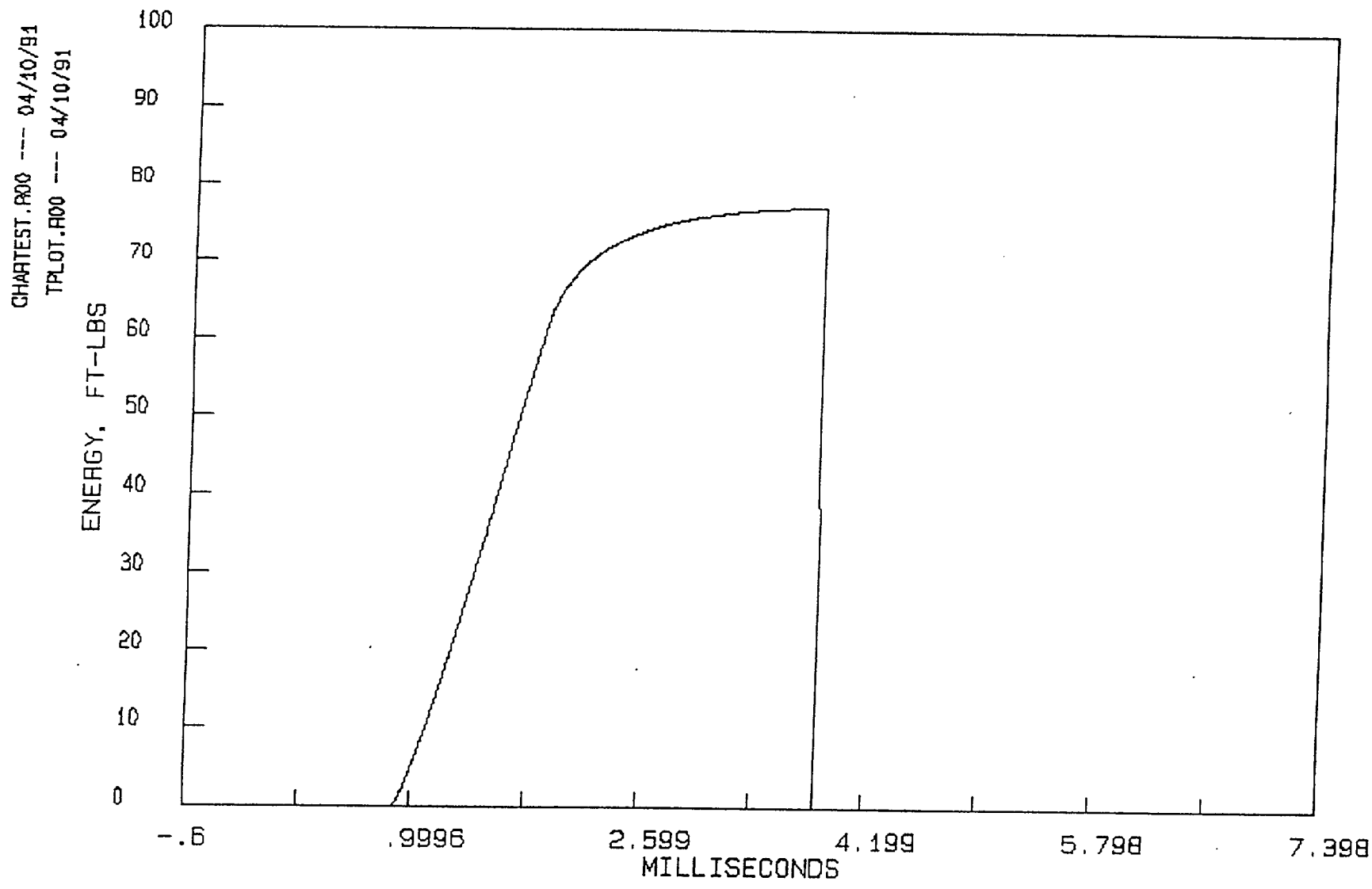

PROJ. NO. 1215-001 QA NO. 99001

LOAD - TIME TRACE FOR SPECIMEN WW41

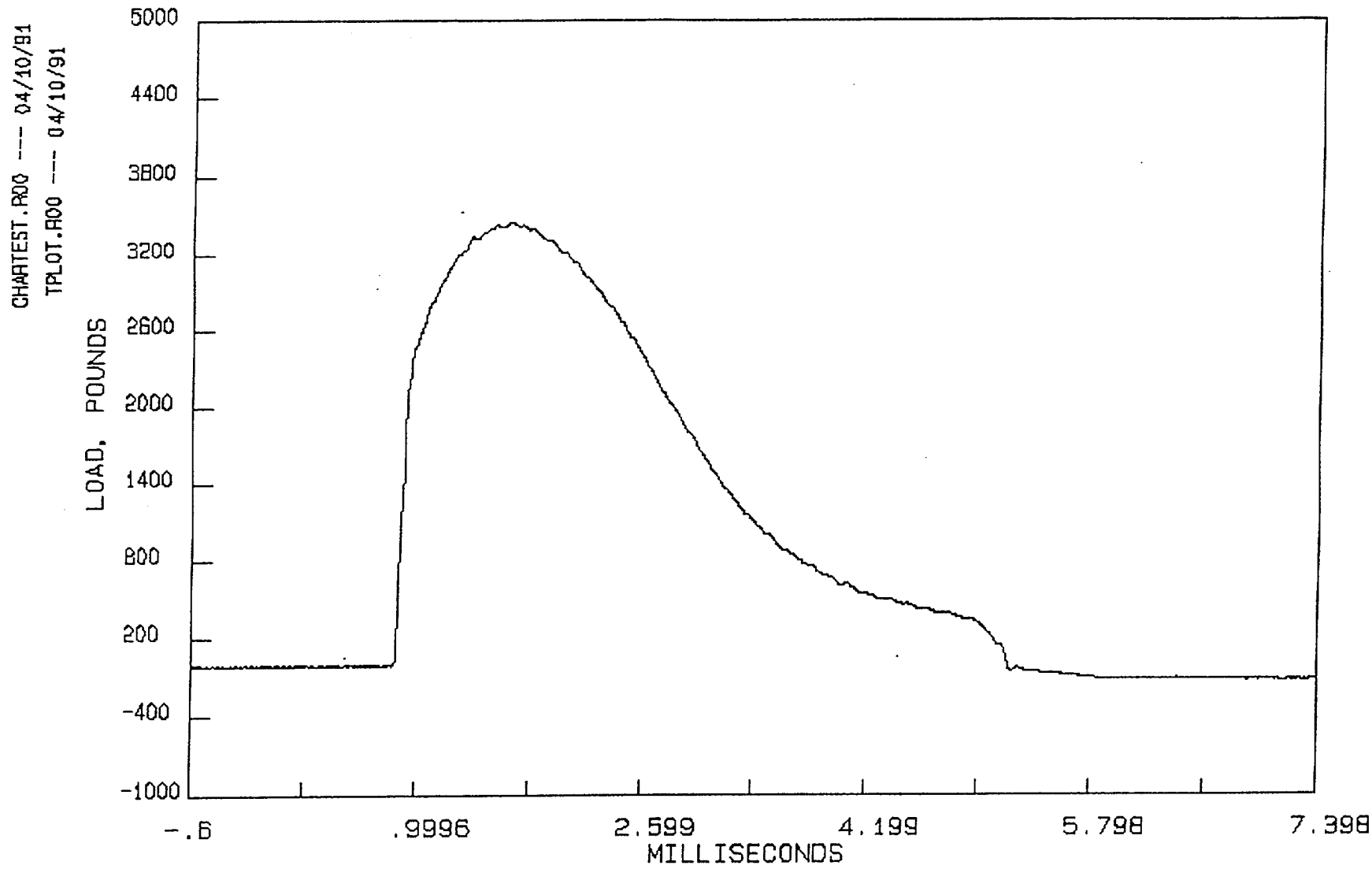

PROJ. NO. 1215-001 QA NO. 99001

ENERGY - TIME TRACE FOR SPECIMEN WW41

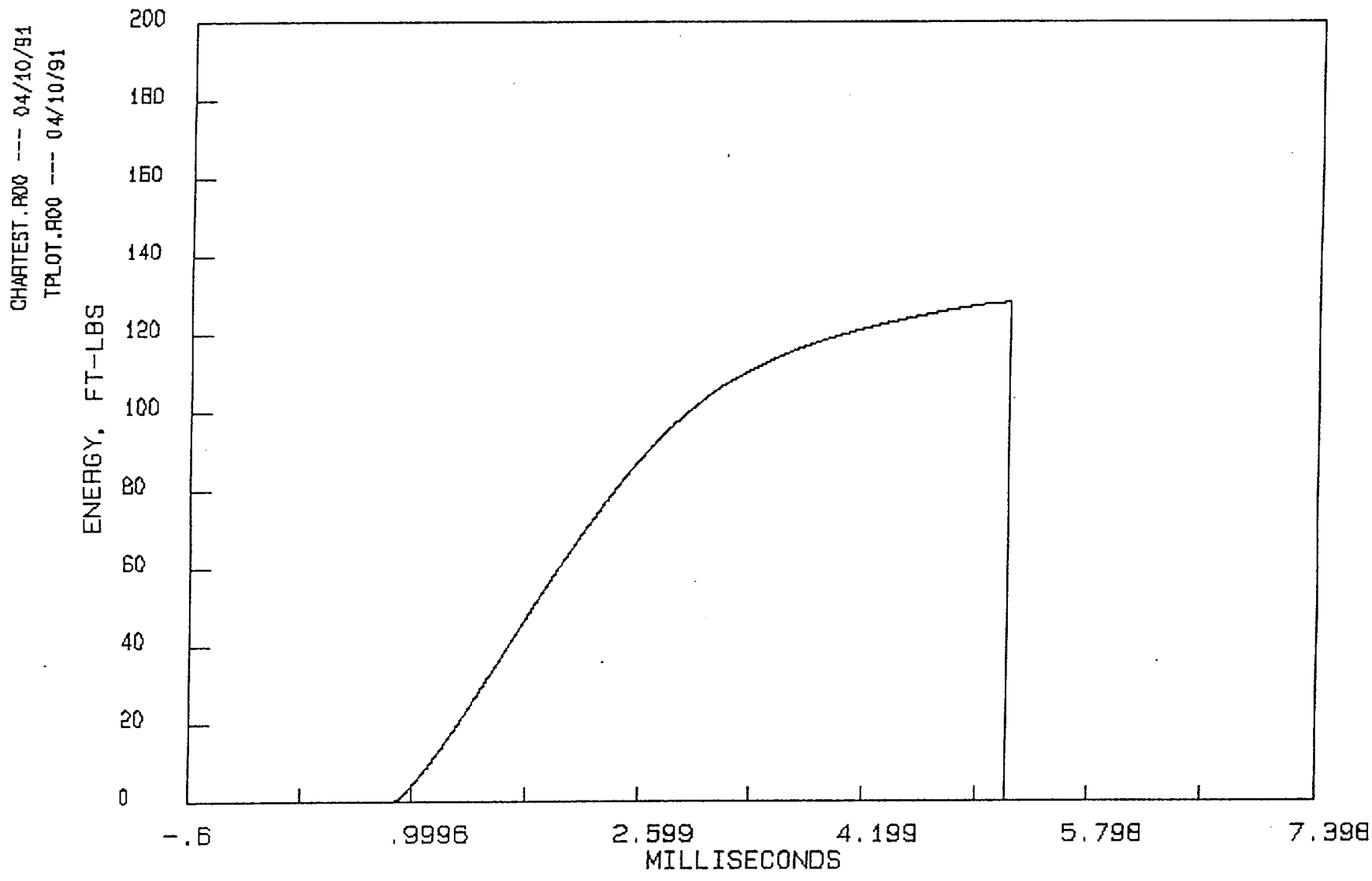

PROJ. NO. 1215-001 QA NO. 99001

LOAD - TIME TRACE FOR SPECIMEN WW33

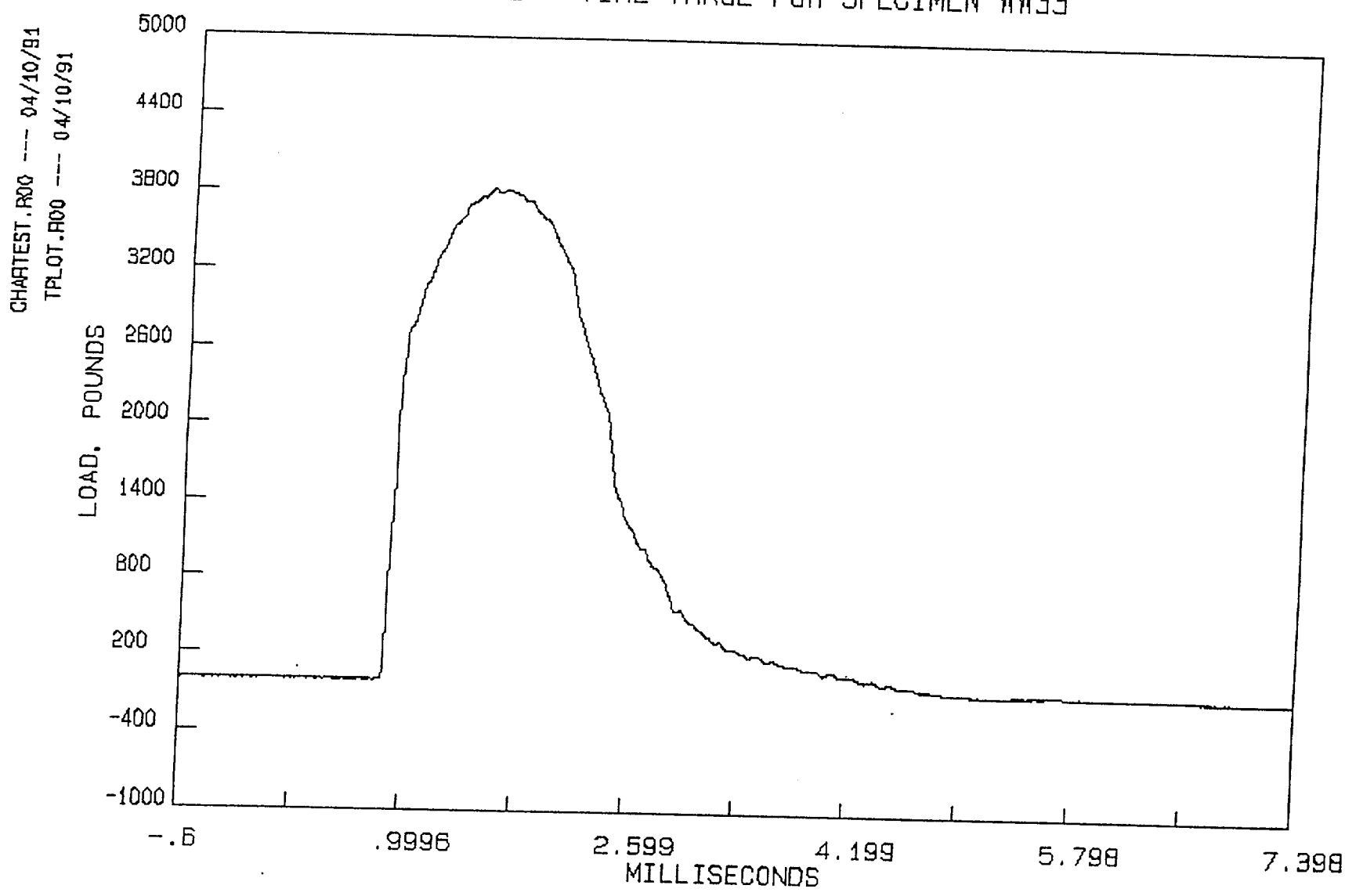

PROJ. NO. 1215-001 QA NO. 99001

ENERGY - TIME TRACE FOR SPECIMEN WW33

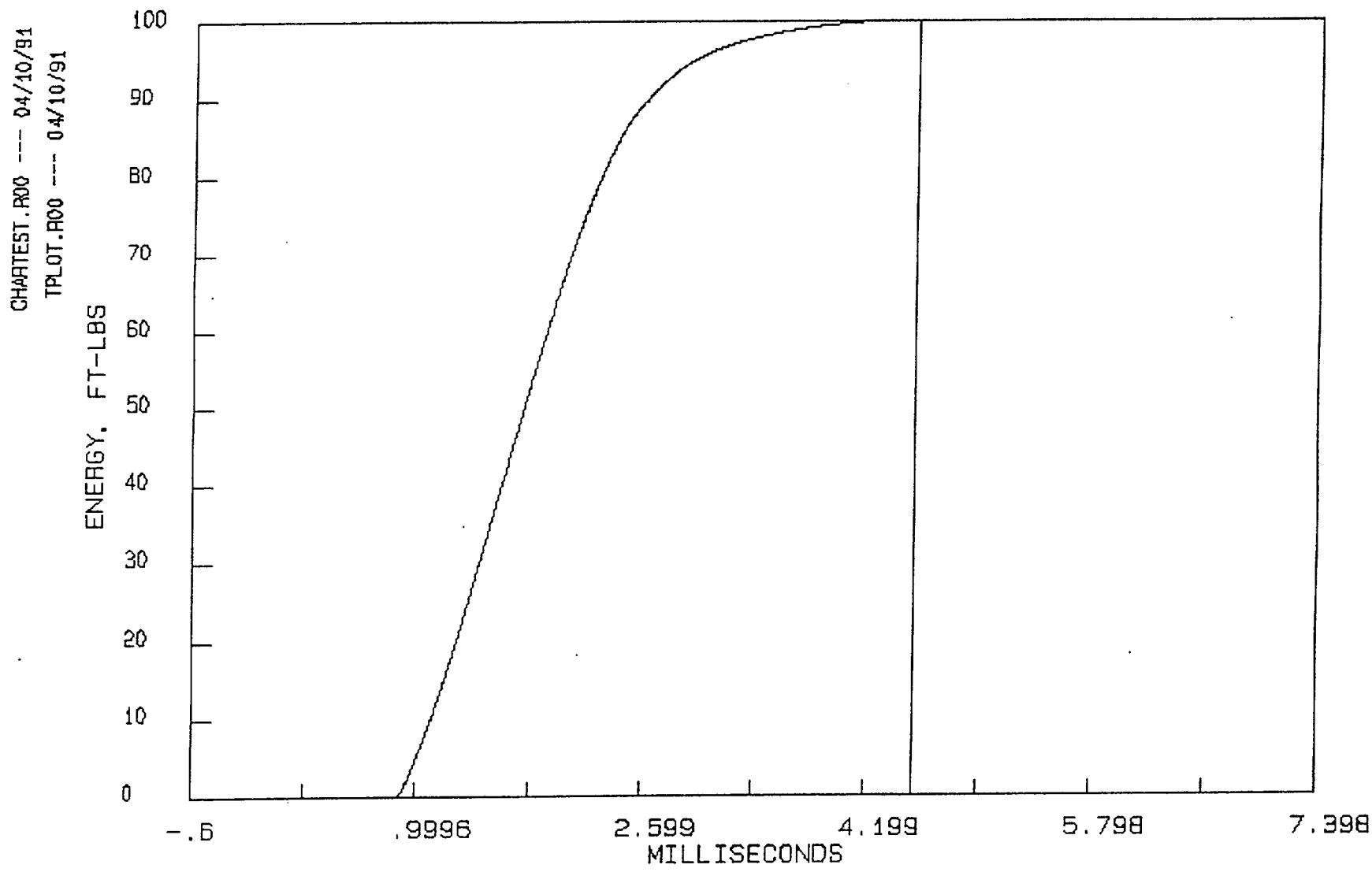

PROJ. NO. 1215-001 QA NO. 99001

LOAD - TIME TRACE FOR SPECIMEN WW34

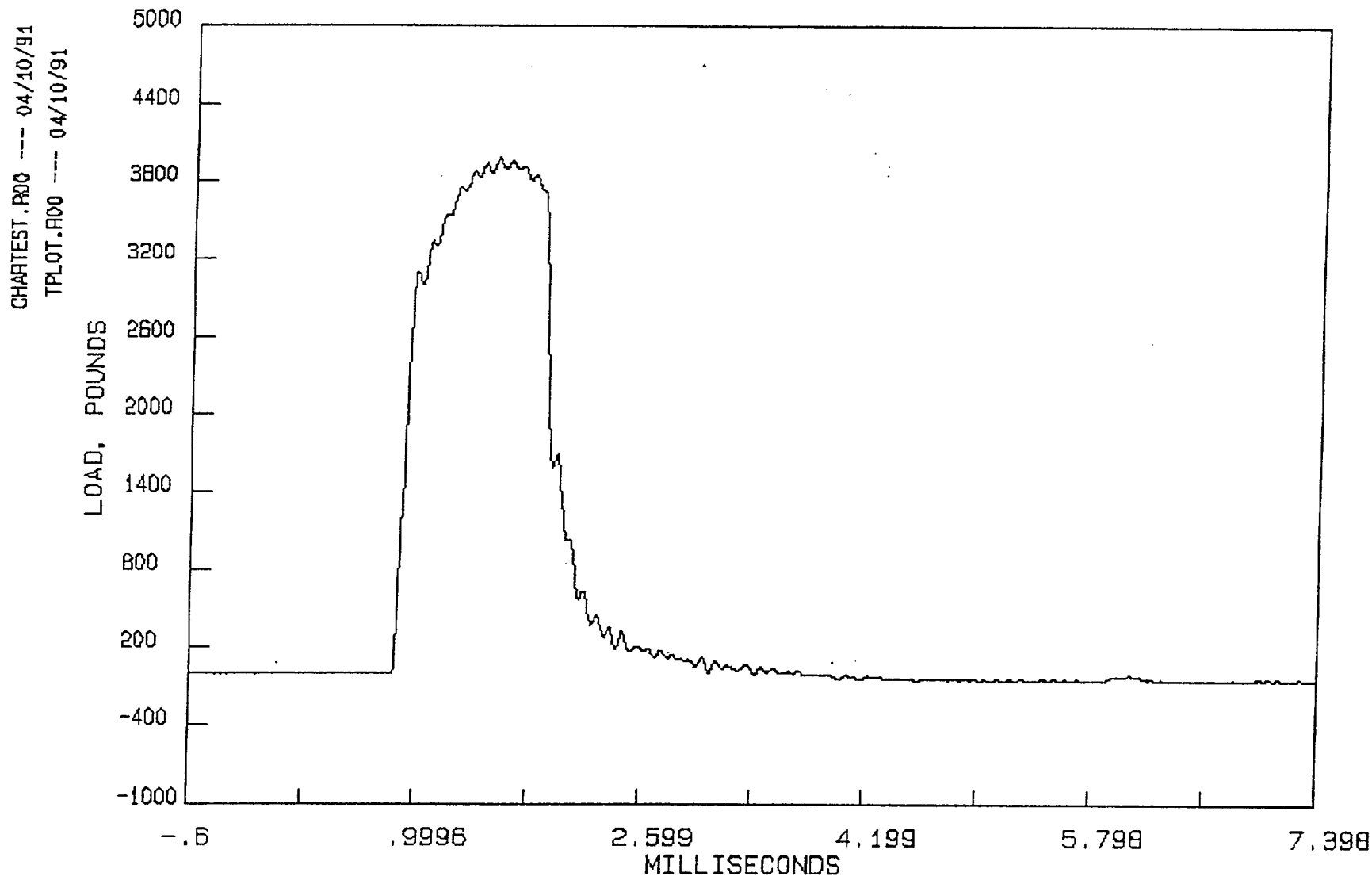

PROJ. NO. 1215-001 QA NO. 99001

ENERGY - TIME TRACE FOR SPECIMEN WW34

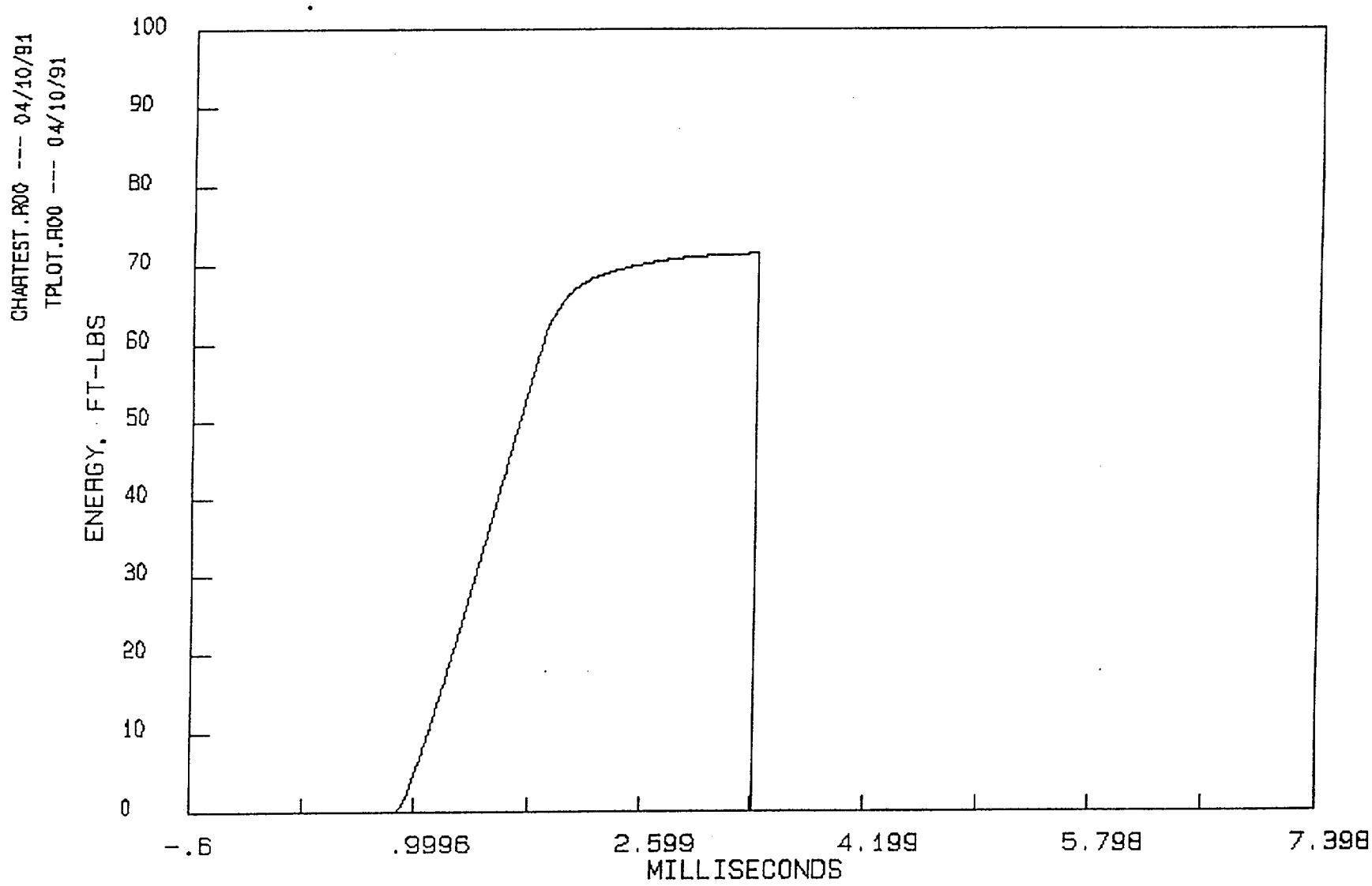

PROJ. NO. 1215-001 QA NO. 99001

LOAD - TIME TRACE FOR SPECIMEN WW45

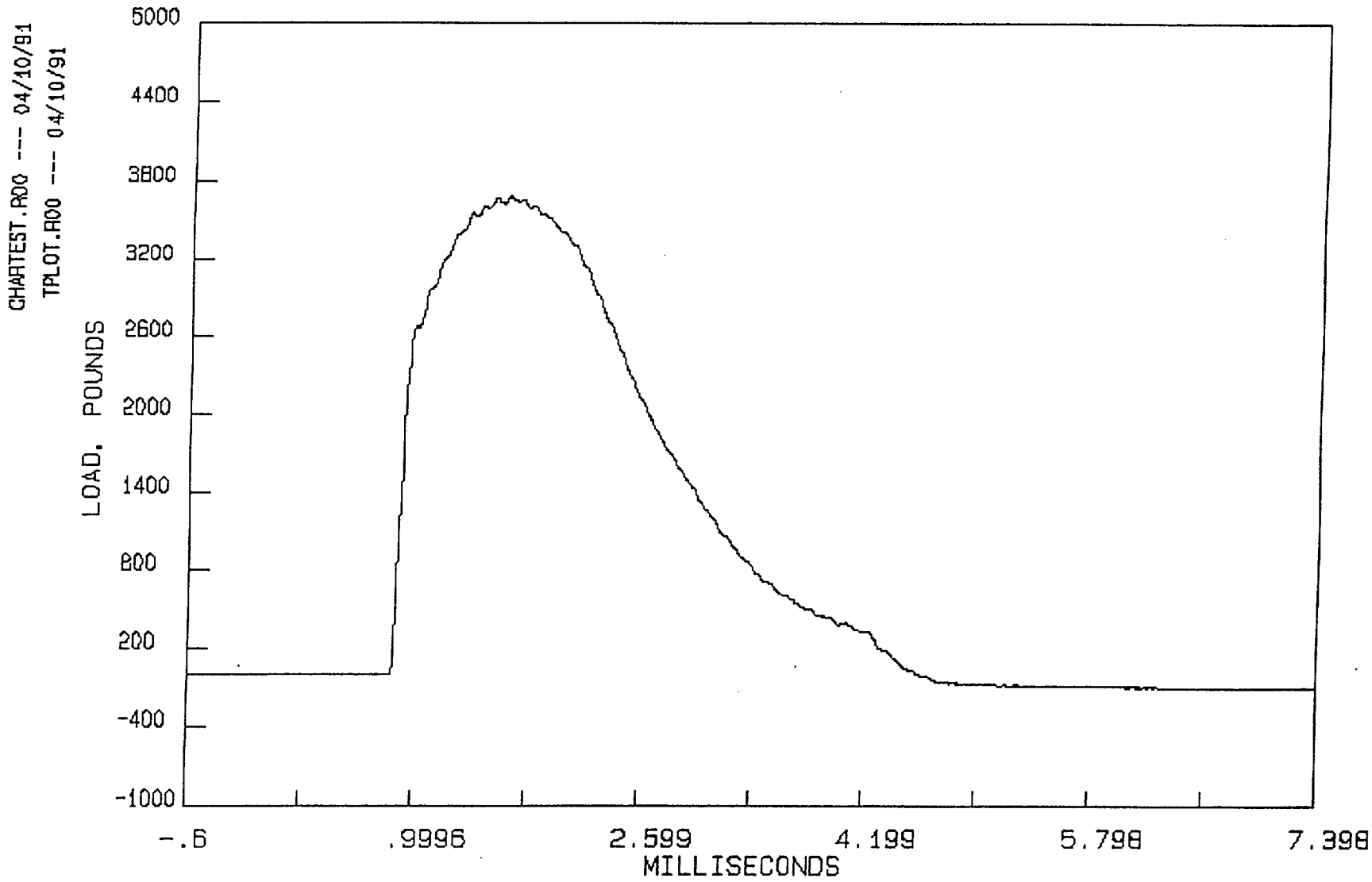

PROJ. NO. 1215-001 QA NO. 99001

ENERGY - TIME TRACE FOR SPECIMEN WW45

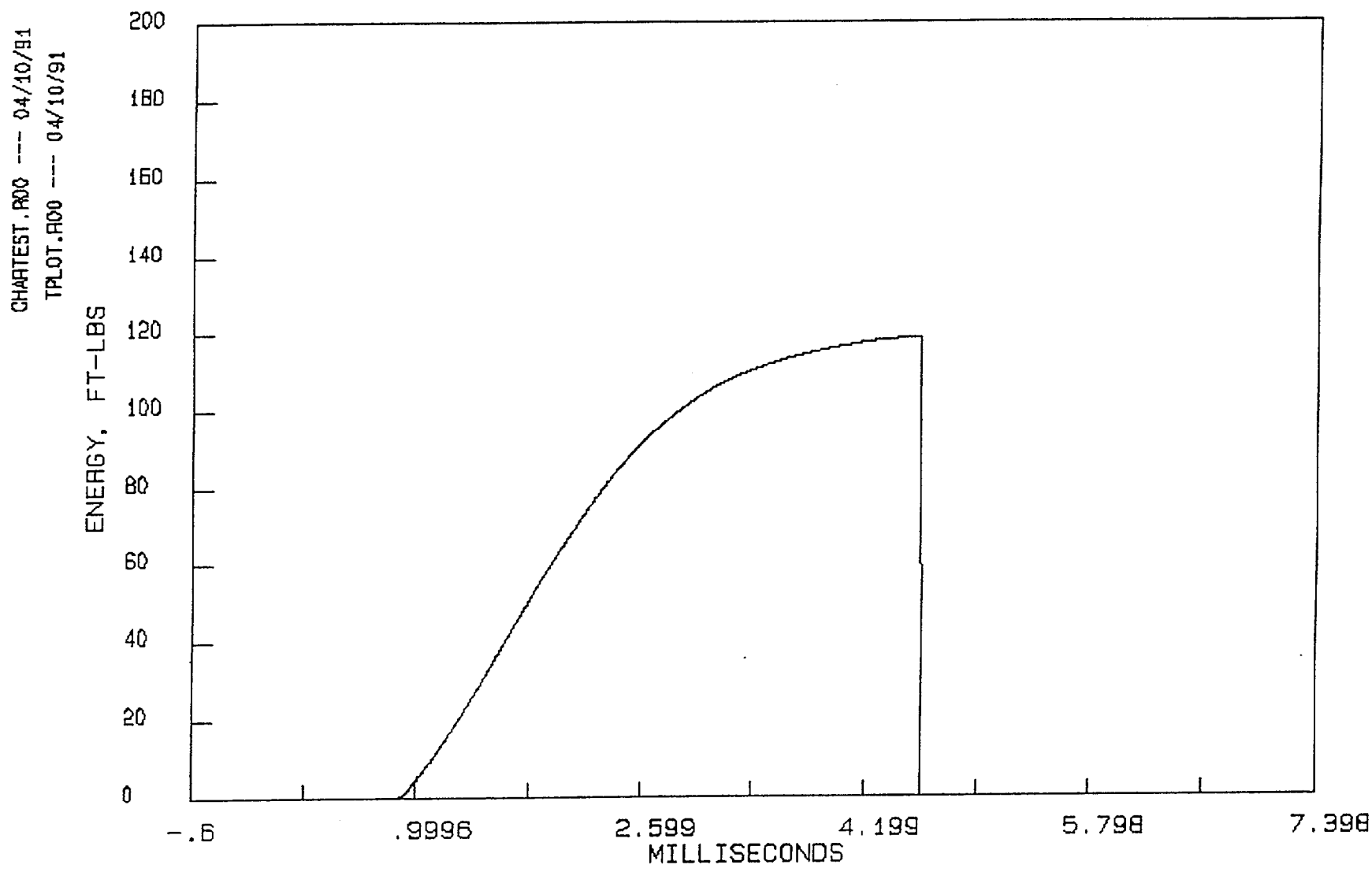

PROJ. NO. 1215-001 QA NO. 00001

LOAD - TIME TRACE FOR SPECIMEN WL32

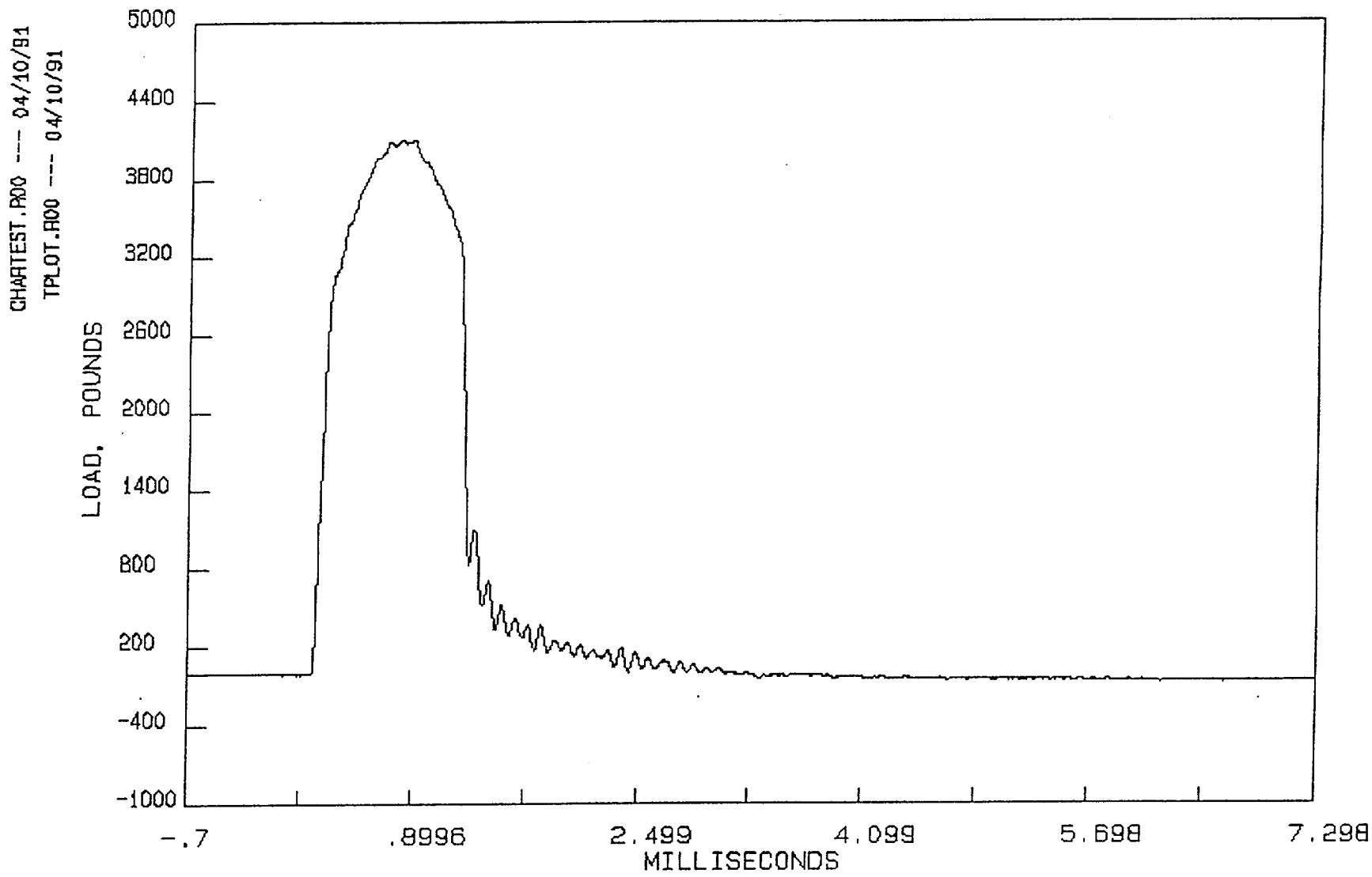

PROJ. NO. 1215-001 QA NO. 00001

ENERGY - TIME TRACE FOR SPECIMEN WL32

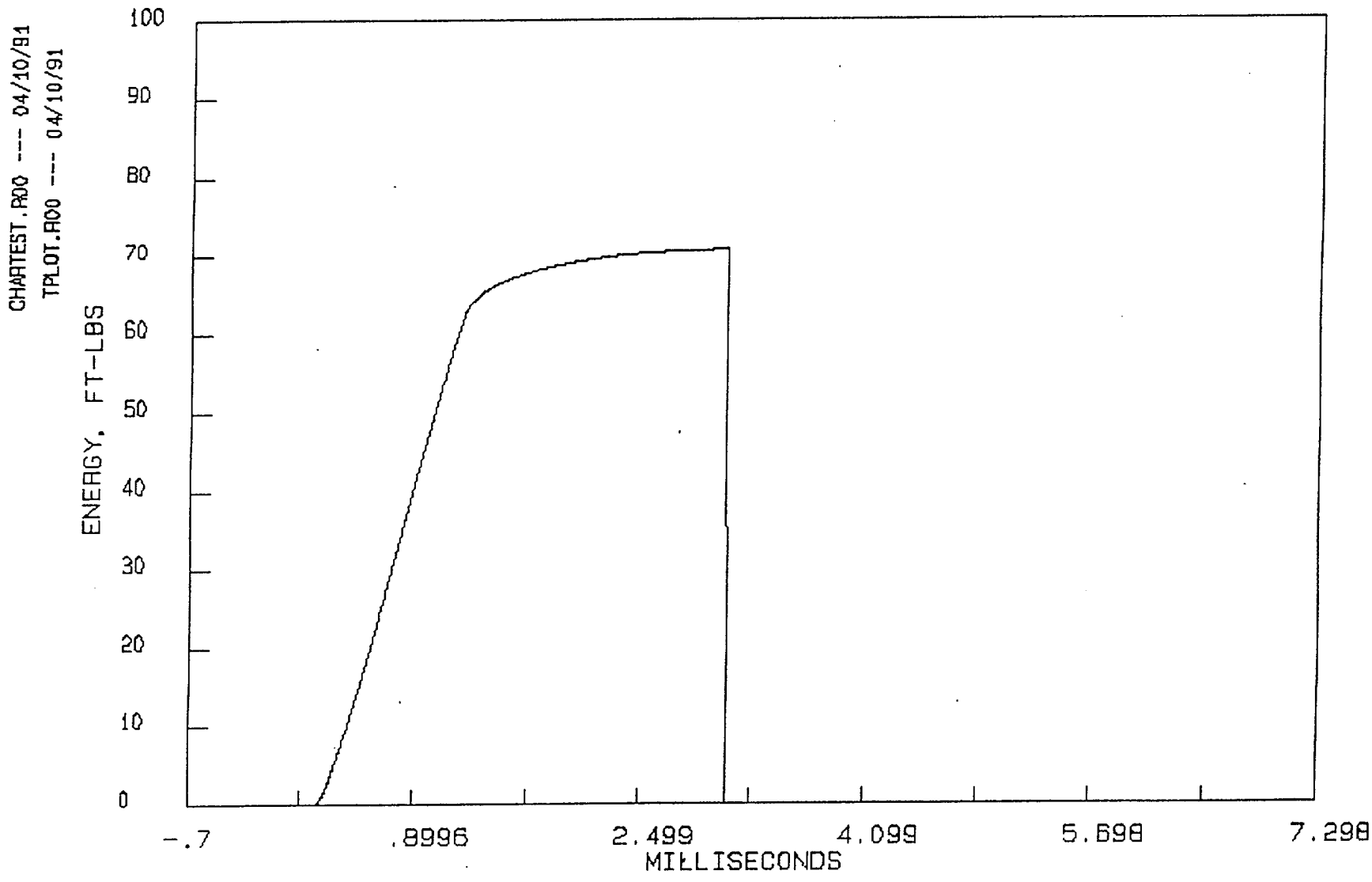

PROJ. NO. 1215-001 QA NO. 00001

LOAD - TIME TRACE FOR SPECIMEN WL41

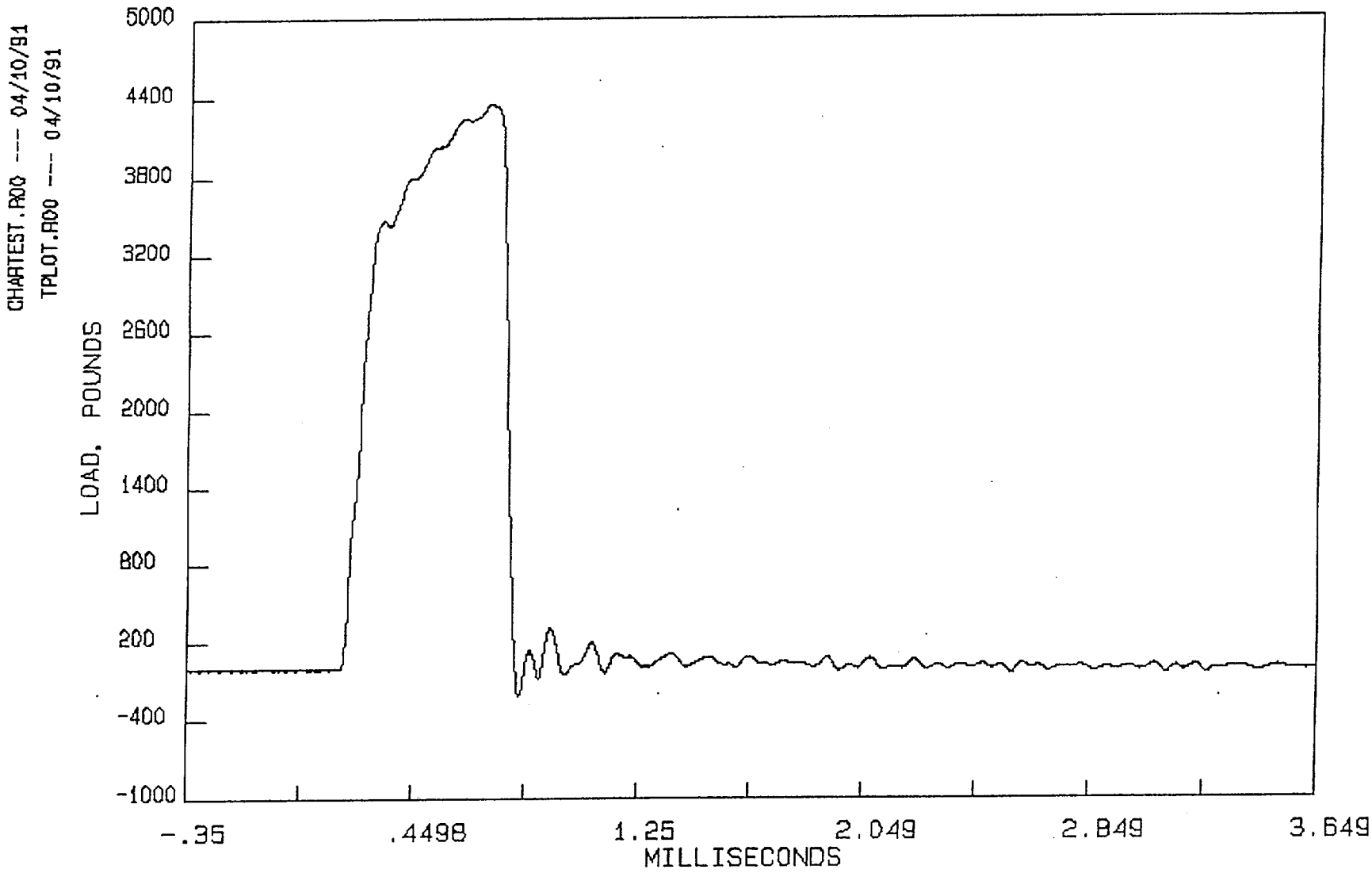

PROJ. NO. 1215-001 QA NO. 00001

LOAD - TIME TRACE FOR SPECIMEN WL42

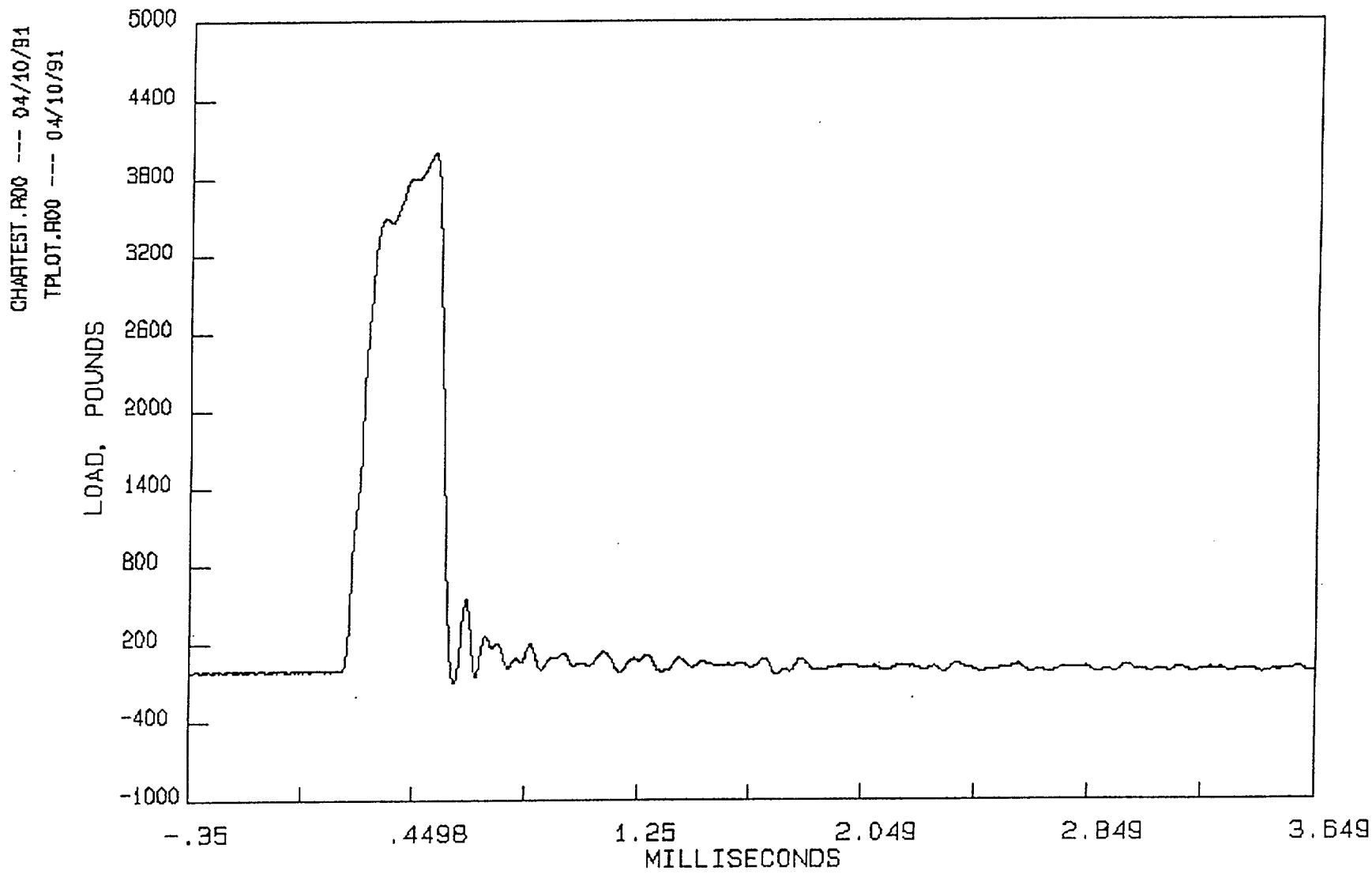

PROJ. NO. 1215-001 QA NO. 00001

ENERGY - TIME TRACE FOR SPECIMEN WL42

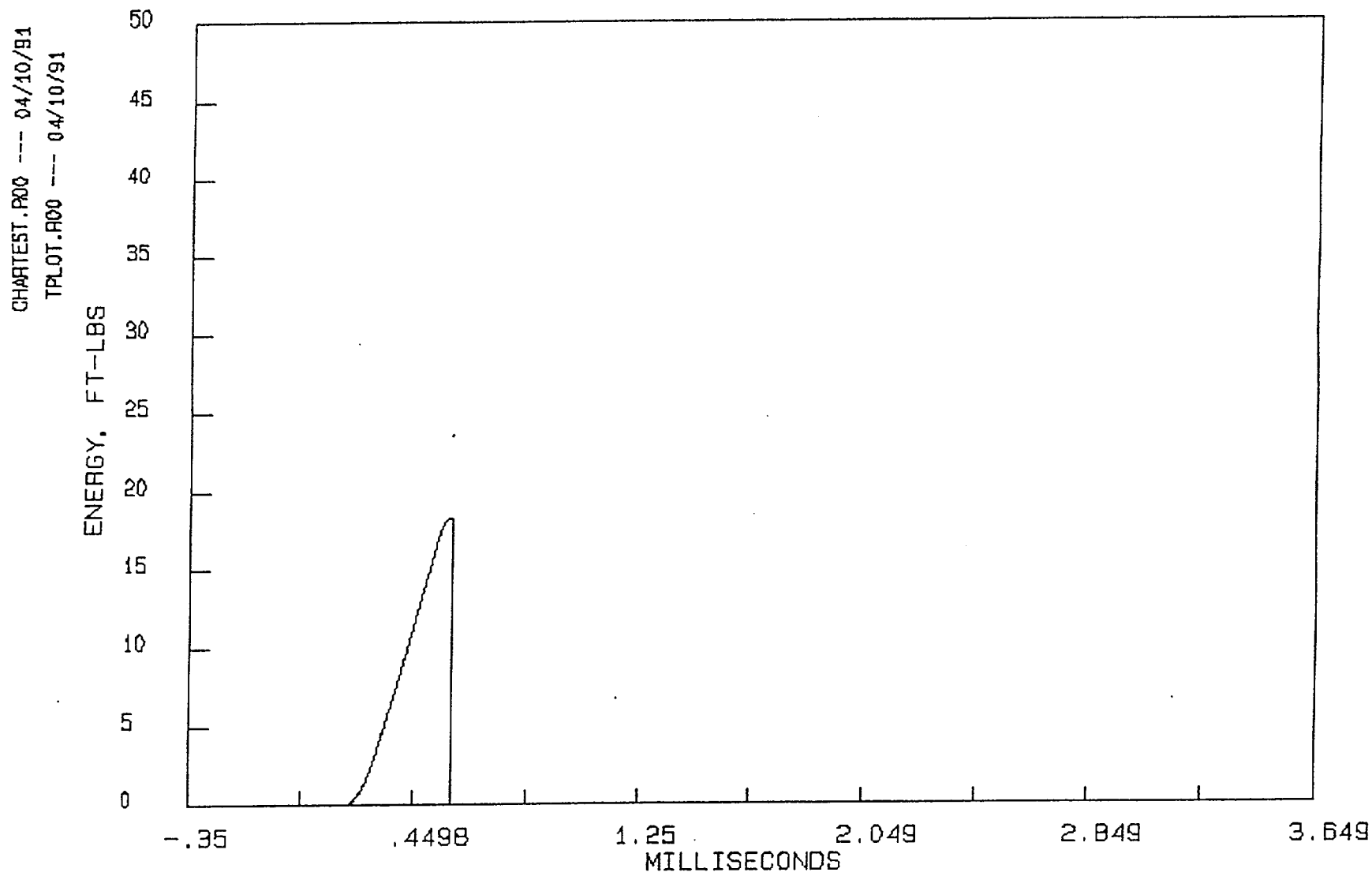

PROJ. NO. 1215-001 QA NO. 00001

LOAD - TIME TRACE FOR SPECIMEN WL39

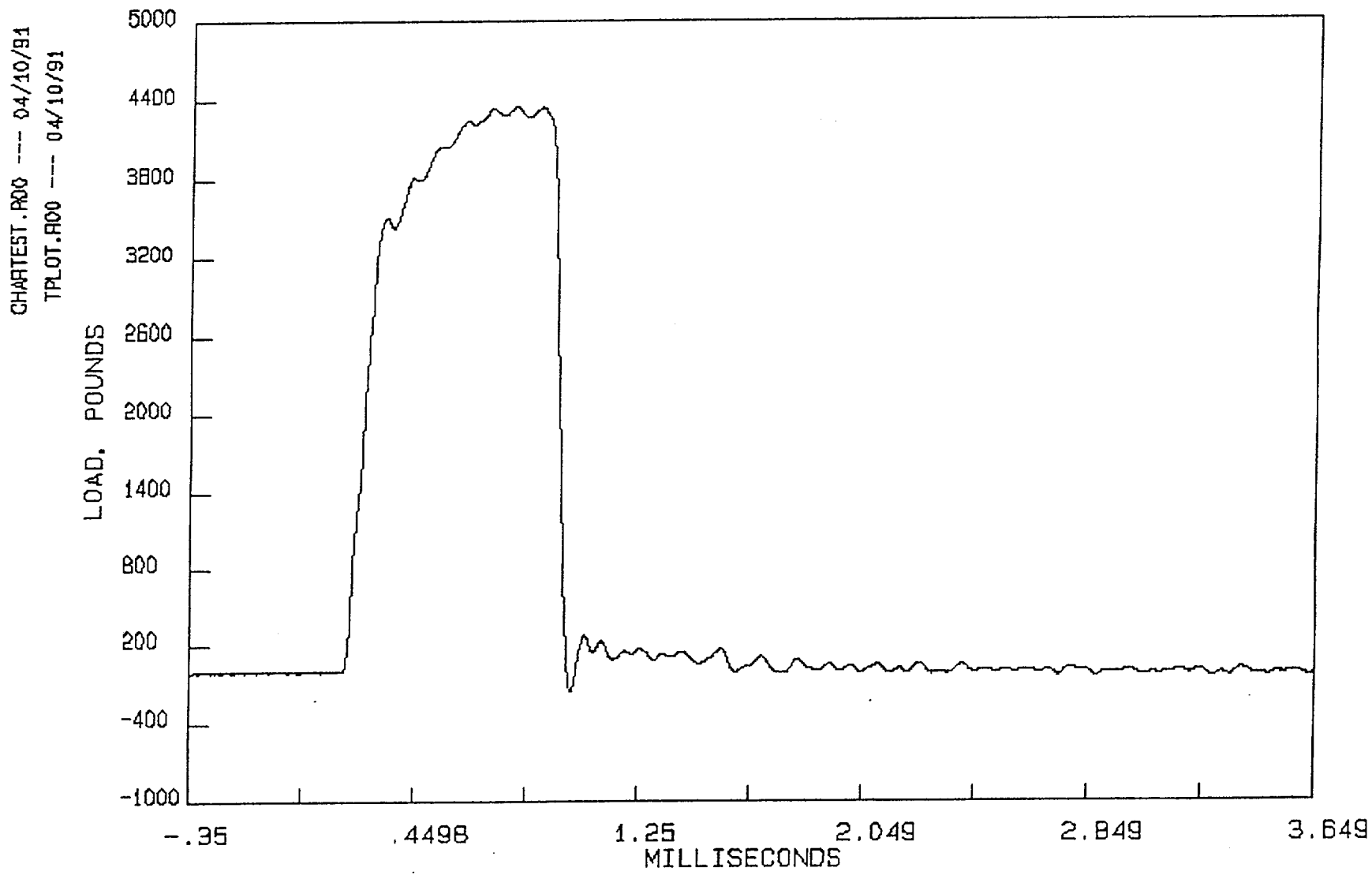

PROJ. NO. 1215-001 QA NO. 00001

ENERGY - TIME TRACE FOR SPECIMEN WL41

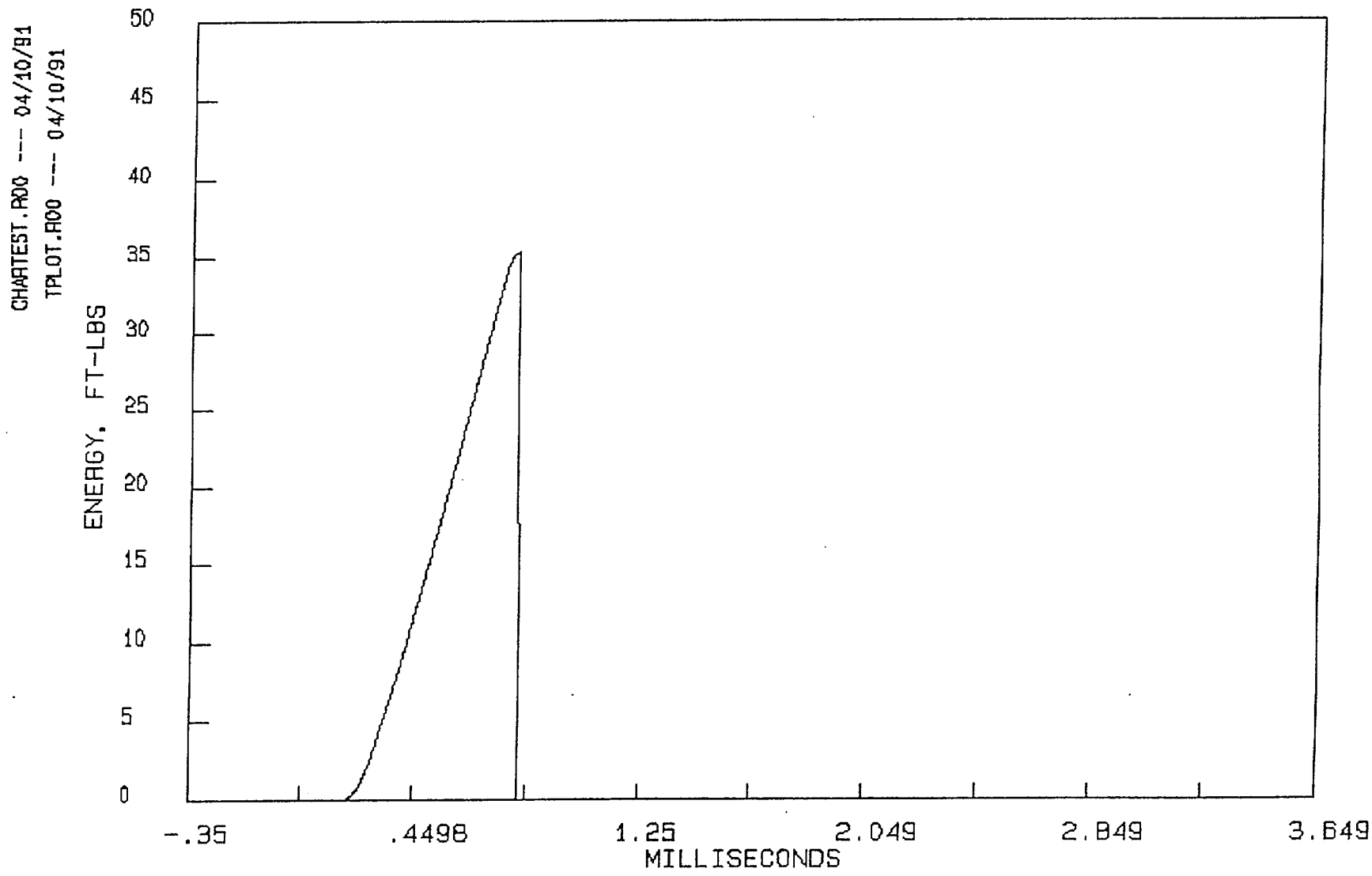

PROJ. NO. 1215-001 QA NO. 00001

ENERGY - TIME TRACE FOR SPECIMEN WL39

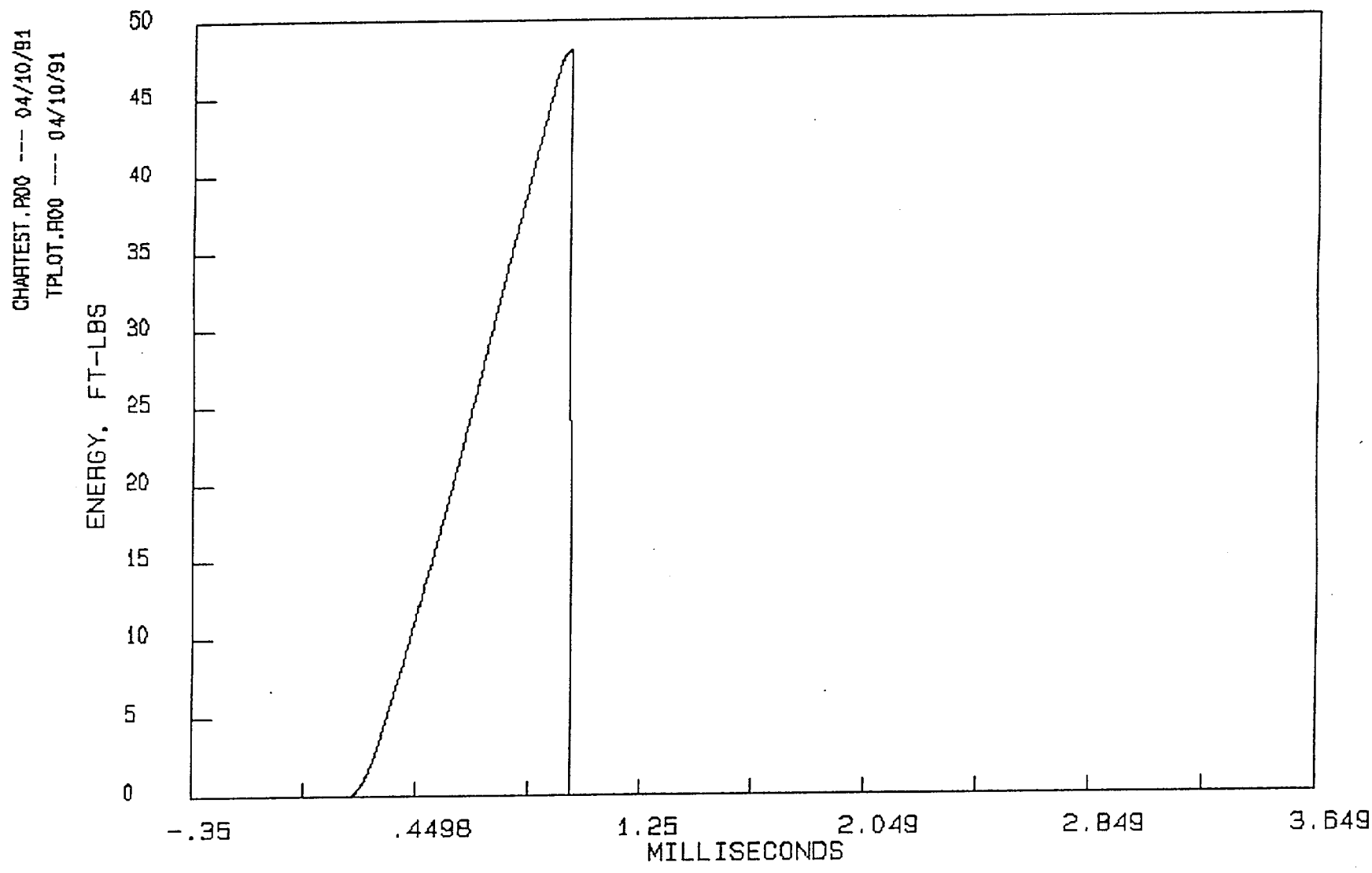

PROJ. NO. 1215-001 QA NO. 00001

LOAD - TIME TRACE FOR SPECIMEN WL45

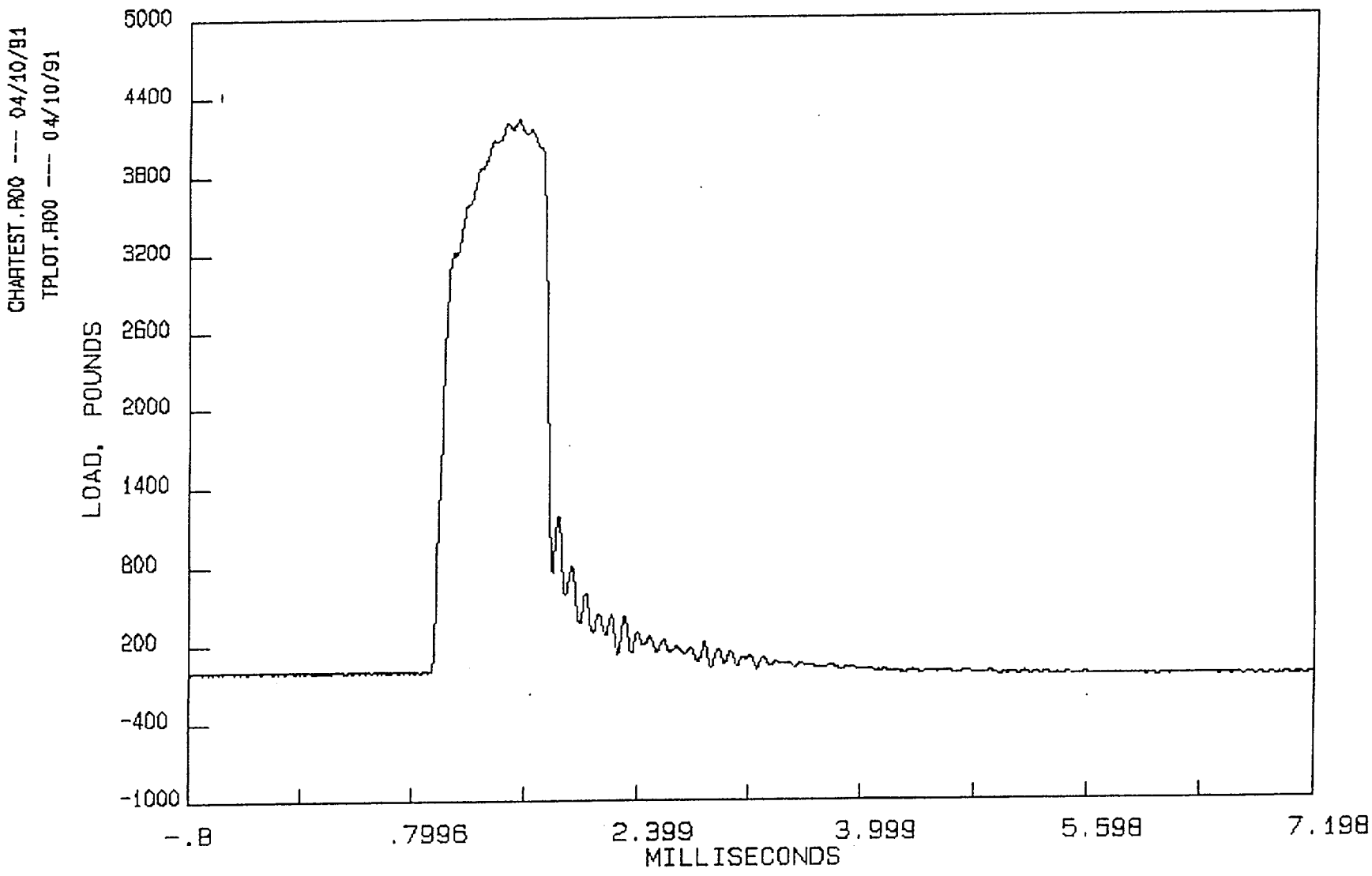

PROJ. NO. 1215-001 QA NO. 00001

ENERGY - TIME TRACE FOR SPECIMEN WL45

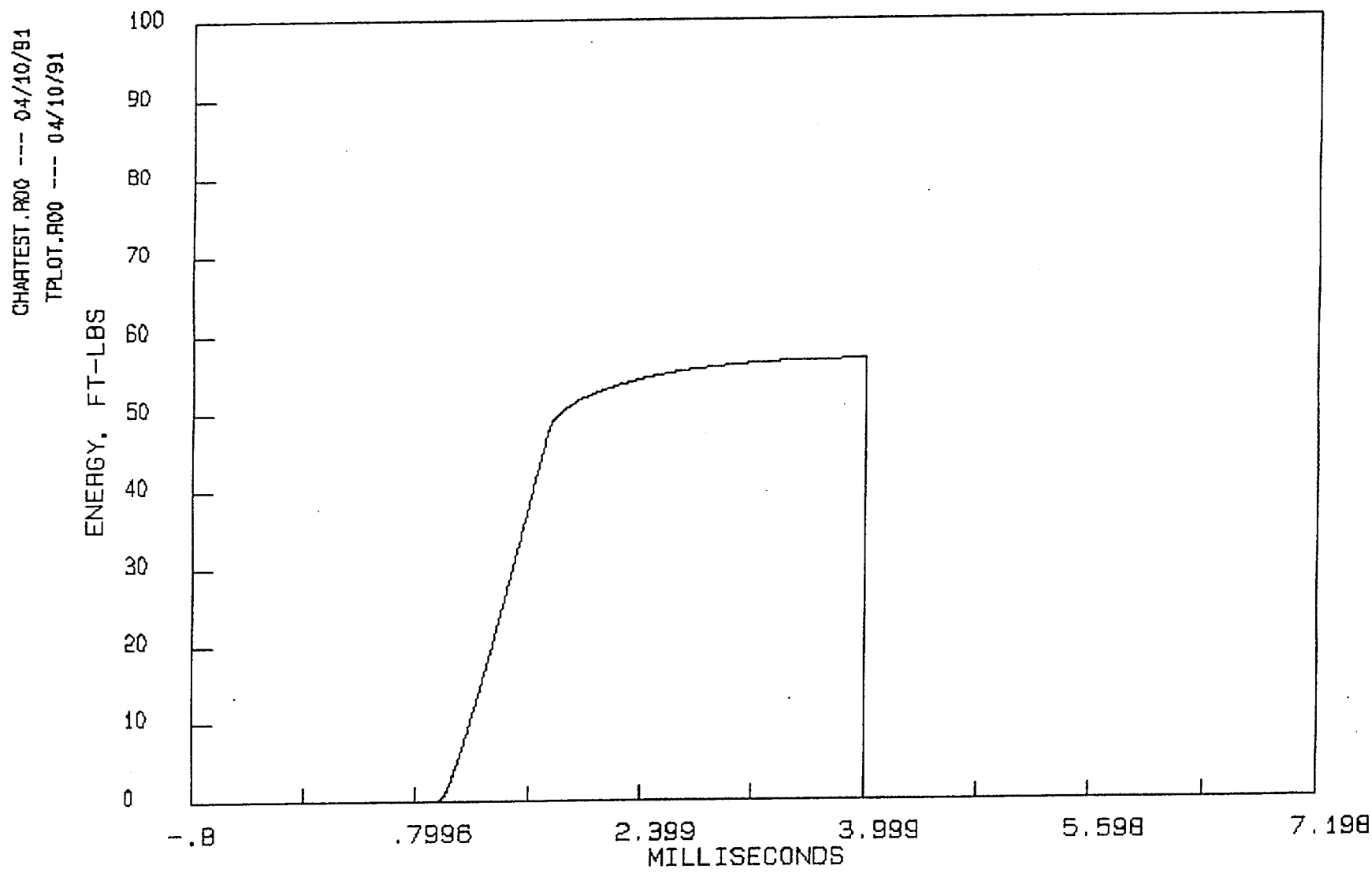

PROJ. NO. 1215-001 QA NO. 00001

LOAD - TIME TRACE FOR SPECIMEN WL34

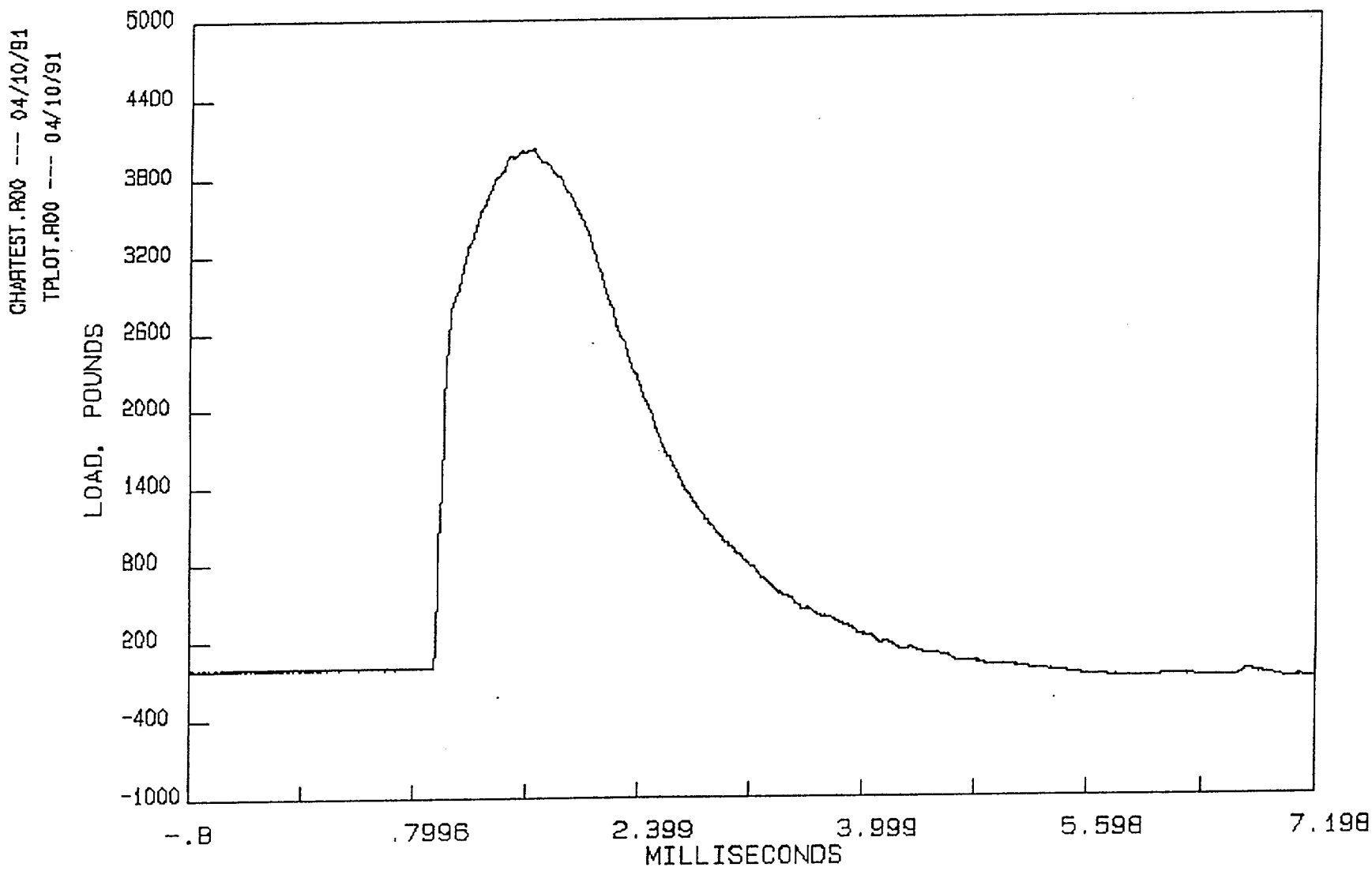

PROJ. NO. 1215-001 QA NO. 00001

ENERGY - TIME TRACE FOR SPECIMEN WL34

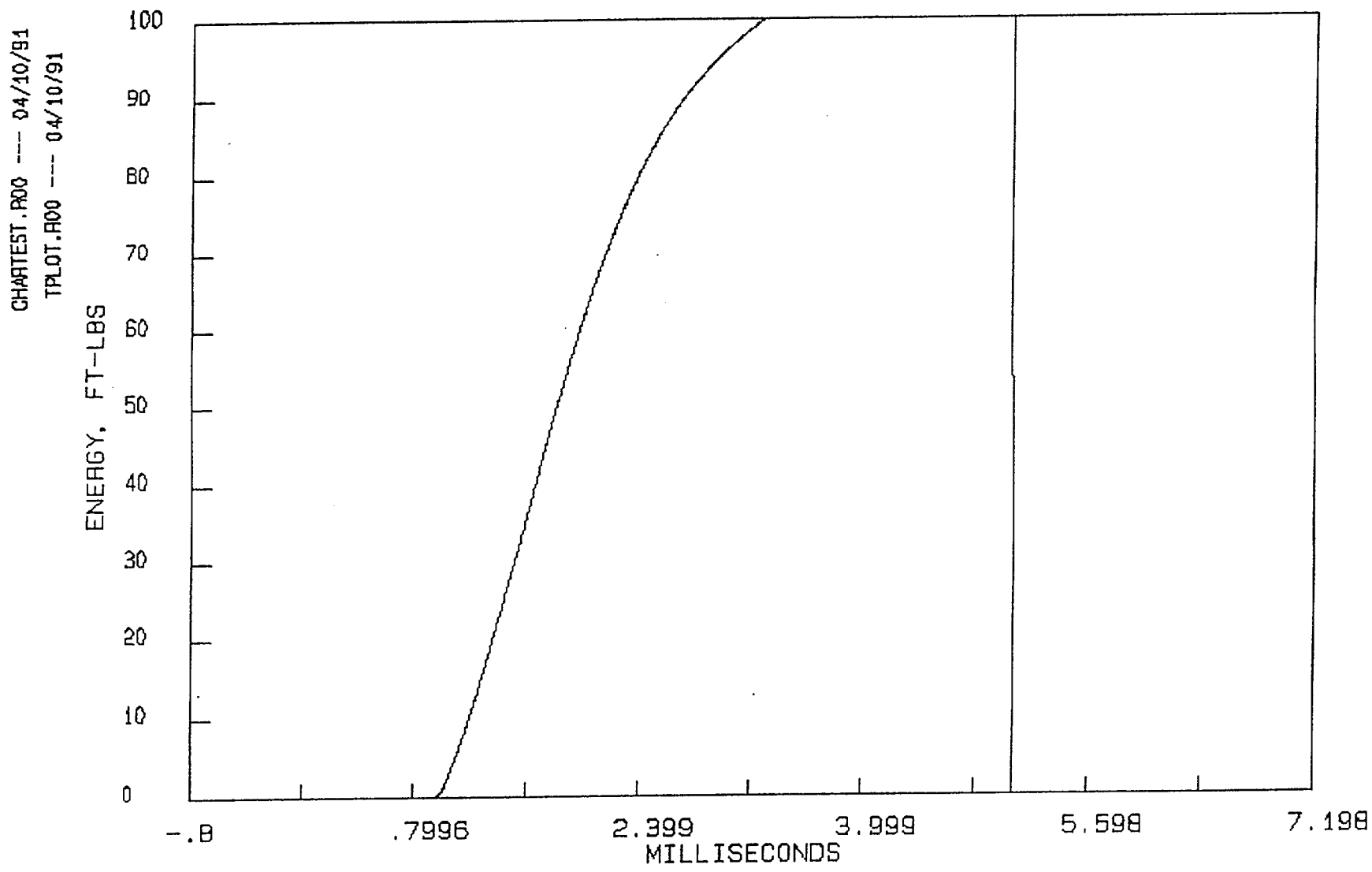

PROJ. NO. 1215-001 QA NO. 00001

LOAD - TIME TRACE FOR SPECIMEN WL35

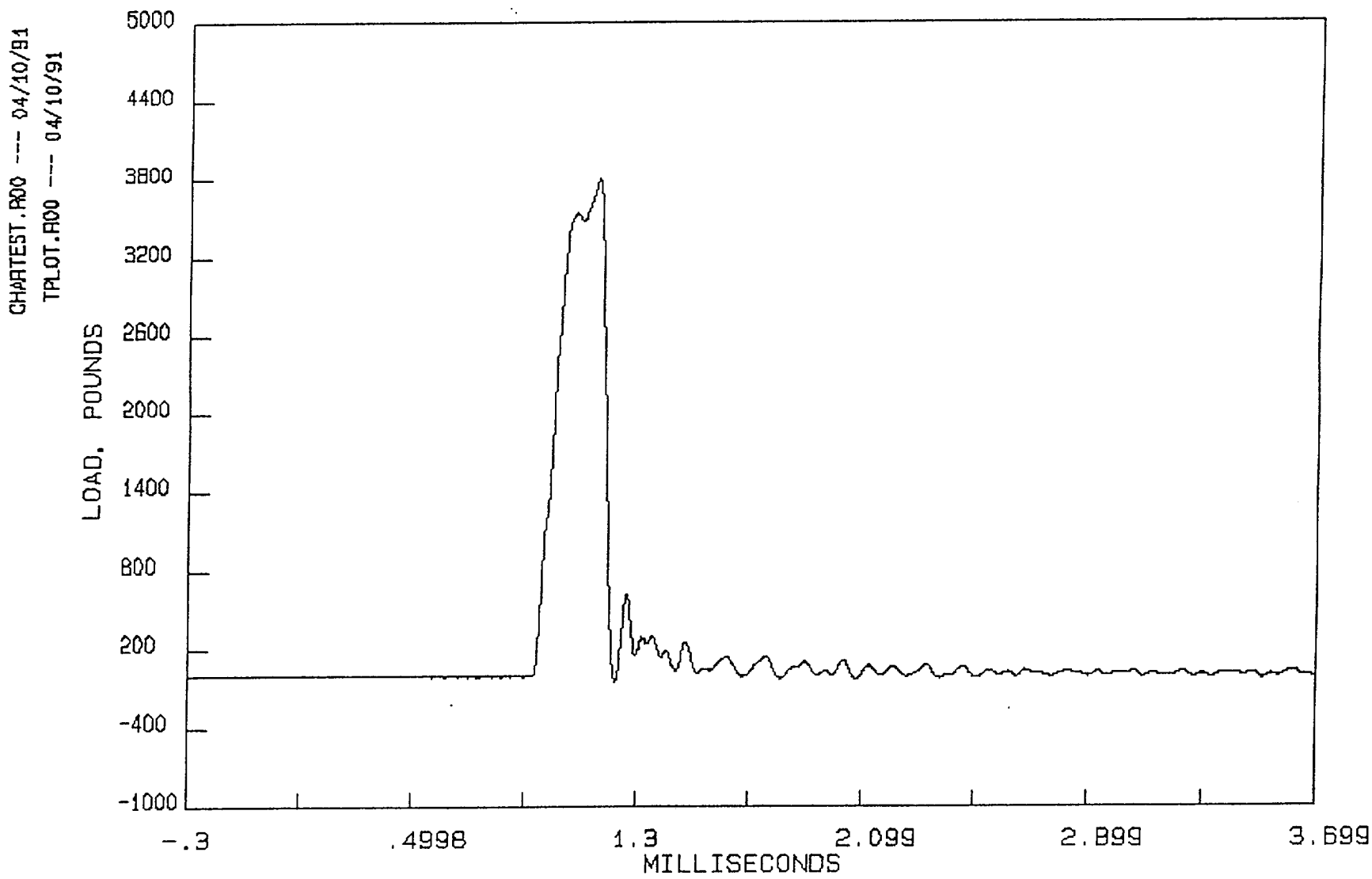

PROJ. NO. 1215-001 QA NO. 00001

ENERGY - TIME TRACE FOR SPECIMEN WL35

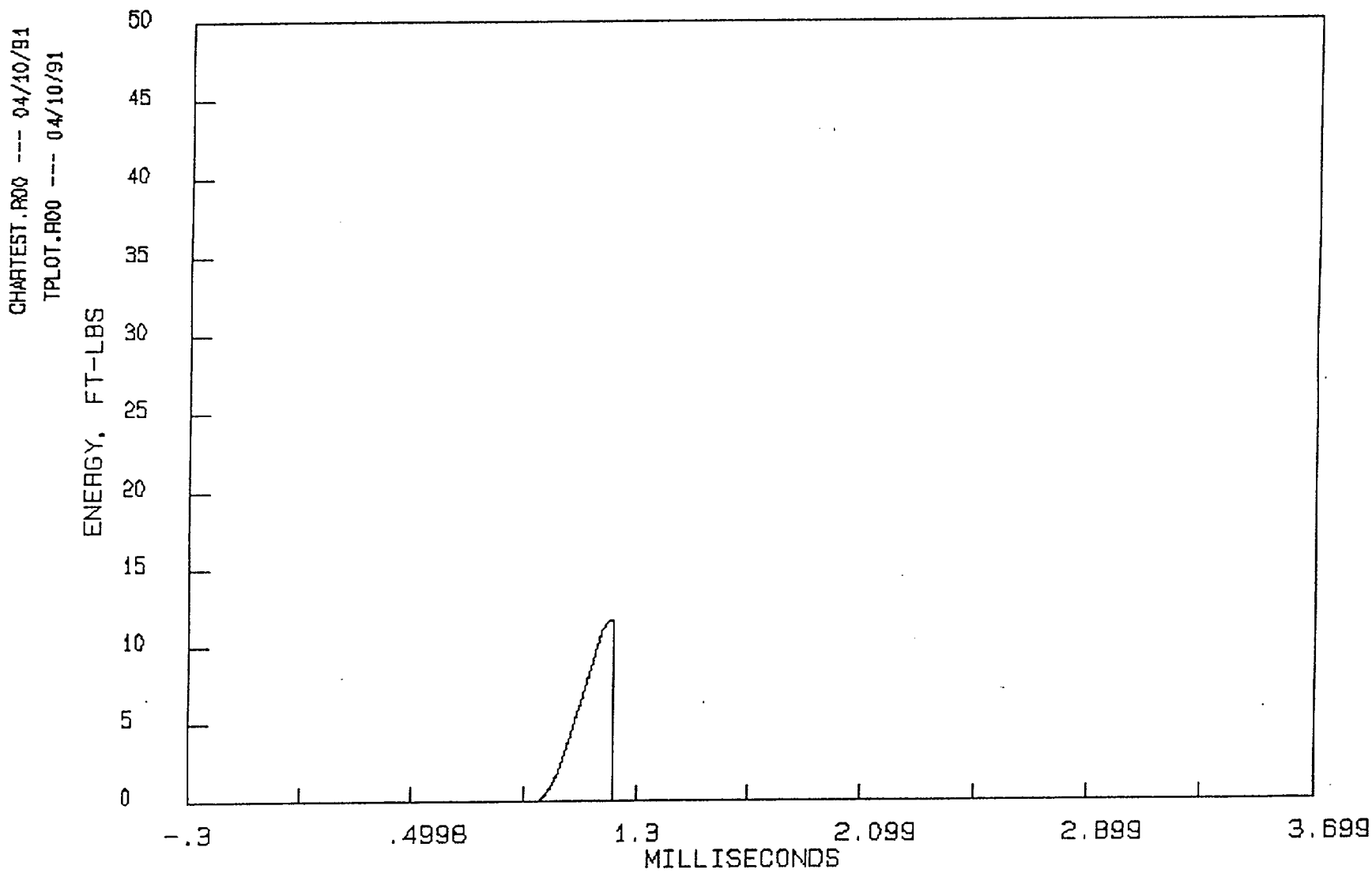

PROJ. NO. 1215-001 QA NO. 00001

LOAD - TIME TRACE FOR SPECIMEN WL36

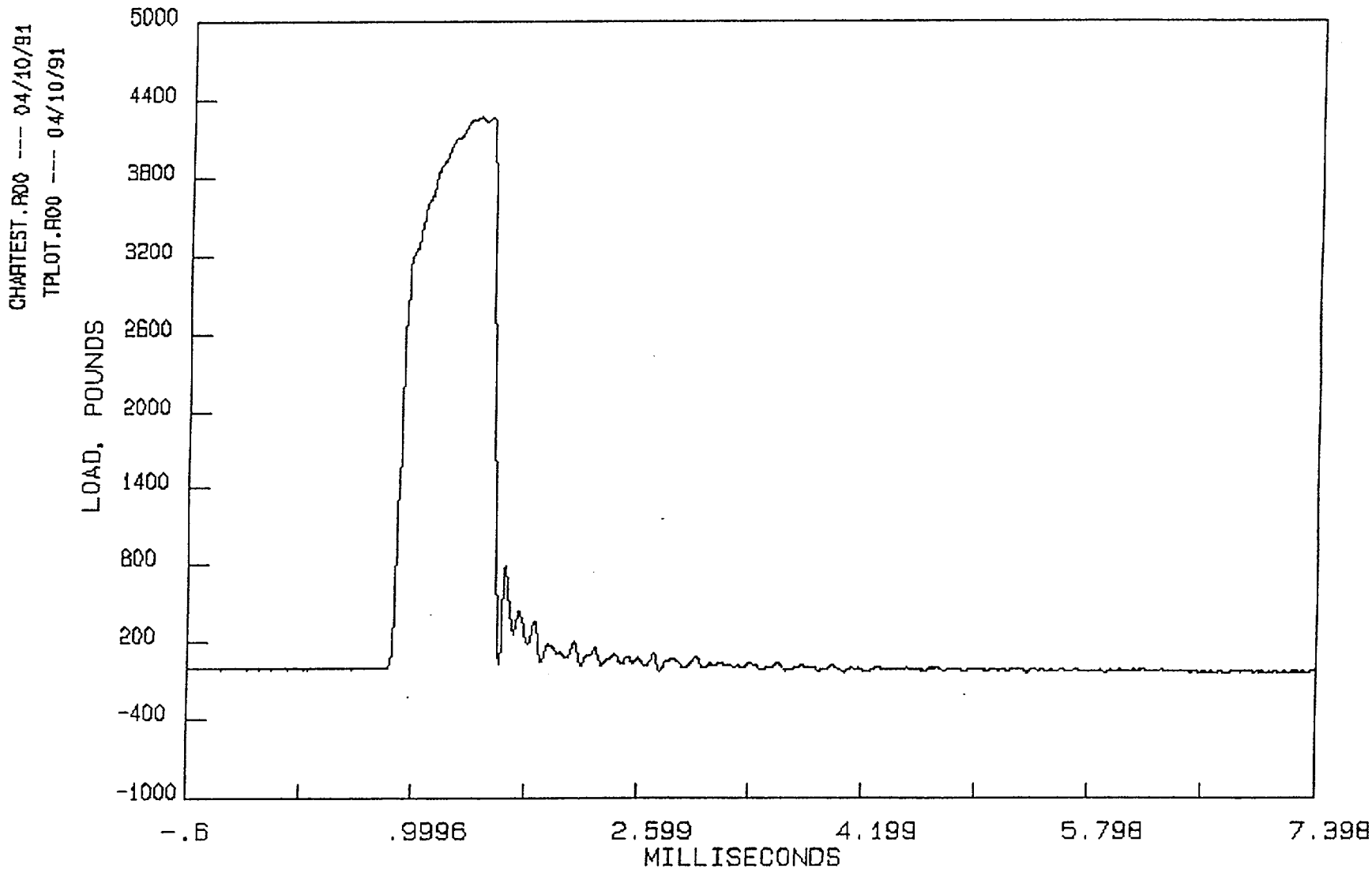

PROJ. NO. 1215-001 QA NO. 00001

ENERGY - TIME TRACE FOR SPECIMEN WL36

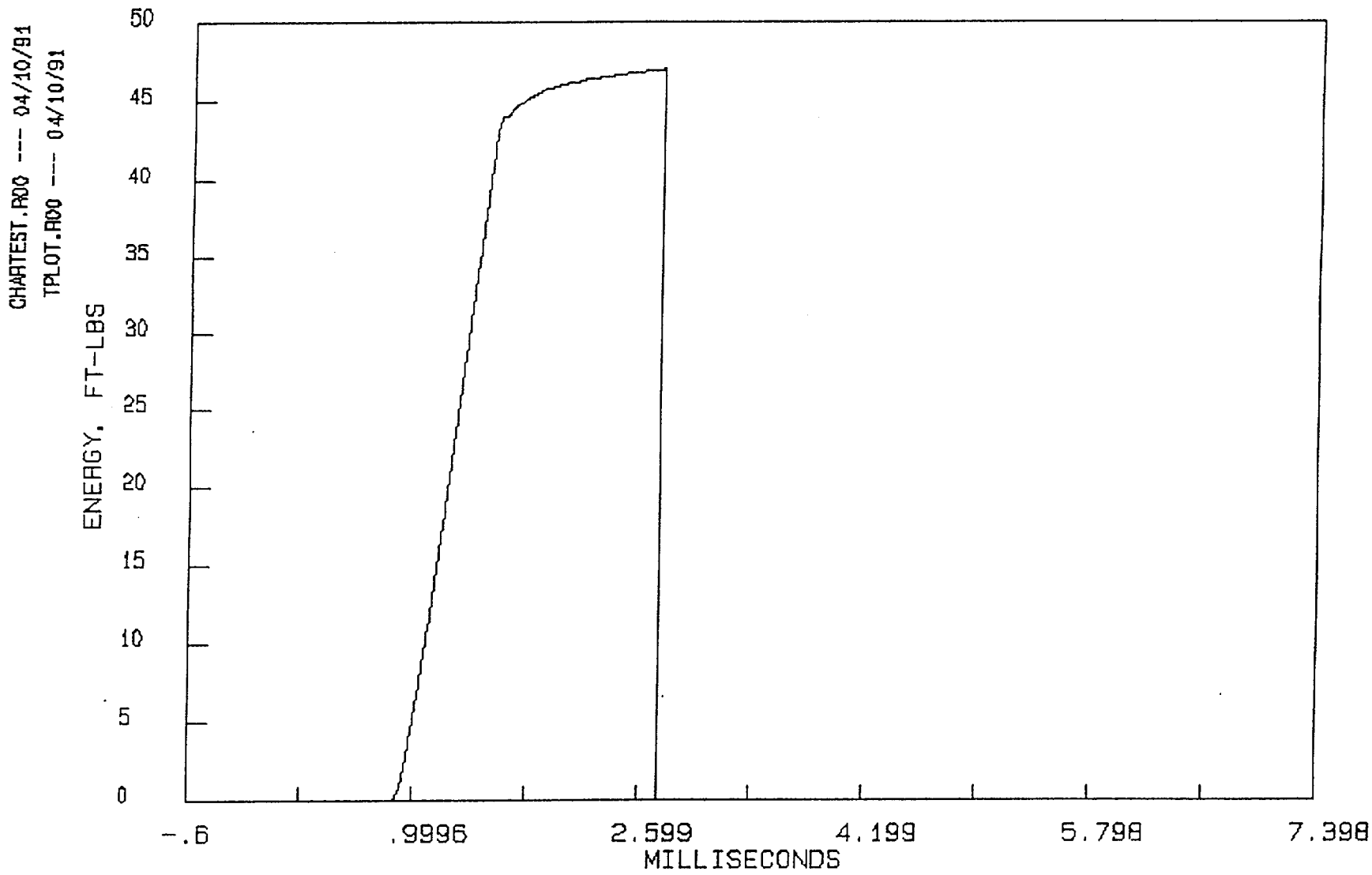

PROJ. NO. 1215-001 QA NO. 00001

LOAD - TIME TRACE FOR SPECIMEN WL43

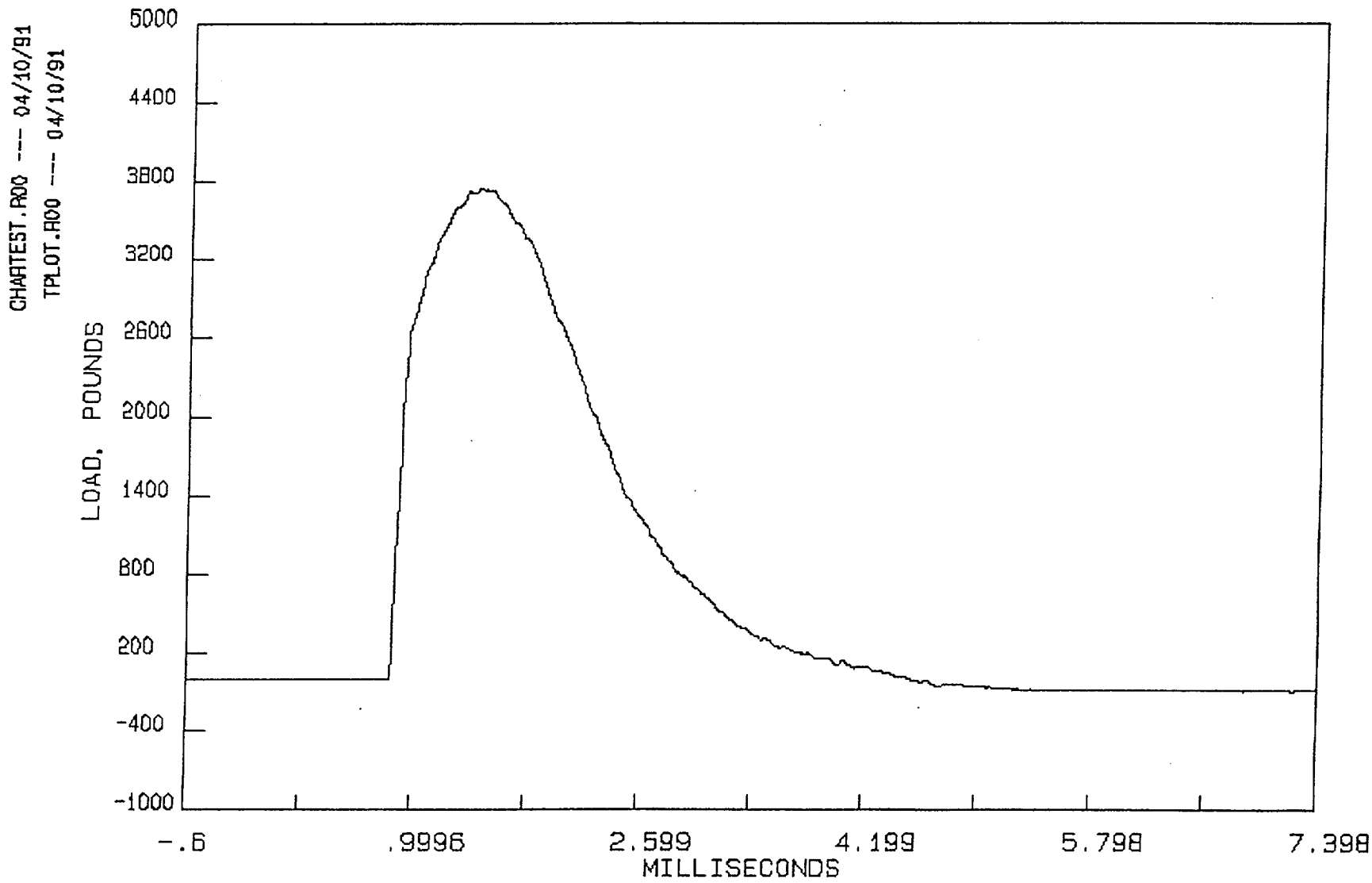

PROJ. NO. 1215-001 QA NO. 00001

ENERGY - TIME TRACE FOR SPECIMEN WL43

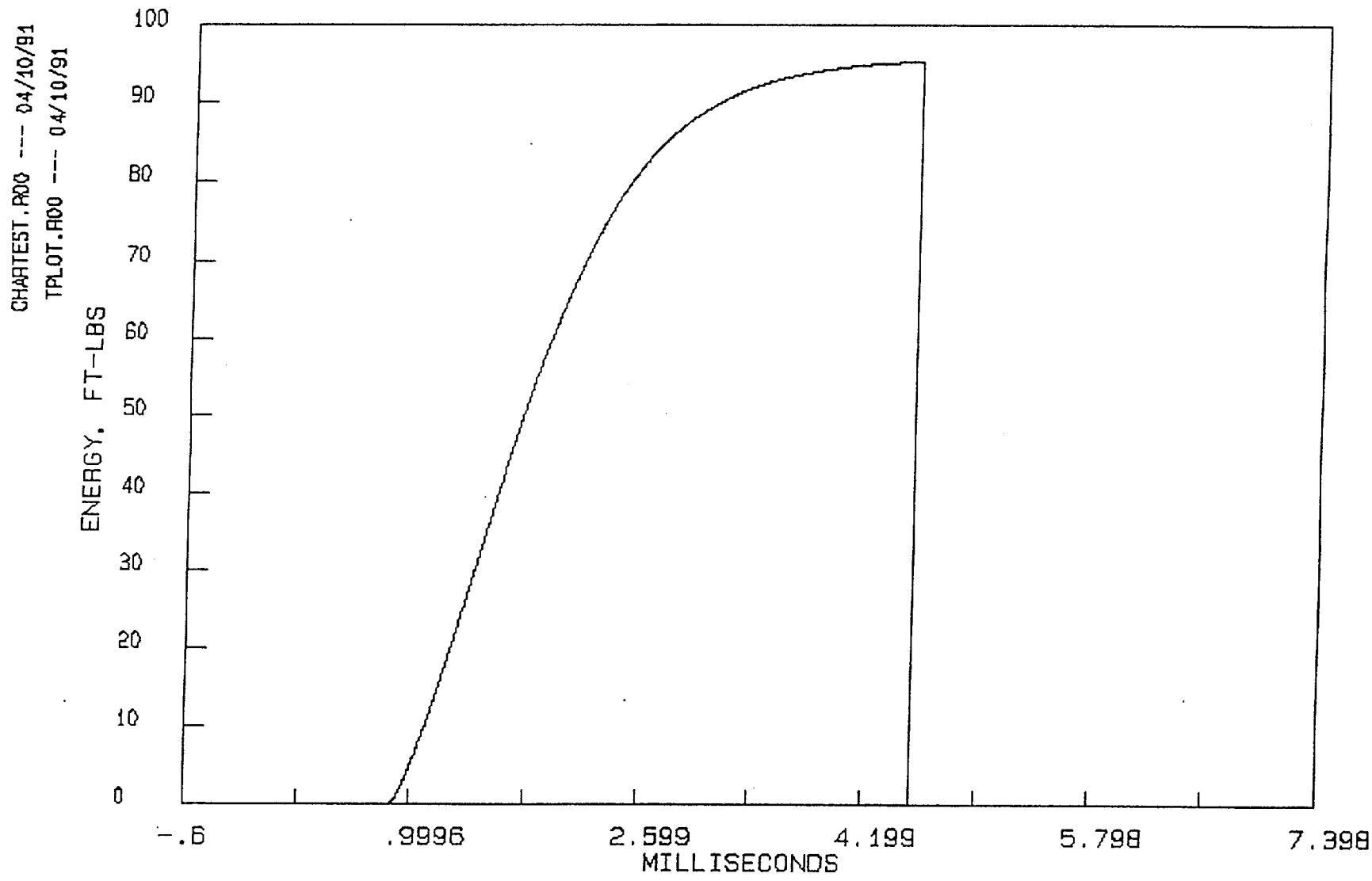

PROJ. NO. 1215-001 QA NO. 00001

LOAD - TIME TRACE FOR SPECIMEN WL37

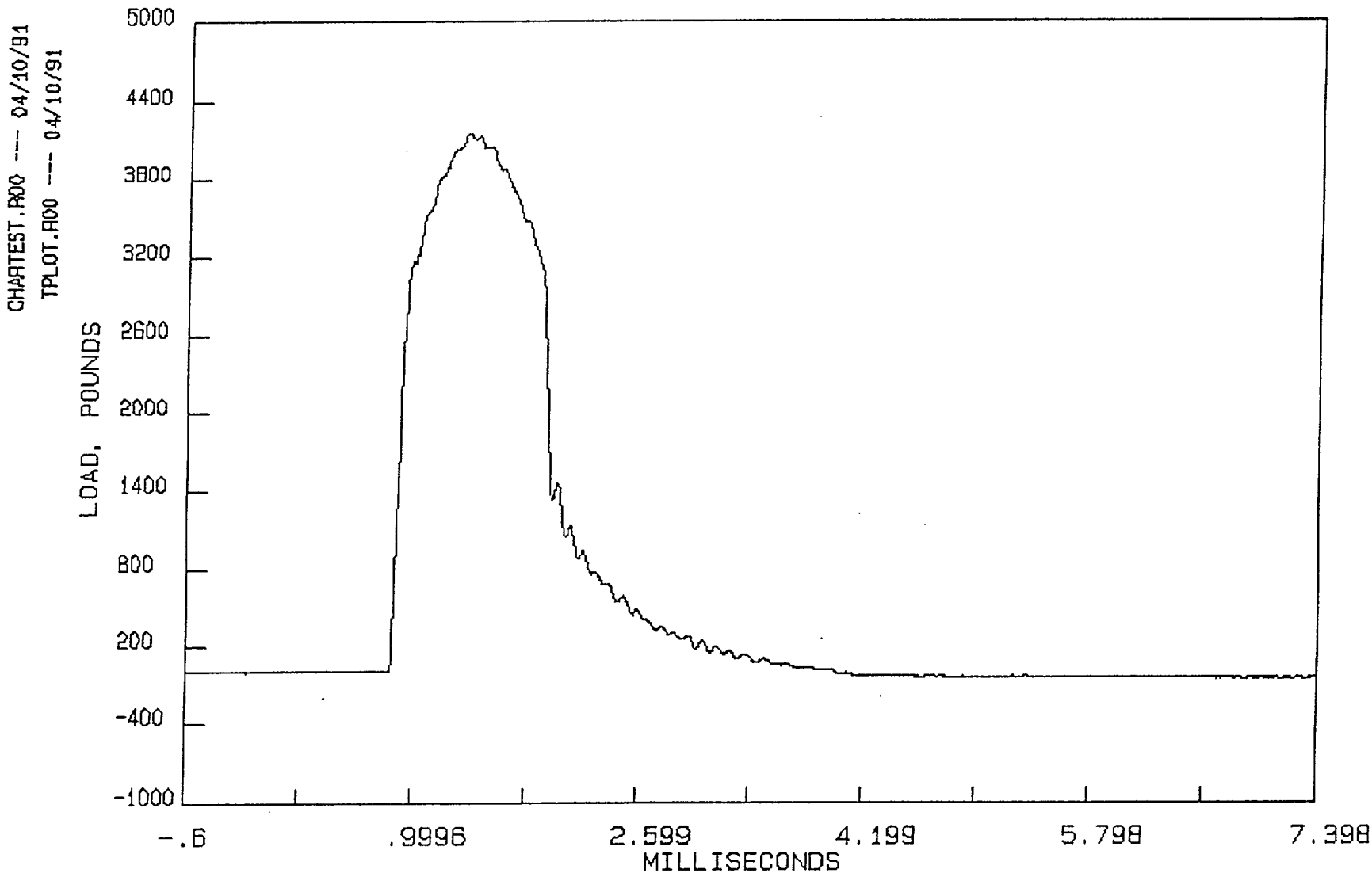

PROJ. NO. 1215-001 QA NO. 00001

ENERGY - TIME TRACE FOR SPECIMEN WL37

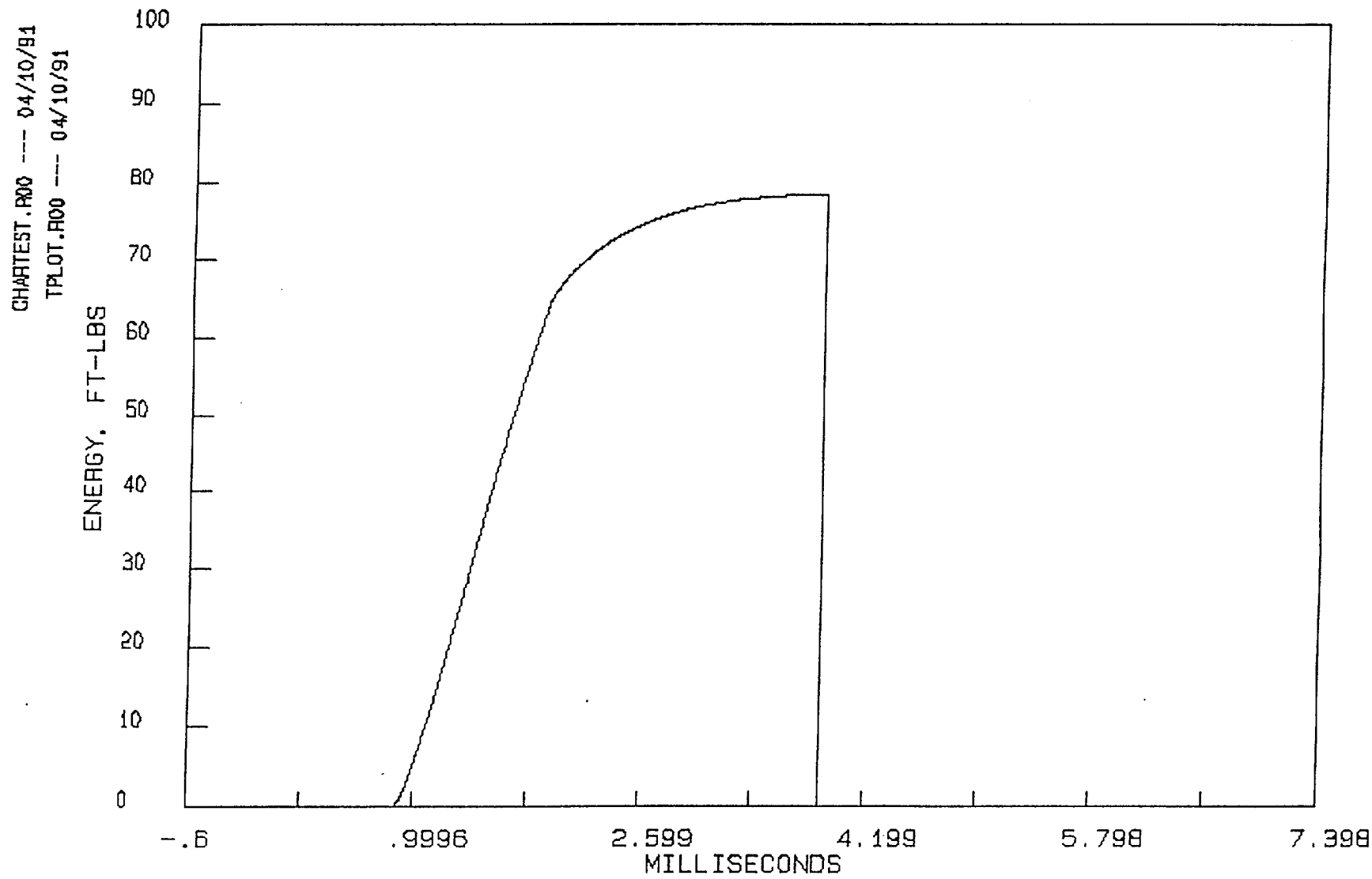

PROJ. NO. 1215-001 QA NO. 00001

LOAD - TIME TRACE FOR SPECIMEN WL40

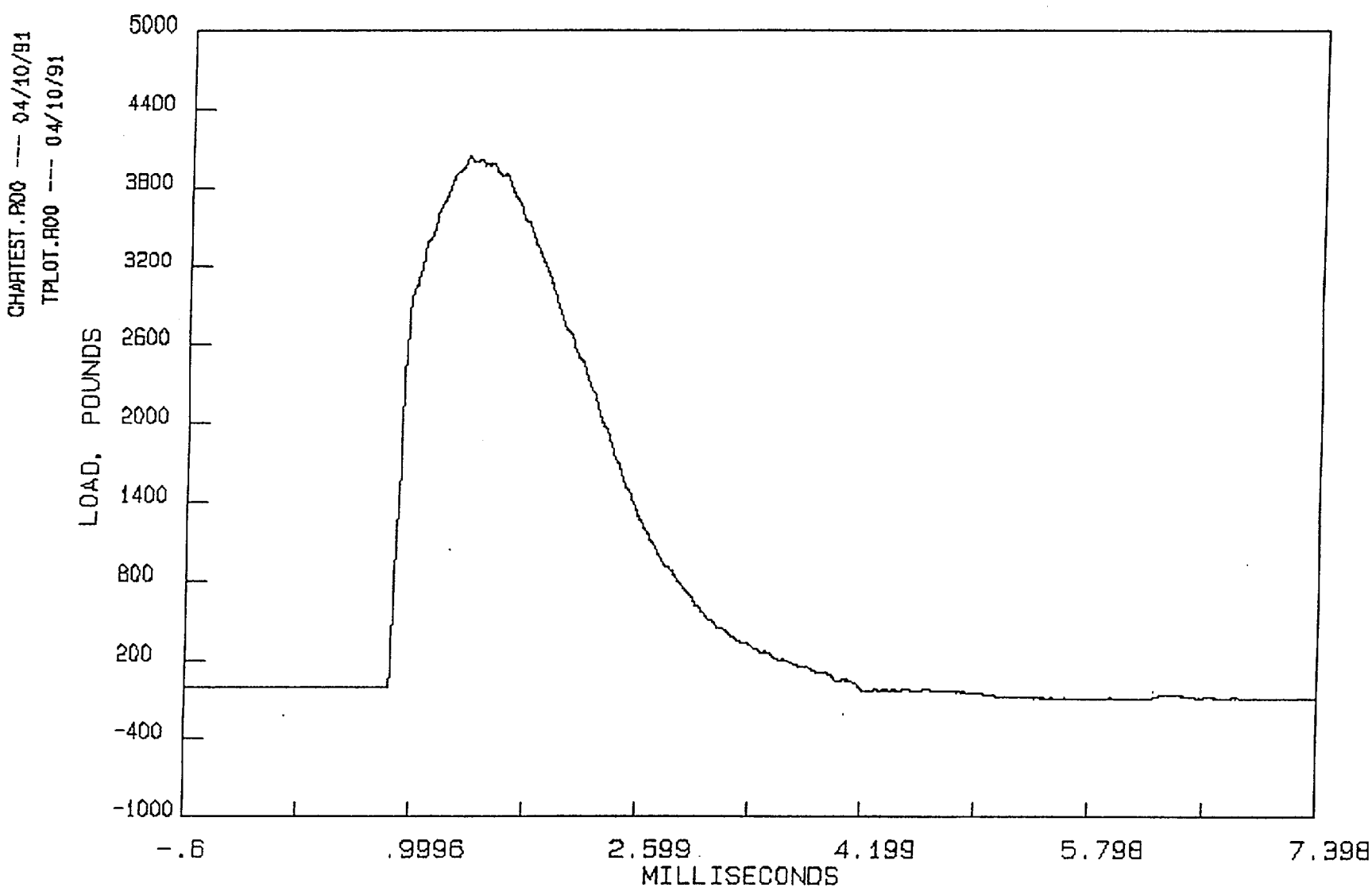

PROJ. NO. 1215-001 QA NO. 00001

ENERGY - TIME TRACE FOR SPECIMEN WL40

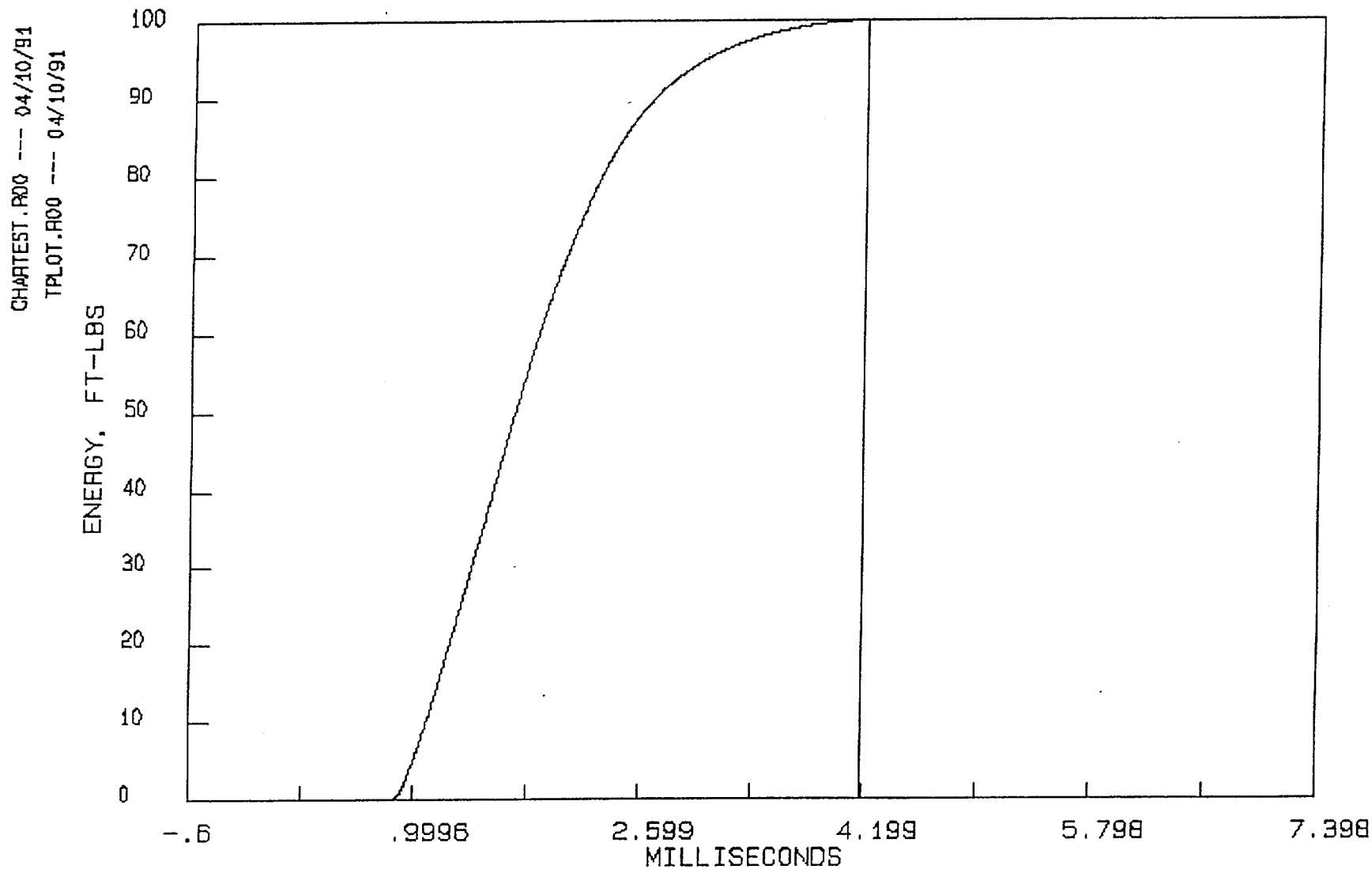

PROJ. NO. 1215-001 QA NO. 00001

LOAD - TIME TRACE FOR SPECIMEN WL38

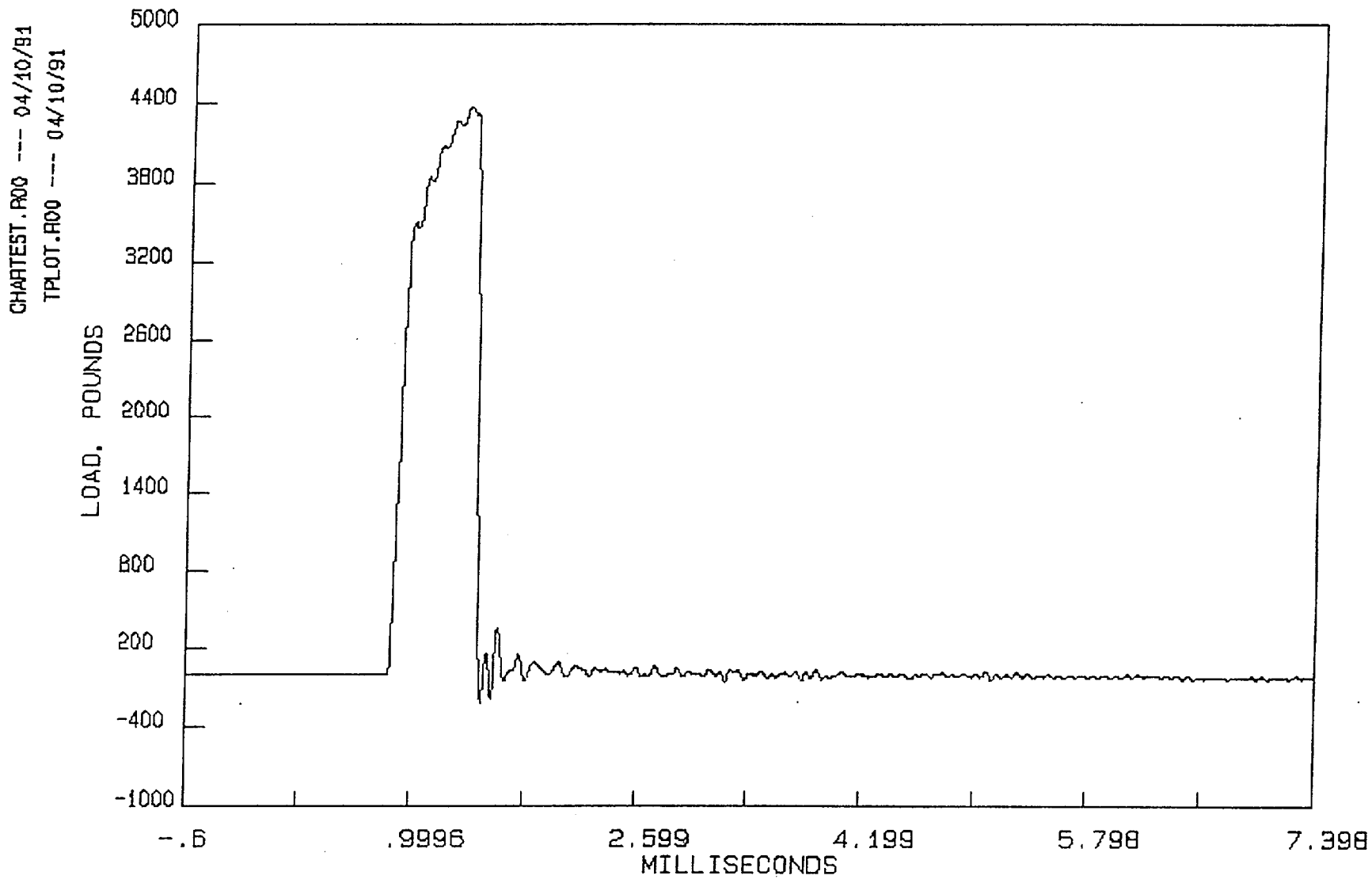

PROJ. NO. 1215-001 QA NO. 00001

ENERGY - TIME TRACE FOR SPECIMEN WL38

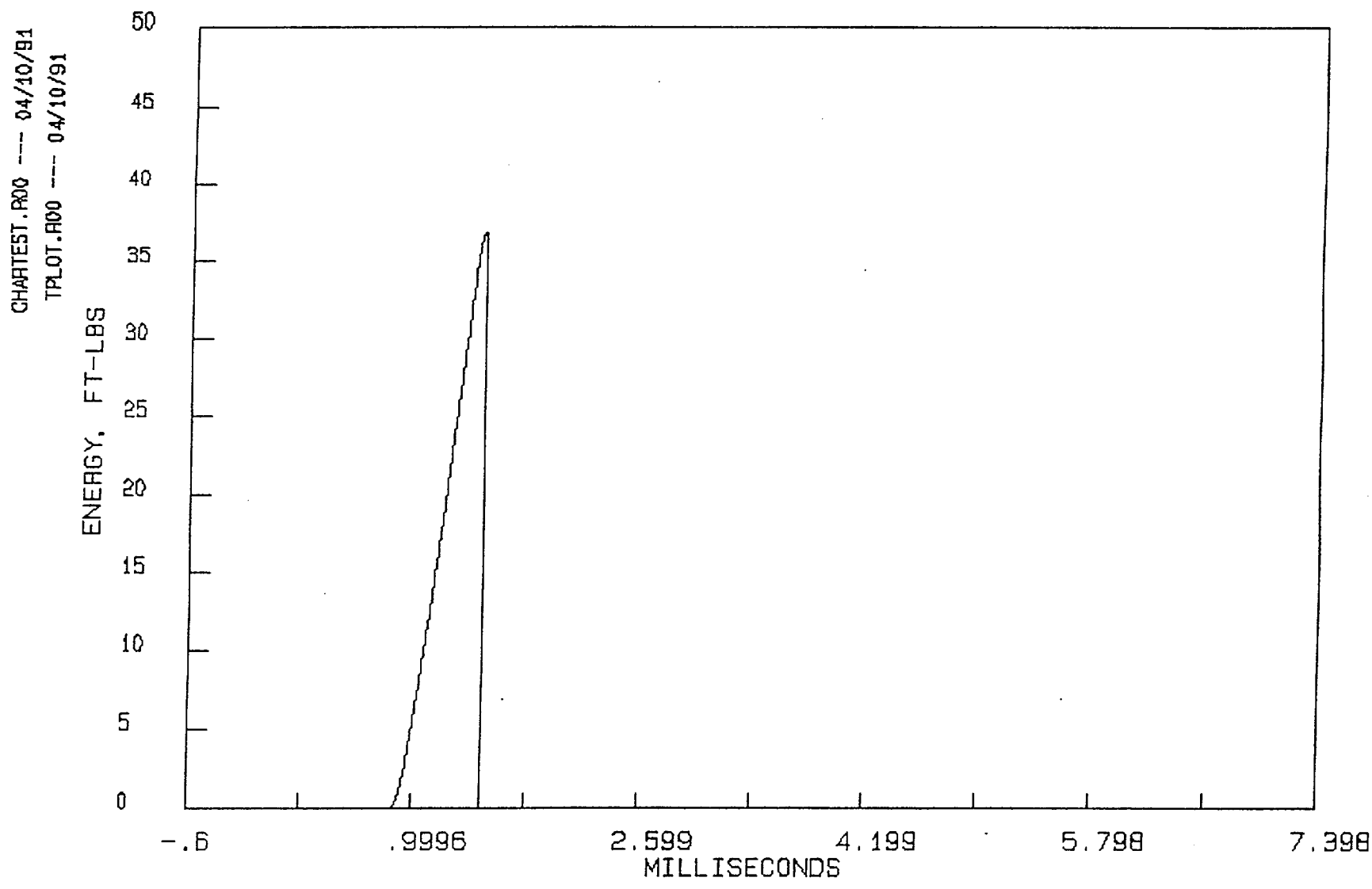

PROJ. NO. 1215-001 QA NO. 00001

LOAD - TIME TRACE FOR SPECIMEN WH36

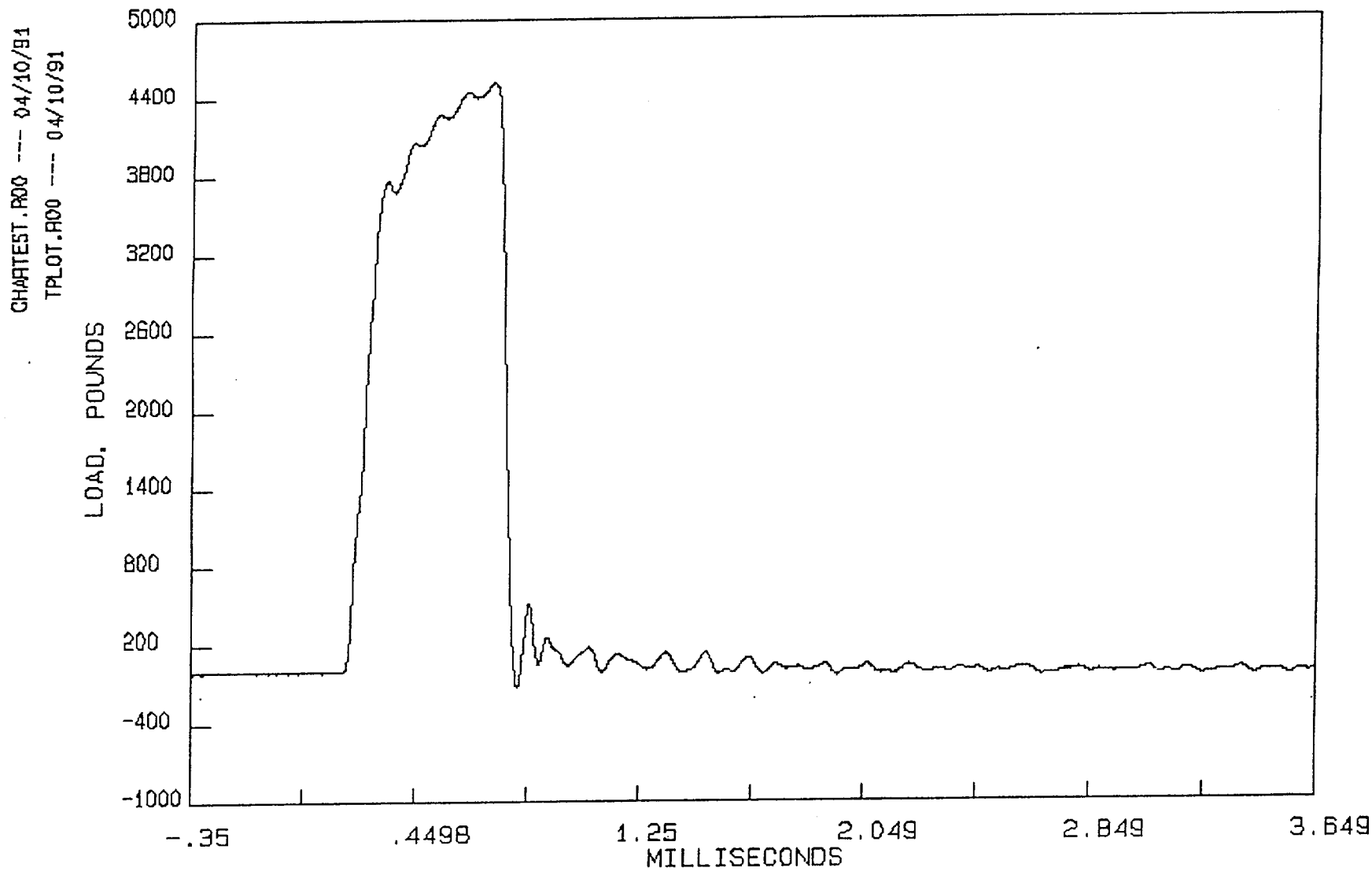

PROJ. NO. 1215-001 QA NO. 00001

ENERGY - TIME TRACE FOR SPECIMEN WH36

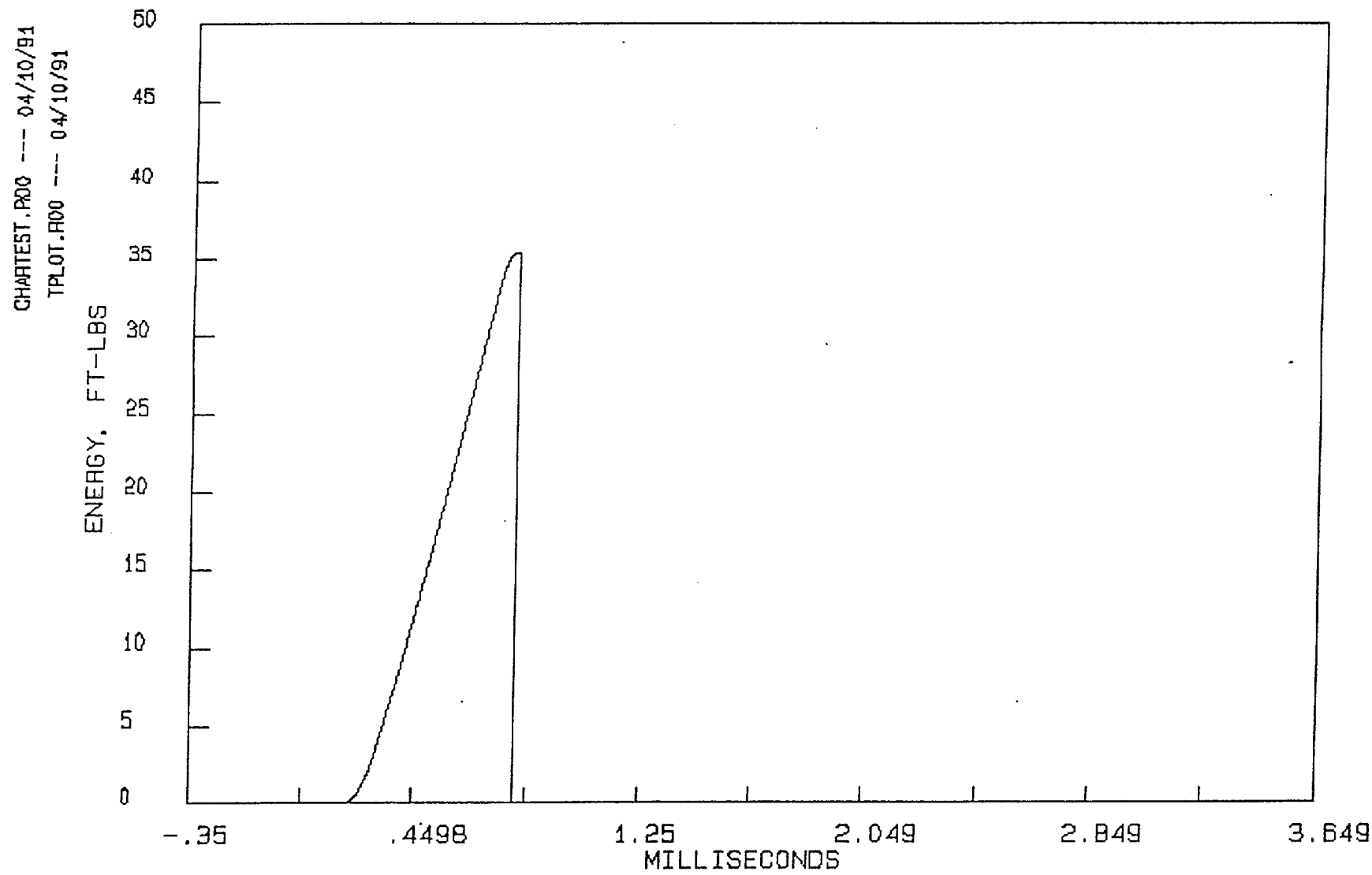

PROJ. NO. 1215-001 QA NO. 00001

LOAD - TIME TRACE FOR SPECIMEN WH38

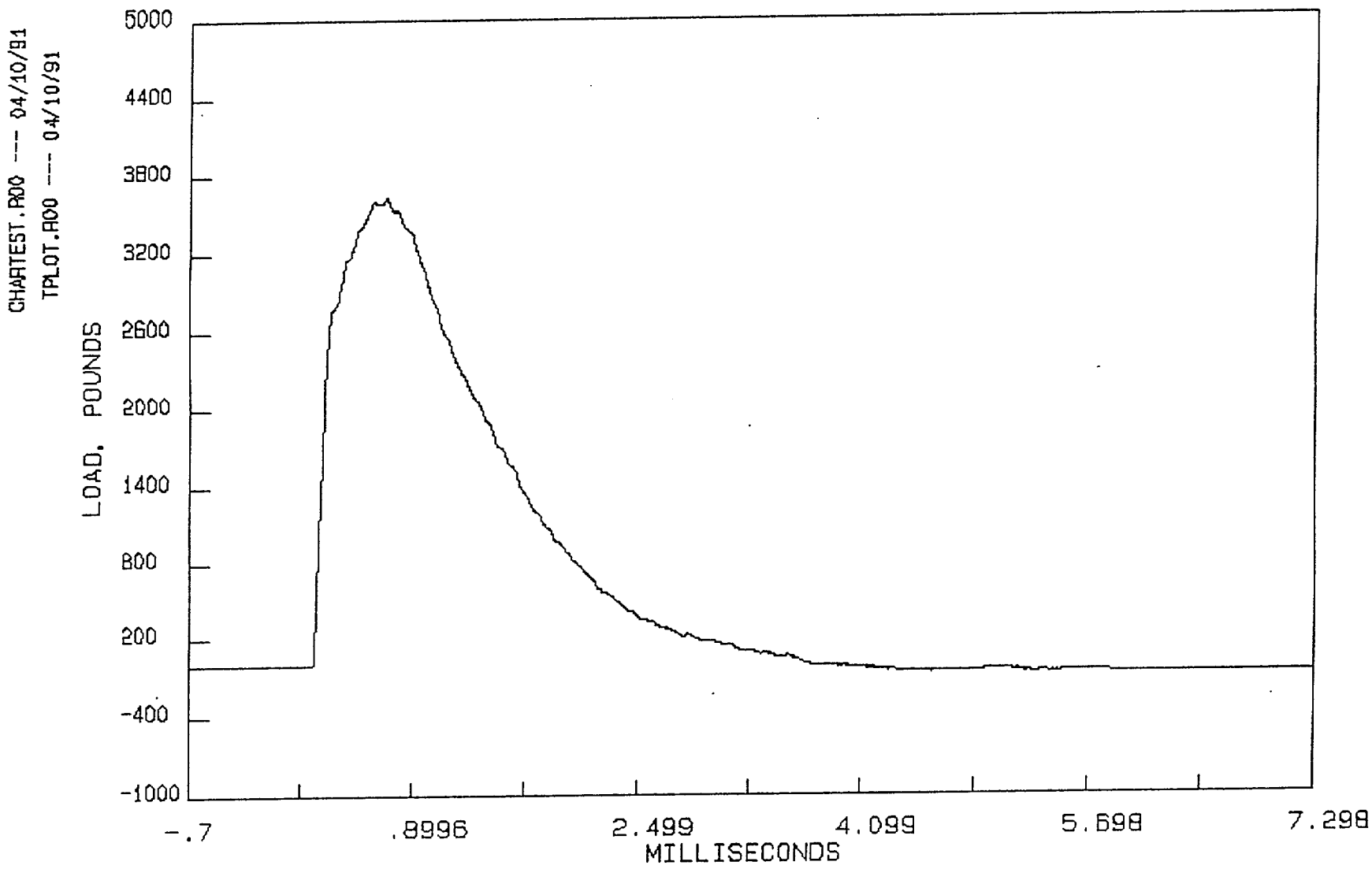

PROJ. NO. 1215-001 QA NO. 00001

ENERGY - TIME TRACE FOR SPECIMEN WH38

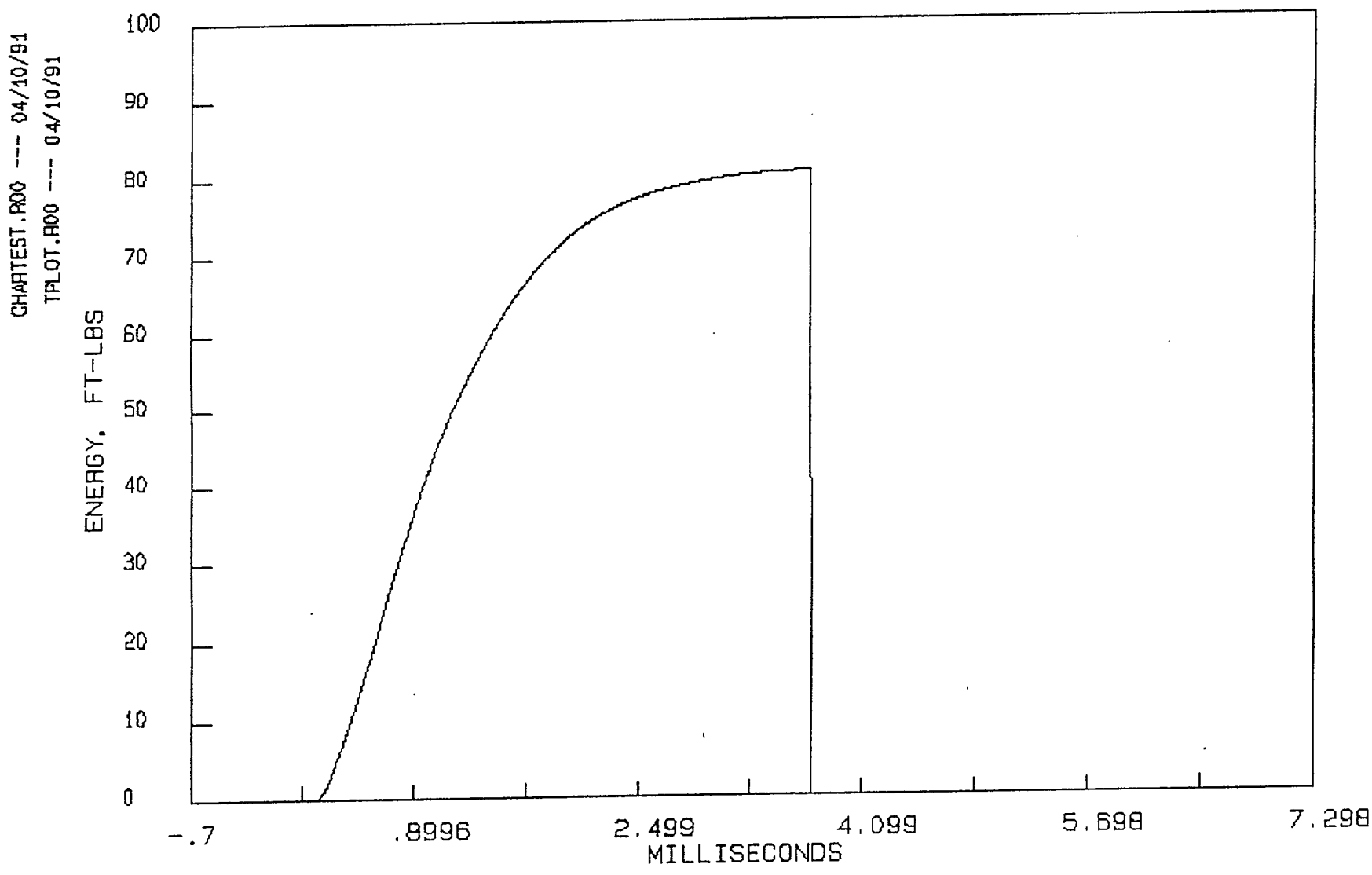

PROJ. NO. 1215-001 QA NO. 00001

LOAD - TIME TRACE FOR SPECIMEN WH40

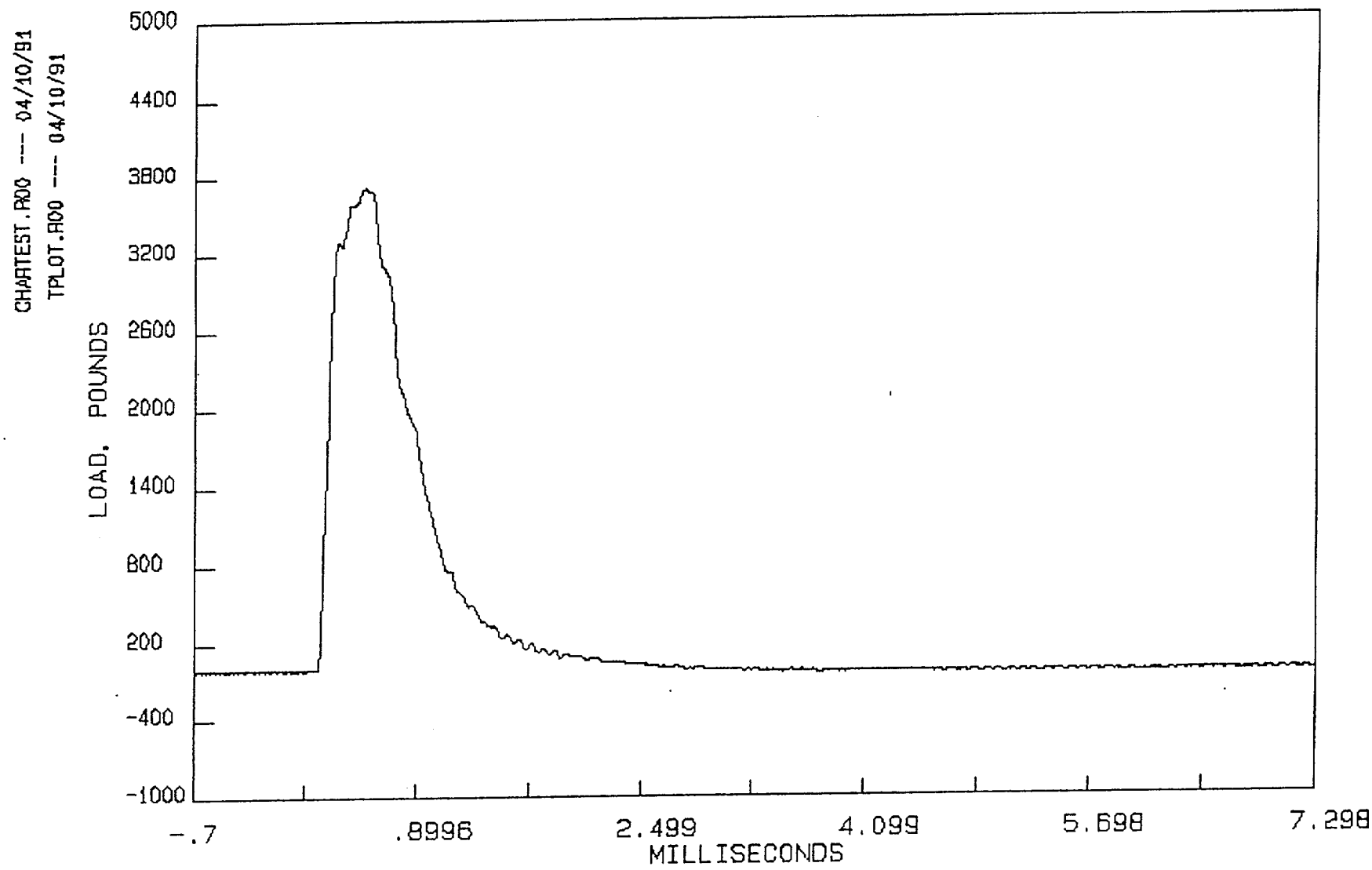

PROJ. NO. 1215-001 QA NO. 00001

ENERGY - TIME TRACE FOR SPECIMEN WH40

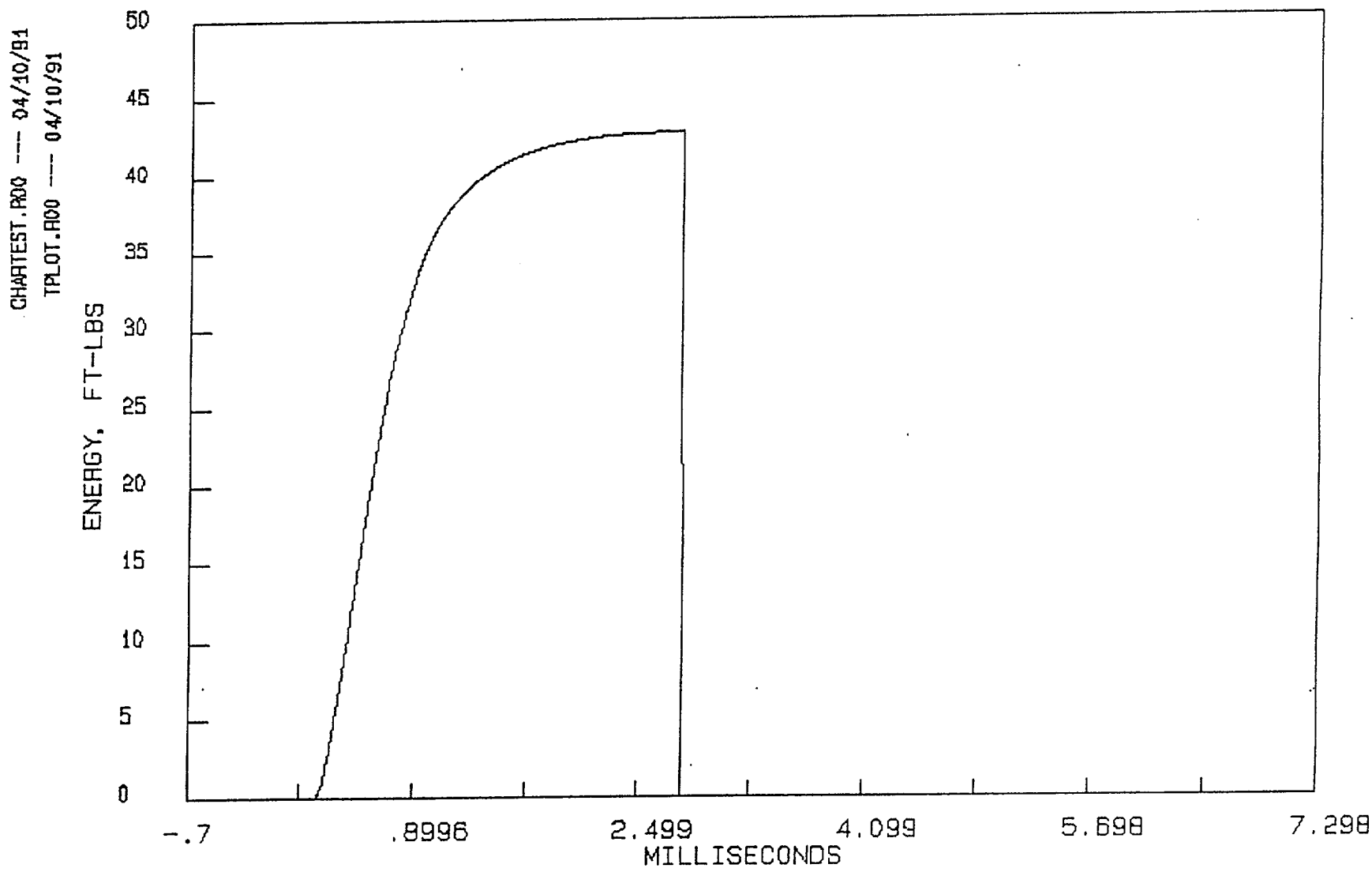

PROJ. NO. 1215-001 QA NO. 00001

LOAD - TIME TRACE FOR SPECIMEN WH33

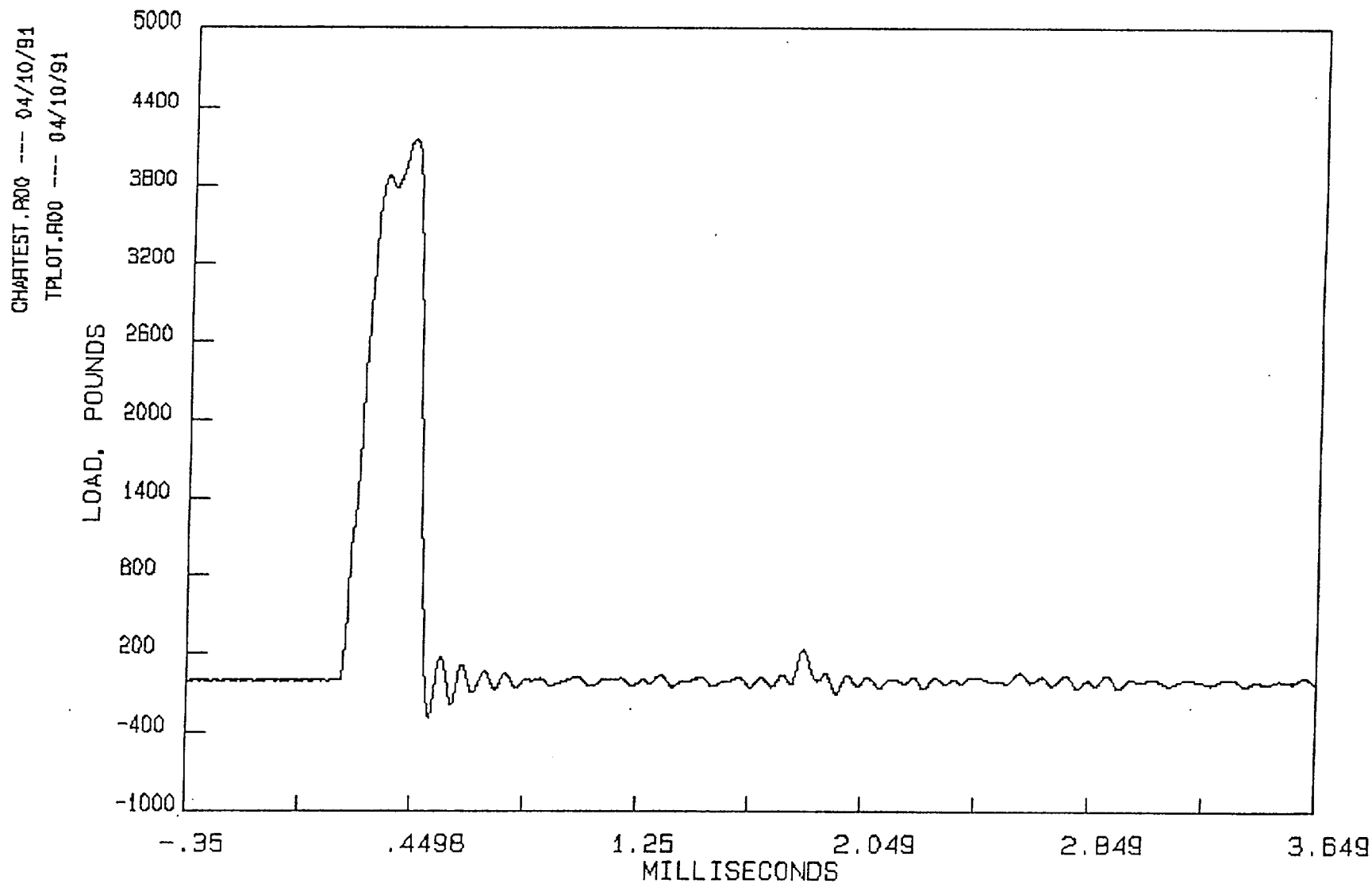

PROJ. NO. 1215-001 QA NO. 00001

ENERGY - TIME TRACE FOR SPECIMEN WH33

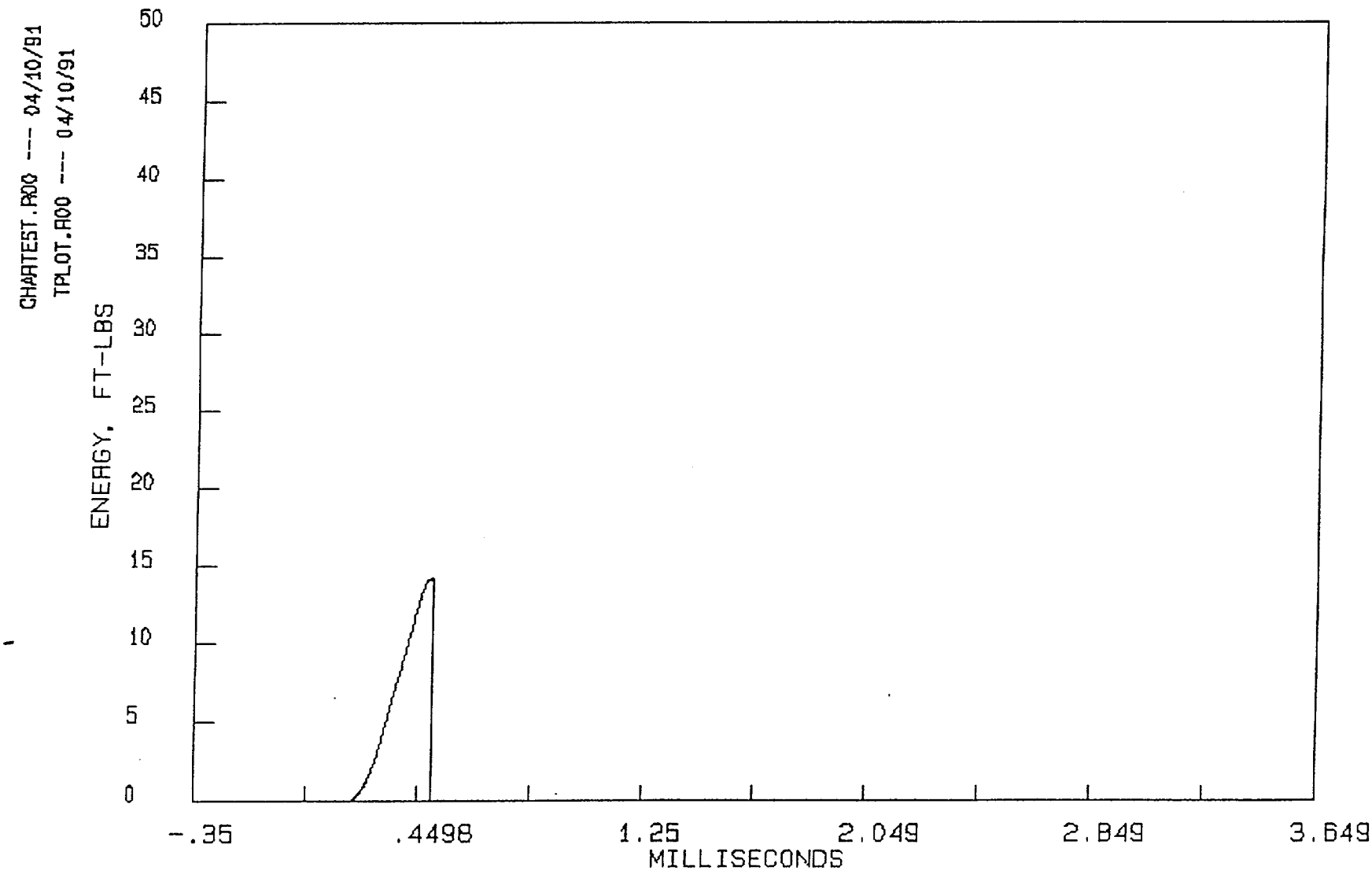

PROJ. NO. 1215-001 QA NO. 00001

LOAD - TIME TRACE FOR SPECIMEN WH37

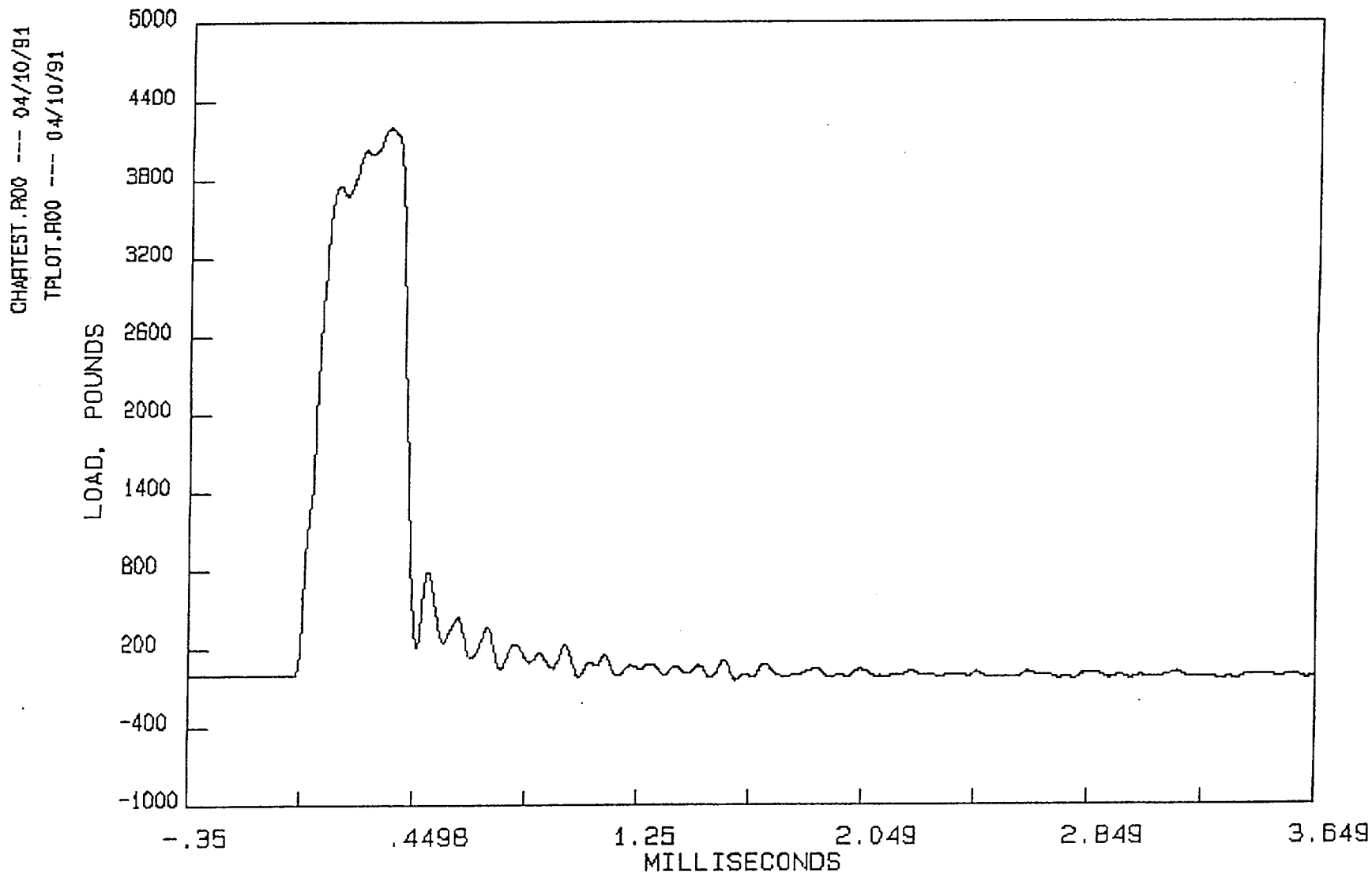

PROJ. NO. 1215-001 QA NO. 00001

ENERGY - TIME TRACE FOR SPECIMEN WH37

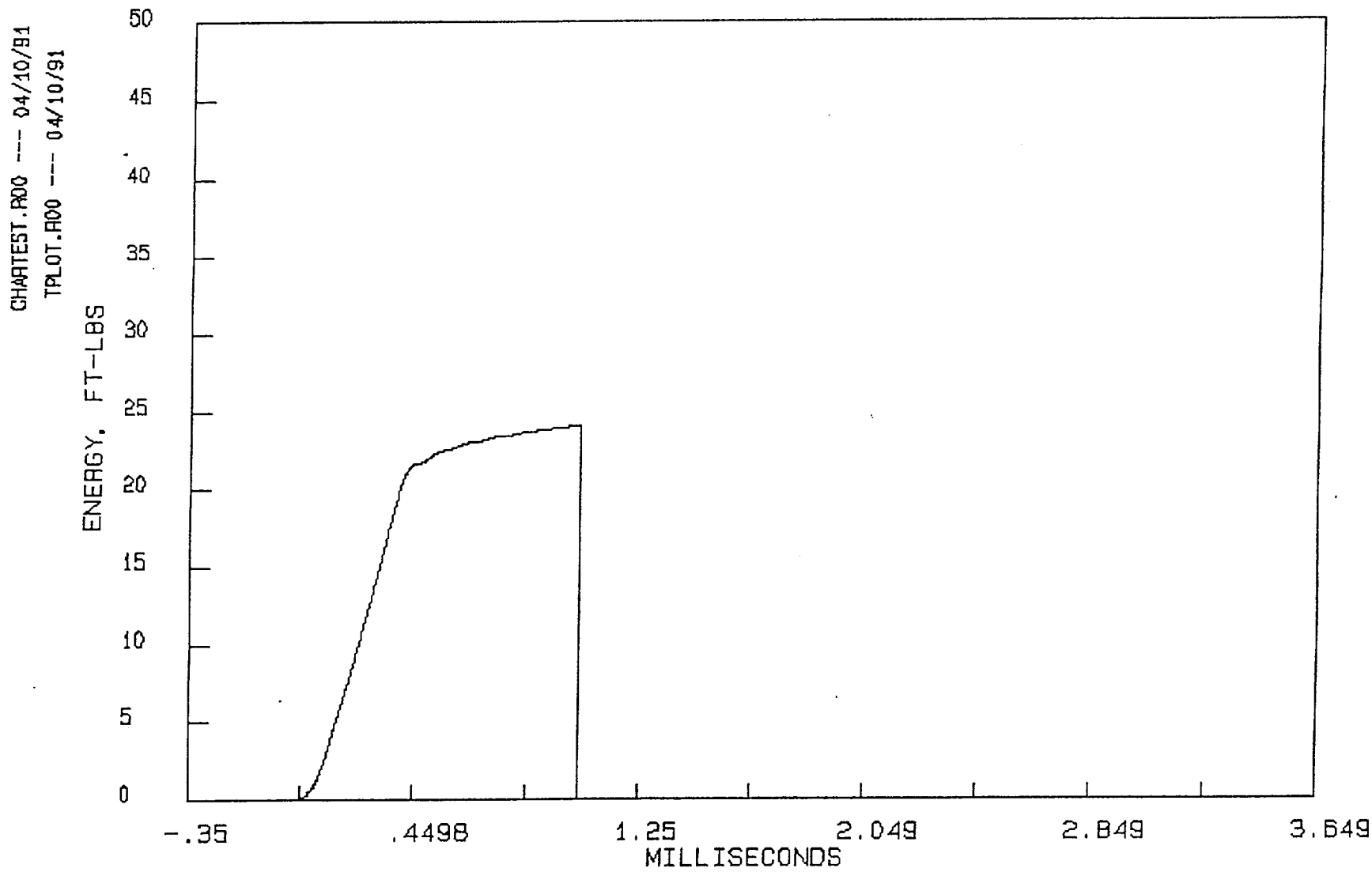

PROJ. NO. 1215-001 QA NO. 00001

LOAD - TIME TRACE FOR SPECIMEN WH41

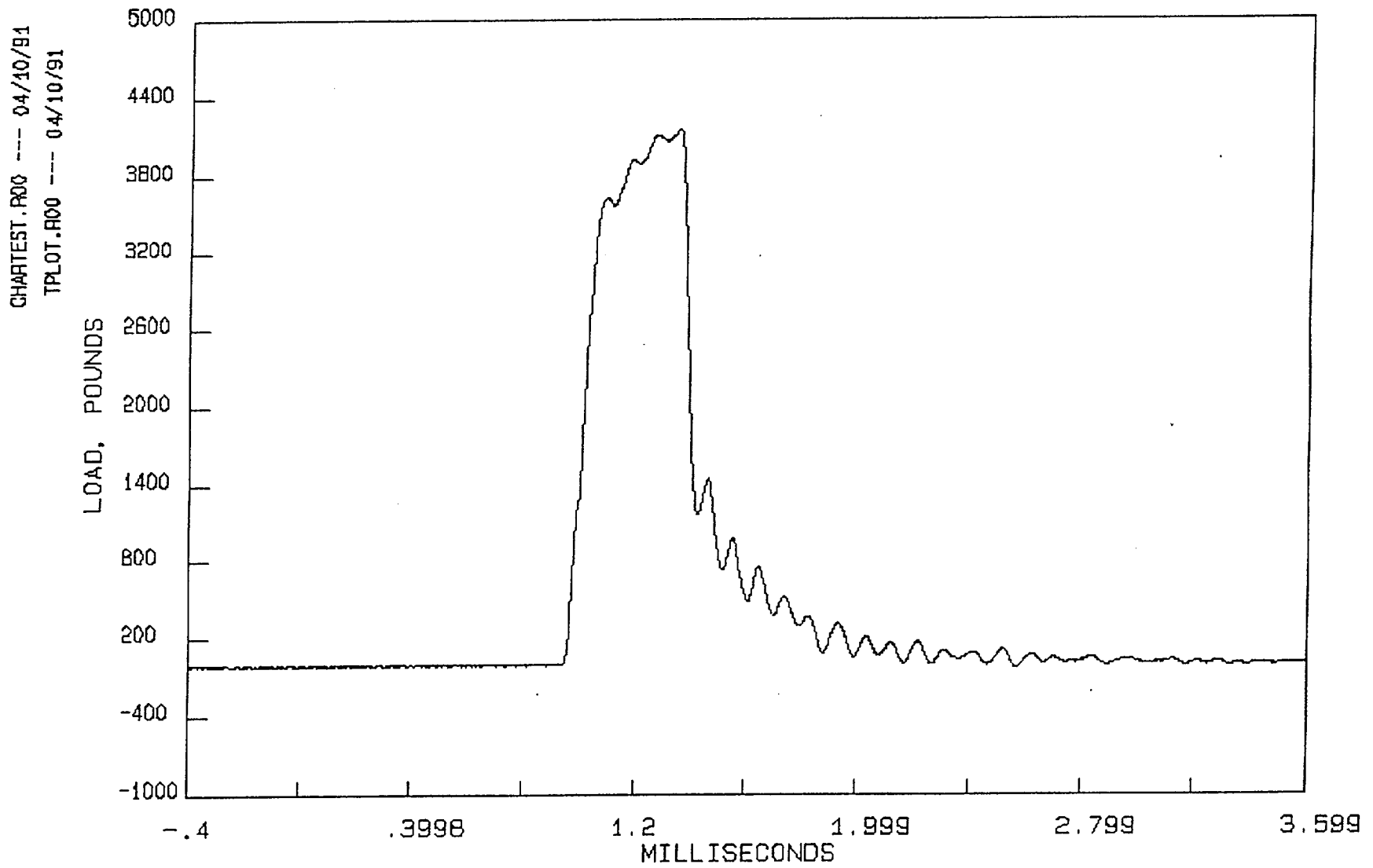

PROJ. NO. 1215-001 QA NO. 00001

ENERGY - TIME TRACE FOR SPECIMEN WH41

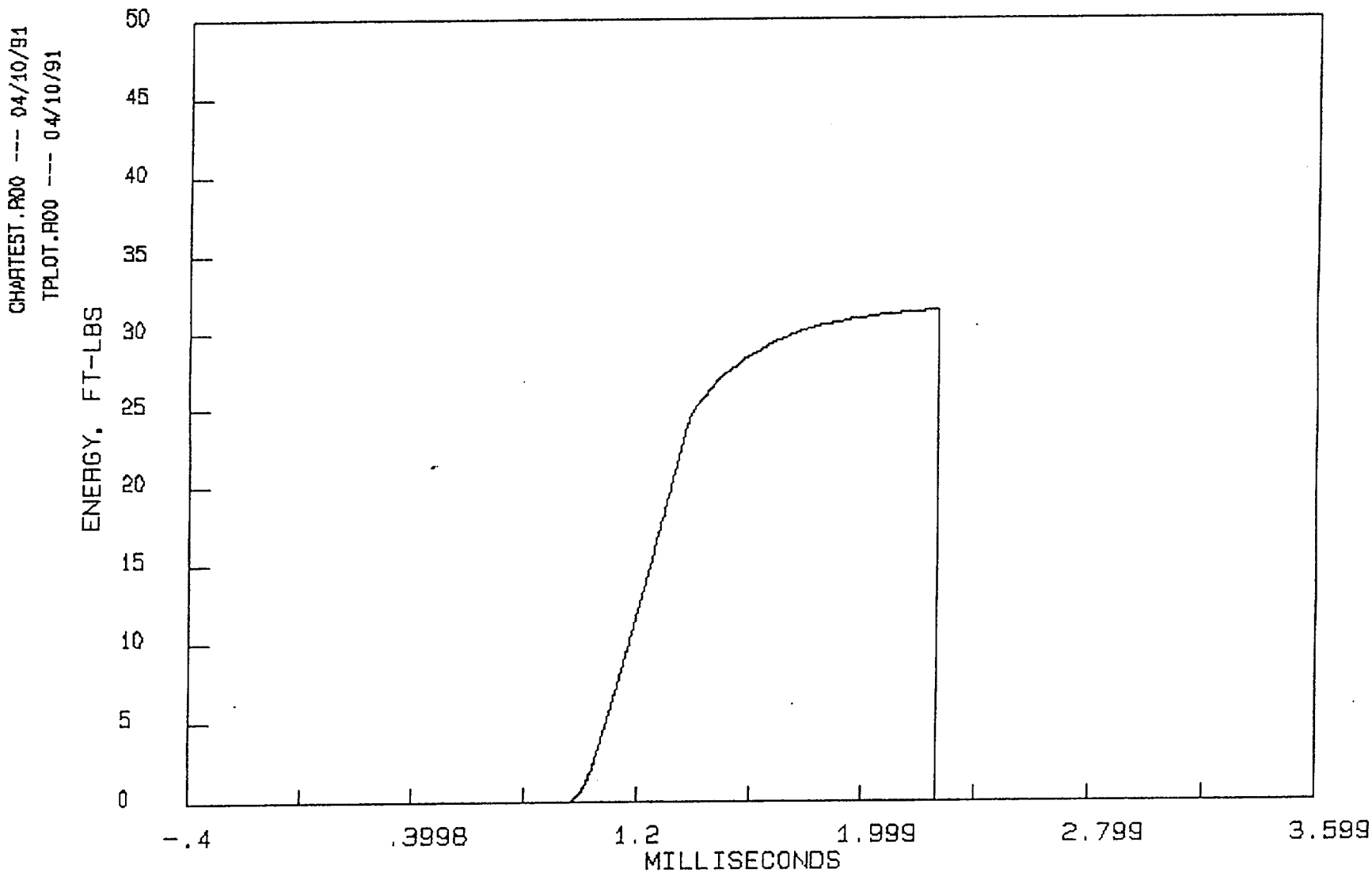

PROJ. NO. 1215-001 QA NO. 00001

LOAD - TIME TRACE FOR SPECIMEN WH44

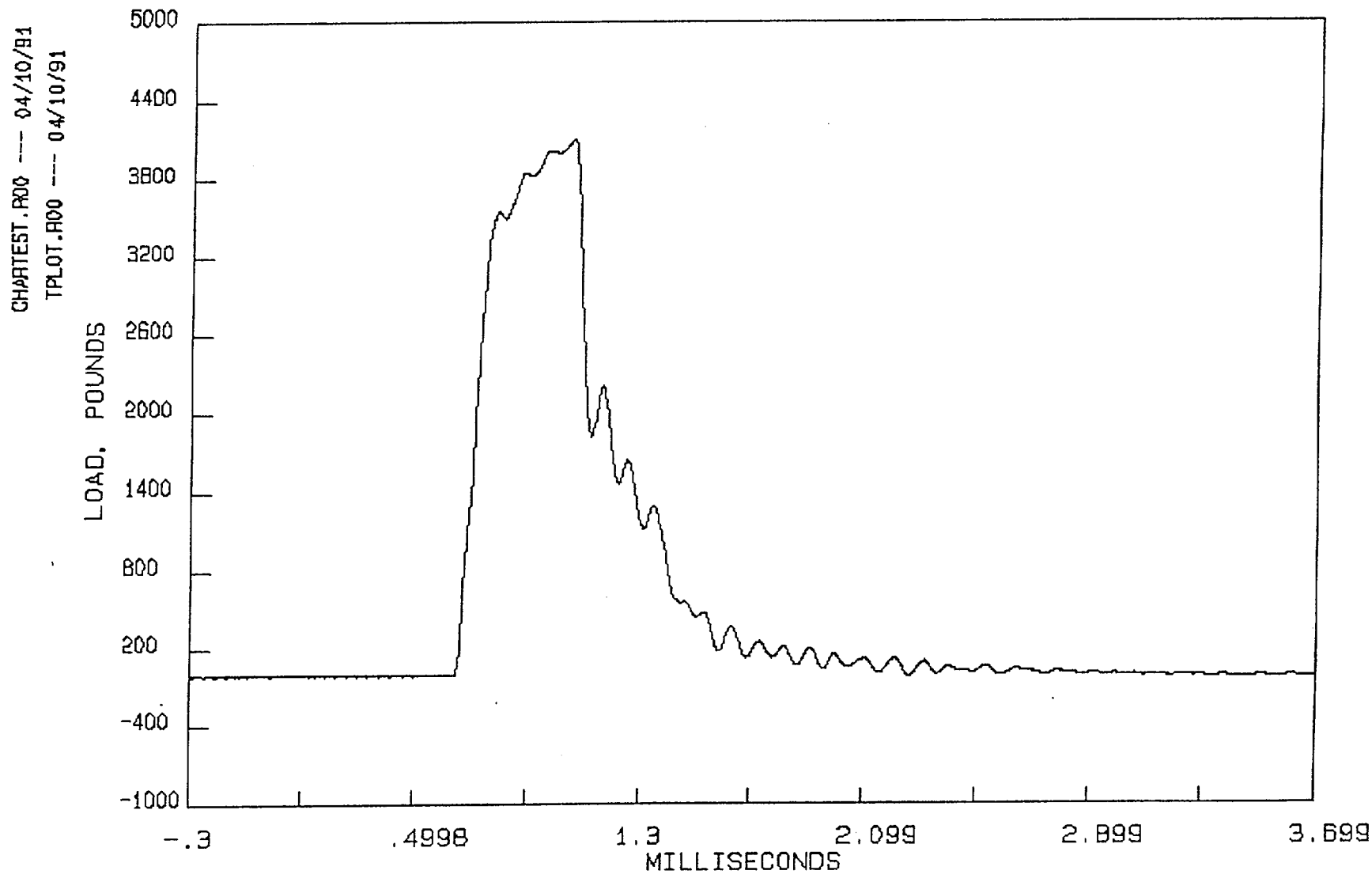

PROJ. NO. 1215-001 QA NO. 00001

ENERGY - TIME TRACE FOR SPECIMEN WH44

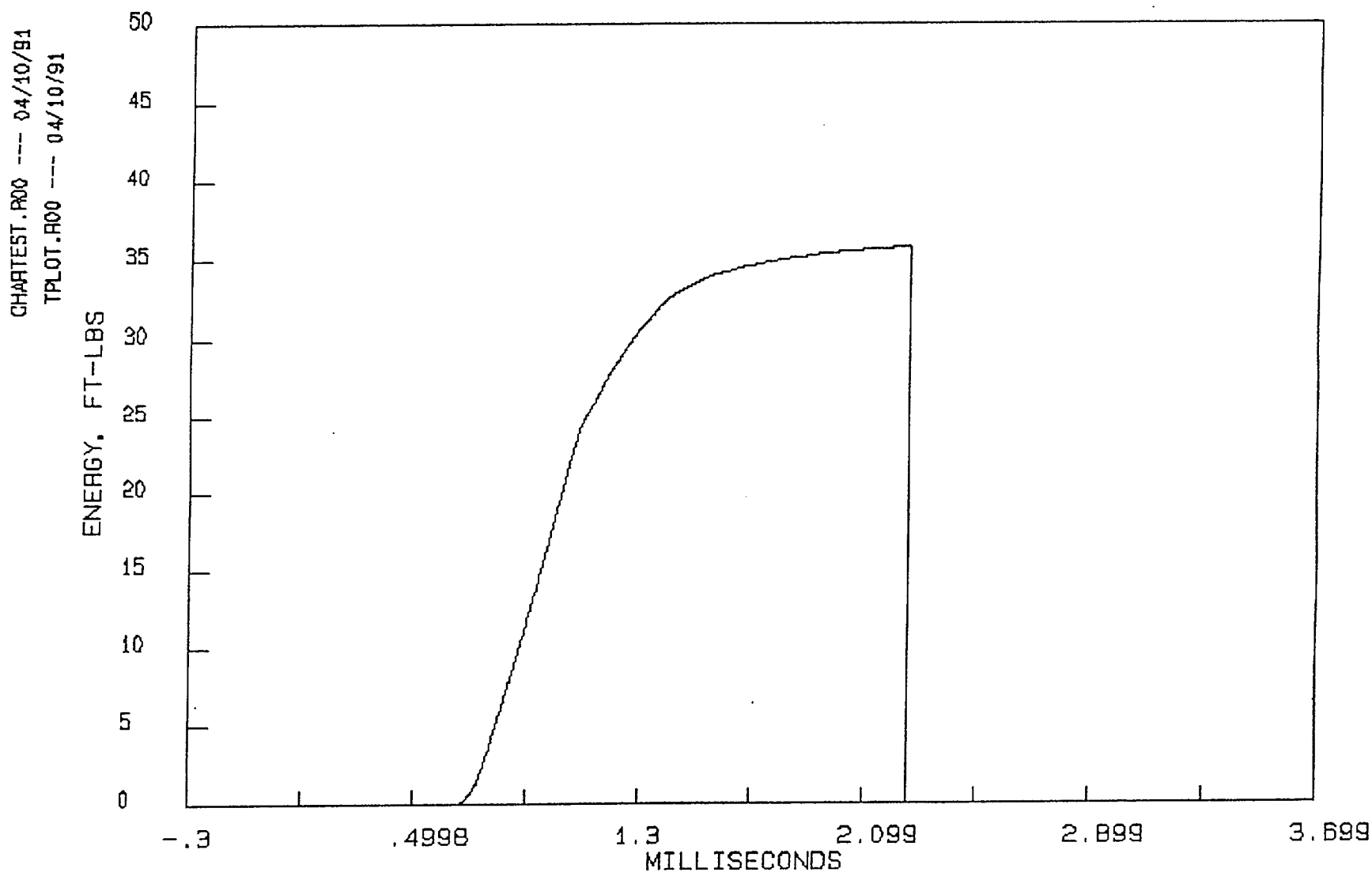

PROJ. NO. 1215-001 QA NO. 00001

LOAD - TIME TRACE FOR SPECIMEN WH34

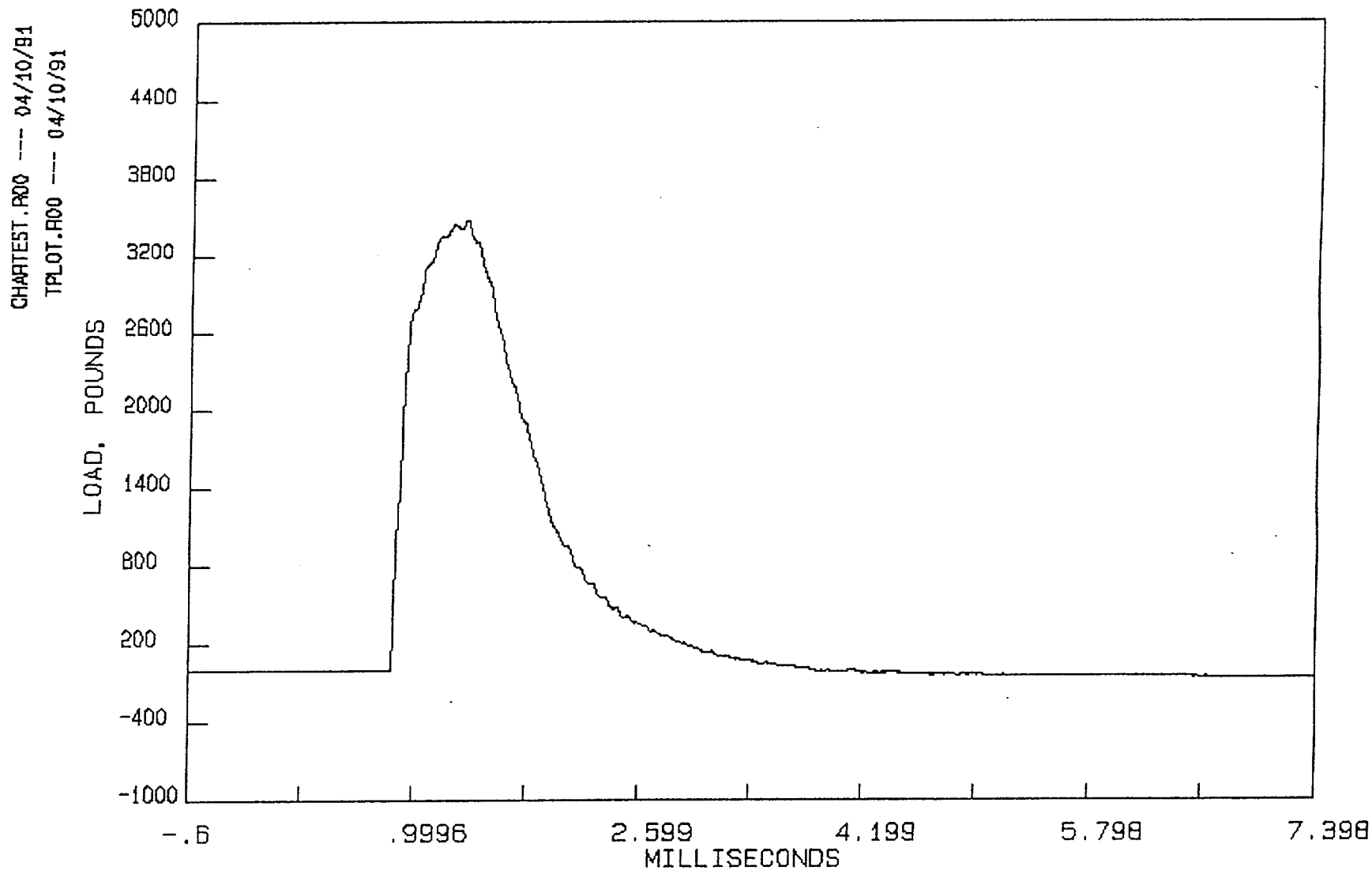

PROJ. NO. 1215-001 QA NO. 00001

ENERGY - TIME TRACE FOR SPECIMEN WH34

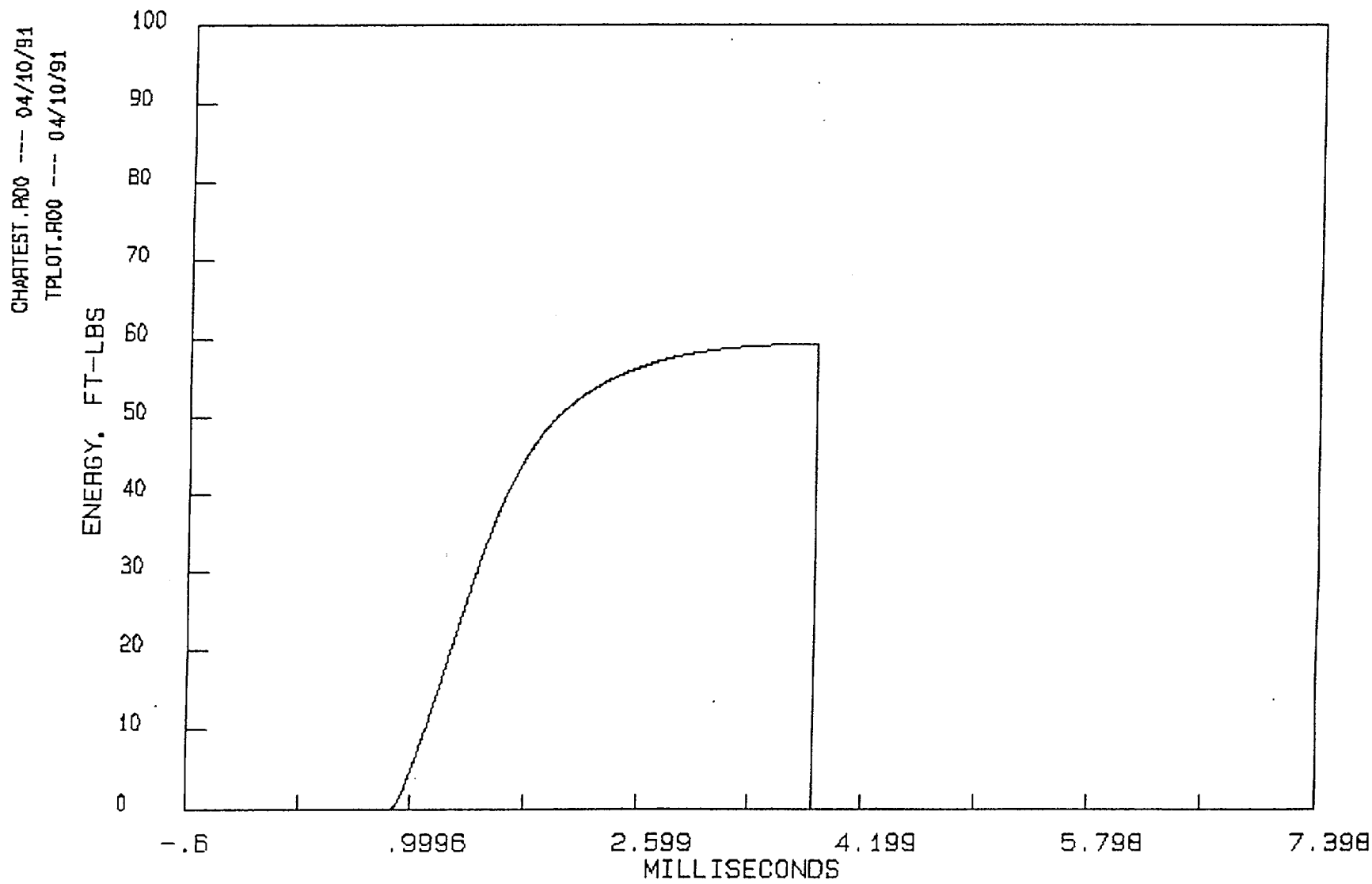

PROJ. NO. 1215-016 QA NO. 00001

LOAD - TIME TRACE FOR SPECIMEN WH43

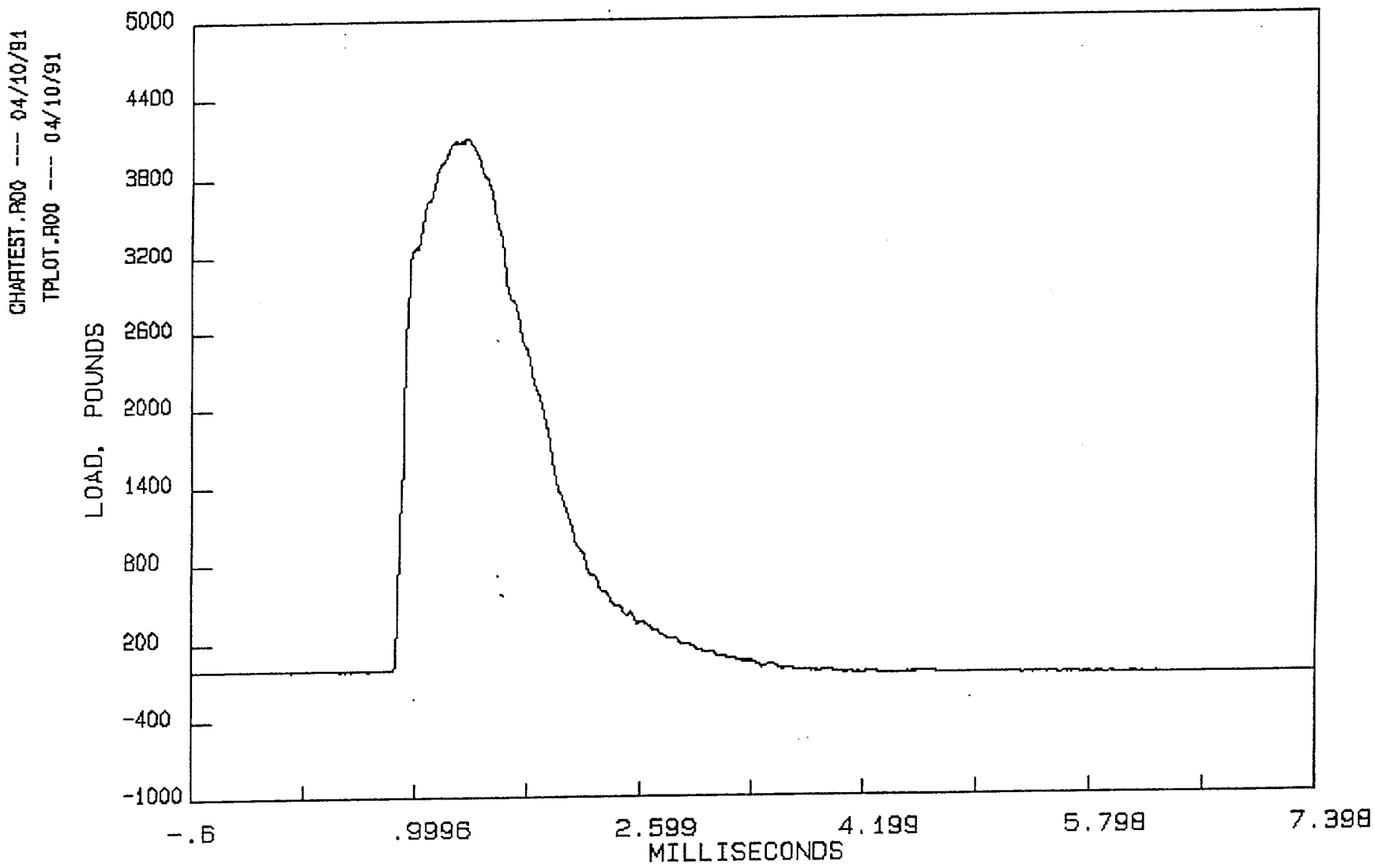

PROJ. NO. 1215-016 QA NO. 00001

ENERGY - TIME TRACE FOR SPECIMEN WH43

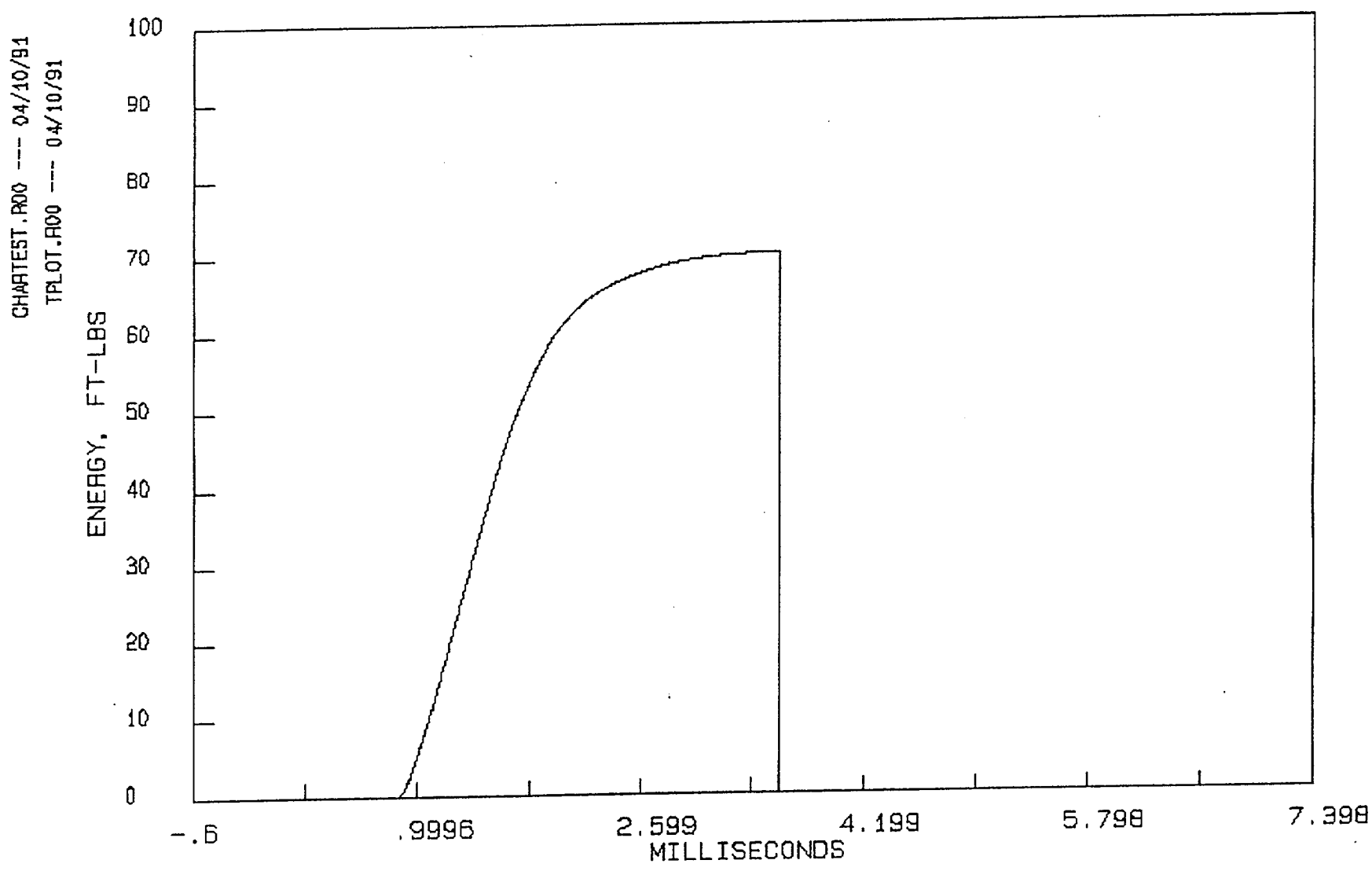

PROJ. NO. 1215-001 QA NO. 00001

LOAD - TIME TRACE FOR SPECIMEN WH39

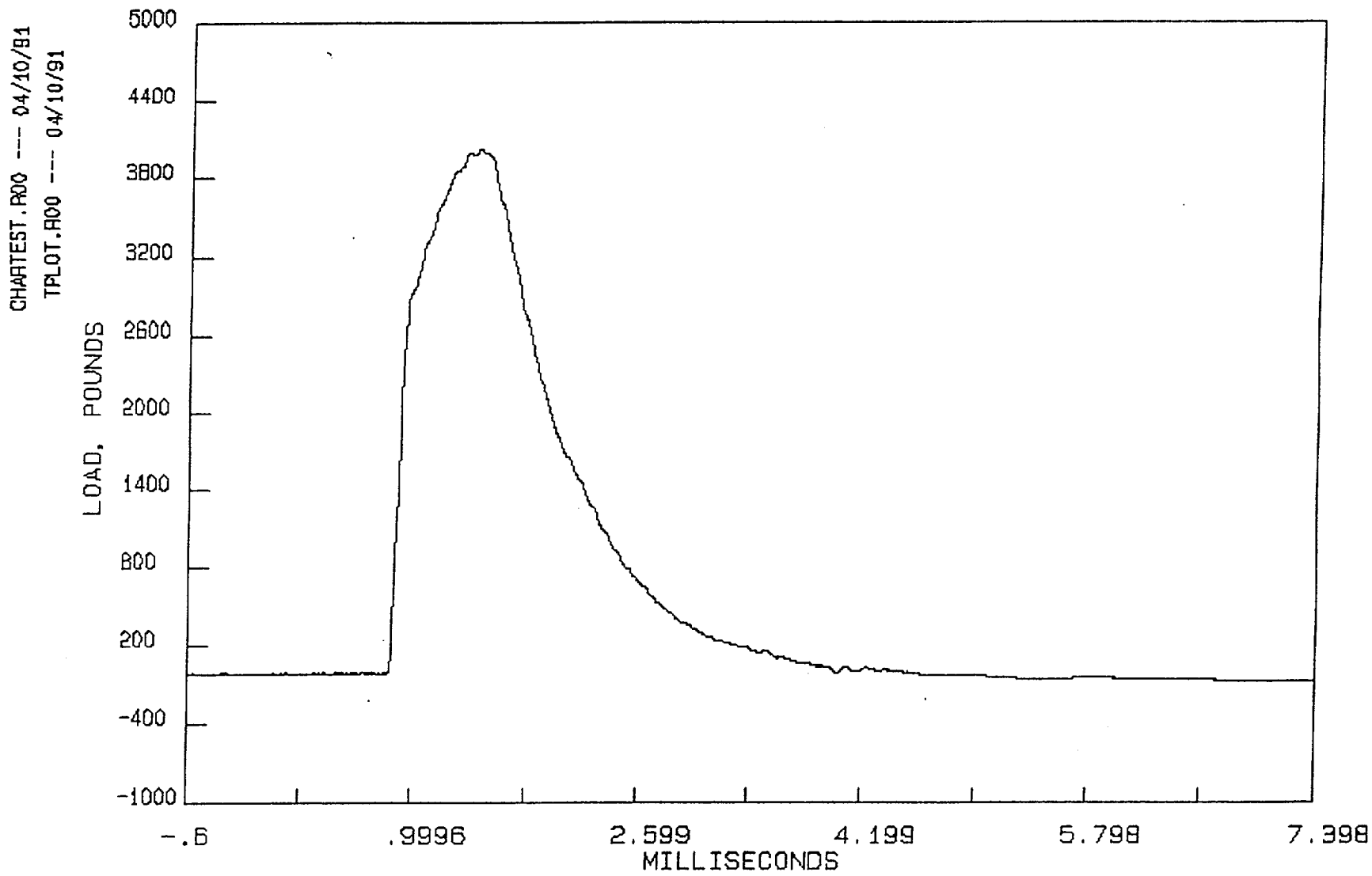

PROJ. NO. 1215-001 QA NO. 00001

ENERGY - TIME TRACE FOR SPECIMEN WH39

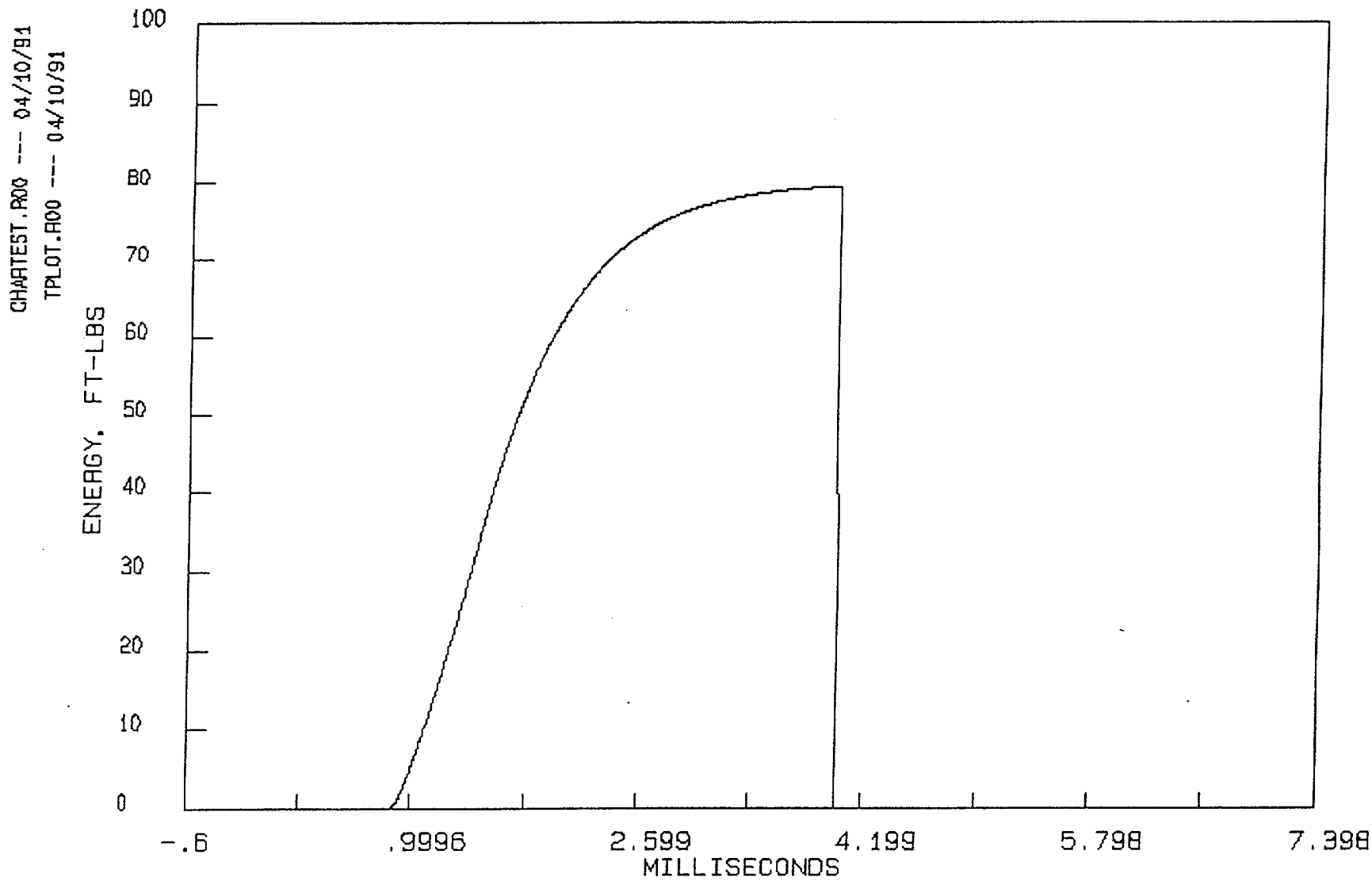

PROJ. NO. 1215-001 QA NO. 00001

LOAD - TIME TRACE FOR SPECIMEN WH31

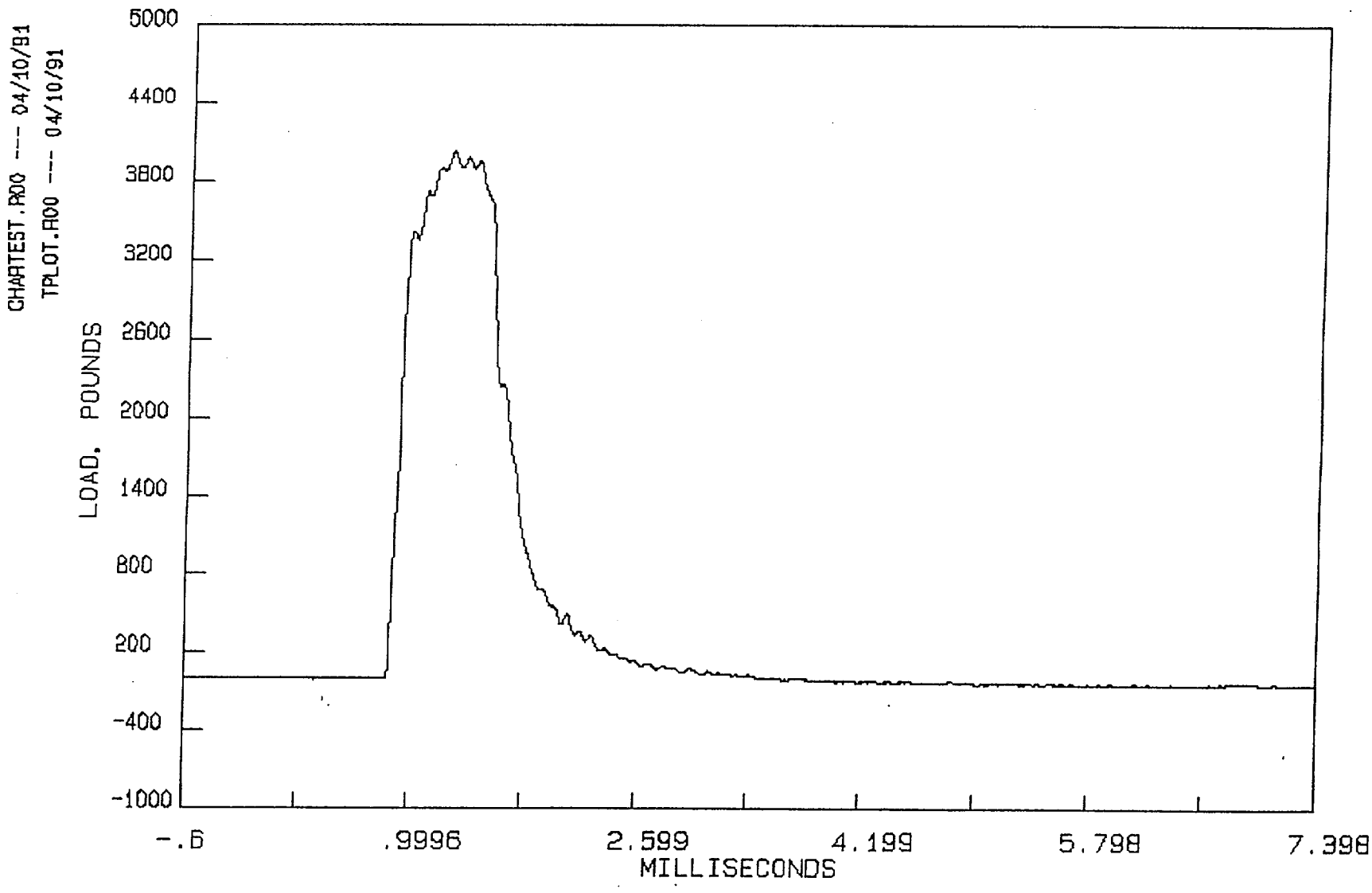

PROJ. NO. 1215-001 QA NO. 00001

ENERGY - TIME TRACE FOR SPECIMEN WH31

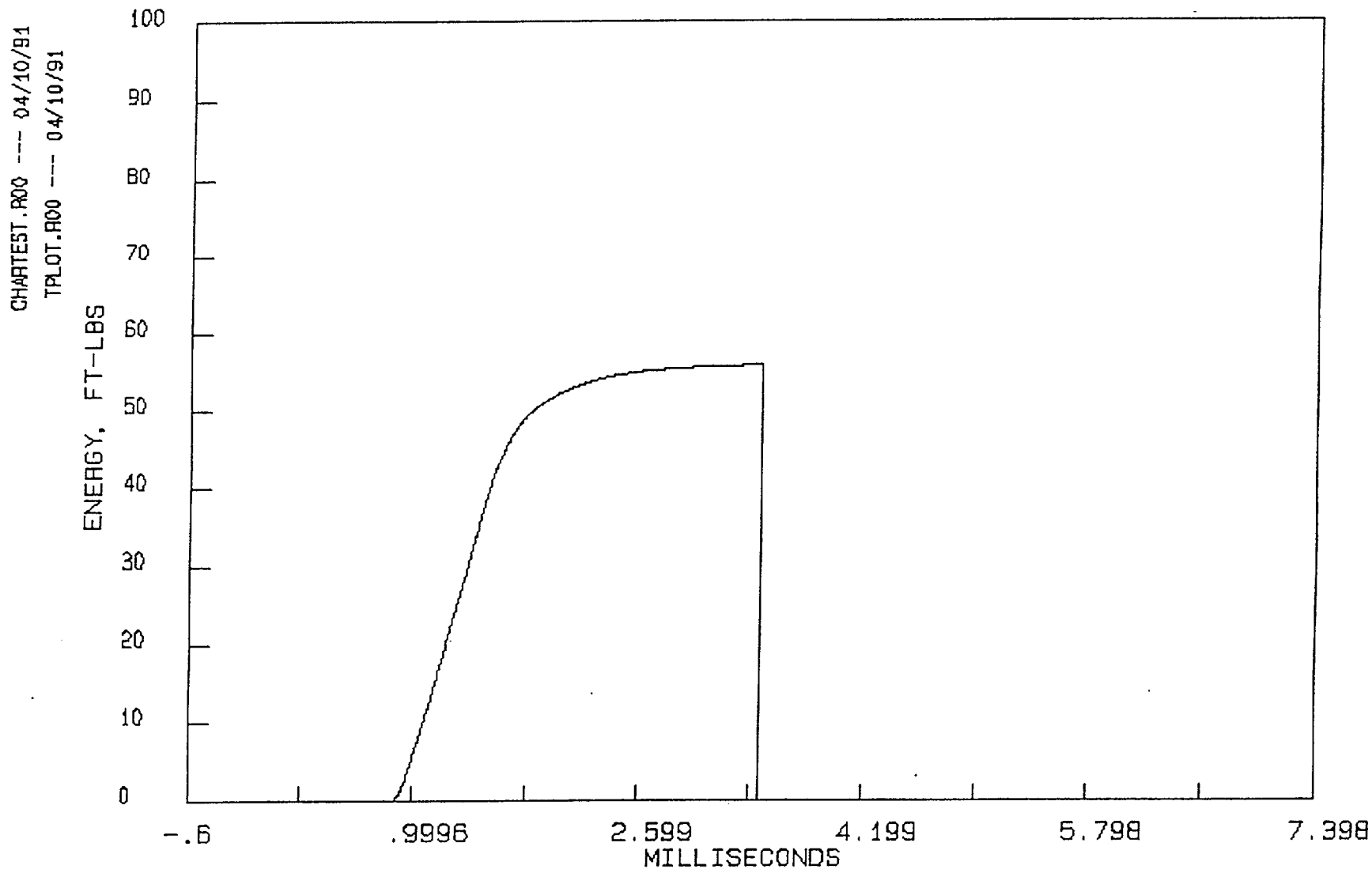

PROJ. NO. 1215-001 QA NO. 00001
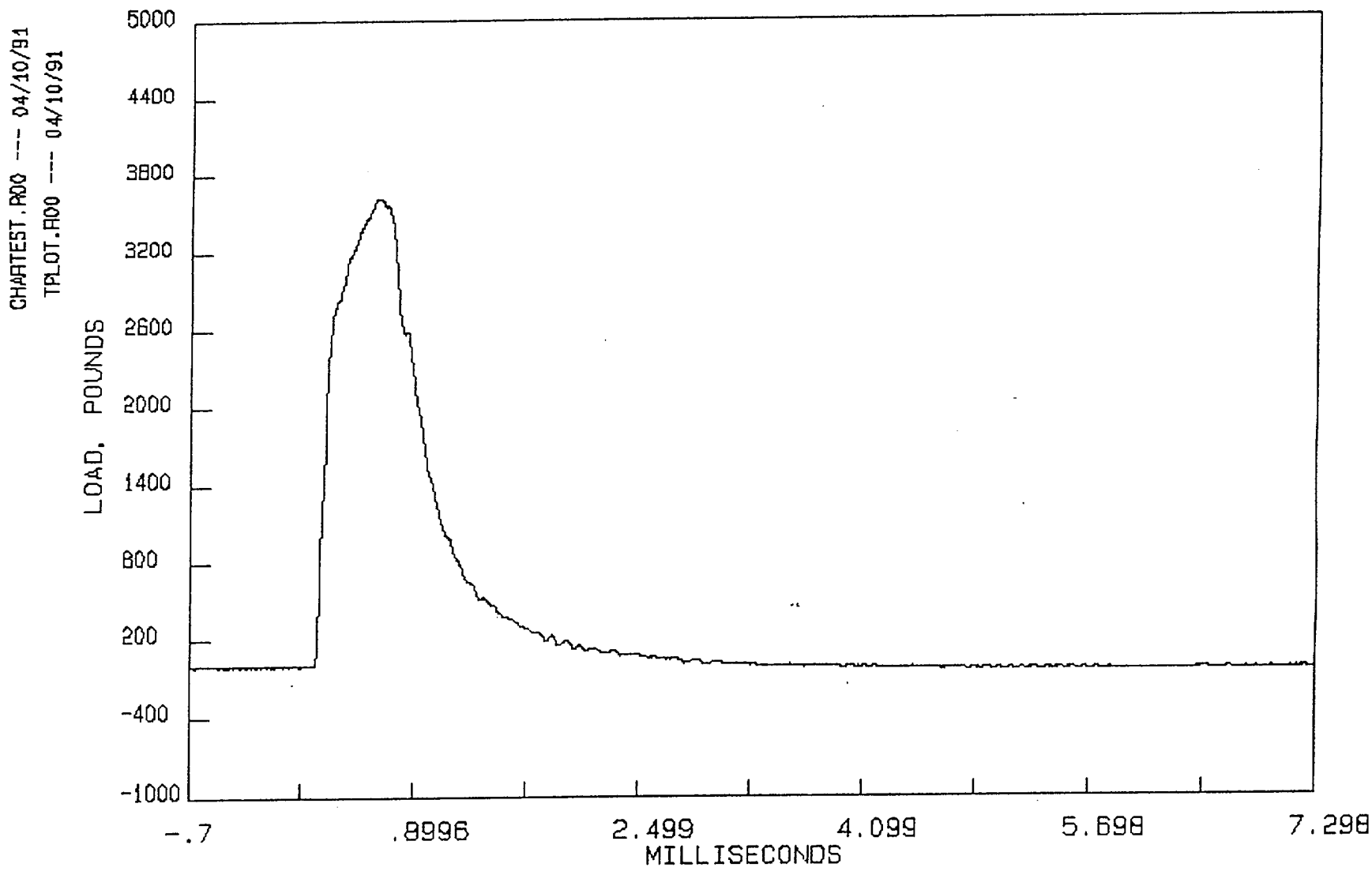
LOAD - TIME TRACE FOR SPECIMEN WT41